Univerzita Karlova v Praze

Lékařská fakulta v Plzni

Šiklův ústav patologie

Doktorská disertační práce

Korelace molekulárně-genetických a morfologických znaků vzácných nádorů slinných žláz

Petr Šteiner

Plzeň 2018

Obor: Patologie

**Školitelka: Prof. MUDr. Skálová Alena, CSc.**

Předmluva

Nádory slinných žláz jsou morfologicky velmi heterogenní a variabilní nádorovou skupinou s častým strukturálním a cytologickým překryvem mezi jednotlivými nádorovými jednotkami. Nádory slinných žláz se vyskytují velmi vzácně s incidencí 5-10 nových případů/ 100 tis. obyvatel, představují asi 6 % nádorů v oblasti hlavy a krku a kolem 0,3 % všech malignit. Nádory slinných žláz postihují jak velké slinné žlázy (příušní, podčelistní a podjazykovou), tak malé slizniční žlázy dutiny ústní, sinonasálního a zažívacího traktu [1, 2]. Mnohé salivární karcinomy jsou nízce maligní, a lze je vyléčit chirurgicky, ale vyskytují se i velmi agresivní primární nádory jako je salivární duktální karcinom, karcinom ex pleomorfní adenom nebo adenoidně cystický karcinom. Vzhledem k morfologické variabilitě a vzácnosti nádorů slinných žláz byla diferenciální diagnostika založená především na histologické klasifikaci vždy velkým dilematem.

Metody molekulární diagnostiky mají v patologii slinných žláz jak diferenciálně diagnostický význam, tak slouží v klasifikaci některých karcinomů, protože mnohé translokace jsou specifické pro určitou nádorovou jednotku. Objevy translokací a fúzních onkogenů, které jsou jejich produktem, změnily přístup ke klasifikaci salivárních karcinomů a do značné míry i diagnostické a interpretační postupy. Některé translokace byly nalezeny především v low-grade primárních karcinomech slinných žláz na základě morfologické analogie s nádory nesalivárního původu nesoucími identické translokace. Tímto způsobem byla objevena například translokace t(12;15)(p13;q25) s fúzním transkriptem *ETV6-NTRK3* u sekrečního karcinomu mamárního typu (mammary analogue secretory carcinoma, MASC) [3], která je identická u morfologicky blízkého sekrečního karcinomu prsu [4] a *EWSR1-ATF1* t(12;22) u hyalinizujícího světlobuněčného karcinomu shodná s některými nádory měkkých tkání [5].

Použití různých zlomových sond z chromosomové oblasti, ve které byla pozorována přestavba pomocí cytologických metod, vedla k identifikaci konkrétních fúzních genů, čehož bylo využito k charakterizaci fúze *MYB-NFIB* u translokace t(6;9)(q22-23;p23-24) adenoidně cystického karcinomu (AdCC) [6] nebo *CRTC1-MAML2* u t(11;19)(q21;p13) mukoepidermoidního karcinomu [7, 8].

Mezi metody, které umožňují detekci specifických translokací, patří především rutinně používané RT-PCR a FISH. V poslední době stále výrazněji také varianty sekvenování nové generace (next generation sequencing - NGS). RT-PCR je zkratkou pro „reverse transcription-polymerase chain reaction". RNA je zpětně přepsána do komplementární cDNA, která je pak amplifikována za použití primerů nasedajících okolo předpokládaného zlomového místa. Nevýhodou metody je nutná znalost přesné sekvence místa zlomu pro správný design primerů. FISH – flouorescenční in-situ hybridizace slouží k identifikaci specifických úseků DNA pomocí in-situ hybridizace s fluorescenčně značenou sondou. K detekci translokací lze využít tzv. „break apart" sond, kdy je jedna část sondy cílena k 5´ části (značena např. oranžovou barvou) genu, druhá k 3´ části genu (značena např. zelenou barvou). Takto lze nepřímo usuzovat na translokaci zjištěním právě zlomů v zúčastněných genech. V negativním případě jsou v mikroskopu vidět 2 složené oranžovo-žluto-zelené signály na jádro (**obr. 1A**), v pozitivním případě jeden složený signál ze zdravé alely a jeden oranžový a zelený signál ze
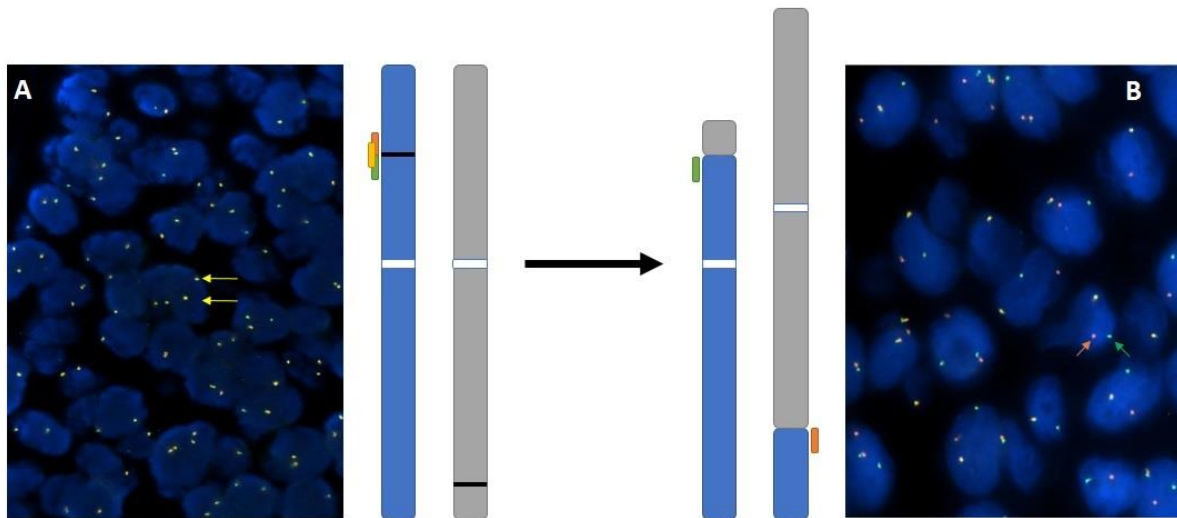
Obrázek 1 – **A.** Negativní „break apart" sonda reprezentovaná dvěva složenými oranžovo-žluto-zelenými signály. **B.** Pozitivní „break apart" sonda reprezentovaná jedním složeným oranžovo-žluto-zeleným signálem ze zdravé alely a separátním oranžovým a zeleným signálem ze zlomené alely.

zlomené alely (**obr. 1B**). Přímý průkaz translokace pomocí FISH je možný za užití fúzní sondy, kdy jedna část sondy překrývá jednoho fúzního partnera a druhá druhého. V negativním případě lze pozorovat 2 separátní oranžové a 2 zelené signály (**obr. 2A**), v pozitivním případě pak lze vidět 1-2 komplexní oranžovo-žluto-zelené signály v pozitivních jádrech (**obr. 2B**).
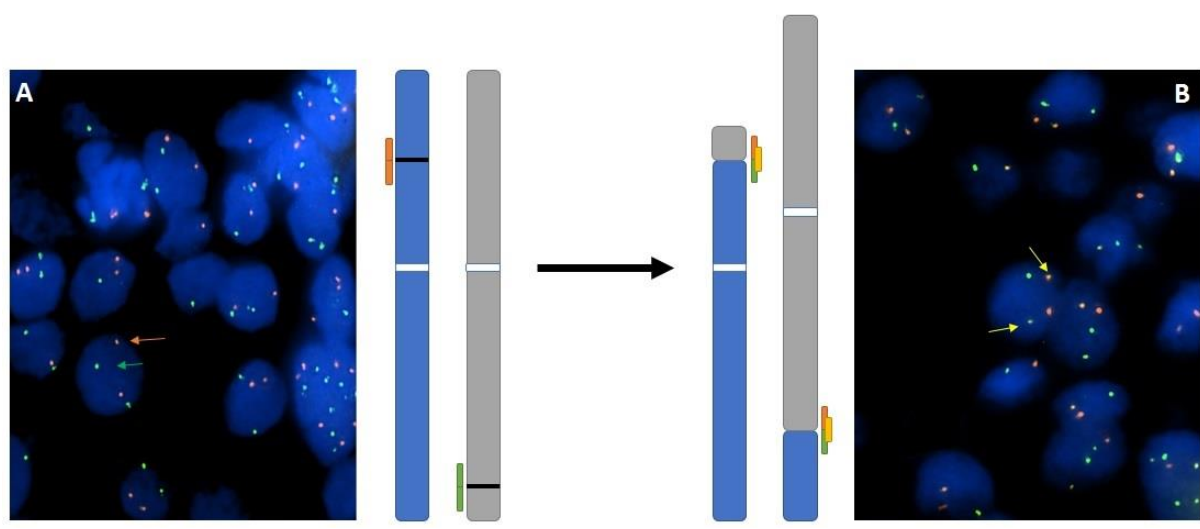
Obrázek 2 – **A.** Negativní „dual fusion" sonda reprezentovaná dvěva složenými oranžovo-žluto-zelenými signály. **B.** Pozitivní „dual fusion" sonda reprezentovaná jedním separátním oranžovým a zeleným signálem ze zdravých alel a 1-2 složenými oranžovo-žluto-zelenými signály jako průkaz fúze.

Nové možnosti v současnosti přináší NGS, které umožňuje detekci kompletní sekvence studované nukleové kyseliny včetně určení míry kvantifikace nukleových kyselin. NGS tím svým způsobem nahrazuje jak klasické Sangerovo sekvenování, tak array-komparativní genomovou hybridizaci (array-comparrative genome hybridization – aCGH),

která slouží k určení početních chromosomálních změn ve studovaném genomu z DNA, tak v případě využití cDNA (reverzně-transkribovaná RNA) včetně detekce míry exprese studovaných RNA a detekci fúzních genů. Mezi další výhody NGS patří též možnost cíleně studovat pouze konkrétní geny, což je oproti sekvenování celých genomů a transkriptomů finančně úspornější varianta, které lze dosáhnout po izolaci nukleové kyseliny, a případném přepsání RNA do cDNA, obohacením oblastí zájmu amplifikací či vychytáváním pomocí hybridizace.

Cíleným RNA sekvenováním byla v naší laboratoři v nedávné době nalezena vzácně se vyskytující fúze *ETV6-RET* u případů MASC negativních na fúzi *ETV6-NTRK3*, ale pozitivních na zlom *ETV6* [9], dále například fúze *NCOA4-RET* a *TRIM27-RET* u intraduktálního karcinomu slinných žláz, což bylo zatím publikováno jako předběžné sdělení na Kongresu amerických a kanadských patologů USCAP 2018 ve formě abstraktu [10].

Předložená doktorská dizertační práce se zabývá především „translokačními karcinomy slinných žláz" a je členěna do čtyř částí. V první části bude diskutována problematika adenoidně cystického karcinomu, v druhé části se práce zabývá sekrečním karcinomem mamárního typu (MASC), třetí část shrnuje publikované přehledové články a ve čtvrté části uvádíme publikaci studující význam *EWSR1* rearanže u vybraných salivárních karcinomů.

Adenoidně cystický karcinom (AdCC) je se svojí 10% četností u nádorů slinných žláz 2. nejčastějším salivárním karcinomem. AdCC je charakteristický svým intra- a perineurálním šířením vyskytujícím se až v 80% případů [11] a svým pomalým růstem. Přestože je často řazen mezi low-grade karcinomy, je jeho typickým projevem dlouhý klinický průběh, opakované recidivy a vysoké riziko rozvoje pozdních vzdálených metastáz. Z dlouhodobého hlediska se jedná o jeden z nejagresivnějších a nejméně předvídatelných nádorů hlavy a krku, vyznačující se vysokou mortalitou ve střednědobém horizontu [2]. Důležitým mezníkem pro diagnostiku AdCC bylo objevení a identifikace translokace t(6;9)(q22-23;p23-24) vyúsťující ve fúzi transkripčních faktorů *MYB* a *NFIB* [6, 12]. V principu díky této fúzi dochází ke stabilní expresi MYB. Té je nejčastěji dosaženo ztrátou jeho 3´ nepřekládané oblasti, která je fyziologicky cílena různými miRNA pro umlčení jeho exprese [6]. Díky rozvoji NGS metodik, byla u *MYB-NFIB* negativních případů nalezena fúze genů *MYBL1-NFIB* a to hned dvěma skupinami v témže roce a dále minoritní fúze genů *YTHDF3* a *RAD51B* s *MYBL1* genem, genů *XRCC4*, *NKAIN2*, *PTPRD* a *AIG1* s genem *NFIB* [13, 14]. Mutační analýzy zjistily nízkou frekvenci mutací u AdCC. Nalezené mutace se týkaly především genu *SPEN*, jehož mutace byly nazeleny u 21 % analyzovaných AdCC a dále mutace zasahující NOTCH signální dráhu patřily mezi nejčastěji pozorované [15].

Sekreční karcinom mamárního typu (mammary analogue secretory carcinoma – MASC) byl v naší laboratoři identifikován jako nový typ salivárního karcinomu v roce 2010 [3] a přijat novou WHO klasifikací v roce 2017 [2]. Pro MASC je typická translokace t(12;15)(p13;q25) vedoucí k fúzi genů *ETV6* a *NTRK3* [16, 17]. MASC je obvykle indolentní, ale lokoregionální recidivy a vzdálené metastázy byly též pozorovány. Důležitý je především vzácný výskyt high-grade transformace, který může vyústit ve smrt v souvislosti o onemocněním [18, 19]. Správná diagnostika MASC a určení fúze *ETV6-NTRK3,* eventuálně *ETV6-RET* jsou nutné k potenciální indikaci cílené biologické léčby inhibitory *NTRK3 (*např. entrectinib) u agresivních nebo neresekovatelných forem karcinomu [20-22].

Předložená doktorská dizertační práce je komentovaným souhrnem dvou prvoautorských článků, které jsou přijaté do tisku [23, 24], z nichž jeden článek bude publikován v impaktovaném časopise a 12 spoluautorských publikací týkajících se tématu nádorů slinných žláz, z čehož 9 bylo publikováno či přijato v impaktovaných časopisech [9, 25-32], zbylé tři jsou publikovány v neimpaktovaných časopisech [33-35]. Autor doktorské dizertace se dále podílel na vzniku dalších osmi publikací [36-43] nesouvisejících s tématem doktorandského studia.

Abstrakt

Doktorská dizertační práce se zabývá vztahem mezi histomorfologickými a molekulárně genetickými nálezy u vybraných nádorů slinných žláz. Autor se jako molekulárně-cytogenetický pracovník ve své práci zaměřoval především na využívání detekce translokací jako diferenciálně diagnostických markerů u karcinomů slinných žláz. Dizertační práce je komentovaným souborem vlastních publikací autora a je rozdělena do 4 částí.

V první části jsou publikace prohlubující znalosti o adenoidně cystickém karcinomu. Bylo prokázáno, že translokace t(6;9)(q22-23;p23-24) vyúsťující ve fúzi transkripčních faktorů *MYB-NFIB*, nebo translokace t(8;9) vyúsťující ve fúzi *MYBL1-NFIB* představují robustní diferenciálně diagnostický marker adenoidně cystického karcinomu. Dále bylo prokázáno, že vzhledem k statisticky významně nižšímu přežívání pacientů se ztrátou lokusu 1p36, může tato delece sloužit jako marker nepříznivé prognózy onemocnění.

Druhá část shrnuje práce zabývající se sekrečním karcinomem mamárního typu (MASC), který byl v naší laboratoři prioritně popsán jako nová jednotka, vyznačující se výskytem translokace t(12;15)(p13;q25) s fúzí genů *ETV6-NTRK3*. Dalším prioritním pozorováním je popis nové fúze *ETV6-RET* u menší části případů MASC. Nově byly popsány první dva případy MASC vycházející ze žlázek v nosní sliznici.

Třetí část tvoří přehledové články, z nichž jeden prvoautorský se zabývá detailním popisem molekulárně-genetických metod používaných ke studiu salivárního adenoidně cystického karcinomu. Další dva spoluautorské shrnují poznatky o biologickém chování, morfologii, prognostice a molekulární-genetice vybraných salivárních karcinomů, především u jednotek vykazujících charakteristické translokace.

Ve čtvrté části je komentována práce zabývající se vztahem mezi zlomem *EWSR1* genu a histomorfologií vybraných salivárních nádorů s převažující světlobuněčnou komponentou. Zlom *EWSR1* se vyskytuje ve spektru nádorových jednotek a není specifický pro hyalinizující světlobuněčný karcinom malých slinných žláz.

Summary

Thesis deals with relationship between histomorphological and molecular-genetic findings of selected salivary gland tumors. Author, as a molecular-cytogeneticist mainly focused on detection of tumor-specific translocations of the salivary gland tumors which can serve as differential diagnostic markers. The thesis is composed as a commented files of authors own publications, and it is divided into four parts.

First part deepens the knowledge of salivary adenoid cystic carcinoma. It was proved, that t(6;9)(q22-23;p23-24) resulting in fusion of transcription factors *MYB-NFIB*, or more rarely t(8;9) resulting in *MYBL1-NFIB* fusion represent robust differential diagnostic marker of adenoid cystic carcinoma. Further it was proved, that the 1p36 deletion can serve as an unfavorable prognostic indicator of adenoid cystic carcinoma, as the patients with 1p36 deletion had significantly lower survival.

Second part summarizes new developments about mammary analogue secretory carcinoma (MASC), which was described by our group as a new salivary tumor entity characterized by translocation t(12;15)(p13;q25) resulting in *ETV6-NTRK3* fusion. Another novel observation is a discovery of *ETV6-RET* fusion in a subset of MASC cases. Further, the first two MASCs of nasal mucosa origin have been described.

Third part consists of review articles. One of them deals with the description of molecular-genetic methods used to study adenoid cystic carcinoma. The latter two articles summarize the knowledge of biological behavior, morphology, prognostics and molecular-genetic of salivary gland carcinomas carrying diagnostic translocations.

In the last section, we comment the paper dealing with relationship of *EWSR1* gene break and histomorphology of selected salivary gland carcinomas with predominant clear cell component. *EWSR1* break occurs in a spectrum of tumor entities, and it is not specific for hyalinizing clear cell carcinoma of small oral salivary gland origin as originally expected.

Poděkování

Na tomto místě bych rád poděkoval prof. MUDr. Aleně Skálové, CSc. za odborné vedení a cenné připomínky k publikacím a při vypracovávání této práce a kolektivu Bioptické laboratoře s.r.o. za pomoc s vlastními analýzami.

Prohlášení

Prohlašuji, že jsem tuto dizertační práci vypracoval samostatně, uvedl jsem všechny použité prameny a literaturu a že práce nebyla použita k získání jiného nebo stejného titulu.

V Plzni dne 8.4.2018   Mgr. Petr Šteiner

Obsah

Seznam použitých zkratek

AdCC	adenoidně cystický karcinom
cDNA	komplementární DNA
CCMC	clear cell myoepithelial carcinoma (světlobuněčný myoepiteliální karcinom)
DNA	deoxyribonukleová kyselina
EMK	epiteliálně-myoepiteliální karcinom
FISH	fluorescenční in-situ hybridizace
ITAC	intestinal-type adenocarcinoma (adenokarcinom intestinálního typu)
MASC	mammary analogue secretory carcinoma (sekreční karcinom mamárního typu)
MCC	myoepiteliální karcinom slinných žláz (myoepithelial cell carcinoma
miRNA	krátké ~22 nukleotidů dlouhé RNA sloužící především k regulaci genové exprese
MC ex PA	myoepithelial carcinoma ex pleomorphic adenoma (myoepiteliální karcinom vznikající z pleomorfního adenomu
NGS	next-generation sequencing (sekvenování nové generace)
non-ITAC	non-intestinal type adenocarcinoma (sinonasální adenokarcinom neintestinálního typu)
PCR	polymerázová řetězová reakce
RNA	ribonukleová kyselina
RT-PCR	reverzně transkripční polymerázová řetězová reakce

Souhrn komentovaných publikací

1. část - Adenoidně cystický karcinom

V první části shrnujeme nové poznatky ze studia adenoidně cystického karcinomu (AdCC) slinných žláz. AdCC je low-grade bazaloidní nádor sestávající z epiteliálních a myoepiteliálních buněk ve variabilních morfologických strukturách [2]. Jedná se o nejčastější karcinom hlavy a krku infiltrující nervy, s peri- a intraneurálním šířením ve 20 - 80 % případů [11]. AdCC je většinou ohraničený, ale neopouzdřený nádor, hluboce infiltrující okolní tkáně především progresí kolem nervů. Je tvořen dvěma hlavními typy buněk, a to duktálními a modifikovanými myoepiteliálními. Jádra jsou hranatá a hyperchromní, cytoplazma často vodojasná. V AdCC se rozlišují tři růstové struktury: tubulární, kribriformní a solidní v různém procentuálním zastoupení [2].

Pro AdCC slinných žláz je typická chromozomální translokace t(6;9)(q22-23;p23-24), která generuje fúzní transkript *MYB-NFIB*. *MYB-NFIB* fúzní onkogen byl poprvé popsán u AdCC Martou Perssonovou et al. v roce 2009 [6]. *MYB-NFIB* fúze nebo přestavba *MYB* genu, které vedou k jeho aktivaci, a tím ke zvýšené expresi MYB-NFIB fúzního proteinu nebo MYB onkoproteinu, byly dosud ze salivárních karcinomů i jiných karcinomů hlavy a krku prokázány pouze u AdCC, a to ve více jak v 80 % případů [17]. Jedná se tak o charakteristický znak těchto maligních sialomů, který se dá využít jako diagnostický marker, s výhodou především u vzdálených metastáz nebo diagnosticky obtížných variant AdCC.

V prvním článku této části „*Adenoidně cystický karcinom slinných žláz. Soubor 27 pacientů*" [34] je řešen především klinický charakter tohoto onemocnění u 27 pacientů léčených v letech 1986 – 2016 ve FN Plzeň, ke kterým byla dostupná klinická data. Soubor je doplněn o výsledky FISH analýzy, konkrétně zlomů genů *MYB* a *NFIB*, fúze *MYB-NFIB* a nakonec ztráty lokusu 1p36. Z výsledků vyplynulo, že AdCC vznikl nejčastěji v malých slinných žlázách ve 41 % případů, metastázy v regionálních uzlinách byly objeveny u 26 % případů a úmrtnost v souvislosti s onemocněním činila 22 %. Molekulární analýza odhalila 79% četnost fúze *MYB-NFIB*, heterozygotní delece lokusu 1p36 se vyskytovala u 3/23 analyzovatelných pacientů.

V publikaci „*Adenoid cystic carcinoma of the salivary gland, lacrimal gland, and breast are morphologically and genetically similar but have distinct microRNA expression profiles*" [31] jsou porovnávány rozdíly v miRNA profilu s výskytem fúzí zahrnujících geny *MYB*, *NFIB* a *MYBL1* mezi AdCC slinných žláz, slzných žláz a prsu. Klastrová analýza miRNA spolehlivě odlišila salivární a slzné AdCC od jejich nenádorových tkání a také odlišila AdCC dle původu (salivární, slzné, prsu), ale ne AdCC prsu od jejich nenádorových tkání. Fúze *MYB-NFIB* se vyskytovala u 55 % pacientů ve všech studovaných lokalizacích. Translokace zahrnující *MYBL1* gen se omezovala jen na salivární AdCC.

V další publikaci „*MicroRNA dysregulation in adenoid cystic carcinoma of the salivary gland in relation to prognosis and gene fusion status: A cohort study*" [29] studující miRNA profil v souboru celkem 184 pacientů s AdCC byly identifikovány například vysoké exprese hsa-mir-21, hsa-mir-181a-2 a hsa-mir-152 jako asociované se sníženým celkovým přežitím a vysoká exprese hsa-miR-374c naopak s lepším přežitím do recidivy. Dále byla u některých miRNA nalezena shoda s již dříve publikovanými výsledky [44]. Tyto výsledky mohou výrazně pomoci k nalezení prognostických faktorů i u vzorků s výrazně degradovaným materiálem, kde miRNA, narozdíl od DNA a RNA, zůstává často dobře zachována [45, 46].

Třetí, prvoautorský, článek „*Prognostic signifikance of 1p36 locus deletion in adenoid cystic carcinoma of the salivary glands*" [24] se detailně zabývá delecí lokusu 1p36 a jejího prognostického významu a možnostem fúzí zahrnující geny *MYB*, *NFIB* a *MYBL1* u celkem 85 analyzovatelných případů salivárních AdCC. Z těchto pochází 23 z registru nádorů Šiklova ústavu a FN Plzeň a dalších 62 z registru nádorů Rigshospitalet v Kodani v Dánsku. Delece lokusu 1p36 byla detekována u 13/85 (15,29 %) pacientů, signifikantně korelovala s vyšším stádiem (3/4) onemocnění v době diagnózy, nižším celkovým přežitím, pro nemoc specifickým přežitím, intervalem do recidivy a přežitím do recidivy. Toto činí z delece 1p36 marker nepříznivé prognózy onemocnění. Translokace zahrnující *MYB*, *NFIB* a *MYBL1* byly identifikovány u celkem 79/85 (92,94 %) pacientů, což z nich činí silný diagnostický nástroj, s výhodou využitelný zvláště u pozdních vzdálených metastáz. Zajímavé bylo též objevení korelace mezi zlomem *MYBL1* a nižším stádiem (1 a 2) onemocnění a zlomu *MYB* s nižším celkovým přežitím a pro nemoc specifickým přežitím. Žádný z 1p36 pozitivních případů nevykazoval rearanži *MYBL1*, které mohou být vzájemně vylučující.

V následující publikaci „ *Small subset of adenoid cystic carcinoma of the skin is associated with alterations of the MYBL1 gene similar to their extracutaneous counterparts*" [32] byly opět studovány fúze zahrnující geny *MYB*, *NFIB* a *MYBL1* u deseti pacientů s kožním AdCC pomocí metody FISH. Dále byla studována přítomnost *MYB-NFIB* transkriptu pomocí RT-PCR. Fúze *MYB-NFIB* byla nalezena u 4 pacientů, *MYB-X* u 2 pacientů a poprvé u kožních AdCC byly též nalezeny rearanže *MYBL1* u dvou pacientů. Fúzní transkript se podařilo prokázat pouze u 1 z 8 studovaných pacientů.

V poslední publikaci této části „*The incidence of MYB gene breaks in adenoid cystic carcinoma of the salivary glands and its prognostic signifikance*" [33] byl studován vztah mezi zlomem *MYB* a prognózou onemocnění u 23 pacientů s AdCC slinných žláz. Zlom *MYB* byl detekován u 15/23 případů (65,22 %). Nepodařilo se však prokázat vztah mezi zlomem *MYB* a žádným ze studovaných klinických parametrů (věku, pohlaví, velikostí nádoru, přítomností metastáz, histologického gradingu a perineurální invaze). Závěrem lze říci, že v diferenciální diagnostice AdCC není vhodné detekovat pouze zlom *MYB*, ale je třeba využít i dalších genů, které se taktéž vyskytují u AdCC (*NFIB*, *MYBL1*). Podařilo se identifikovat první potenciální prognostický marker AdCC a sice deleci lokusu 1p36.

Adenoidně cystický karcinom slinných žláz. Soubor 27 pacientů

(Původní práce – retrospektivní studie)

Adenoid Cystic Carcinoma of Salivary Glands. Case Series of 27 Patients

(Original Article – Retrospective Study)

Hauer L.[1], Skálová A.[2,3], Šteiner P.[3], Hrušák D.[1], Andrle P.[1], Hostička L.[1], Sebera O.[4]

[1]Stomatologická klinika LF UK a FN, Plzeň
[2]Šiklův ústav patologie LF UK a FN, Plzeň
[3]Bioptická laboratoř s.r.o., Plzeň
[4]ORL klinika LF UK a FN, Plzeň

SOUHRN

Úvod a cíl práce: Adenoidně cystický karcinom (AdCC) je druhým nejčastějším salivárním karcinomem. Tento maligní sialom je charakteristický svým pomalým růstem, a přestože se histologicky jedná o low--grade nádor, typickým jevem je častý prolongovaný klinický průběh trvající zpravidla roky, opakované recidivy, vznik především vzdálených metastáz a vysoká smrtnost onemocnění. V posledních několika letech byly zjištěny nejen nové skutečnosti ohledně biologického chování AdCC, ale byly objeveny i molekulárně genetické znaky, které jsou pravděpodobně zodpovědné za jeho kancerogenezi. S ohledem na tato fakta autoři v předkládané práci vyhodnocují vlastní soubor pacientů s AdCC.
Metody: Do retrospektivní klinické studie bylo zahrnuto 27 pacientů s AdCC, kteří byli léčeni ve FN v Plzni v posledních 30 letech (01/1986 až 01/2016). Byly sledovány klinické i demografické parametry. Soubor byl navíc vyšetřen pomocí fluorescenční in situ hybridizace na průkaz nádorově specifického MYB-NFIB fúzního onkogenu a na deleci 1p36.
Výsledky: AdCC vznikl ve 41 % v malých slinných žlázách, v 26 % ve žláze podčelistní, v 22 % v žláze příušní a v 11 % v žláze podjazykové. První stadium bylo zaznamenáno v 26 % případů, 2. stadium v 18 %, 3. stadium v 26 % a 4. stadium v 30 % případů. Metastázy v regionálních lymfatických uzlinách byly diagnostikovány u 26 %, vzdálené metastázy pak u 30 % pacientů (podle lokalizace – plíce 55 %, játra 27 %, kosti 9 %, peritoneum 9 %). Průměrný follow-up byl 76,4 ± 67,0 měsíců (v rozmezí 7–287 měsíců). Za dobu dispenzarizace bylo 59 % pacientů bez jakýchkoli příznaků choroby, 22 % zemřelo v důsledku AdCC a 19 % žilo s tímto onemocněním, ať již v podobě recidivy či metastáz. Fúzní onkogen MYB-NFIB byl prokázán v 79 % případů (19/24) a 1p36 delece pak ve 13 % případů (3/23).
Závěr: AdCC slinných žláz vykazuje vyšší tendenci k zakládání regionálních uzlinových metastáz, než se dříve soudilo. MYB-NFIB fúze je hlavní nádorově specifickou onkogenní událostí u AdCC s vysokou úspěšností detekce. Tento fúzní onkogen je možné v současné době potenciálně využít pouze jako pomocný diagnostický nástroj u histopatologicky sporných případů, především pak u pozdních vzdálených metastáz.
Klíčová slova: *adenoidně cystický karcinom – fúzní onkogen – biomarker – MYB-NFIB*

SUMMARY

Aim of the study: Adenoid cystic carcinoma (AdCC) is the second most common salivary gland cancer. This malignant tumor is characterized by its slow growth and in spite of the fact that it has a histological low - grade appearance, a prolonged clinical course usually lasting for years, repeated recurrences,

Hauer L., Skálová A., Šteiner P., Hrušák D., Andrle P., Hostička L., Sebera O.

development of distant metastases and high mortality rate are typical signs. New facts of its biological behavior as well as new fusion oncogenes probably responsible for its carcinogenesis were described in the last few years. In light of these facts, the authors evaluate their own case series of patients suffering from AdCC in this manuscript.

Methods: The retrospective case series included 27 patients with AdCC, who were treated at the University Hospital in Pilsen in the last 30 years (01/1986–01/2016). Clinical and demographic parameters were identified and evaluated. Detection of the 1p36 deletion and the tumor-specific MYB–NFIB fusion oncogene by fluorescence in situ hybridization were performed.

Results: The incidence of AdCC in minor salivary glands, submandibular gland, parotid gland and sublingual gland was 41%, 26%, 22 % and 11% respectively. The following staging was observed: the 1st stage in 26%, the 2nd stage in 18%, the 3rd stage in 26% and the 4th stage in 30% of cases. Metastases to regional lymph nodes were diagnosed in 26% and distant metastases in 30% of patients (55% to lung, 27% to liver, 9% to bones and 9% of peritoneal metastases). The average follow-up was 76.4 ± 67.0 months (range 7–287 months). An outcome of the treatment during follow-up was as follows: 59% of patients were with no evidence of the disease, 22% of patients died because of the disease and 19% of patients were alive with a recurrence or metastases of AdCC. The MYB-NFIB fusion transcript was detected in 79% of cases (19/24) and the 1p36 deletion in 13% of cases (3/23).

Conclusion: The AdCC of salivary glands shows a greater tendency to development of regional lymph node metastases than previously thought. The MYB-NFIB gene fusion is the major tumor-specific oncogenic event in AdCC with high detection rate. The MYB-NFIB fusion oncogene could currently only be used as a potential diagnostic tool in difficult histopathological cases of AdCC, especially in late distant metastases.

Keywords: *adenoid cystic carcinoma – fusion oncogene – biomarker – MYB-NFIB*

ÚVOD

Adenoidně cystický karcinom (AdCC) je bazaloidní nádor sestávající se z epiteliálních a myoepiteliálních buněk v různých morfologických konfiguracích, tvořících tubulární, kribriformní a solidní struktury [6]. Jedná se o nejčastější karcinom hlavy a krku s peri- a intraneurálním šířením (20–80 % případů), a to i diskontinuálním způsobem (skip lesions), což je příčinou zasahování tumoru za klinické a radiologické hranice s vysokým rizikem pro recidivy nádoru (i za předpokladu dosažení negativních resekčních okrajů) [4, 23]. Ve srovnání s ostatními salivárními karcinomy je u AdCC popsáno v lidském těle nejvíce možných lokalizací, kde může tento nádor primárně vznikat. Kromě slinných žláz postihuje i žlázu slznou, zvukovod a žlázy v horním aerodigestivním traktu (hrtan, nos a paranazální dutiny). Může ale vzácně vznikat i ve vzdálenějších orgánech, jako je trachea, bronchy, prsní žláza, prostata, kůže, ovaria, děložní hrdlo nebo Bartoliniho žlázy [19, 28]. Biologické chování a prognóza AdCC se v jednotlivých lokalizacích liší [19, 20, 22]. AdCC slinných žláz je charakteristický svým pomalým růstem, a přestože se histologicky jedná o low-grade nádor, typickým jevem je častý prolongovaný klinický průběh trvající zpravidla roky, opakované recidivy, vznik především vzdálených metastáz a vysoká smrtnost onemocnění.

Incidence salivárního AdCC se uvádí 3–4,5 případů/1 milion obyvatel/rok (pro západní Evropu se uvádí rozmezí 0,14–0,64/100 000 obyvatel/rok) [8, 9]. Představuje asi 1 % všech malignit hlavy a krku [9] a tvoří 10 % všech sialomů a 20 % všech salivárních karcinomů [28]. Je tak po mukoepidermoidním karcinomu druhou nejčastější salivární malignitou. AdCC je nejčastějším maligním sialomem žlázy podčelistní a pravděpodobně i jazyka [23]. Je také považován za nejčastější karcinom malých slinných žláz, kde představuje asi 30 % ze všech nádorů postihujících tyto žlázy (někdy se uvádí až na druhém místě po mukoepidermoidním karcinomu) [28]. Vzniká především na patře, druhou nejčastější lokalizací jsou žlázy sliznice vedlejších nosních dutin (obr. 1). Tvoří 12–15 % salivárních karcinomů příušní žlázy, 30–60 % žlázy podčelistní a 32–71 % karcinomů malých slinných žláz [28].

AdCC postihuje všechny věkové skupiny, nejvyšší incidence je ale u pacientů ve věku 40 až 60 let. Z hlediska výskytu u jednotlivých pohlaví není popsána významnější predilekce kromě AdCC podčelistních žláz, který vzniká téměř výhradně u žen [23].

V posledních několika letech byly zjištěny nejen nové skutečnosti ohledně biologického chování AdCC, ale byly objeveny i molekulárně genetické znaky, které jsou pravděpodobně zodpovědné za jeho kancerogenezi.

Obr. 1 Adenoidně cystický karcinom malé slinné žlázy tvrdého patra vpravo

a hlavní genetickou událost AdCC, velmi pravděpodobně zodpovědnou za jeho kancerogenezi. *MYB-NFIB* fúze nebo rearanže *MYB* genu, které vedou k jeho aktivaci, a tím ke zvýšené expresi *MYB–NFIB* fúzního proteinu nebo *MYB* onkoproteinu, byly dosud ze salivárních karcinomů i jiných karcinomů hlavy a krku prokázány pouze u AdCC, a to ve více než v 80 % případů [33]. Jedná se tak o charakteristický znak těchto maligních sialomů, že se u něj v současnosti zkoumají možnosti využití jako diagnostického, prognostického a terapeutického biomarkeru. Zcela recentně byl u AdCC popsán i nový fúzní onkogen *MYBL1-NFIB* jako následek translokace t(8;9) [26]. Translokace t(8;9) a jiné rearanže genu *MYBL1* byly zjištěny u 35 % AdCC negativních na translokaci t(6;9) [26].

S ohledem na tato fakta autoři v předkládané práci vyhodnocují vlastní soubor pacientů s AdCC.

MATERIÁL A METODY

Pomocí klinických informačních systémů PC DENT (CompuGroup Medical Česká republika s.r.o., verze 3.1.1, revize:6), WinMedicalc (Medicalc software s.r.o., Česká republika, verze 2.10.8.46) a WinZis (Prodata Praha s.r. o., Česká Republika) byli vyhledáni všichni pacienti s diagnózou AdCC, kteří byli léčeni ve FN v Plzni (Stomatologická a ORL klinika) a u kterých byly dohledatelné klinické údaje o dispenzarizaci trvající nejméně šest měsíců. Bylo identifikováno 27 pacientů za období 01/1986 až 01/2016, tedy za 30 let. Ve stanoveném souboru byly sledovány tyto ukazatele: věk, pohlaví, lokalizace nádoru, klinické stadium v době diagnózy podle 7. vydání TNM klasifikace, přítomnost metastáz v regionálních lymfatických uzlinách a vzdálených metastáz, grading, průměrná doba dispenzarizace, léčba a její výsledky.

Metodika detekce *MYB-NFIB* fúze pomocí FISH

Čtyři mikromilimetry silné řezy tkáně formalínem fixované, v parafínu zalité (FFPE) byly naneseny na povrch pozitivně nabitých podložních skel. Neobarvené standardně deparafinizované preparáty byly inkubovány v 1x Target Retrieval Solution Citrate pH 6 (Dako, Glostrup, Německo) při 95 °C/40 minut a ve stejném roztoku chlazeny po dobu 20 minut při pokojové teplotě. Skla byla následně omyta v destilované vodě po dobu pěti minut při pokojové teplotě, natrávena v roztoku pepsinu (Sigma Aldrich, St. Louis, MO, USA) o koncentraci 0,5 mg/ml v 0,01M HCl při 37 °C/25 minut a omývána v destilované vodě po dobu pěti minut při pokojové teplotě. Následovala dehydratace vzestupnou alkoholovou řadou (70 %,

Lymfogenní metastázování do regionálních lymfatických uzlin se u AdCC tradičně považuje za vzácné (6–10 %), vznikající jen při nekontrolovaném pokročilém či recidivujícím onemocnění [2]. Jedná se ale pravděpodobně o nesprávný údaj. Podle recentní multicentrické studie se ukazuje, že regionální uzlinové postižení je u tohoto karcinomu častějším jevem, než se dříve soudilo, a to v 29 % případů (79/270). Především u orálních AdCC malých slinných žláz jsou metastázy v krčních lymfatických uzlinách relativně časté (37 %, 55/148 pacientů) oproti AdCC velkých slinných žláz (19 %, 18/95 pacientů) [2]. Metastázy nejčastěji vznikají v uzlinových oblastech I až III, nehledě na lokalizaci primárního nádoru (85 % pacientů s metastázami orálních AdCC, 55 % s metastázami AdCC velkých slinných žláz). Při elektivních krčních disekcích byly prokazovány okultní mikrometastázy v 15–44 % případů [34]. Nejčastější postižení klinicky nedetekovatelnými metastázami v lymfatických uzlinách bylo zaznamenáno u AdCC malých slinných žláz (22 % u orálních tumorů a 16 % u karcinomů paranazálních dutin) [2]. U AdCC s high-grade transformací se vyskytují metastázy v regionálních lymfatických uzlinách ve více než 50 % případů [13, 29]. Vyšší incidence nodálních metastáz se udává i u solidní varianty AdCC (grade 3).

Pro AdCC slinných žláz je typická chromozomální translokace t(6;9)(q22-23;p23-24), poprvé popsaná v roce 2009, která generuje fúzní onkogen MYB-NFIB [33]. Jedná se o recidivující a nenáhodnou translokaci

59

85 % a 96 % à dvě minuty) a vysušení preparátu na vzduchu.

Pro detekci fúze *MYB-NFIB* byla použita komerčně dostupná break-apart FISH sonda ZytoLight® SPEC MYB Dual Color Break Apart Probe (ZytoVision GmbH, Bremerhaven, Německo) a dále sondy vlastního designu, break-apart sonda SureFish NFIB Break Apart Probe a fúzní sonda SureFish MYB-NFIB Fusion Probe (Agilent Technologies, Santa Clara, California, USA). Oligonukleotidy NFIB break-apart sondy byly lokalizovány v oblasti chromozomu 9 na pozici 13740671-14140560 a 14340306-14740560. U *MYB-NFIB* fúzní sondy byly oligonukleotidy v oblasti chromozomu 6 lokalizovány na pozici 135271234-135771043 a v oblasti chromozomu devět na pozici 13990266--14490285 (vše Build GRCh37).

Hybridizační směs SureFish sond byla připravena z jednoho μl oranžově a jednoho μl zeleně značených částí sond, jednoho μl destilované vody a sedmi μl LSI pufru (Vysis/Abbott Molecular, IL, USA). Sonda MYB Dual Color Break Apart Probe byla již z výroby připravena k přímé aplikaci.

Podle velikosti řezu bylo na preparáty aplikováno potřebné množství sondy a přikryto sklem, jehož okraje byly zalepeny lepidlem. Pak byla skla inkubována v přístroji ThermoBrite™ (StatSpin/Iris Sample Processing, Westwood, MA, USA) s následujícím programem: kodenaturace při 85 °C/8 minut a hybridizace při 37 °C/16 hodin. Po vyjmutí skel z přístroje byla odstraněna krycí sklíčka a preparáty byly omyty v post-hybridizačním roztoku 2xSSC + 0,3% NP-40 při 72 °C/2 minuty. Po oschnutí skel ve tmě byly preparáty podbarveny 4 ', 6 ' -diamidino-2-phenylindolem – DAPI (Vysis/Abbott Molecular) a přikryty novým krycím sklíčkem.

Interpretace FISH

Preparáty byly prohlédnuty v epifluorescenčním mikroskopu Olympus BX51 (Olympus Corporation, Tokyo, Japonsko) při stonásobném zvětšení se sety filtrů Triple Band Pass (DAPI/SpectrumGreen/SpectrumOrange), Dual Band Pass (SpectrumGreen/SpectrumOrange) a Single Band Pass (SpectrumGreen nebo SpectrumOrange).

V každém preparátu bylo hodnoceno 100 náhodně vybraných nepřekrývajících se jader v cílové oblasti. Jako pozitivní byl u break-apart sond hodnocen nález separátního zeleného nebo oranžového signálu v jádře, u fúzní sondy byl pozitivní nález značen přítomností fúzního oranžovo-žluto-zeleného signálu v jádře.

Cut-off hodnoty byly určeny u vlastní kontrolní skupiny s normálním histologickým nálezem, kde byla hodnocena jádra s abnormálním nálezem, stanoven jejich průměr a směrodatná odchylka. Cut-off byla definována jako hodnota součtu průměru + tři standardní odchylky. Pro obě break-apart sondy byla cut-off hodnota 10 % pozitivních jader, u fúzní sondy 20 %.

VÝSLEDKY

Soubor 27 pacientů s AdCC a sledované parametry shrnuje tabulka 1. Průměrný věk pacientů byl 55,8 ± 17,4 let (v rozmezí 24 – 84 let). Poměr zastoupení mužů a žen byl 1 : 1,7. AdCC vznikl v malých slinných žlázách (nebo v jim podobných žlázách horního aerodigestivního traktu) v 41 %, v podčelistní žláze v 26 %, v příušní žláze v 22 % a v podjazykové žláze pak v 11 % případů.

V době diagnózy bylo zaznamenáno první klinické stadium v 26 %, druhé stadium v 18 %, třetí stadium v 26 % a čtvrté stadium v 30 % případů. Metastázy v regionálních lymfatických uzlinách byly v době diagnózy detekovány u šesti pacientů, z toho u jednoho nemocného se jednalo o přímé prorůstání karcinomu z podčelistní žlázy do uzliny. U jednoho pacienta s AdCC příušní žlázy byla diagnostikována metastáza v intraglandulární parotické uzlině, která ale podle pravidel TNM klasifikace nebyla započítána. Celkem se metastázy v regionálních lymfatických uzlinách vyskytovaly u 26 % pacientů (7/27). Vzdálené metastázy byly diagnostikovány u 30 % pacientů, u tří nemocných v době diagnózy. Nejdelší období od diagnózy AdCC do diagnózy vzdálených metastáz (plicních) bylo 11 let u pacientky bez lokoregionální recidivy. Nejčastější lokalizací vzdálených metastáz byly plíce (55 %), játra (27 %), kosti (9 %) a peritoneum (9 %). U dvou pacientů byly diagnostikovány vzdálené metastázy ve více lokalizacích. Grading byl popsán jen u 21 pacientů, a to grade 1 v 5 % případů, grade 2 v 67 % případů a grade 3 v 28 % případů. Průměrná doba dispenzarizace byla 76,4 ± 67,0 měsíců (v rozmezí 7–287 měsíců).

Všichni pacienti kromě jednoho (pacient se synchronní nádorovou triplicitou s generalizací – karcinom ledviny, tračníku a AdCC) byli primárně léčeni chirurgicky, u jedné pacientky byl proveden pouze debulking. Celkem 61 % chirurgických výkonů s cílem radikálního odstranění AdCC mělo histologicky blízké nebo pozitivní okraje resekátu. Všichni pacienti (kromě čtyř – nemocní se vzdálenými metastázami v době diagnózy a jedna nemocná, která odmítla léčbu) poté podstoupili adjuvantní radioterapii nebo chemoradioterapii. V případě jinak neléčitelného progresivního onemocnění pak byla indikována paliativní chemoterapie.

Tab. 1 Soubor pacientů s AdCC léčených ve FN v Plzni v letech 1986 až 2016

Č.	Věk/ Pohlaví	Lokalizace (místo vzniku)	Staging/ Grading	Chirurgická terapie	Onkol. terapie	Výsledky, další vývoj	Follow-up (m)
1	57/Ž	příušní žláza	T3N0M0/Gx, 3. st.	superficiální parotidektomie	RT	NED	48
2	32/M	podčelistní žláza	T1N0M0/G2, 1.st.	ND Ib	RT	NED	62
3	84/M	dolní vestibulum	T4N2bM1/Gx, 4. st.	- (triplicita)	-	DOD	9
4	58/Ž	měkké patro	T2N0Mx/G3, 2. st.	excize	CHRT	NED	135
5	60/Ž	horní vestibulum	T1N0M0/G2, 1. st.	excize	-	rT4N0M0, odmítla Th AWD	91
6	48/Ž	měkké patro	T2N0M0/G3, 2. st.	excize	CHRT	NED	115
7	57/M	příušní žláza	T4N2bM0/G3, 4. st.	totální parotidektomie RND	RT, CHT	rT3N0M1, DOD	18
8	48/Ž	podčelistní žláza	T3N0M0/G2, 3. st.	ND Ib	CHRT, CHT	rT4N0M1, DOD	137
9	47/Ž	podčelistní žláza	T1N0M0/G2, 1. st.	exstirpace, RND - T0N2bM0	CHRT, CHT	T0N0M1, DOD	44
10	28/Ž	příušní žláza	T1N0M0/G2, 1. st.	exstirpace	CHRT	NED	92
11	65/M	podjazyk. žláza	T1N0Mx/G2, 1. st.	excize, ND I	RT	NED	80
12	45/M	příušní žláza	T3N0M0/G2, 3. st.	totální parotidektomie RND	RT	NED	75
13	56/Ž	příušní žláza	T3N0Mx/G2, 3. st.	totální parotidektomie	RT	rT4N0M1, AWD	190
14	79/Ž	patrová tonzila	T4N1M0/G2, 4. st.	debulking	RT	DOD	7
15	28/Ž	čelistní dutina	T4N0M0/G2, 4. st.	etmoidektomie, subtotální maxillektomie	CHRT	rT4N0M0, DOD	63
16	77/Ž	příušní žláza	T2N0M0/G3, 2. st.	totální parotidektomie	RT	NED	55
17	49/Ž	podčelistní žláza	T3N0M0/G2, 3. st.	ND Ib, rT2N0M0 – ND Ia	RT, CHT	NED	193
18	76/Ž	podjazyk. žláza	T3N1M0/G3, 3. st.	excize, ND Ib	RT	NED	29
19	54/Ž	podčelistní žláza	T1N0M0/Gx, 1. st.	exstirpace	RT	T0N0M1, AWD	130
20	82/Ž	podjazyk. žláza	T2N0M0/Gx, 2. St	excize	RT	NED	48
21	51/M	čelistní dutina	T4N2bM0/Gx, 4. st.	- rT4N0M0 - subtotální maxillektomie	RT	NED	86
22	24/M	podčelistní žláza	T1N0M0/Gx, 1. st.	ND I	RT	NED	287
23	63/M	dolní vestibulum	T3N0M0/G3, 3. st.	excize	RT	NED	26
24	77/Ž	nosní dutina	T4N0M1/G1, 4. st.	subtotální maxillektomie	-	T0N0M1, AWD	10
25	32/Ž	tvrdé patro	T4N0M0/G2, 4. st.	alveolo-palatinální resekce	RT	NED	15
26	79/M	podčelistní žláza	T3N1M1/G2, 4. st.	ND Ib	CHT	T0N0M1, AWD	12
27	50/M	čelistní dutina	T2N0M0/G2, 2.st	etmoidektomie, subtotální maxillektomie	RT	NED	7

(R)ND – (radical) neck dissection, (radikální) krční disekce, Th – terapie, RT – radioterapie, CHT – chemoterapie, CHRT – chemoradioterapie,

NED – no evidence of disease, bez příznaků onemocnění, AWD - alive with disease, žije s onemocněním, DOD – dead of disease, smrt v důsledku onemocnění

61

Tab. 2 Genetické vyšetření souboru pacientů s AdCC léčených ve FN v Plzni v letech 1986 až 2016

Č.	1p36 delece	MYBba	NFIBba	MYB/NFIB fúze
1	Neg.	+	+	+
2	Neg.	+	+	+
3	+	+	+	+
4	Neg.	+	+	+
5	Neg.	+	+	+
6	Neg.	+	+	+
7	+	+	+	+
8	Neg.	+	+	+
9	+	+	+	+
10	Neg.	+	+	+
11	Neg.	+	+	+
12	Neg.	Neg.	+	Neg.
13	Neg.	+	+	+
14	Neg.	+	+	+
15	///	///	///	///
16	Neg.	+	+	+
17	Neg.	Neg.	+	Neg.
18	Neg.	Neg.	Neg.	///
19	N/A	N/A	N/A	///
20	Neg.	Neg.	Neg.	///
21	N/A	Neg.	N/A	N/A
22	Neg.(NH)	+	+	+
23	N/A	N/A	N/A	N/A
24	Neg.	Neg.	Neg.	+
25	Neg.	+	+	+
26	Neg.	+	+	+
27	Neg.	+	+	+

Neg. - negativní, + pozitivní, /// - nevyšetřeno, NH - nerovnoměrná hybridizace, N/A – nelze analyzovat

Za dobu dispenzarizace bylo 59 % pacientů bez jakýchkoliv příznaků choroby, 22 % zemřelo v důsledku AdCC a 19 % žilo s tímto onemocněním, ať již v podobě recidivy, či metastáz.

Genetické vyšetření souboru 26 pacientů s AdCC shrnuje tabulka 2. Při FISH vyšetření pomocí MYB break-apart sondy byla pozitivita zaznamenána v 75 % (18/24), pomocí NFIB break-apart sondy byla v 87 % (20/23) a pomocí MYB/NFIB fúzní sondy pak v 90 % případů (19/21). Souhrnná detekce fúzního onkogenu MYB-NFIB byla zaznamenána v 79 % případů (19/24) a 1p36 delece pak ve 13 % případů (3/23). U jedné pacientky bylo FISH vyšetření pomocí MYB break-apart a NFIB break-apart sond negativní, ale přesto byla potvrzena MYB- NFIB fúze. U dvou pacientů bylo vyšetření pomocí MYB break-apart sond negativní, ale NFIB break-apart pozitivní, s negativními MYB-NFIB fúzemi u obou z nich.

DISKUSE

Na většině pracovišť je u operabilních AdCC „zlatým standardem“ léčby primárně chirurgická terapie s adjuvantní radioterapií nebo chemoradioterapií s cílem zlepšit lokoregionální kontrolu onemocnění. Efekt této adjuvantní onkologické léčby je však v odborné literatuře popisován kontroverzně, především z důvodu minimálního vlivu na celkové nebo nádorově specifické přežití pacientů, což je způsobeno neovlivněním častých vzdálených metastáz [35]. Při samostatné radioterapii (většinou u inoperabilních nádorů) není AdCC kurabilní [24].

Paliativní chemoterapie (především monoterapie mitoxantronem, vinorelbinem nebo antracyklinovými cytostatiky) by měla být vyhrazena jen pro minoritní část pacientů s jinak neřešitelným pokročilým onemocněním, které je rychle progredující a/nebo symptomatické, a to po zvážení všech rizikových faktorů (komorbidity, toxicita léků, preference pacienta aj.), eventuálně i jiných způsobů terapie (paliativní radioterapie, metastatektomie solitárních lézí) [18].

Vznik lokálních recidiv AdCC je považován za závažnou známku nevyléčitelnosti tohoto karcinomu a udává se v 16–85 % případů, a to i pět let po terapii [3, 6]. V prezentovaném souboru jsme v souladu s recentní literaturou [3, 9] potvrdili vysokou tendenci AdCC k lokálním recidivám (26 %, 7/27), která je způsobena především obtížnou radikální chirurgickou léčbou vzhledem k časté peri- a intraneurální invazi (61 % resekátů AdCC s histologicky blízkým nebo pozitivním okrajem). Podle jedné studie 80 % AdCC v oblasti baze lební mělo po excizi pozitivní resekční okraje, i přes to, že tyto karcinomy byly preoperačně označeny zkušeným chirurgem za radikálně operabilní [7]. Pozitivní resekční okraje jsou prokazovány v 5,9–29,4 % případů a blízké okraje (< 5 mm) pak v 1,4–74,3 % případů [10].

Metastázování hematogenní cestou jsme zaznamenali jako časný (11 % pacientů v době diagnózy) i pozdní projev AdCC, který je nezávislý na lokoregionální kontrole onemocnění (plicní metastázy až 11 let od stanovení diagnózy při lokoregionální remisi). Obecně jsou vzdálené metastázy u AdCC častým jevem (20–60 % případů) [28]. Relativně často jsou detekovány již v době diagnózy, a to i v případě karcinomů malých rozměrů (podle jedné studie nejméně 20 % případů časných stadií AdCC, které nebyly recidivami) [11, 23]. U AdCC se tak ukazuje, že potenciál k nádorovému růstu a schopnost metastá-

zovat jsou dvě nezávislé vlastnosti nádoru [23]. Ani pozdní vzdálené metastázy AdCC nejsou ojedinělé. U 20 % pacientů vznikají mezi osmým až 20. rokem po stanovení diagnózy [11]. Nejčastějším místem hematogenního rozesevu AdCC jsou plíce (v jedné studii 74,5 % ze 145 pacientů se vzdálenými metastázami), kam se nádor šíří cestou vnitřní jugulární žíly. Méně časté je pak postižení skeletu (6,9 %), jater (3,4 %) nebo mozku (2,1 %). Více než jedna lokalizace byla diagnostikována u 13,1 % pacientů [11].

V kontrastu s dřívějšími názory na AdCC jsme zjistili vysokou incidenci metastáz do regionálních lymfatických uzlin (26 %, 7/27), čímž jsme potvrdili i výsledky jiných současných prací [2, 25]. Podhodnocení výskytu regionálních nodálních metastáz je nejspíše způsobeno relativně častým okultním postižením a také z důvodu nepříliš obvyklého provádění krčních disekcí (elektivní nejsou standardně doporučovány), a tím i absencí histopatologického vyšetření [9]. Elektivní blokové disekce jsou obecně u spinaliomů hlavy a krku prováděny z důvodu odstranění okultních uzlinových mikrometastáz, a to při riziku výskytu více než 15–20 % [12]. Při recentně prokazované vysoké incidenci okultních mikrometastáz u AdCC by již elektivní krční disekce, a to ipsilaterální v rozsahu I–III (okultní nodální metastázy byly zjištěny pouze v těchto lokalizacích), byly ospravedlnitelné a mohly by být indikovány. Podle studie s 457 pacienty s AdCC slinných žláz, kdy 226 pacientů (49 %) podstoupilo kromě odstranění primárního nádoru i elektivní krční disekci a u 231 nemocných (51 %) byl pouze resekován primární tumor, se zjistilo, že pětileté celkové přežití je u první skupiny 72 % a u druhé 79 % a pětileté nádorově specifické přežití pak 74 % resp. 81 % [5]. Takže statistická analýza neukázala žádné výhody z hlediska přežití u pacientů podstupujících elektivní krční disekci. Vzhledem k tomu, že tyto preventivní výkony by měly být indikovány nejen podle rizika incidence okultních metastáz v lymfatických uzlinách, ale i podle očekávaného vlivu léčby na přežití, nejsou podle výsledků dosud prezentovaných studií elektivní krční disekce u AdCC slinných žláz nadále standardně indikovány [5]. U AdCC s high-grade transformací nebo histologicky verifikovanou angio-/lymfangioinvazí a u AdCC v rizikových lokalizacích (baze jazyka), pokud není plánována adjuvantní radioterapie, by ale měly být tyto výkony zvažovány [13, 34]. U N0 pacientů, kde je pooperační radioterapie indikována například z důvodu pokročilého nádoru (T3/T4), se zdá být účelná ipsilaterální elektivní iradiace krku, bez krční disekce [34].

V průměru po více než šesti letech dispenzarizace bylo v našem souboru 59 % pacientů v kompletní remisi a 41 % nemocných zemřelo v důsledku AdCC nebo žije s pokročilým, jinak neřešitelným onemocněním, což odpovídá výsledkům léčby v jiných studiích i prognóze tohoto novotvaru, přestože v řadě případů chirurgická léčba v našem souboru neodpovídala současným doporučením (např. krční disekce v rozsahu I–III pro AdCC submandibulární žlázy) [23, 28]. Pětileté přežití se u AdCC udává 75 %, desetileté přežití 20–40 % a patnáctileté přežití pak 10–25 % [23, 28]. Mezi hlavní nezávislé negativní prognostické faktory patří: klinické stadium onemocnění, které je nadřazené gradingu, primární lokalizace nádoru, grading, pozitivita resekčních okrajů, intraneurální invaze a věk ≥ 70 let [3, 4, 6].

V případě výskytu vzdálených metastáz mají výrazně horší prognózu pacienti s postižením mozku a kostí oproti nemocným s metastázami plic nebo jater [3]. Průměrné přežití nemocného se vzdálenými metastázami AdCC jsou tři roky, pouze 20 % pacientů přežije pět let [6, 18]. Obecně lze říci, že více než polovina pacientů se vzdálenými metastázami zemře v průběhu deseti let po stanovení diagnózy (třetina pacientů umírá do dvou let od vzniku metastáz). Až 10 % pacientů ale přežívá více než deset let při pomalém růstu např. plicních metastáz [11, 18], což staví klinického lékaře před otázku, zda tyto pacienty lokoregionálně léčit chirurgicky.

Naopak více než polovina pacientů bez vzdálených metastáz pak přežívá více než 20 let [11].

Fúzní onkogen *MYB-NFIB* byl v našem souboru detekován u 79 % pacientů s AdCC (19/24). V současné době se v zahraničních studiích dosahuje většinou výsledků 50–80 % [26, 27, 30, 32]. U dvou nemocných, u kterých bylo vyšetření pomocí MYB break-apart sondy negativní a NFIB break-apart sondy pozitivní současně s negativními *MYB-NFIB* fúzemi, lze předpokládat jiného fúzního partnera, pravděpodobně *MYBL1*, což bude předmětem dalšího výzkumu. Deleci 1p36 jsme zaznamenali ve 13 % případů (3/23). V práci z roku 2008 bylo zjištěno zvýšení incidence této genetické změny 44 % u 53 vyšetřených AdCC se závěrem, že se jedná o nejčastější genetickou změnu signifikantně spojenou s horší prognózou pacientů [31]. Všichni tři pacienti z našeho souboru s diagnostikovanou delecí 1p36 zemřeli v důsledku AdCC v období 9–44 měsíců od stanovení diagnózy a léčby. Vzhledem k malému souboru pacientů a nízké incidenci delece 1p36, navíc při nádorové triplicitě jednoho z nemocných, nelze blíže statisticky hodnotit klinicko-patologickou korelaci tohoto markeru.

Na základě současných znalostí zatím nemůže *MYB–NFIB* fúze a/nebo *MYB* aktivace sloužit jako prognostický ani terapeutický biomarker [33]. U sali-

63

várních AdCC dosud neexistuje účinná cílená léčba, která by poskytovala větší benefit pro pacienta než klasická chemoterapie. Nejperspektivněji by se jevily léky cílené proti *MYB* a *MYB-NFIB*, které ale dosud nebyly vyvinuty (velmi obtížné vzhledem k tomu, že se jedná o transkripční faktory).

Při probíhajících studiích využívajících preparáty inhibující některé signální dráhy zapojené do regulace *MYB* a *MYB-NFIB* bylo zatím nejlepších výsledků cílené terapie dosaženo při léčbě dovitinibem, lapatinibem, cetuximabem, sunitinibem, everolimem a nebo axitinibem [1, 14, 15, 16, 17, 21]. *MYB-NFIB* fúzní onkogen lze u AdCC v současnosti využít pouze jako diagnostický biomarker, a to hlavně u pozdních vzdálených metastáz při lokoregionální remisi onemocnění. Ty již často nebývají dávány do souvislosti s AdCC a mohou být mylně považovány za primární nádory daných lokalizací (např. adenokarcinomy plic) nebo za metastázy neznámého origa (např. v játrech), což pak může vést klinického lékaře k dalším chybám v diagnosticko-léčebném postupu. Problémem v těchto případech bývá i to, že se biopsie z těchto orgánů primárně nedostávají k patologům specializujícím se na diagnostiku NSŽ.

ZÁVĚR

AdCC slinných žláz vykazuje vyšší tendenci k zakládání regionálních uzlinových metastáz, než se dříve soudilo. *MYB-NFIB* fúze je hlavní nádorově specifickou onkogenní událostí u AdCC s vysokou úspěšností detekce. Tento fúzní onkogen je možné v současné době potenciálně využít pouze jako pomocný diagnostický nástroj u histopatologicky sporných případů, především pak u pozdních vzdálených metastáz.

LITERATURA

1. **Agulnik, M., Cohen, E. W., Cohen, R. B., Chen, E. X., Vokes, E. E., Hotte, S. J., Winquist, E., Laurie, S., Hayes, D. N., Dancey, J. E., Brown, S., Pond, G. R., Lorimer, I., Daneshmand, M., Ho, J., Tsao, M. S., Siu, L. L.:** Phase II study of lapatinib in recurrent or metastatic epidermal growth factor receptor and/or erbB2 expressing adenoid cystic carcinoma and non adenoid cystic carcinoma malignant tumors of the salivary glands. J. Clin. Oncol., roč. 25, 2007, č. 25, s. 3978–3984.

2. **Amit, M., Binenbaum, Y., Sharma, K., Ramer, N., Ramer, I., Agbetoba, A., Glick, J., Yang, X., Lei, D., Bjørndal, K., Godballe, C., Mücke, T., Wolff, K. D., Fliss, D., Eckardt, A. M., Copelli, C., Sesenna, E., Palmer, F., Ganly, I., Patel, S., Gil, Z.:** Incidence of cervical lymph node metastasis and its association with outcomes in patients with adenoid cystic carcinoma. An international collaborative study. Head Neck, roč. 37, 2015, č. 7, s. 1032–1037.

3. **Amit, M., Binenbaum, Y., Sharma, K., Ramer, N., Ramer, I., Agbetoba, A., Miles, B., Yang, X., Lei, D., Bjøerndal, K., Godballe, C., Mücke, T., Wolff, K. D., Fliss, D., Eckardt, A. M., Copelli, C., Sesenna, E., Palmer, F., Patel, S., Gil, Z.:** Analysis of failure in patients with adenoid cystic carcinoma of the head and neck. An international collaborative study. Head Neck, roč. 36, 2014, č. 7, s. 998–1004.

4. **Amit, M., Binenbaum, Y., Trejo-Leider, L., Sharma, K., Ramer, N., Ramer, I., Agbetoba, A., Miles, B., Yang, X., Lei, D., Bjørndal, K., Godballe, C., Mücke, T., Wolff, K. D., Eckardt, A. M., Copelli, C., Sesenna, E., Palmer, F., Ganly, I., Patel, S., Gil, Z.:** International collaborative validation of intraneural invasion as a prognostic marker in adenoid cystic carcinoma of the head and neck. Head Neck, roč. 37, 2015, č. 7, s. 1038–1045.

5. **Amit, M., Na'ara, S., Sharma, K., Ramer, N., Ramer, I., Agbetoba, A., Glick, J., Yang, X., Lei, D., Bjoerndal, K., Godballe, C., Mücke, T., Klaus-Dietrich, W., Eckardt, A. M., Copelli, C., Sesenna, E., Palmer, F., Ganly, I., Gil, Z.:** Elective neck dissection in patients with head and neck adenoid cystic carcinoma: an international collaborative study. Ann. Surg. Oncol., roč. 22, 2015, č. 4, s. 1353–1359.

6. **Barnes, L., Eveson, J. W., Reichart, P., Sidransky, D.:** World Health Organization classification of tumours: Pathology and genetics of head and neck tumours. Lyon, IARC Press, 2005, s. 209–281.

7. **Casler, J. D., Conley, J. J.:** Surgical management of adenoid cystic carcinoma in the parotid gland. Otolaryngol. Head Neck Surg., roč. 106, 1992, č. 4, s. 332–338.

8. **Ciccolallo, L., Licitra, L., Cantú, G., Gatta, G.; EUROCARE Working Group.:** Survival from salivary glands adenoid cystic carcinoma in European populations. Oral Oncol., roč. 45, 2009, č. 8, s. 669–674.

9. **Coca-Pelaz, A., Rodrigo, J. P., Bradley, P. J., Vander Poorten, V., Triantafyllou, A., Hunt, J. L., Strojan, P., Rinaldo, A., Haigentz, M. Jr., Takes, R. P., Mondin, V., Teymoortash, A., Thompson, L. D., Ferlito, A.:** Adenoid cystic carcinoma of the head and neck – An update. Oral Oncol., roč. 51, 2015, č. 7, s. 652–661.

10. **Ganly, I., Amit, M., Kou, L., Palmer, F.L., Migliacci, J., Katabi, N., Yu, C., Kattan, M. W., Binenbaum, Y., Sharma, K., Naomi, R., Abib, A., Miles, B., Yang, X., Lei, D., Bjoerndal, K., Godballe, C., Mücke, T., Wolff, K. D., Fliss, D., Eckardt, A. M., Chiara, C., Sesenna, E., Ali, S., Czerwonka, L., Goldstein, D. P., Gil, Z., Patel, S. G.:** Nomograms for predicting survival and recurrence in patients with adenoid cystic carcinoma. An international collaborative study. Eur. J. Cancer, roč. 51, 2015, č. 18, s. 2768–2776.

11. **Gao, M., Hao, Y., Huang, M. X., Ma, D. Q., Luo, H. Y., Gao, Y., Peng, X., Yu, G. Y.:** Clinicopathological study of distant metastases of salivary adenoid cystic carcinoma. Int. J. Oral Maxillofac. Surg., roč. 42, 2013, č. 8, s. 923–928.

12. **Hauer, L.:** Dentoalveolární chirurgie. Test 10: Zhoubný nádor dutiny ústní – spinocelulární karcinom jazyka. LKS, roč. 25, 2015, č. 10, s. 203–207.

13. **Hellquist, H., Skálová, A., Barnes, L., Cardesa, A., Thompson, L. D., Triantafyllou, A., Williams, M. D., Devaney, K. O., Gnepp, D. R., Bishop, J. A., Wenig, B .M., Suárez, C., Rodrigo, J. P., Coca-Pelaz, A., Strojan, P., Shah, J. P., Hamoir, M., Bradley, P. J., Silver, C. E., Slootweg, P. J., Vander Poorten, V., Teymoortash, A., Medina, J. E., Robbins, K. T., Pitman, K. T., Kowalski, L. P., de Bree, R., Mendenhall, W. M., Eloy, J. A., Takes, R. P., Rinaldo, A., Ferlito, A.:** Cervical lymph node metastasis in high-grade transformation of head and neck adenoid cystic carcinoma: a collective international review. Adv. Ther., 2016 [Epub ahead of print].

14. **Ho, A. L., Sherman, E. J., Fury, M. G., Baxi, S. S., Haque, S., Sima, C. S., Antonescu, C. R., Katabi, N., Pfister, D. G.:** Phase II

study of axitinib in patients with progressive, recurrent/metastatic adenoid cystic carcinoma. J. Clin. Oncol., roč. 32, 2014, č. 15, Suppl., s. 6093.

15. **Chau, N. G., Hotte, S. J., Chen, E. X., Chin, S. F., Turner, S., Wang, L., Siu, L. L.:** A phase II study of sunitinib in recurrent and/or metastatic adenoid cystic carcinoma (ACC) of the salivary glands: current progress and challenges in evaluating molecularly targeted agents in ACC. Ann. Oncol., roč. 23, 2012, č. 6, s. 1562–1570.

16. **Keam, B., Kim, S. B., Shin, S. H., Cho, B. C., Lee, K. W., Kim, M. K., Yun, H. J., Lee, S. H., Yoon, D. H., Bang, Y. J.:** Phase 2 study of dovitinib in patients with metastatic or unresectable adenoid cystic carcinoma. Cancer, roč. 121, 2015, č. 15, s. 2612–2617.

17. **Kim, D. W., Oh, D. Y., Shin, S. H., Kang, J. H., Cho, B. C., Chung, J. S., Kim, H., Park, K. U., Kwon, J. H., Han, J. Y., Kim, M. J., Bang, Y. J.:** A multicenter phase II study of everolimus in patients with progressive unresectable adenoid cystic carcinoma. BMC Cancer, roč. 14, 2014, s. 795.

18. **Laurie, S. A., Ho, A. L., Fury, M. G., Sherman, E., Pfister, D. G.:** Systemic therapy in the management of metastatic or locally recurrent adenoid cystic carcinoma of the salivary glands: a systematic review. Lancet Oncol., roč.12, 2011, č. 8, s. 815–824.

19. **Li, N., Xu, L., Zhao, H., El-Naggar, A. K., Sturgis, E. M.:** A comparison of the demographics, clinical features, and survival of patients with adenoid cystic carcinoma of major and minor salivary glands versus less common sites within the Surveillance, Epidemiology, and End Results registry. Cancer, roč. 118, 2012, č. 16, s. 3945–3953.

20. **Lin, Y. C., Chen, K. C., Lin, C. H., Kuo, K. T., Ko, J. Y., Hong, R. L.:** Clinicopathological features of salivary and non-salivary adenoid cystic carcinomas. Int. J. Oral Maxillofac. Surg., roč. 41, 2012, č. 3, s. 354–360.

21. **Locati, L. D., Bossi, P., Perrone, F., Potepan, P., Crippa, F., Mariani, L., Casieri, P., Orsenigo, M., Losa, M., Bergamini, C., Liberatoscioli, C., Quattrone, P., Calderone, R. G., Rinaldi, G., Pilotti, S., Licitra, L.:** Cetuximab in recurrent and/or metastatic salivary gland carcinomas: A phase II study. Oral Oncol., roč. 45, 2009, č. 7, s. 574–578.

22. **Marchiò, C., Weigelt, B., Reis-Filho, J. S.:** Adenoid cystic carcinomas of the breast and salivary glands (or ‚The strange case of Dr Jekyll and Mr Hyde' of exocrine gland carcinomas). J. Clin. Pathol., roč. 63, 2010, č. 3, s. 220–228.

23. **Marx, R. E., Stern, D.:** Oral and maxillofacial pathology: A rationale for diagnosis and treatment. 2. vyd., Quintessence Pub. Co., 2012, s. 547 – 598.

24. **Mendenhall, W. M., Morris, C. G., Amdur, R. J., Werning, J. W., Hinerman, R. W., Villaret, D. B.:** Radiotherapy alone or combined with surgery for adenoid cystic carcinoma of the head and neck. Head Neck, roč. 26, 2004, č. 2, s. 154–162.

25. **Min, R., Siyi, L., Wenjun, Y., Ow, A., Lizheng, W., Minjun, D., Chenping, Z.:** Salivary gland adenoid cystic carcinoma with cervical lymph node metastasis: a preliminary study of 62 cases. Int. J. Oral Maxillofac. Surg., roč. 41, 2012, č. 8, s. 952–957.

26. **Mitani, Y., Liu, B., Rao, P. H., Borra, V. J., Zafereo, M., Weber, R. S., Kies, M., Lozano, G., Futreal, P. A., Caulin, C., El-Naggar, A. K.:** Novel MYBL1 gene rearrangements with recurrent MYBL1-NFIB fusions in salivary adenoid cystic carcinomas lacking t(6;9) translocations. Clin. Cancer Res., roč. 22, 2016, č. 3, s. 725–733.

27. **Mitani, Y., Rao, P. H., Futreal, P. A., Roberts, D. B., Stephens, P. J., Zhao, Y. J., Zhang, L., Mitani, M., Weber, R. S., Lippman, S. M., Caulin, C., El-Naggar, A. K.:** Novel chromosomal rearrangements and break points at the t(6;9) in salivary adenoid cystic carcinoma: association with MYB-NFIB chimeric fusion, MYB expression, and clinical outcome. Clin. Cancer Res., roč. 17, 2011, č. 22, s. 7003–7014.

28. **Myers, E. N., Ferris, R. L.:** Salivary gland disorders. 1. vyd., Berlin, Springer-Verlag, 2007, s. 59–62.

29. **Nagao, T.:** „Dedifferentiation" and high-grade transformation in salivary gland carcinomas. Head Neck Pathol., roč. 7, 2013, Suppl. 1, s. S37–S47.

30. **Persson, M., Andrén, Y., Moskaluk, C. A., Frierson, H. F. Jr., Cooke, S. L., Futreal, P. A., Kling, T., Nelander, S., Nordkvist, A., Persson, F., Stenman, G.:** Clinically significant copy number alterations and complex rearrangements of MYB and NFIB in head and neck adenoid cystic carcinoma. Genes Chromosomes Cancer, roč. 51, 2012, č. 8, s. 805–817.

31. **Rao, P. H., Roberts, D., Zhao, Y. J., Bell, D., Harris, C. P., Weber, R. S., El-Naggar, A. K.:** Deletion of 1p32-p36 is the most frequent genetic change and poor prognostic marker in adenoid cystic carcinoma of the salivary glands. Clin. Cancer Res., roč. 14, 2008, č. 16, s. 5181–5187.

32. **Rettig, E. M., Tan, M., Ling, S., Yonescu, R., Bishop, J. A., Fakhry, C., Ha, P. K.:** MYB rearrangement and clinicopathologic characteristics in head and neck adenoid cystic carcinoma. Laryngoscope, roč. 125, 2015, č. 9, s. E292–E299.

33. **Stenman, G., Persson, F., Andersson, M. K.:** Diagnostic and therapeutic implications of new molecular biomarkers in salivary gland cancers. Oral Oncol., roč. 50, 2014, č. 8, s. 683–690.

34. **Suárez, C., Barnes, L., Silver, C. E., Rodrigo, J. P., Shah, J. P., Triantafyllou, A., Rinaldo, A., Cardesa, A., Pitman, K. T., Kowalski, L. P., Robbins, K. T., Hellquist, H., Medina, J. E., de Bree, R., Takes, R. P., Coca-Pelaz, A., Bradley, P. J., Gnepp, D. R., Teymoortash, A., Strojan, P., Mendenhall, W. M., Eloy, J. A., Bishop, J. A., Devaney, K. O., Thompson, L. D. R., Hamoir, M., Slootweg, P. J., Vander Poorten, V., Williams, M. D., Wenig, B. M., Skálová, A., Ferlito, A.:** Cervical lymph node metastasis in adenoid cystic carcinoma of oral cavity and oropharynx: A collective international review. Auris Nasus Larynx, 2016, článek v tisku.

35. **Subramaniam, T., Lennon, P., O'Neill, J. P.:** Ongoing challenges in the treatment of adenoid cystic carcinoma of the head and neck. Ir. J. Med. Sci., roč. 184, 2015, č. 3, s. 583–590.

MUDr. et. MUDr. Lukáš Hauer, Ph.D.
Stomatologická klinika LF UK a FN
Oddělení ústní, čelistní a obličejové chirurgie
Alej Svobody 80
304 60 Plzeň
e-mail: hauerl@fnplzen.cz

22

ARTICLE

Adenoid cystic carcinomas of the salivary gland, lacrimal gland, and breast are morphologically and genetically similar but have distinct microRNA expression profiles

Simon Andreasen [1,2] · Qihua Tan[3] · Tina Klitmøller Agander[4] · Petr Steiner[5,6] · Kristine Bjørndal[7] · Estrid Høgdall[8] ·
Stine Rosenkilde Larsen[9] · Daiva Erentaite[10] · Caroline Holkmann Olsen[11] · Benedicte Parm Ulhøi[12] ·
Sarah Linéa von Holstein[13,14] · Irene Wessel[2] · Steffen Heegaard[4,13] · Preben Homøe[1]

Abstract

Adenoid cystic carcinoma is among the most frequent malignancies in the salivary and lacrimal glands and has a grave prognosis characterized by frequent local recurrences, distant metastases, and tumor-related mortality. Conversely, adenoid cystic carcinoma of the breast is a rare type of triple-negative (estrogen and progesterone receptor, HER2) and basal-like carcinoma, which in contrast to other triple-negative and basal-like breast carcinomas has a very favorable prognosis. Irrespective of site, adenoid cystic carcinoma is characterized by gene fusions involving *MYB*, *MYBL1*, and *NFIB*, and the reason for the different clinical outcomes is unknown. In order to identify the molecular mechanisms underlying the discrepancy in clinical outcome, we characterized the phenotypic profiles, pattern of gene rearrangements, and global microRNA expression profiles of 64 salivary gland, 9 lacrimal gland, and 11 breast adenoid cystic carcinomas. All breast and lacrimal gland adenoid cystic carcinomas had triple-negative and basal-like phenotypes, while salivary gland tumors were indeterminate in 13% of cases. Aberrations in *MYB* and/or *NFIB* were found in the majority of cases in all three locations, whereas *MYBL1* involvement was restricted to tumors in the salivary gland. Global microRNA expression profiling separated salivary and lacrimal gland adenoid cystic carcinoma from their respective normal glands but could not distinguish normal breast adenoid cystic carcinoma from normal breast tissue. Hierarchical clustering separated adenoid cystic carcinomas of salivary gland origin from those of the breast and placed lacrimal gland carcinomas in between these. Functional annotation of the microRNAs differentially expressed between salivary gland and breast adenoid cystic carcinoma showed these as regulating genes involved in metabolism, signal transduction, and genes involved in other cancers. In conclusion, microRNA dysregulation is the first class of molecules separating adenoid cystic carcinoma according to the site of origin. This highlights a novel venue for exploring the biology of adenoid cystic carcinoma.

✉ Simon Andreasen
Simon@Andreasen.pm

1 Department of Otorhinolaryngology and Maxillofacial Surgery, Zealand University Hospital, Køge, Denmark

2 Department of Otorhinolaryngology Head and Neck Surgery and Audiology, Rigshospitalet, Copenhagen, Denmark

3 Department of Clinical Research, Unit of Human Genetics, University of Southern Denmark, Odense, Denmark

4 Department of Pathology, Rigshospitalet, Copenhagen, Denmark

5 Department of Pathology, Faculty of Medicine, Charles University in Prague, Pilsen, Czech Republic

6 Bioptic Laboratory Ltd, Molecular Pathology Laboratory, Pilsen, Czech Republic

7 Department of ORL–Head and Neck Surgery, Odense University Hospital, Odense, Denmark

8 Department of Pathology, Herlev Hospital, University of Copenhagen, Herlev, Denmark

9 Department of Pathology, Odense University Hospital, Odense, Denmark

10 Department of Pathology, Aalborg University Hospital, Aalborg, Denmark

11 Department of Pathology, Zealand University Hospital, Roskilde, Denmark

12 Department of Pathology, Aarhus University Hospital, Aarhus, Denmark

13 Department of Ophthalmology, Rigshospitalet-Glostrup, Copenhagen, Denmark

14 Department of Ophthalmology, Zealand University Hospital, Roskilde, Denmark

SPRINGER NATURE

Introduction

Adenoid cystic carcinoma is among the most frequent malignancies in the salivary and lacrimal gland, and is clinically characterized by frequent local invasion, distant metastatic spread, and a dismal prognosis, with 10-year disease-specific survival rates of 75% and 52%, respectively [1, 2]. In the breast, adenoid cystic carcinoma is rare and belongs to the basal-like (estrogen receptor and human epidermal growth factor receptor 2 (HER2) negative, CK5/6 and/or epidermal growth factor receptor (EGFR) positive) and triple-negative (negative for estrogen receptor, progesterone receptor, and HER2) subtypes [3]. The phenotypic classification of breast carcinoma (i.e., luminal, basal-like, and HER2 phenotypes) carries significant prognostic and therapeutic implications in breast cancer and has been shown to apply to at least a subset of salivary and lacrimal gland carcinomas [3–6]. The phenotypic profile of adenoid cystic carcinoma has not been characterized, which constitutes a significant gap in the context of phenotypic correlations between tumors of the salivary gland, lacrimal gland, and breast. Triple-negative breast carcinoma is generally regarded as a clinically aggressive group of malignancies without available targeted therapies, but in contrast to this and the behavior of adenoid cystic carcinoma in salivary and lacrimal gland, adenoid cystic carcinoma in the breast is a notable exception since recurrences and tumor-related deaths are exceptionally rare for these tumors [7, 8]. In addition to having morphology in common, the genetic landscape is highly similar in adenoid cystic carcinoma regardless of site, including pattern of copy-number alterations, low mutational burden, and the *MYB-NFIB* gene fusion [9–16]. This phenomenon of similarities in morphology and genetics but discrepancy in clinical behavior has earned adenoid cystic carcinoma the title as the Dr. Jekyll and Mr. Hyde of exocrine gland carcinomas [3].

The occurrence of salivary-like carcinomas in the lacrimal gland and breast is well known and includes several entities besides adenoid cystic carcinoma, namely, acinic cell carcinoma, mucoepidermoid carcinoma, secretory carcinoma, ductal carcinoma, and other more rare types, which collectively is highly suggestive of a common pathogenesis irrespective of site [5, 17–19]. Indeed, it is firmly established that histologically identical tumors are genetically similar in all three sites and that, despite the rarity of some type of salivary-like breast carcinomas, the aggressiveness is largely similar, with the notable exception of adenoid cystic carcinoma [5, 9–11, 15, 19–21].

Despite the inadequacy of genetic studies to explain the differences in clinical course of adenoid cystic carcinoma according to site, intrinsic differences in tumor biology remain the most likely explanations. Epigenetic mechanisms have been shown to be potent regulators of gene expression and involved in numerous malignancies of different organs [22, 23]. Among these, microRNAs (miR-NAs) are short non-coding RNAs ~22 nucleotides in length, functioning as potent post-transcriptional regulators of gene expression by causing either degradation or translational blockage of target mRNAs [24, 25]. MicroRNAs have been demonstrated as prognostic markers in salivary gland adenoid cystic carcinoma, whereas the involvement in lacrimal gland and breast adenoid cystic carcinoma is unknown [26, 27].

Searching for molecular mechanisms to explain the differences in clinical behavior between adenoid cystic carcinoma of the salivary gland, lacrimal gland, and breast, we characterize their phenotypic profile, distribution of genetic rearrangements, and global miRNA expression profile. For the first time, these findings shed light on the molecular background for this discordance in clinical behavior.

Materials and methods

Patient material

The Biospecimen Reporting for Improved Study Quality (BRISQ) was used as a guideline for this study [28]. Patients diagnosed with adenoid cystic carcinoma of the salivary gland, lacrimal gland, or breast were identified by searching the Danish Pathology Registry and the Eye Pathology Institute files [29]. Material was fixed in 10% neutral-buffered formalin immediately following surgery and subsequently embedded in paraffin. Material from 64 salivary gland adenoid cystic carcinomas (13 from parotid, 28 from submandibular, 3 from sublingual, nine from sinonasal tract, and 11 from oral, pharyngeal, and laryngeal minor salivary/ glands), nine lacrimal gland adenoid cystic carcinomas, and 11 breast adenoid cystic carcinomas stored at room temperature were sectioned and reviewed for diagnostic accuracy [30]. Sinonasal carcinomas were tested for presence of human papillomavirus (HPV) to exclude HPV-related multiphenotypic carcinoma and palatal carcinomas and tested for *PRKD1* c.2130 mutation to exclude polymorphous adenocarcinoma, respectively [31, 32]. Adjacent normal gland from 10, seven, and six salivary gland, breast, and lacrimal gland adenoid cystic carcinomas, respectively, were included for miRNA expression profiling. Clinicopathologic details and outcomes were collected from patient files and from the Danish Patient Registry, the Danish Cancer Registry, and the Danish Pathology Registry, as previously described [1]. Staging was performed according to the American Joint Committee on Cancer (AJCC), 8th edition [33]. The Regional Ethics Committee (H-6-2014-086) and the Danish Data Protection Agency (Journal no. REG-94-2014) approved this protocol.

Histology, immunohistochemistry, phenotypic profiling, and survival statistics

From all cases, 4-μm-thick formalin-fixed and paraffin-embedded sections were cut and stained with hematoxylin and eosin (H&E) according to standard protocols, or subjected to immunohistochemical staining on the Ventana Benchmark Ultra platform (Ventana Medical Systems, Tucson, AZ) as previously described [34]. Primary antibodies included androgen receptor (clone AR441, 1:400, Dako (Glostrup, Denmark)), CK5/6 (clone D5/16, 1:20, Dako), EGFR (clone E30, 1:200, Dako), estrogen receptor (clone SP1, ready-to-use (RTU), Roche (Basel, Switzerland)), HER2 (clone 4B5, RTU, Roche), ki-67 (clone MIB1, 1:100, Dako), MYB (clone ER769Y, 1:150, AbCam (Cambridge, UK)), and progesterone receptor (clone 1E2, RTU, Roche). Positive controls as suggested on datasheets were used on each slide, and the expected reaction was confirmed. Negative controls were included on all slides. HER2 and EGFR was evaluated according to ASCO guidelines [35]. MYB positivity was defined as nuclear reaction in at least 5% of tumor cells [36]. CK 5/6 was regarded as positive when >10% of cells were positive while androgen receptor, estrogen receptor, and progesterone receptor were regarded as positive when Allred score was >2 as previously described [37, 38]. The HER2 phenotype was defined as membranous HER2 positivity of 3+ or 2+ with concurrent *HER2* gene amplification regardless of other markers. Luminal phenotype was defined as HER2-negativity but with expression of estrogen receptor and/or progesterone receptor. Luminal androgen receptor-positive was defined as negativity for HER2, estrogen receptor, and progesterone receptor and positivity for androgen receptor. Basal-like phenotype was defined as negativity for HER2, estrogen receptor, progesterone receptor, and androgen receptor along with either 1) EGFR at 3+ or 2+ with concurrent *EGFR* gene amplification and/or 2) positivity for CK5/6. Cases negative for all markers were categorized as indeterminate [6, 39]. Nottingham grade was determined for breast carcinomas and architectural grade as described by Ro et al. on H&E-stained sections [40, 41]. Comparison of overall survival between basal-like and indeterminate phenotypes was performed using the Kaplan–Meier method and compared by the log-rank test in SPSS v.22.0 (SPSS, Chicago, IL) with a *p* value of ≤0.05 considered significant.

Fluorescence in situ hybridization

The 4-μm-thick formalin-fixed and paraffin-embedded sections from each case were placed onto positively charged slides. Hematoxylin and eosin stained slides were examined for determination of areas for counting. Fluorescence in situ hybridization (FISH) on all salivary gland cases and lacrimal gland and breast cases was performed using break-apart probes for *MYB* (ZytoVision GmbH, Bremerhaven, Germany), *MYBL1* (custom probe oligonucleotides chr8:67076230-67474559 and chr8:67526335-68426199 (Agilent Technologies, Santa Clara, CA)/[Empire Genomics, Buffalo, NY]), and *NFIB* (custom probe oligonucleotides chr9:13740671-14140560 and chr9:14340306-14740560 (Agilent Technologies)/(Empire Genomics)) and an *MYB-NFIB* fusion probe (custom probe oligonucleotides chr6:135271234-135771043 and chr9:13990266-14490285 (Agilent Technologies)/(Cytotest, Rockville, MD), according to the manufacturers' protocol as previously described [20, 31]. Nuclei were counterstained with 4′,6-diamidino-2-phenylindole (DAPI) II (ZytoVision). Break-apart signal in ≥10% of cells was considered to represent rearrangement and fused signals in ≥20% of cells was considered to represent fusion [42]. Amplification was defined as ≥3 signals/cell in ≥10% of cells. In case of equivocal (2+) EGFR immunohistochemistry, the *EGFR* (ZytoVision) numeric probe was employed according to ASCO guidelines as previously described [5, 35]. One hundred nuclei were counted, and only nuclei where the entire nuclear membrane could be visualized were scored.

RNA extraction

To maximize tumor content, a one 1 mm core was obtained from each tumor after identification of a representative tumor area from an H&E slide. The QiaCube (Qiagen, Valencia, CA) was used for automated isolation of miRNA with the miRNeasy FFPE Kit (Qiagen) according to the manufacturer's instructions [43]. Total RNA concentration was measured using the NanoDrop ND-1000 (Thermo Scientific, Wilmington, DE), and ranged from 294 to 1648 ng/μl with A260/A280 ratio ranging from 1.7 to 2.7, indicating high nucleic acid purity. RNA quality, as estimated by RNA integrity number (RIN), was measured on the 10 oldest samples using the Agilent 2100 Bioanalyzer platform (Agilent Technologies, Santa Clara, CA) using the Agilent RNA 6000 Nano Kit (Agilent) with RIN ranging from 0.9 to 1.6 (median 1.1).

MicroRNA array

The Affymetrix miRNA 4.1 array platform (Affymetrix, Santa Clara, CA) was used, covering all entries in Sanger miRbase database v.20, including 2,578 mature and 2,025 immature human miRNAs with a dynamic range of 4 logs. For miRNA analysis, 300 μg of total RNA was labeled with the FlashTag Biotin HSR RNA Labeling kit (Affymetrix) according to the manufacturer's instructions. To eliminate batch variation, all cases were run in a single batch. Array

Table 1 Demographics, clinicopathologic characteristics, and phenotypic profiling of patients with adenoid cystic carcinoma of the salivary gland, lacrimal gland, and breast

	Salivary gland	Lacrimal gland	Breast
n	64	9	11
Sex (male/female)	31/33	4/5	0/11
Median age (range, years)	55 (14–83)	41 (23–67)	63 (53–81)
Stage (%)[a]			
I	28%	T2a: 33%	73%
II	36%	T2b: 11%	18%
III	16%	T3a:11%	9%
IV	20%	T4c: 44%	0%
Treatment and outcome			
Surgery[b]			
R0	22%[c]	0%	73%
R1	73%	89%	27%
R2	5%	11%	0%
Lymph node excision[d]	67%	0%	90%
Radiotherapy	94%	89%	82%[e]
Local recurrence or distant metastasis	39%	89%	0%
Median follow-up (range, months)	92 (1–322)	123 (36–334)	81 (47–146)
Histopathological characteristics and immunohistochemistry			
Perineural invasion	85%	100%	30%
Architectural grade[f]			
I	68%	11%	27%/27%
II	21%	67%	64%/55%
III	11%	22%	9%/18%
Estrogen receptor	2%	0%	0%
Progesterone receptor	0%	0%	0%
Androgen receptor	0%	0%	0%
Cytokeratin 5/6	84%	100%	100%
EGFR	9%	0%	0%
HER2	0%	0%	0%
Phenotypic profile			
Basal-like	86%	100%	100%
Luminal	2%	0%	0%
Indeterminate	13%	0%	0%

[a]TNM is listed for lacrimal gland ACC as no staging system exists. All patients were without nodal or distant involvement at diagnosis

[b]R0 = complete resection, R1 = only microscopic residual tumor, R2 = macroscopic residual tumor

[c]Radicality was not possible to assess in two patients with sinonasal tumors and were considered involved.

[d]Lymph nodes had micrometastases in 11/43 salivary gland ACC and in 1/10 breast ACC. Lymph nodes were not excised in patients with lacrimal gland ACC

[e]Eight received combined chemoradiation

[f]Architectural grade/Nottingham grade is stated for breast adenoid cystic carcinoma

plates were washed, stained, and scanned on the GeneTitan Instrument (Affymetrix).

MicroRNA data analysis

Raw global miRNA expression data were normalized by using the quantile normalization method implemented in the free R package *preprocessCore* [44]. The normalized data were then log-transformed with base 2 to ensure normal or approximately normal distribution before statistical analysis. For each miRNA, linear regression models were fitted, regressing the log-transformed miRNA expression level on the tumor indicator variable (tumor = 1, normal = 0) for each of the three tissue types, or on tumor type variable (salivary, lacrimal, breast, with breast as reference). Correction for multiple testing was done by estimating the Benjamini−Hochberg adjusted p values (false discovery rate, FDR). MiRNAs with FDR ≤ 0.05 were considered to be statistically significant. All statistical analysis were performed using the free R software (https://cran.r-project.org/).

Pathway analysis and functional annotation

Pathway analysis of miRNAs was performed with DIANA-miRPath v3.0 software available from http://snf-515788.vm.okeanos.grnet.gr/. [45] The DIANA-TarBase v7.0 was selected as miRNA target prediction algorithm [46]. For functional annotation, the Kyoto Encyclopedia of Genes and Genomes (KEGG) pathways were used and enrichment score for KEGG pathways presented by −ln (p value) [47].

Results

Patient demographics and clinicopathologic characteristics

Stage at diagnosis in salivary gland adenoid cystic carcinoma ranged from I to IV, and all lacrimal gland cases presented with N0M0 disease with T-stage ranging from 2a to 4c (Table 1). In the breast, all cases were stage I or II, except in one patient with stage III (case 7) due to multiple ipsilateral axillary lymph node metastases (pN2a). Radical surgery was performed in the majority of patients with breast adenoid cystic carcinoma, while this was the case in 23% and 0% of salivary gland and lacrimal gland adenoid cystic carcinoma, respectively. Median follow-up was 81, 92, and 123 months for breast, salivary gland, and lacrimal gland cases, respectively (Table 1). Perineural invasion (PNI) was identified in 30%, 85%, and 100% of breast, salivary gland, and lacrimal gland carcinomas, respectively. In the salivary gland, 9/64 (14%) experienced local recurrence, 16/64 (25%) distant
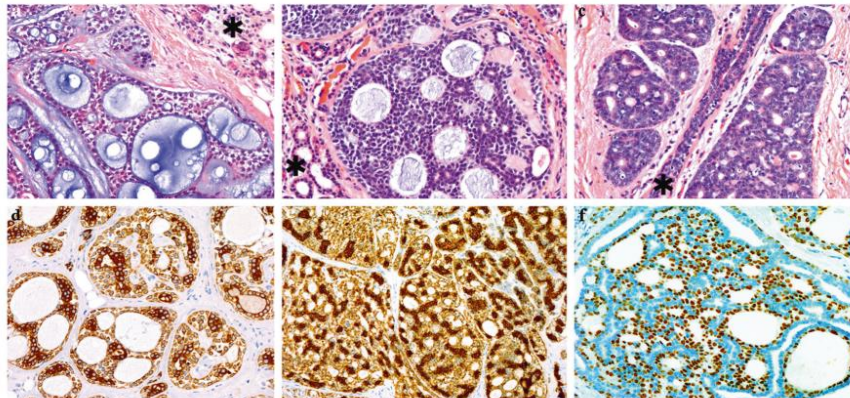
Fig. 1 Histological features of fusion-positive adenoid cystic carcinoma of the salivary gland, lacrimal gland, and breast. **a** Adenoid cystic carcinoma of the submandibular gland with tubular and cribriform areas with accumulation of basal membrane material in pseudoluminae. Normal ducts and acinar cells are seen in the upper right corner (asterisk). **b** Adenoid cystic carcinoma of the lacrimal gland with normal ducts and acinar cells in the lower left corner (asterisk) and **c** adenoid cystic carcinoma of the breast surrounding a normal duct (asterisk). **d** Cytokeratin 5/6 in salivary gland and **e** breast adenoid cystic carcinoma with intense cytoplasmic reaction in luminal cells, and **f** nuclear p63 reaction in abluminal cells lining pseudoluminae
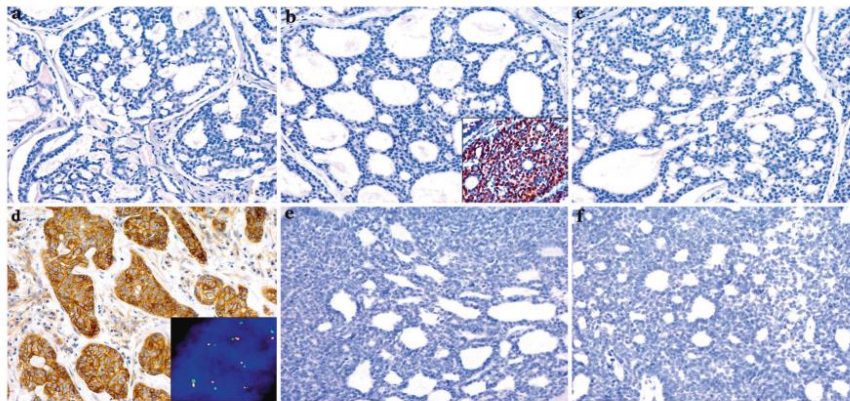
Fig. 2 Phenotypic profiling of adenoid cystic carcinoma of the salivary gland, lacrimal gland, and breast. **a** Androgen receptor was uniformly negative in adenoid cystic carcinoma irrespective of site (a salivary gland specimen is shown). **b** Estrogen receptor was negative in all cases irrespective of site (a breast specimen is shown), with the exception of one salivary gland case (inset) with intense expression in 60% of tumor cells. **c** Progesterone receptor was uniformly negative in tumors of all three sites (a salivary gland specimen is shown). **d** Membranous EGFR expression (3+) was identified exclusively in a subset of salivary gland carcinomas, and (inset) all cases with 2+ scores showed intact *EGFR* copy number status with fluorescent in situ hybridization. **e** HER2 was consistently negative in adenoid cystic carcinoma at all three sites, with a salivary gland (**f**) and breast specimen shown

metastases, and 27/64 (42%) died of disease. In patients with lacrimal gland adenoid cystic carcinoma, 5/9 (56%) experienced each of these events. None of the breast carcinomas recurred.

Histology and phenotypic profiling

Irrespective of site, all tumors displayed the histological hallmark features of adenoid cystic carcinoma with

Table 2 Rearrangements, fusions, and copy-number status of the *MYB*, *NFIB*, and *MYBL1* genes in adenoid cystic carcinoma of the salivary gland, lacrimal gland, and breast

Split probe				Fusion probe	Amplification	Wild type
n	MYB	NFIB	MYBL1	MYB–NFIB	MYB	
Salivary gland adenoid cystic carcinoma						
63	39	49	13	37	3	7
Lacrimal gland adenoid cystic carcinoma						
9	5	5	0	5	1	3
Breast adenoid cystic carcinoma						
11	4	6	0	4	0	4

Summary of fluorescent in situ hybridization in adenoid cystic carcinoma using break apart and fusion probes. *MYB* and *NFIB* demonstrated split signals in the majority of cases, and the majority of these had fused *MYB–NFIB* signals. *MYBL1* split signals were exclusively found in salivary gland carcinomas. Amplification of *MYB* was a rare event. Only a minority of cases were wild type

combinations of tubular, cribriform, and solid areas (Fig. 1a–c). Architectural grade ranged from I to III at all three sites, with grade III (i.e., "solid histology") in 1/11 (9%), 7/62 (11%), and 2/9 (22%) of breast, salivary gland, and lacrimal gland tumors, respectively (Table 1). Immunohistochemistry identified dual populations of luminal and abluminal cells in varying proportions in tumors at all three sites (Fig. 1d–f). The results of phenotypic profiling are summarized in Table 1 and further specified in Table S1. The majority of cases at all sites were CK5/6 positive, most intensely in the luminal cells (Fig. 1d, e). Androgen receptor and progesterone receptor were consistently negative, while 1/64 (2%) carcinomas from the salivary gland expressed estrogen receptor (Fig. 2a–c). EGFR was positive (3+) in 6/64 (9%) of salivary gland tumors and in none of the lacrimal gland or breast tumors (Fig. 2d). All EGFR 2+ cases (five in the salivary gland) had intact *EGFR* copy number by FISH (Fig. 2d, insert). HER2 was consistently negative (Fig. 2e, f). This categorized 55/64 (86%) of salivary gland adenoid cystic carcinomas as basal-like, 8/64 (13%) as indeterminate, and 1/64 (2%) as luminal type due to estrogen receptor expression (Case 32, Fig. 2b insert). There was no difference in overall survival between basal-like and indeterminate phenotypes ($p = 0.59$) (Figure S2). All lacrimal gland and breast adenoid cystic carcinomas were basal-like.

MYB, MYBL1, and NFIB gene status in adenoid cystic carcinoma of the salivary gland, lacrimal gland, and breast

Concurrent rearrangement of *MYB* and *NFIB* was the most frequent finding in tumors at all sites, with *MYB–NFIB* fusion found in all of these (Table 2, Fig. 3a–c). The

second most frequent finding was concurrent rearrangement of *MYBL1* and *NFIB*, which was seen exclusively in salivary gland adenoid cystic carcinoma (Table 2, Fig. 3d). More rare events included *MYB* amplification and isolated rearrangements of *MYB* (*MYB-X*), *NFIB* (*NFIB-X*), and *MYBL1* (*MYBL1-X*) (Table 2, Fig. 3e, g). There was no difference in overall survival between patients with *MYB* and *MYBL1* involvement ($p = 0.92$) (Figure S3). Among non-salivary sites, one lacrimal gland case had *MYB* amplification and two breast cases had isolated *NFIB* rearrangement (*NFIB-X*). All cases without detectable genetic abnormalities were intensely positive for MYB protein (Fig. 3f, Table 2).

MicroRNA expression profiling of adenoid cystic carcinoma of the salivary gland, lacrimal gland, and breast

After establishing morphological and genetic similarities between adenoid cystic carcinoma irrespective of site, the miRNA expression profiles of the tumor and normal tissue were compared. This identified 22 upregulated and 25 downregulated miRNAs in salivary gland adenoid cystic carcinoma (Table S2), and eight upregulated miRNAs in lacrimal gland adenoid cystic carcinoma. Among these differentially expressed miRNAs, hsa-miR-455-5p and hsa-miR-181d-5p were upregulated in carcinomas of both salivary and lacrimal gland (Fig. 4, Table S2, and Table S3). In contrast, adenoid cystic carcinoma of the breast did not separate from normal breast until increasing FDR to <0.27 (Fig. 4, Table S4). Comparing adenoid cystic carcinoma from the salivary gland and breast identified 31 upregulated and 62 downregulated miRNAs (Table 3). Hierarchical clustering identified two main clusters, with the largest cluster being composed exclusively of salivary gland carcinomas (51/64, 80%) (Fig. 5). The other main cluster divided into two subclusters, with one being composed exclusively of 8 breast adenoid cystic carcinomas (8/11, 73%) and the other harboring all 9 (9/9, 100%) lacrimal gland carcinomas, plus the remaining 13 (13/64, 20%) salivary gland carcinomas and 3 (3/11, 27%) breast carcinomas (Fig. 5). Among the miRNAs identified by hierarchical clustering as being differentially expressed between salivary gland and breast adenoid cystic carcinoma, none were differentially expressed between the corresponding normal glands, excluding tissue-specific differences as the cause for the differences found. Functional annotation of miRNAs differentially expressed between salivary gland and breast adenoid cystic carcinoma identified their involvement in several different biological processes, including the Kyoto Encyclopedia of Genes and Genomes (KEGG) categories: metabolism, signal transduction, and cancers (Table S5).
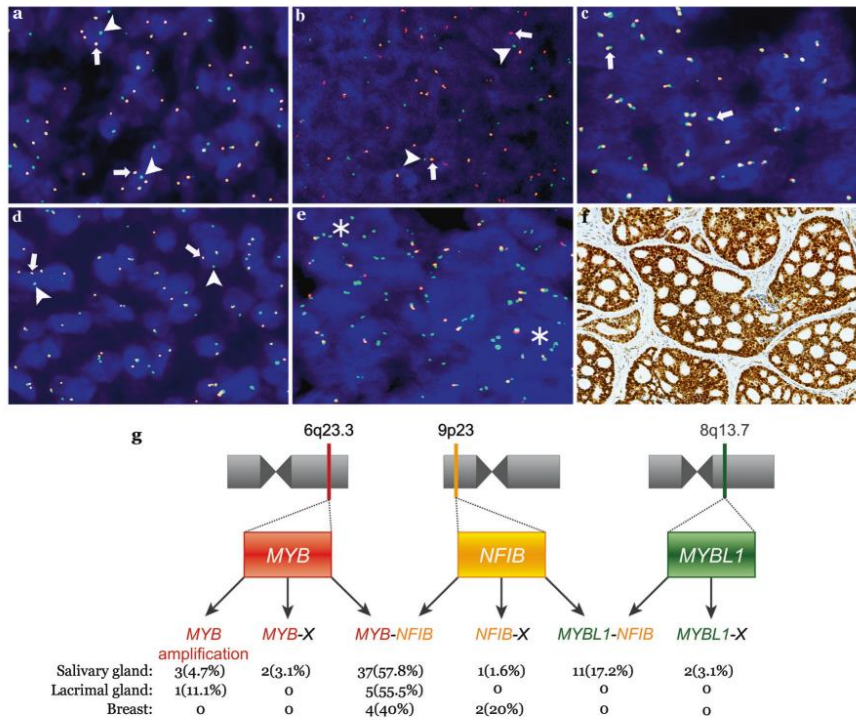
Fig. 3 Genetic characterization of adenoid cystic carcinoma of the salivary gland, lacrimal gland, and breast. **a** Fluorescent in situ hybridization using break-apart probes for *MYB* and **b** *NFIB* showing separate red (arrows) and green (arrowheads) signals, indicating rearrangement in a breast adenoid cystic carcinoma. **c** The fusion probe demonstrates the presence of the *MYB–NFIB* fusion in the same specimen. **d** Break-apart probe demonstrating *MYBL1* rearrangement that was identified exclusively in a subset of salivary gland carcinomas. **e** In a subset of non-rearranged cases, numerous green signals were found which is consistent with amplification of the 5′ part of the *MYB* gene. **f** In the non-rearranged carcinomas, all cases overexpressed MYB protein. **g** Overview of the genetic spectrum in salivary gland, lacrimal gland, and breast adenoid cystic carcinoma. *MYB* and *NFIB* involvement was seen in adenoid cystic carcinoma of all three organs, while *MYBL1* was exclusively found in the salivary gland

Discussion

While being by far most common in the salivary gland, adenoid cystic carcinoma is found at other sites including the lacrimal gland, lung, breast, and skin [9, 10, 48]. Adenoid cystic carcinoma of the salivary gland, lacrimal gland, and lung has a protracted but relentless clinical course, contrasting with cutaneous and breast adenoid cystic carcinoma which are indolent neoplasms [1, 3, 9, 48]. The contrast in clinical outcome between adenoid cystic carcinoma of the salivary and lacrimal gland on one side and breast on the other is confirmed in the present series (Table 1). While it could be speculated that this paradox is simply due to a morphological overlap of different entities, combined immunohistochemical phenotyping and pattern of genetic rearrangements uniformly rejects this theory.

Hence, the genetic cause of the majority of adenoid cystic carcinoma irrespective of site is unquestioned, but does not explain the site-dependent difference in clinical behavior. Through recent years, several studies on the genetics of especially salivary gland adenoid cystic carcinoma have demonstrated a low mutational burden as compared to other cancers [12, 14, 49–52]. However, none of these have been shown to be independent prognostic factors, nor do they apply to the majority of patients with this malignancy.

The indolent nature of breast adenoid cystic carcinoma not only stand out in this type of malignancy across different anatomical sites but also among triple-negative and basal-like breast carcinomas, which are otherwise known to be associated with an aggressive clinical course [4, 7]. In the breast, phenotypic classification places adenoid cystic carcinoma in the basal-like and triple-negative categories,
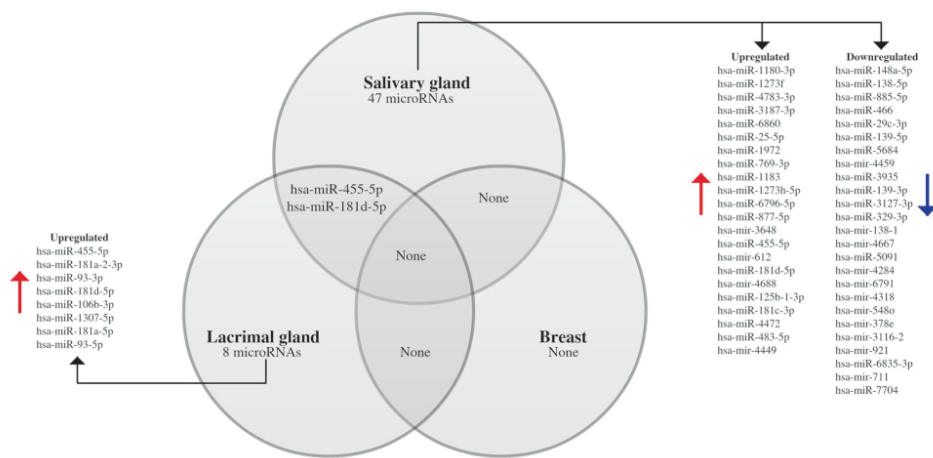
Fig. 4 Venn diagram illustrating the number of microRNAs differentially expressed in adenoid cystic carcinoma of each site compared with their normal tissue counterpart and how they overlap with each other (FDR < 0.05)

and gene expression profiling is in accordance with adenoid cystic carcinoma being similar to other basal-like carcinomas [15, 53, 54]. Our results are in agreement with the exclusively basal-like and triple-negative phenotype of breast adenoid cystic carcinoma, and this finding also applied to lacrimal gland tumors. However, salivary gland tumors were triple negative in all cases, but despite being basal-like in the majority of these, a substantial proportion was negative for all markers and thereby of indeterminate phenotype (Fig. 5, Table S4). In the breast, indeterminate phenotypes are more aggressive than basal-like phenotypes, but this was not the case between these two groups of salivary gland adenoid cystic carcinomas (Figure S1) [4]. Hence, the significance of phenotypic profiling in salivary gland tumors, if any, is not straightforward and deserves further investigation.

While gene fusions in salivary gland adenoid cystic carcinoma have been studied in great detail, the fusion status of much fewer cases from the lacrimal gland and breast have been reported [9, 10, 15, 55, 56]. In agreement with previous studies, we identified a spectrum of genetic abnormalities in salivary gland carcinomas, including two cases with isolated *MYB* rearrangement of which one was estrogen receptor-positive [57]. To the best of our knowledge, an estrogen receptor-positive salivary gland adenoid cystic carcinoma has not previously been described. In contrast, a much narrower selection of genetic rearrangements was found in lacrimal gland and breast adenoid cystic carcinomas. Lacrimal gland abnormalities were restricted to *MYB–NFIB* fusions and *MYB* amplification, while a somewhat larger proportion of breast adenoid

cystic carcinomas had normal *MYB* and *NFIB* genes or had isolated *NFIB* rearrangement (*NFIB-X*). To our knowledge, isolated *NFIB* rearrangement have not previously been described in breast adenoid cystic carcinoma [10, 15, 56]. Also, *MYBL1* rearrangements seem to be unique to salivary gland adenoid cystic carcinoma, and, in agreement with the literature, we did not find a difference in overall survival between cases with *MYB* and *MYBL1* involvement (Figure S2) [58]. An intriguing observation is that, among the different genetic aberrations identified, *NFIB* was the most consistently involved (Figs. 3 and 5). The function of *NFIB* is poorly characterized but is crucial for salivary gland embryonic development and paradoxically serves as a metastatic driver in some cancers while having a tumor suppressor function others [59–63]. It is interesting that the salivary gland and breast are the two tissues in which *NFIB* is expressed in the highest level among a large selection of human tissues in the Genotype-Tissue Expression project (GTEx) (Figure S3) [64]. Although shown to be involved in other types of salivary gland malignancies, further clarification of *NFIB* function in these organs is warranted [65].

Post-transcriptional regulation of gene expression by miRNAs is known to be involved in a number of human malignancies, but the two previous studies comparing miRNA expressions in salivary gland adenoid cystic carcinoma and normal salivary gland have identified widely different patterns of miRNA dysregulation [26, 66, 67]. Also, only little agreement is found between these studies and our findings, and the general discrepancy in miRNA expression between studies is well known [68]. To improve

Table 3 Differentially expressed miRNA between salivary gland and breast adenoid cystic carcinoma

Upregulated						Downregulated					
miRBase accession	miRBase symbol	FDR	Fold change	Genomic location	Host gene	miRBase accession	miRBase symbol	FDR	Fold change	Genomic location	Host gene
MIMAT0027353	hsa-miR-6726-5p	0.02	1.70	1p36.33	ACAP3	MIMAT0001080	hsa-miR-196b-5p[a]	<0.001	0.38	7p15.2	Intergenic
MIMAT0017990	hsa-miR-3613-5p	0.012	1.58	13q14.2	Intergenic	MIMAT0003283	hsa-miR-615-3p[a]	<0.001	0.42	12q13.13	HOXC5
MIMAT0027640	hsa-miR-6870-5p	<0.001	1.54	20p12.2	JAG1	MIMAT0000253	hsa-miR-10a-5p	0.001	0.44	17q21.32	HOXB3
MIMAT0018105	hsa-miR-3679-3p	0.030	1.49	2q21.2	MGAT5	MIMAT0004749	hsa-miR-424-3p	0.012	0.45	Xq26.3	Intergenic
MI0300022574	hsa-mir-6729	0.012	1.47	1p36.22	MIIP	MIMAT0001635	hsa-miR-452-5p	0.002	0.47	Xq28	GABRE
MIMAT0018101	hsa-miR-3677-3p	0.033	1.40	16p13.3	Intergenic	MIMAT0000459	hsa-miR-193a-3p	0.026	0.47	17q11.2	Intergenic
MI0003179	hsa-mir-527	0.016	1.39	19q13.42	Intergenic	MIMAT0009198	hsa-miR-224-3p	0.017	0.49	Xq28	GABRE
MI0006656	hsa-mir-1197	0.002	1.36	15q26.2	Intergenic	MIMAT0000281	hsa-miR-224-5p	<0.001	0.47	Xq28	GABRE
MI0020358	hsa-mir-6081	0.047	1.28	9q22.32	C9orf3	MIMAT0000765	hsa-miR-335-5p	<0.001	0.47	7q32.2	MEST
MI0016772	hsa-mir-4432	0.040	1.27	2p16.1	Intergenic	MIMAT0000254	hsa-miR-10b-5p	0.001	0.48	2q31.1	HOXD4
MI0006375	hsa-mir-548f-2	0.018	1.26	2q34	ERBB4	MIMAT0002874	hsa-miR-503-5p	0.021	0.48	Xq26.3	Intergenic
MI0006339	hsa-mir-1206	0.024	1.26	8q24.21	Intergenic	MIMAT0000083	hsa-miR-26b-5p	0.009	0.50	2q35	CTDSP1
MIMAT0027383	hsa-miR-6741-5p	0.022	1.24	1q42.12	Intergenic	MI0014146	hsa-mir-3128	0.001	0.52	2q312	NFE2L2
MI0003823	hsa-mir-449c	0.038	1.24	5q11.2	CDC20B	MIMAT0015030	hsa-miR-3156-5p	<0.001	0.53	NA	Multiple stemloops[b]
MIMAT0027563	hsa-miR-6831-3p	0.043	1.22	5q31.3	APBB3	MIMAT0019068	hsa-miR-4529-3p	<0.001	0.53	18q21.2	TCF4
MI0022589	hsa-mir-6744	0.026	1.20	11p15.5	MUC5B	MIMAT0014991	hsa-miR-3128	0.031	0.53	2q31.2	NFE2L2
MI0016426	hsa-mir-3150b	0.039	1.19	8q22.1	NDUFAF6	MIMAT0004698	hsa-miR-135b-3p	0.018	0.54	1q32.1	LEMD1
MI0005544	hsa-mir-147b	0.038	1.18	15q21.1	C15orf48	MIMAT0018179	hsa-miR-3907	0.016	0.57	7q36.1	CRYGN
MI0016857	hsa-mir-4495	0.041	1.18	12q23.1	Intergenic	MIMAT0000096	hsa-miR-98-5p	0.016	0.60	Xp11.22	HUWE1
MI0017281	hsa-mir-4653	0.039	1.16	7q22.1	AP1S1	MIMAT0019954	hsa-miR-4786-5p	0.011	0.63	2q37.3	Intergenic
MIMAT0023710	hsa-miR-6085	0.001	1.15	15q22.2	Intergenic	MIMAT0004955	hsa-miR-374b-5p	0.004	0.64	Xq13.2	Intergenic
MIMAT0019027	hsa-miR-4492	0.002	1.11	11q23.3	BCL9L	MI0025513	hsa-mir-6516	0.039	0.64	17q25.2	SEC14L1
MIMAT0026622	hsa-miR-619-5p	0.037	1.11	12q24.11	SSH1	MI0025751	hsa-mir-7975	0.002	0.66	19q13.42	Intergenic
MIMAT0030999	hsa-miR-8072	<0.001	1.10	12q24.31	SBNO1	MI0022733	hsa-mir-6886	0.038	0.66	19p13.2	LDLR

Table 3 (continued)

Upregulated						Downregulated					
miRBase accession	miRBase symbol	FDR	Fold change	Genomic location	Host gene	miRBase accession	miRBase symbol	FDR	Fold change	Genomic location	Host gene
MIMAT0005582	hsa-miR-1228-5p	0.005	1.09	12q13.3	LRP1	MIMAT0026636	hsa-miR-668-5p	0.016	0.67	14q32.31	Intergenic
MIMAT0018994	hsa-miR-4467	0.009	1.09	7q22.1	LRWD1	MIMAT0019231	hsa-miR-3944-5p	0.010	0.69	10q26.3	ECHS1
MIMAT0007881	hsa-miR-1908-5p	0.002	1.08	11q12.2	FADS1	MI0000077	hsa-mir-21	0.028	0.69	17q23.1	Intergenic
MIMAT0022946	hsa-miR-1237-5p	0.016	1.06	11q13.1	RPS6KA4	MIMAT0004552	hsa-miR-139-3p	0.045	0.69	11q13.4	PDE2A
MIMAT0023252	hsa-miR-5787	0.017	1.06	3p21.31	GNAI2	MI0000082	hsa-mir-25	0.027	0.71	7q22.1	MCM7
MIMAT0019032	hsa-miR-4497	0.037	1.04	12q24.11	Intergenic	MIMAT0019830	hsa-miR-4717-3p	0.027	0.71	16p13.3	Intergenic
MIMAT0030019	hsa-miR-7704	0.045	1.02	2q31.1	HOXD1	MIMAT0026606	hsa-miR-511-3p	0.002	0.72	10p12.33	MRC1
						MIMAT0005895	hsa-miR-548f-3p	0.003	0.72	NA	Multiple stemloops[c]
						MI0015849	hsa-mir-4320	0.010	0.72	18q21.1	MYO5B
						MI0014250	hsa-mir-3201	0.011	0.73	22q13.32	Intergenic
						MI0017310	hsa-mir-4679-1	0.010	0.74	10q23.31	Intergenic
						MIMAT0018942	hsa-miR-4427	0.031	0.74	1q42.2	KCNK1
						MI0003634	hsa-mir-620	0.031	0.74	12q24.21	MED13L
						MI0015999	hsa-mir-3609	0.009	0.76	7q22.1	TRRAP
						MI0003628	hsa-mir-615	0.042	0.76	12q13.13	HOXC5
						MIMAT0015053	hsa-miR-3176	<0.001	0.77	16p13.3	CAPN15
						MIMAT0018950	hsa-miR-4434	0.011	0.78	2p14	AFTPH
						MI0003514	hsa-mir-539	0.017	0.78	14q32.31	Intergenic
						MIMAT0019726	hsa-miR-4659a-5p	0.031	0.78	8p23.1	AGPAT5
						MIMAT0015018	hsa-miR-3146	0.009	0.79	7p21.1	TWISTNB
						MIMAT0000226	hsa-miR-196a-5p	<0.001	0.8	NA	Multiple stemloops[d]
						MIMAT0003289	hsa-miR-620	0.010	0.80	12q24.21	MED13L
						MI0025901	hsa-mir-8065	0.012	0.80	16p13.3	RBFOX1
						NA[e]	hsa-miR-3673	0.039	0.80	—	—
						MI0000253	hsa-mir-148a	0.012	0.81	7p15.2	Intergenic
						MIMAT0025460	hsa-miR-6502-5p	0.031	0.81	12q14.3	IRAK3

Table 3 (continued)

Upregulated						Downregulated					
miRBase accession	miRBase symbol	FDR	Fold change	Genomic location	Host gene	miRBase accession	miRBase symbol	FDR	Fold change	Genomic location	Host gene
						MI0016800	hsa-mir-4454	0.043	0.81	4q32.2	Intergenic
						MI0000471	hsa-mir-126	0.043	0.81	9q34.3	EGFL7
						MIMAT0002172	hsa-miR-376b-3p	0.007	0.82	14q32.31	Intergenic
						MIMAT0018094	hsa-miR-3671	0.017	0.82	1p31.3	LOC107983962
						MIMAT0026473	hsa-miR-95-5p	0.040	0.83	4p16.1	ABLIM2
						MIMAT0031176	hsa-miR-7973	0.047	0.83	15q21.2	CYP19A1
						MIMAT0019030	hsa-miR-4495	0.047	0.83	12q23.1	Intergenic
						MIMAT0019745	hsa-miR-4668-5p	0.010	0.84	9q31.3	UGCG
						MIMAT0017991	hsa-miR-3613-3p	0.012	0.84	13q14.2	Intergenic
						MI0005775	hsa-mir-297	0.042	0.84	4q25	Intergenic
						MI0016074[e]	hsa-mir-3673	0.036	0.85	—	—
						MIMAT000250	hsa-miR-139-5p	0.024	0.90	11q13.4	PDE2A

[a] Also downregulated in lacrimal gland adenoid cystic carcinoma as compared to breast hsa-miR-196b-5p fold change 0.41 (FDR <0.001) and hsa-miR-615-3p fold change 0.39 (FDR = 0.003)

[b] hsa-mir-3156-1, hsa-mir-3156-2, and hsa-mir-3156-3

[c] hsa-mir-548f-1, hsa-mir-548f-2, hsa-mir-548f-3, hsa-mir-548f-4, and hsa-mir-548f-5

[d] hsa-mir-196a-1 and hsa-mir-196a-2

[e] Removed from miRBase
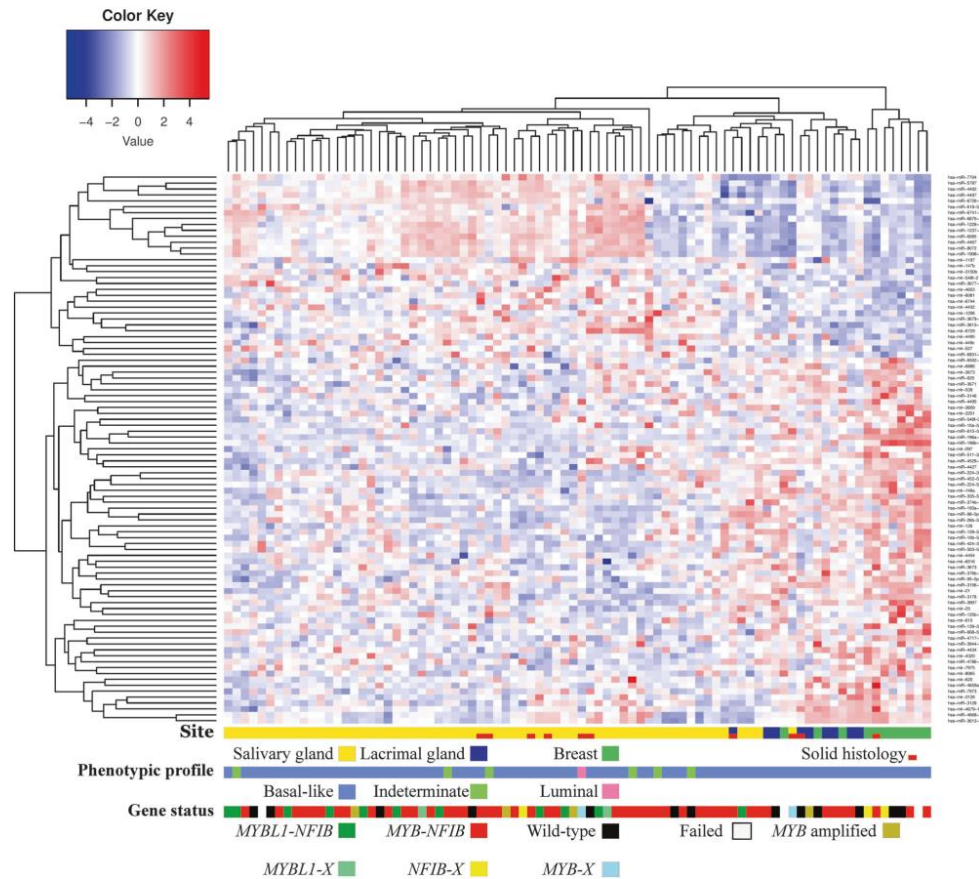
Fig. 5 MicroRNA expression profiling separates most breast from salivary gland adenoid cystic carcinoma irrespective of phenotypic profile and genetic status. Unsupervised hierarchical clustering of adenoid cystic carcinoma of the salivary gland, lacrimal gland, and breast clustered the majority of salivary gland carcinomas (51/64) and breast carcinomas (8/11) at each end of the spectrum. All lacrimal gland cases (9/9) clustered between the pure salivary gland and breast clusters. The lacrimal gland cluster included the remaining subset of salivary gland (11/64) and breast carcinomas (3/11). Clustering of cases occurred irrespective of architectural grade (solid), phenotypic profile, and gene status

transparency, we conducted this study according to BRISQ guidelines and sought to minimize the influence of external factors by sampling pure tumor tissue, assuring the quality of extracted miRNA, use of a comprehensive and validated array, and inclusion of a large number of samples. The fact that miRNA expression could not distinguish between breast adenoid cystic carcinoma and normal breast tissue, while pronounced dysregulation was found between tumor tissue and normal tissue from both salivary and lacrimal gland, goes well in hand with the differences in malignant potential (Fig. 4). Indeed, despite characterizing only nine cases from the lacrimal gland, an overlap in tumor-specific

miRNA expression was found between lacrimal and salivary gland adenoid cystic carcinoma. These two miRNAs (hsa-miR-455-5p, hsa-miR-181d-5p) have been repeatedly found to be overexpressed in other malignancies [69–71]. In unsupervised hierarchical clustering, global miRNA expression profiling separated salivary gland from breast adenoid cystic carcinoma with high accuracy and placed lacrimal gland tumors in between these two (Fig. 5). Importantly, this separation was not caused by tissue-specific expression but by differences between the tumors, and the plausibility of these differentially expressed miR-NAs as being responsible for the difference in clinical

behavior is strengthened by their involvement in the regulation of genes in several KEGG orthology categories frequently involved in cancer (Table S5). In addition to being the first class of molecules able to separate adenoid cystic carcinoma according to site of origin, this lends support to miRNA as having a role in the clinical behavior of these tumors. The mechanism for this miRNA dysregulation is currently unknown, as none of these are located to chromosomal regions involved in recurrent copy number alterations in adenoid cystic carcinoma, and needs to be further studied (Table 3) [72].

In conclusion, we present a comparative study of adenoid cystic carcinoma of the salivary gland, lacrimal gland, and breast and corroborate the histological and genetic similarity between these lesions despite the large variations in clinical behavior. We show that global miRNA expression profiling separates these tumors according to site of origin, and that differentially expressed miRNAs are involved in regulation of cellular processes that could be responsible for a more aggressive clinical course in salivary gland adenoid cystic carcinoma as compared to those in the breast. These findings are helpful in directing studies for prognostication, intensity of treatment and monitoring of patients with salivary gland adenoid cystic carcinoma.

Compliance with ethical standards

Conflict of interest The authors declare that they have no conflict of interest.

References

1. Bjørndal K, Krogdahl A, Therkildsen MH, et al. Salivary adenoid cystic carcinoma in Denmark 1990–2005: outcome and independent prognostic factors including the benefit of radiotherapy. Results of the Danish Head and Neck Cancer Group (DAHANCA). Oral Oncol. 2015;51:1138–42.
2. Andreoli MT, Aakalu V, Setabutr P. Epidemiological trends in malignant lacrimal gland tumors. Otolaryngol Head Neck Surg. 2015;152:279–83.
3. Marchiò C, Weigelt B, Reis-Filho JS. Adenoid cystic carcinomas of the breast and salivary glands (or "The strange case of Dr Jekyll and Mr Hyde" of exocrine gland carcinomas). J Clin Pathol. 2010;63:220–28.
4. Voduc KD, Cheang MC, Tyldesley S, et al. Breast cancer subtypes and the risk of local and regional relapse. J Clin Oncol. 2010;28:1684–91.
5. Andreasen S, Grauslund M, Heegaard S. Lacrimal gland ductal carcinomas: clinical, morphological and genetic characterization and implications for targeted treatment. Acta Ophthalmol. 2017;95:299–6.
6. Di Palma S, Simpson RH, Marchió C, et al. Salivary duct carcinomas can be classified into luminal androgen receptor-positive, HER2 and basal-like phenotypes. Histopathology. 2012;61:629–43.
7. Badve S, Dabbs DJ, Schnitt SJ, et al. Basal-like and triple-negative breast cancers: a critical review with an emphasis on the implications for pathologists and oncologists. Mod Pathol. 2011;24:157–67.
8. Miyai K, Schwartz MR, Divatia MK, et al. Adenoid cystic carcinoma of breast: recent advances. World J Clin Cases. 2014;2:732–41.
9. von Holstein SL, Fehr A, Persson M, et al. Adenoid cystic carcinoma of the lacrimal gland: MYB gene activation, genomic imbalances, and clinical characteristics. Ophthalmology. 2013;120:2130–38.
10. Martelotto LG, De Filippo MR, Ng CK, et al. Genomic landscape of adenoid cystic carcinoma of the breast. J Pathol. 2015;237:179–89.
11. Persson M, Andrén Y, Mark J, et al. Recurrent fusion of MYB and NFIB transcription factor genes in carcinomas of the breast and head and neck. Proc Natl Acad Sci USA. 2009;106:18740–44.
12. Stephens PJ, Davies HR, Mitani Y, et al. Whole exome sequencing of adenoid cystic carcinoma. J Clin Invest. 2013;123:2965–68.
13. Persson M, Andrén Y, Moskaluk CA, et al. Clinically significant copy number alterations and complex rearrangements of MYB and NFIB in head and neck adenoid cystic carcinoma. Genes Chromosomes Cancer. 2012;51:805–17.
14. Ho AS, Kannan K, Roy DM, et al. The mutational landscape of adenoid cystic carcinoma. Nat Genet. 2013;45:791–98.
15. Wetterskog D, Lopez-Garcia MA, Lambros MB, et al. Adenoid cystic carcinomas constitute a genomically distinct subgroup of triple-negative and basal-like breast cancers. J Pathol. 2012;226:84–96.
16. Horlings HM, Weigelt B, Anderson EM, et al. Genomic profiling of histological special types of breast cancer. Breast Cancer Res Treat. 2013;142:257–69.
17. Andreasen S, Esmaeli B, von Holstein SL, et al. An update on tumors of the lacrimal gland. Asia-Pac J Ophthalmol. 2017;6:159–72.
18. Pia-Foschini M, Reis-Filho JS, Eusebi V, et al. Salivary gland-like tumours of the breast: surgical and molecular pathology. J Clin Pathol. 2003;56:497–6.
19. Dalin MG, Desrichard A, Katabi N, et al. Comprehensive molecular characterization of salivary duct carcinoma reveals actionable targets and similarity to apocrine breast cancer. Clin Cancer Res. 2016;22:4623–33.
20. Skálová A, Vanecek T, Sima R, et al. Mammary analogue secretory carcinoma of salivary glands, containing the ETV6-NTRK3 fusion gene: a hitherto undescribed salivary gland tumor entity. Am J Surg Pathol. 2010;34:599–8.
21. Krings G, Joseph NM, Bean GR, et al. Genomic profiling of breast secretory carcinomas. Mod Pathol. 2017;30:1086–99.
22. Lu J, Getz G, Miska EA, et al. MicroRNA expression profiles classify human cancers. Nature. 2005;435:834–38.
23. Iorio MV, Croce CM. microRNA involvement in human cancer. Carcinogenesis. 2012;33:1126–33.
24. Filipowicz W, Bhattacharyya SN, Sonenberg N. Mechanisms of post-transcriptional regulation by microRNAs: are the answers in sight? Nat Rev Genet. 2008;9:102–14.

25. Ul Hussain M. Micro-RNAs (miRNAs): genomic organisation, biogenesis and mode of action. Cell Tissue Res. 2012;349:405–13.

26. Mitani Y, Roberts DB, Fatani H, et al. MicroRNA profiling of salivary adenoid cystic carcinoma: association of miR-17-92 upregulation with poor outcome. PLoS One. 2013;8:e66778.

27. Kiss O, Tőkés AM, Spisák S, et al. Breast- and salivary gland-derived adenoid cystic carcinomas: potential post-transcriptional divergencies. A pilot study based on miRNA expression profiling of four cases and review of the potential relevance of the findings. Pathol Oncol Res. 2015;21:29–4.

28. Moore HM, Kelly AB, Jewell SD, et al. Biospecimen reporting for improved study quality (BRISQ). J Proteome Res. 2011;10:3429–38.

29. Erichsen R, Lash TL, Hamilton-Dutoit SJ, et al. Existing data sources for clinical epidemiology: The Danish National Pathology Registry and Data Bank. Clin Epidemiol. 2010;2:51–56.

30. Andreasen S, Bjørndal K, Agander TK, et al. Tumors of the sublingual gland: a national clinicopathologic study of 29 cases. Eur Arch Otorhinolaryngol. 2016;273:3847–56.

31. Andreasen S, Bishop JA, Hansen TV, et al. Human papillomavirus-related carcinoma with adenoid cystic-like features of the sinonasal tract: clinical and morphological characterization of 6 new cases. Histopathology. 2017;70:880–88.

32. Andreasen S, Melchior LC, Kiss K, et al. The PRKD1 E710D hotspot mutation is highly specific in separating polymorphous adenocarcinoma of the palate from adenoid cystic carcinoma and pleomorphic adenoma on FNA. Cancer. 2017 [Epub ahead of print] doi:10.1002/cncy.21959

33. Amin MB, Edge SB, Greene FL et al. AJCC cancer staging manual. 8th ed. New York: Springer-Verlag; 2017.

34. Andreasen S, Therkildsen MH, Grauslund M, et al. Activation of the interleukin-6/Janus kinase/STAT3 pathway in pleomorphic adenoma of the parotid gland. APMIS. 2015;123:706–15.

35. Wolff AC, Hammond ME, Hicks DG, et al. Recommendations for human epidermal growth factor receptor 2 testing in breast cancer: American Society of Clinical Oncology/College of American Pathologists clinical practice guideline update. J Clin Oncol. 2013;31:3997–13.

36. Brill LB 2nd, Kanner WA, Fehr A, et al. Analysis of MYB expression and MYB-NFIB gene fusions in adenoid cystic carcinoma and other salivary neoplasms. Mod Pathol. 2011;24:1169–76.

37. Harvey JM, Clark GM, Osborne CK, et al. Estrogen receptor status by immunohistochemistry is superior to the ligand-binding assay for predicting response to adjuvant endocrine therapy in breast cancer. J Clin Oncol. 1999;17:1474–81.

38. Tan DS, Marchió C, Jones RL, et al. Triple negative breast cancer: molecular profiling and prognostic impact in adjuvant anthracycline-treated patients. Breast Cancer Res Treat. 2008;111:27–44.

39. Nielsen TO, Hsu FD, Jensen K, et al. Immunohistochemical and clinical characterization of the basal-like subtype of invasive breast carcinoma. Clin Cancer Res. 2004;10:5367–74.

40. Elston C, Ellis I. Pathological prognostic factors in breast cancer. I. The value of histological grade in breast cancer. Experience from a large study with long-term follow-up. Histopathology. 1991;19:403–10.

41. Ro JY, Silva EG, Gallager HS. Adenoid cystic carcinoma of the breast. Hum Pathol. 1987;18:1276–81.

42. Hudson JB, Collins BT. MYB gene abnormalities t(6;9) in adenoid cystic carcinoma fine-needle aspiration biopsy using fluorescence in situ hybridization. Arch Pathol Lab Med. 2014;138:403–9.

43. Howe K. Extraction of miRNAs from formalin-fixed paraffin-embedded (FFPE) tissues. Methods Mol Biol. 2017;1509:17–24.

44. Bolstad BM, Irizarry RA, Astrand M, et al. A comparison of normalization methods for high density oligonucleotide array data based on variance and bias. Bioinformatics. 2003;19:185–93.

45. Vlachos IS, Zagganas K, Paraskevopoulou MD, et al. DIANA-miRPathv3.0: deciphering microRNA function with experimental support. Nucleic Acids Res. 2015;43:W460–66.

46. Vlachos IS, Paraskevopoulou MD, Karagkouni D, et al. DIANA-TarBasev7.0: Indexing more than half a million experimentally supported miRNA:mRNA interactions. Nucleic Acids Res. 2015;43:D153–59.

47. Ogata H, Goto S, Sato K, et al. KEGG: Kyoto encyclopedia of genes and genomes. Nucleic Acids Res. 1999;27:29–34.

48. Li N, Xu L, Zhao H, et al. A comparison of the demographics, clinical features, and survival of patients with adenoid cystic carcinoma of major and minor salivary glands versus less common sites within the Surveillance, Epidemiology, and End Results registry. Cancer. 2012;118:3945–53.

49. Liu B, Mitani Y, Rao X, et al. Spatio-temporal genomic heterogeneity, phylogeny, and metastatic evolution in salivary adenoid cystic carcinoma. J Natl Cancer Inst. 2017;109:jx033. https://doi.org/10.1093/jnci/djx033.

50. Rettig EM, Talbot CC Jr, Sausen M, et al. Whole-genome sequencing of salivary gland adenoid cystic carcinoma. Cancer Prev Res. 2016;9:265–74.

51. Kato S, Elkin SK, Schwaederle M, et al. Genomic landscape of salivary gland tumors. Oncotarget. 2015;6:25631–45.

52. Ross JS, Wang K, Rand JV, et al. Comprehensive genomic profiling of relapsed and metastatic adenoid cystic carcinomas by next-generation sequencing reveals potential new routes to targeted therapies. Am J Surg Pathol. 2014;38:235–38.

53. Weigelt B, Horlings HM, Kreike B, et al. Refinement of breast cancer classification bymolecular characterization of histological special types. J Pathol. 2008;216:141–50.

54. Shah SP, Roth A, Goya R, et al. The clonal and mutational evolution spectrum of primary triple-negative breast cancers. Nature. 2012;486:395–99.

55. Chen TY, Keeney MG, Chintakuntlawar AV, et al. Adenoid cystic carcinoma of the lacrimal gland is frequently characterized by MYB rearrangement. Eye. 2017;31:720–25.

56. Argani P, Ning Y, Cimino-Mathews A. MYB labeling by immunohistochemistry is more sensitive and specific for breast adenoid cystic carcinoma than MYB labeling by FISH. Am J Surg Pathol. 2017;41:973–79.

57. Fujii K, Murase T, Beppu S, et al. MYB, MYBL1, MYBL2, and NFIB gene alterations and MYC overexpression in salivary gland adenoid cystic carcinoma. Histopathology. 2017;71:823–34.

58. Mitani Y, Liu B, Rao PH, et al. Novel MYBL1 gene rearrangements with recurrent MYBL1-NFIB fusions in salivary adenoid cystic carcinomas lacking t(6;9) translocations. Clin Cancer Res. 2016;22:725–33.

59. Mellas RE, Kim H, Osinski J, et al. NFIB regulates embryonic development of submandibular glands. J Dent Res. 2015;94:312–19.

60. Semenova EA, Kwon MC, Monkhorst K, et al. Transcription factor NFIB is a driver of small cell lung cancer progression in mice and marks metastatic disease in patients. Cell Rep. 2016;16:631–43.

61. Fane ME, Chhabra Y, Hollingsworth DE, et al. NFIB mediates BRN2 driven melanoma cell migration and invasion through regulation of EZH2 and MITF. EBioMedicine. 2017;16:63–5.

62. Becker-Santos DD, Thu KL, English JC, et al. Developmental transcription factor NFIB is a putative target of oncofetal miRNAs and is associated with tumour aggressiveness in lung adenocarcinoma. J Pathol. 2016;240:161–72.

63. Stringer BW, Bunt J, Day BW, et al. Nuclear factor one B (NFIB) encodes a subtype-specific tumour suppressor in glioblastoma. Oncotarget. 2016;7:29306–20.

64. The GTEx Consortium. The Genotype-Tissue Expression (GTEx) project. Nat Genet. 2013;45:580–85. https://gtexportal.org/home/gene/NFIB.

65. Andreasen S, Persson M, Kiss K, et al. Genomic profiling of a rare case of combined large-cell neuroendocrine carcinoma of the submandibular gland. Oncol Rep. 2016;35:2177–82.

66. Croce CM. Causes and consequences of microRNA dysregulation in cancer. Nat Rev Genet. 2009;10:704–14.

67. Gao R, Cao C, Zhang M, et al. A unifying gene signature for adenoid cystic cancer identifies parallel MYB-dependent and MYB-independent therapeutic targets. Oncotarget. 2014;5: 12528–42.

68. Andorfer CA, Necela BM, Thompson EA, et al. MicroRNA signatures: clinical biomarkers for the diagnosis and treatment of breast cancer. Trends Mol Med. 2011;17:313–19.

69. Wong N, Khwaja SS, Baker CM, et al. Prognostic microRNA signatures derived from The Cancer Genome Atlas for head and neck squamous cell carcinomas. Cancer Med. 2016;5:1619–28.

70. Cheng CM, Shiah SG, Huang CC, et al. Up-regulation of miR-455-5p by the TGF-β–SMAD signalling axis promotes the proliferation of oral squamous cancer cells by targeting UBE2B. J Pathol. 2016;240:38–49.

71. Yan LX, Huang XF, Shao Q, et al. MicroRNA miR-21 over-expression in human breast cancer is associated with advanced clinical stage, lymph node metastasis and patient poor prognosis. RNA. 2008;14:2348–60.

72. Zhang L, Mitani Y, Caulin C, et al. Detailed genome-wide SNP analysis of major salivary carcinomas localizes subtype-specific chromosome sites and oncogenes of potential clinical significance. Am J Pathol. 2013;182:2048–57.

37

Virchows Archiv

MicroRNA dysregulation in adenoid cystic carcinoma of the salivary gland in relation to prognosis and gene fusion status: A cohort study

--Manuscript Draft--

Manuscript Number:	
Full Title:	MicroRNA dysregulation in adenoid cystic carcinoma of the salivary gland in relation to prognosis and gene fusion status: A cohort study
Article Type:	Original Article
Corresponding Author:	Simon Andreasen, MD Zealand University Hospital Køge, DENMARK
Corresponding Author Secondary Information:	
Corresponding Author's Institution:	Zealand University Hospital
Corresponding Author's Secondary Institution:	
First Author:	Simon Andreasen, MD
First Author Secondary Information:	
Order of Authors:	Simon Andreasen, MD
	Qihua Tan, MD, PhD
	Tina Klitmøller Agander, MD, PhD
	Thomas van Overeem Hansen, PhD
	Petr Steiner
	Kristine Bjørndal, MD, PhD
	Estrid Høgdall, PhD, DMSc
	Stine Rosenkilde Larsen, MD
	Daiva Erentaite, MD
	Caroline Holkmann Olsen, MD
	Benedicte Parm Ulhøi, MD
	Steffen Heegaard, MD, DMSc
	Irene Wessel, MD, PhD
	Preben Homøe, MD, PhD, DMSc
Order of Authors Secondary Information:	

Abstract:	Adenoid cystic carcinoma (ACC) is among the most frequent malignancies of the salivary gland, and is notorious for its prolonged clinical course characterized by frequent recurrences often years after initial treatment. No molecular marker has been shown to have independent prognostic value in ACC, including characteristic gene fusions involving MYB, MYBL1, and NFIB. MicroRNA has been shown to be associated with clinical outcome in numerous malignancies, including one study of ACC, warranting further validation of this class of markers in this disease. Here, we investigate the prognostic value of microRNA in two ACC cohorts: a training cohort (n=64) and a validation cohort (n=120) with microarray and qPCR. In the training cohort, multivariate analysis of microarray data found high expression of hsa-miR-6835-3p to be associated with reduced recurrence-free survival (RFS) (p=0.016). Measuring the highest ranking microRNAs identified in survival analysis in the same cohort, qPCR identified high expression of hsa-miR-4676 to be associated with reduced overall survival (OS) and high expression of hsa-mir-1180 to be associated with improved RFS. This was not confirmed in the validation cohort, in which qPCR identified high expression of hsa-mir-21, hsa-mir-181a-2, and hsa-mir-152 to be associated with reduced OS and high expression of hsa-miR-374c to be associated with improved RFS. Interestingly, two distinct subsets of ACC separated in microRNA expression irrespective of gene fusion status, but without significant difference in outcome. Collectively, qPCR identified several microRNAs associated with OS and RFS, and different subsets of ACC separated according to microRNA expression, suggestive of ACC being a heterogeneous group of malignancies in its microRNA profile.
Suggested Reviewers:	Morten Grauslund, PhD Skane University Hospital Morten.Grauslund@skane.se Mr. Grauslund has worked with the utility of microRNA as diagnostic and prognostic markers in cancer. Furthermore, he has published several papers on salivary gland carcinoma.
	Albina Altemani, MD Professor, Faculdade de Medicina - UNICAMP aaltemani@uol.com.br Professor Altemani has published extensively on the molecular features of salivary gland carcinoma, including adenoid cystic carcinoma. She has the background for evaluating a study like this.
	Abbas Agaimy, MD Professor, Universitatsklinikum Erlangen Abbas.Agaimy@uk-erlangen.de Professor Agaimy has published extensively on salivary gland malignancies as well as on the prognostic value of microRNA.
Opposed Reviewers:	

MicroRNA dysregulation in adenoid cystic carcinoma of the salivary gland in relation to

prognosis and gene fusion status: A cohort study

Simon Andreasen[1,2], Qihua Tan[3], Tina Klitmøller Agander[4], Thomas v.O. Hansen[5], Petr Steiner[6,7], Kristine Bjørndal[8], Estrid Høgdall[9], Stine Rosenkilde Larsen[10], Daiva Erentaite[11], Caroline Holkmann Olsen[12], Benedicte Parm Ulhøi[13], Steffen Heegaard[4,14], Irene Wessel[2], Preben Homøe[1]

[1] Department of Otorhinolaryngology and Maxillofacial Surgery, Zealand University Hospital, Køge, Denmark

[2] Department of Otorhinolaryngology Head and Neck Surgery & Audiology, Rigshospitalet, Copenhagen, Denmark

[3] Unit of Human Genetics, Department of Clinical Research, University of Southern Denmark, Odense, Denmark

[4] Department of Pathology, Rigshospitalet, Copenhagen, Denmark

[5] Genomic Medicine, Rigshospitalet, Copenhagen University Hospital, Copenhagen, Denmark,

[6] Department of Pathology, Charles University in Prague, Faculty of Medicine, Pilsen, Czech Republic

[7] Bioptic Laboratory Ltd, Molecular Pathology Laboratory, Pilsen, Czech Republic

[8] Department of ORL – Head and Neck Surgery, Odense University Hospital, Odense, Denmark

[9] Department of Pathology, Herlev Hospital, University of Copenhagen, Herlev, Denmark

[10] Department of Pathology, Odense University Hospital, Odense, Denmark

[11] Department of Pathology, Aalborg University Hospital, Aalborg, Denmark

[12] Department of Pathology, Zealand University Hospital, Roskilde, Denmark

[13] Department of Pathology, Aarhus University Hospital, Aarhus, Denmark

[14] Department of Ophthalmology, Rigshospitalet-Glostrup, Copenhagen, Denmark

Word count: 3,207

Corresponding author:

Simon Andreasen, MD

Department of Otorhinolaryngology and Maxillofacial Surgery, Zealand University Hospital, Køge,

Denmark

Mail: Simon@Andreasen.pm

Phone: +45 22610764

ORCID: 0000-0002-1528-4988

2

Abstract

Adenoid cystic carcinoma (ACC) is among the most frequent malignancies of the salivary gland,

and is notorious for its prolonged clinical course characterized by frequent recurrences often years

after initial treatment. No molecular marker has been shown to have independent prognostic value

in ACC, including characteristic gene fusions involving *MYB*, *MYBL1*, and *NFIB*. MicroRNA has

been shown to be associated with clinical outcome in numerous malignancies, including one study

of ACC, warranting further validation of this class of markers in this disease. Here, we investigate

the prognostic value of microRNA in two ACC cohorts: a training cohort (n=64) and a validation

cohort (n=120) with microarray and qPCR. In the training cohort, multivariate analysis of

microarray data found high expression of hsa-miR-6835-3p to be associated with reduced

recurrence-free survival (RFS) (p=0.016). Measuring the highest ranking microRNAs identified in

survival analysis in the same cohort, qPCR identified high expression of hsa-miR-4676 to be

associated with reduced overall survival (OS) and high expression of hsa-mir-1180 to be associated

with improved RFS. This was not confirmed in the validation cohort, in which qPCR identified

high expression of hsa-mir-21, hsa-mir-181a-2, and hsa-mir-152 to be associated with reduced OS

and high expression of hsa-miR-374c to be associated with improved RFS. Interestingly, two

distinct subsets of ACC separated in microRNA expression irrespective of gene fusion status, but

without significant difference in outcome. Collectively, qPCR identified several microRNAs

associated with OS and RFS, and different subsets of ACC separated according to microRNA

expression, suggestive of ACC being a heterogeneous group of malignancies in its microRNA

profile.

Key words: Adenoid cystic carcinoma; Salivary gland; microRNA; Prognosis; MYB; MYBL1

3

Introduction

Adenoid cystic carcinoma (ACC) is among the most frequent salivary gland carcinomas and is enigmatic among head and neck malignancies for its unpredictable clinical course [1]. Clinically, the most challenging feature of ACC is its ability to recur both locally and with distant metastases often many years after primary treatment. The treatment is surgical resection while the use of adjuvant radiotherapy (RT) is an area of controversy [1–5]. Despite adjuvant RT being administered in most cases, more than one third of patients experience local or distant recurrence [1]. Importantly, local recurrences lead to repeated surgeries with significant associated morbidity, and non-resectable recurrences and distant metastases are usually fatal as conventional chemotherapy is largely ineffective [1,6,7].

The biologically most prominent feature of ACC are mutually-exclusive gene fusions involving the *MYB* or *MYBL1* [8,9]. Besides structural genetic abnormalities, mutations in ACC are few and diverse but with a predilection for NOTCH pathway genes [10,11]. Involvement of the NOTCH pathway is especially prevalent in the 10% of ACCs with solid histology, which has a particularly aggressive clinical course [12,13]. However, despite the scrutinization of the molecular background of ACC over recent years, a major deficit is the lack of findings with independent prognostic value. Recently, a subgroup of ACC with poor overall-survival was found to have a distinct gene expression profile, lending hope to improvements in prognostication and treatment based on studies of ACC biology [14]. Currently, clinicopathological variables such as stage, margins, solid histology, and vascular invasion are the classic clinicopathological characteristics with prognostic value used in clinical practice [1]. Still, ACCs with apparently favorable characteristics can have fulminant clinical courses, which makes reliable prognostic markers highly warranted for tailoring individual follow-up programs [15].

4

MicroRNA (miRNA) is a class of short non-coding RNAs ~22 nucleotides in length, functioning as potent post-transcriptional regulators of gene expression by causing either degradation or translational blockage of target mRNAs [16,17]. MiRNA has been shown to be involved in numerous human malignancies and to be of prognostic value in several tumor types [18–20]. Making miRNA especially interesting in the context of ACC is that binding sites for miRNAs are lost with the formation of fusion genes, thereby relieving miRNA-mediated inhibition of especially *MYB* [8]. Previously, one study on salivary gland ACC has shown a large number of miRNAs to be associated with adverse outcome, but currently this finding stands unchallenged and needs further confirmation [21].

In order to provide an understanding of the value of miRNA in prognostication of salivary gland ACC as well as the correlation between miRNA expression and gene fusion status, we perform global miRNA expression profiling of a large material with long-term follow-up and validate candidate prognostic miRNAs in a large external cohort.

Materials and methods

Patient material and clinicopathological variables

The study adheres to the REporting recommendations for tumor MARKer prognostic studies

(REMARK) and Biospecimen Reporting for Improved Study Quality (BRISQ) guidelines as

specified in supplementary materials and methods [22,23]. Patients with ACC in the period 1

January 1990 – 31 December 2014 were identified in the Danish Pathology Registry (Patobank)

with codes for ACC combined with topographical codes for the major and minor salivary glands

[24]. Only patients treated with curative intent were included. Formalin-fixed paraffin-embedded

(FFPE) specimens from cases not previously revised in a previous study on salivary gland

carcinomas were retrieved for central histological revision by an experienced head and neck

pathologist (TKA) according to the current WHO classification [25–27]. To exclude potential

mimics, sinonasal cases were screened for human papillomavirus to exclude HPV-related

multiphenotypic sinonasal carcinoma, and palatal cases underwent *PRKD1* hotspot sequencing to

exclude polymorphous adenocarcinoma [28–30]. All Danish residents have a unique personal

identification number (CPR number), and this number was cross-referenced with the Danish Cancer

Registry, the Danish Patient Registry, and the Danish Register of Causes of Death to identify date

and cause of death [31,32]. Clinicopathologic data from a subset of patients have been collected for

a previous study, and data on the remaining patients were collected in the same way from the

Danish Pathology Data Bank, the Danish Cancer Registry, the Danish Patient Registry, and hospital

registries [25]. Sample size for this hypothesis was based on using all available samples, and 184

ACCs with clinical information were available for inclusion. Sixty-four patients were randomly

selected to constitute the training cohort and the remaining 120 cases comprised the validation

cohort. The study was approved by the Regional Ethics Committee (H-6-2014-086) and the Danish

Data Protection Agency (REG-94-2014).

RNA extraction

To avoid admixture of normal cells, one 1mm core was obtained from each tumor block after

identification of a representative tumor area from a H&E-stained slide [33]. The QiaCube (Qiagen,

Valencia, CA) was used for automated isolation of miRNA with the miRNeasy FFPE Kit (Qiagen)

according to the manufacturer's instructions [33]. Total RNA concentration was measured using the

NanoDrop ND-1000 (Thermo Scientific, Wilmington, DE) (range: 300–1536 ng/µl) and nucleic

acid content (A260/A280, range: 1.7–2.7), indicating high nucleic acid purity. In the training

cohort, RNA integrity number (RIN) was measured in 10 samples >15 years old using the Agilent

2100 Bioanalyzer platform (Agilent Technologies, Santa Clara, CA) and the RNA 6000 Nano Kit

(Agilent) with RIN ranging from 0.9–1.6 (median 1.1), which is suitable for miRNA profiling.

MicroRNA microarray

The Affymetrix miRNA 4.1 microarray platform (Affymetrix, Santa Clara, CA) was used, covering

all entries in Sanger miRbase v.20, including 2,578 mature and 2,025 immature human miRNAs.

For miRNA analysis, 300 µg of total RNA was labelled with the FlashTag Biotin HSR RNA

Labelling kit (Affymetrix) according to the manufacturer's instructions. Microarrays from the same

batch were used to avoid batch variation. Microarray plates were washed, stained, and scanned on

the GeneTitan Instrument (Affymetrix). Raw data are available as Table S1.

MicroRNA data analysis

Following background correction, raw data were first normalized using the quantile

normalization function implemented in the free R package *preprocessCore* [34]. A linear

regression model was applied by regressing the log-transformed miRNA expression on group

membership, and correction for multiple testing was done by estimating the false discovery rate

(FDR), with FDR ≤ 0.05 defined as statistically significant. Hierarchical clustering was

performed with the significant miRNAs using the clustering function in the R package *gplots* (https://cran.r-project.org/web/packages/ggplot2s) by calculating the Euclidean distance. Survival curves were constructed by the Kaplan–Meier method and compared with the log-rank test, with significance defined as $p < 0.05$. High expression was defined as above the median and low expression as below the median. Hazard ratios were calculated in the Cox regression analysis after adjusting for clinical variables. Significant miRNAs were validated by comparing microarray and qPCR data using Pearson's correlation. Statistical analyses were done using R (https://www.r-project.org) and SPSS 20 (SPSS Inc., Chicago, IL, USA).

Quantitative polymerase chain reaction

Briefly, complementary DNA (cDNA) was made using 3.3ng miRNA as template. For pri-miRNAs, the High-Capacity cDNA Reverse Transcription Kit (Thermo Fisher Scientific, Waltham, MA) was used. For mature miRNAs, cDNA was prepared with the TaqMan MicroRNA Reverse Transcription Kit (Thermo Fisher). Preamplification was performed using the TaqMan PreAmp Master Mix (Thermo Fisher). Quantitative PCR (qPCR) was performed in triplicates on the Fluidigm Dynamic Array Chips (Fluidigm, San Francisco, CA) platform with the TaqMan Gene Expression Master Mix (Thermo Fisher Scientific) on the Fluidigm BioMark platform (Fluidigm) according to the manufacturer's instructions. Mean values were used for subsequent analysis. Arrays from the same batch were used to avoid batch variation. Non-enzyme controls (negative controls) and ath-miR-159a (positive controls) were included for all reactions. Data were analyzed in the Fluidigm Real-Time PCR analysis program v. 4.1.3 with baseline settings at linear (derivative) and Ct threshold methods at detectors. Detailed descriptions of PCR conditions are available in supplementary materials and methods.

8

Fluorescence in situ hybridization

Four-μm-thick FFPE sections from each case of the training cohort were placed onto positively-charged slides, and hematoxylin and eosin-stained slides were examined for determination of areas for counting. Fluorescence *in situ* hybridization was performed using break-apart probes for *MYB* (ZytoVision GmbH, Bremerhaven, Germany), *MYBL1* (Agilent Technologies, Santa Clara, CA/Empire Genomics, Buffalo, NY), and *NFIB* (Agilent Technologies/Empire Genomics) and an *MYB-NFIB* fusion probe (Agilent Technologies/Cytotest, Rockville, MD) according to the manufacturers' protocol as previously described and stated in detail in supplementary materials and methods [28,35]. Nuclei were counterstained with DAPI II (ZytoVision). Break-apart signals in ≥ 10% of cells was considered to represent rearrangement and fused signals in ≥20% of cells was considered to represent fusion [36].

9

Results

Clinicopathological characteristics of the two cohorts

A total of 184 patients were included; 64 in the training cohort and 120 in the validation cohort with

median follow-up of 92 and 71 months, respectively (Table 1). In the training cohort, there was a

larger proportion of female patients, submandibular gland tumors, tumors with tubulocribriform

histology, tumors without vascular invasion, and patients receiving radiotherapy as compared to the

validation cohort (Table 1). By comparison, the validation cohort had more males and tumors in the

parotid gland and oral minor salivary glands.

Thirty-six (56%) of the patients had recurrence (25 [39%]) and/or died (27 [42%]) during

follow-up in the training cohort. Eighty-eight (73.3%) of patients had recurrence (63 [53%]) and/or

died (59 [49%]) during follow-up in the validation cohort. There was no difference in overall or

recurrence-free survival between the training and validation cohorts (p=0.11 and 0.17, respectively)

(Fig. 1).

Prognostic value of clinicopathological parameters

High stage and vascular invasion were associated with decreased overall and recurrence-free

survival in both cohorts (Table 2). Solid histology was associated with reduced overall survival in

the validation cohort only but with reduced recurrence-free survival in both cohorts. Close or

involved surgical margins were associated with reduced recurrence-free survival in both cohorts,

whereas radiotherapy and perineural invasion was not associated with overall or recurrence-free

survival in any of the cohorts (Table 2).

microRNA as a prognostic marker in ACC

10

ACC and normal salivary gland tissue separated with 47 differentially expressed miRNA (Table

S2). A multivariate Cox regression model incorporating the significant variables listed in Table 2

for overall and recurrence-free survival was performed with microarray data from the training

cohort. No miRNA was associated with overall survival but high levels of hsa-miR-6835-3p was

associated with reduced recurrence-free survival (p=0.016). In order to validate this, qPCR was

performed on the 32 highest-ranking miRNAs in survival analysis despite the majority of these not

reaching significance (Table S3). Positive controls worked in all cases but 14/32 candidate miRNAs

had an insufficient number of cases with measureable levels to perform statistical analysis, and no

correlation was found between the expression levels of the remaining 18 miRNAs measured with

microarray and qPCR (R=-0.72 – 0.28)(Table S4). However, in multivariate analysis qPCR

identified high expression of hsa-miR-4676 as being associated with reduced overall survival and

high expression of hsa-mir-1180 to be associated with improved recurrence-free survival in the

training cohort, but not in the validation cohort (Fig 2, Table 3). In contrast, among the 18 miRNAs

measured with qPCR, high expression of three miRNAs (hsa-mir-21, hsa-mir-181a-2, and hsa-mir-

152) were associated with reduced overall survival, and high expression of hsa-miR-374c was

associated with improved recurrence-free survival in the validation cohort in multivariate analysis

(Fig. 2, Table 3). There were no differentially expressed miRNAs between solid and

tubulocribriform ACCs.

microRNA expression signatures separate ACC into two groups

Unsupervised hierarchical clustering was performed in order to identify groups with differences in

outcome. This identified two distinct groups composed of 11 (Group 1) and 53 (Group 2) tumors,

which separated due to differential expression of 1,658 miRNAs (Fig. 3A, 3B, Table S5).

Comparing the outcome of these two groups showed no difference between the groups for overall

11

survival (p=0.17) or recurrence-free survival (p=0.32) (Fig. 4). Interestingly, the clusters consisted

of tumors with aberrations of *MYB, MYBL1*, as well as tumors without involvement of either of the

two genes. The similarities in miRNA expression regardless of rearrangement status is further

illustrated by a complete overlap in principal component analysis (Fig. 5). None of the miRNAs

known to target *MYB* (hsa-miR-150, hsa-miR-16, hsa-miR-15a) or *MYBL1* (hsa-miR-223) were

differentially expressed in *MYB*- and *MYBL1*-rearranged ACCs compared to tumors without these

aberrations.

Discussion

While there is a direct therapeutic benefit in discovering directly targetable molecular alterations, markers able to identify high-risk patients can be transferred into clinical practice by initiating more intensive and/or prolonged follow-up programs for high-risk patient groups. Due to the lack of effective alternatives to surgery in ACC patients, early detection is of paramount importance for successful treatment. However, studying the biology of ACC is complicated by its relative rarity and the lack of validated cell lines. In addition, prognostic studies require studying relatively old samples due to the protracted clinical course of ACC, which is complicated by degradation of DNA and long RNA molecules in archival FFPE material [37]. However, shorter RNA molecules such as miRNA are well-preserved in FFPE samples for many years, and are therefore well-suited for this purpose [38,39].

Numerous miRNAs have been shown to be predictive for increased risk of recurrence in several types of carcinoma including lung, prostate, colorectal, and breast [40–42]. Similar findings have been made in one study of ACC, but this has stood alone until now [21]. In the present study of the largest molecularly profiled cohort of ACC reported to date, we found the classic clinicopathological parameters stage, solid growth, and vascular invasion to be associated with reduced overall survival, and these along with close/involved resection margins to be associated with reduced disease-specific survival (Table 2). This is in agreement with previous studies, and makes the material well-suited for further analysis [1]. Interestingly, we did not find any association between RT and outcome in neither of the cohorts. A very high proportion of patients received this treatment, and we found the majority of the patients who did not to have completely resected low-stage disease in the majority of cases. Based on these considerations, it cannot be excluded that the influence of RT on prognosis would have been different if a similar material of RT non-receivers was available for comparison. Ideally, a randomized controlled trial is needed in order to elute this

13

controversial area, but also a case-control study could contribute valuable information on this topic. Also, we find perineural invasion to be without prognostic value. Together with the same findings in two other major ACC cohorts, this lends strong support to abandoning this as being indicative of particular aggressive disease [1,44,45].

ACC separated from normal salivary gland tissue in miRNA expression, and comparing these findings with those previously obtained by Mitani et al. revealed that hsa-miR-455-5p and three closely-related miRNAs were upregulated in both our materials (hsa-miR-25-5p, hsa-miR-181d-5p, and hsa-miR-181c-3p) [21]. Similarly, five closely-related miRNAs were found to be downregulated in both our studies (hsa-miR-148a-5p, hsa-miR-138-5p, hsa-miR-885-5p, hsa-miR-29c-3p, and hsa-miR-329-3p) (Table S2). However, in contrast to the findings by Mitani et al., we did not find differences between solid and tubulocribriform ACCs [21]. As the particularly aggressive clinical course of solid ACC is apparent from our material, this finding suggests that at least this feature occurs unrelated to miRNA (Table 2).

As measured by microarray in the training cohort, high expression of one miRNA, hsa-miR-6835-3p, was found to be associated with reduced recurrence-free survival. In *in vitro* studies, this otherwise poorly-characterized miRNA has been found to be downregulated in lung carcinoma in response to IGFR1 silencing, which was recently shown to result in reduced *MYB-NFIB* transcription and reduced proliferation in ACC [46,47]. However, qPCR did not confirm this finding in either of the two cohorts (Table 3). Rather, qPCR and microarray did not correlate in any of the 18 miRNAs measured, which disrupts the concept of using microarray data in directing further exploration by qPCR. Others have made a head-to-head comparison between miRNA expression levels in FFPE samples measured with the two platforms used in the present study, and each platform was found to produce highly reproducible results, whereas the correlation between platforms was only moderate [48]. We performed qPCR in triplicates and found only miniscule

14

variation in measurements from individual samples. Although known to increase sensitivity, some

bias could be introduced by the preamplification step preceding qPCR which is an especially

vulnerable step for miRNAs expressed in low levels [49]. Another possibility could be the

fundamentally different principles for gene expression measurements in the two methods [49,50].

While the measurements of microarrays rely on complete labeling and high specificity of

hybridization between plate and labeled targets, the TaqMan-based method of qPCR depends on the

specificity of the primer to discriminate among highly-conserved miRNA target sequences. Despite

these discrepancies between methods, high expression of three miRNAs (hsa-mir-21, hsa-mir-181a-

2, hsa-mir-152) were associated with reduced overall survival, whereas high expression of hsa-miR-

374c was associated with improved recurrence-free survival in the validation cohort (Fig 2, Table

3). Notably, none of these were found in the other microarray-based study of miRNA in ACC [21].

However, hsa-mir-21 is among the most well-characterized miRNAs in human cancer and is known

to be involved in malignancies of the breast, lung, colon, and glioblastoma [18]. This lends support

to the involvement of miRNAs showing prognostic value in the validation cohort.

Interestingly, we found that ACC separated into two major groups based on miRNA

expression (Fig. 3). There was no statistically significant difference in outcome between these two

groups, but the smaller of these (Group 1) was composed of only 11 cases and the survival of this

subgroup of ACC with distinctly different miRNA expression needs further study including

additional cases. Also, we noted that several larger subgroups formed within Group 2 regardless of

gene fusion status and solid histology, which suggests that several molecularly separate subtypes

are present within the ACC category of tumors. The difference in miRNA expression between

Group 1 and Group 2 was substantial, caused by no less than 1,658 miRNAs expressed in

significantly different levels, which corresponds well with findings in transcriptomic studies of

ACC [14]. In agreement with numerous genomic studies demonstrating a diverse mutational

15

landscape of this disease, these findings imply that the ACC diagnosis encompass a variety of different molecular subtypes with only few mutual gene fusions in the majority of cases [10]. The biological significance of many of these rest on reports of a very limited number of cases in several different reports [8–11]. This illustrates two challenges in the current state of knowledge in ACC, as i) data from relatively few cases are available, ii) no studies employing more than one or two different molecular methods have been performed on the same material (i.e. investigating mutations, mRNA expression, miRNA expression, methylation patterns, protein expression on tumor and matched normal tissue) which is important to gain further insight into, what now appears to be a diverse group of tumors. Yet another consideration for these studies would be to take intratumoral heterogeneity into account [11].

In conclusion, we found several miRNAs to be associated with outcome in salivary gland ACC collected from nation-wide registries with up to 25 years of follow-up. Also, distinct groups of ACC formed based on global miRNA expression but irrespective of gene fusion status and growth pattern. At present, the most unifying feature of ACC remains the involvement of *MYB*, which makes the efforts in development of MYB-targeted therapies, directly or indirectly, ever more important [47].

Acknowledgements

Conflicts of interest

The authors declare no conflict of interest.

Funding

17

References

1. Bjørndal K, Krogdahl A, Therkildsen MH, Charabi B, Kristensen CA, Andersen E, Schytte S, Primdahl H, Johansen J, Pedersen HB, Andersen LJ, Godballe C. Salivary adenoid cystic carcinoma in Denmark 1990–2005: Outcome and independent prognostic factors including the benefit of radiotherapy. Results of the Danish Head and Neck Cancer Group (DAHANCA). Oral Oncol 51:1138–1142. doi: 10.1016/j.oraloncology.2015.10.002

2. Kokemueller H, Eckardt A, Brachvogel P, Hausamen JE. Adenoid cystic carcinoma of the head and neck—a 20 years experience. Int J Oral Maxillofac Surg 33:25–31. 10.1054/ijom.2003.0448

3. Oplatek A, Ozer E, Agrawal A, Bapna S, Schuller DE. Patterns of recurrence and survival of head and neck adenoid cystic carcinoma after definitive resection. Laryngoscope 120:65–70. 10.1002/lary.20684

4. Chen AM, Bucci MK, Weinberg V, Garcia J, Quivey JM, Schechter NR, Phillips TL, Fu KK, Eisele DW. Adenoid cystic carcinoma of the head and neck treated by surgery with or without postoperative radiation therapy: Prognostic features of recurrence. Int J Radiat Oncol Biol Phys 66:152–159. 10.1016/j.ijrobp.2006.04.014

5. Balamucki CJ, Amdur RJ, Werning JW, Vaysberg M, Morris CG, Kirwan JM, Mendenhall WM. Adenoid cystic carcinoma of the head and neck. Am J Otolaryngol 33:510–518. 10.1016/j.amjoto.2011.11.006

6. Adelstein DJ, Koyfman SA, El-Naggar AK, Hanna EY. Biology and Management of Salivary Gland Cancers. Semin Radiat Oncol 22:245–253. 10.1016/j.semradonc.2012.03.009

18

7. Dillon PM, Chakraborty S, Moskaluk CS, Joshi PJ, Thomas CY. Adenoid cystic carcinoma: A review of recent advances, molecular targets, and clinical trials. Head Neck 38:620–627. 10.1002/hed.23925

8. Persson M, Andrén Y, Mark J, Horlings HM, Persson F, Stenman G. Recurrent fusion of MYB and NFIB transcription factor genes in carcinomas of the breast and head and neck. Proc Natl Acad Sci U S A 106:18740–18744. 10.1073/pnas.0909114106

9. Mitani Y, Liu B, Rao PH, Borra VJ, Zafereo M, Weber RS, Kies M, Lozano G, Futreal A, Caulin C, El-Naggar AK. Novel MYBL1 Gene Rearrangements with Recurrent MYBL1-NFIB Fusions in Salivary Adenoid Cystic Carcinomas Lacking t(6;9) Translocations. Clin Cancer Res 22:725–733. 10.1158/1078-0432.CCR-15-2867-T

10. Ho AS, Kannan K, Roy DM et al. The mutational landscape of adenoid cystic carcinoma. Nat Genet 45:791–798. 10.1038/ng.2643

11. Liu B, Mitani Y, Rao X, Zafereo M, Zhang J, Zhang J, Futreal A, Lozano G, El-Naggar AK. Spatio-Temporal Genomic Heterogeneity, Phylogeny, and Metastatic Evolution in Salivary Adenoid Cystic Carcinoma. JNCI J Natl Cancer Inst 10.1093/jnci/djx033

12. Sajed DP, Faquin WC, Carey C, Severson EA, Afrogheh A, Johnson C, Blacklow SC, Chau NG, Lin DT, Krane JF, Jo VY, Garcia JJ, Scholl LM, Aster JC. Diffuse Staining for Activated NOTCH1 Correlates with NOTCH1 Mutation Status and Is Associated with Worse Outcome in Adenoid Cystic Carcinoma. Am J Surg Pathol 41:1473–1482. 10.1097/PAS.0000000000000945

13. Ferrarotto R, Mitani Y, Diao L et al Activating NOTCH1 Mutations Define a Distinct Subgroup of Patients With Adenoid Cystic Carcinoma Who Have Poor Prognosis, Propensity to Bone and Liver Metastasis, and Potential Responsiveness to Notch1 Inhibitors. J Clin Oncol 35:352–360. 10.1200/JCO.2016.67.5264

14. Frerich CA, Brayer KJ, Painter BM, Kang H, Mitani Y, El-naggar AK, Ness SA. Transcriptomes define distinct subgroups of salivary gland adenoid cystic carcinoma with different driver mutations and outcomes. Oncotarget 9:7341–7358. doi.org/10.18632/oncotarget.23641

15. Spiro RH. Distant metastasis in adenoid cystic carcinoma of salivary origin. Am J Surg. 174:495–8.

16. Filipowicz W, Bhattacharyya SN, Sonenberg N. Mechanisms of post-transcriptional regulation by microRNAs: are the answers in sight? Nat Rev Genet 9: 102–114. 10.1038/nrg2290

17. Ul Hussain M. Micro-RNAs (miRNAs): genomic organisation, biogenesis and mode of action. Cell Tissue Res. 349:405–413. 10.1007/s00441-012-1438-0

18. Calin GA, Croce CM. MicroRNA signatures in human cancers. Nat Rev Cancer 6:857–866. 10.1038/nrc1997

19. Thomson JM, Newman M, Parker JS, Morin-Kensicki EM, Wright T, Hammond SM. Extensive post-transcriptional regulation of microRNAs and its implications for cancer. Genes Dev 20:22022207. 10.1101/gad.1444406

20. Kong YW, Ferland-McCollough D, Jackson TJ, Bushell M. MicroRNAs in cancer management. Lancet Oncol 13: e249–e258. 10.1016/S1470-2045(12)70073-6.

21. Mitani Y, Roberts DB, Fatani H, Weber RS, Kies MS, Lippman SM, El-Naggar AK. MicroRNA Profiling of Salivary Adenoid Cystic Carcinoma: Association of miR-17-92 Upregulation with Poor Outcome. PLoS One 8:e66778. 10.1371/journal.pone.0066778

22. McShane LM, Altman DG, Sauerbrei W, Taube SE, Gion M, Clark GM. REporting recommendations for tumour MARKer prognostic studies (REMARK). Br J Cancer 93:387–91. 10.1038/sj.bjc.6602678

20

23.   Moore HM, Kelly AB, Jewell SD, McShane LM, Clark DP, Greenspan R, Hayes DF,

Hainaut P, Kim P, Mansfield E, Potapova O, Riegman P, Rubinstein Y, Seijo E, Somiari S,

Watson P, Weier HU, Zhu C, Vaught J. Biospeciment reporting for improved study quality

(BRISQ). J Proteome Res 10:3429–38. 10.1021/pr200021n

24.   Erichsen R, Lash TL, Hamilton-Dutoit SJ, Bjerregaard B, Vyberg M, Pedersen L. Existing

data sources for clinical epidemiology: The Danish National Pathology Registry and Data

Bank. Clin Epidemiol 2010:51–56.

25.   Bjørndal K, Krogdahl A, Therkildsen MH, Overgaard J, Johansen J, Kristensen CA,

Homøe P, Sørensen CH, Andersen E, Bundgaard T, Primdahl H, Lambertsen H, Andersen

LJ, Godballe C. Salivary gland carcinoma in Denmark 1990-2005: a national study of

incidence, site and histology. Results of the Danish Head and Neck Cancer Group

(DAHANCA). Oral Oncol 47:677–682. 10.1016/j.oraloncology.2011.04.020

26.   Stenman G, Licitra L, Said-Al-Naief N, van Zante A, Yarborough W. Adenoid cystic

carcinoma. In: El-Naggar A, Chan J, Grandis J, Takata T, Slootweg P (eds) World Health

Organization Classification of Tumours. IARC Press, Lyon, 164–165.

27.   Andreasen S, Bjørndal K, Agander TK, Wessel I, Homøe P. Tumors of the sublingual

gland: a national clinicopathologic study of 29 cases. Eur Arch Otorhinolaryngol

273:3847–3856. 0.1007/s00405-016-4000-y

28.   Andreasen S, Bishop JA, Hansen TV, Westra WH, Bilde A, von Buchwald C, Kiss K.

Human Papillomavirus-related Carcinoma with Adenoid Cystic-like Features of the

Sinonasal Tract: Clinical and Morphological Characterization of 6 New Cases.

Histopathology 70:880–888. 10.1111/his.13162

29.   Bishop JA, Andreasen S, Hang JF et al. HPV-related Multiphenotypic Sinonasal

Carcinoma. Am J Surg Pathol 41:1690–1701. 10.1097/PAS.0000000000000944

21

30. Andreasen S, Melchior LC, Kiss K, Bishop JA, Høgdall E, Grauslund M, Wessel I, Homøe P, Agander TK. The PRKD1 E710D hotspot mutation is highly specific in separating polymorphous adenocarcinoma of the palate from adenoid cystic carcinoma and pleomorphic adenoma on FNA. Cancer 10.1002/cncy.21959

31. Pedersen CB. The Danish Civil Registration System. Scand J Public Health. 39:22–25. 10.1177/1403494810387965

32. Helweg-Larsen K. The Danish Register of Causes of Death. Scand J Public Health 39:26–29. 10.1177/1403494811399958

33. Howe K. Extraction of miRNAs from Formalin-Fixed Paraffin-Embedded (FFPE) Tissues. Methods Mol Biol 10.1007/978-1-4939-6524-3_3

34. Bolstad BM, Irizarry RA, Astrand M, Speed TP. A Comparison of Normalization Methods for High Density Oligonucleotide Array Data Based on Variance and Bias. Bioinformatics 19:185–193.

35. Skálová A, Vanecek T, Sima R, Laco J, Weinreb I, Perez-Ordonez B, Starek I, Geierova M, Simpson RH, Passador-Santos F, Ryska A, Leivo I, Kinkor Z, ichal M. Mammary analogue secretory carcinoma of salivary glands, containing the ETV6-NTRK3 fusion gene: a hitherto undescribed salivary gland tumor entity. Am J Surg Pathol 34:599–608. 10.1097/PAS.0b013e3181d9efcc

36. Hudson JB, Collins BT. MYB Gene Abnormalities t(6;9) in Adenoid Cystic Carcinoma Fine-Needle Aspiration Biopsy Using Fluorescence In Situ Hybridization. Arch Pathol Lab Med 138:403–409. 10.5858/arpa.2012-0736-OA

37. Bass BP, Engel KB, Greytak SR, Moore HM. A Review of Preanalytical Factors Affecting Molecular, Protein, and Morphological Analysis of Formalin-Fixed, Paraffin-Embedded

(FFPE) Tissue. How Well Do You Know Your FFPE Specimen? Arch Pathol Lab Med 138:1520–1530. 10.5858/arpa.2013-0691-RA

38. Hall JS, Taylor J, Valentine HR, Irlam JJ, Eustace A, Hoskin PJ, Miller CJ, West CM. Enhanced stability of microRNA expression facilitates classification of FFPE tumour samples exhibiting near total mRNA degradation. Br J Cancer 107:684–894. 10.1038/bjc.2012.294

39. Xi Y, Nakajima G, Gavin E, Morris CG, Kudo K, Hayashi K, Ju J. Systematic analysis of microRNA expression of RNA extracted from fresh frozen and formalin-fixed paraffin-embedded samples. RNA 13:1668–1674. 10.1261/rna.642907

40. Yu SL, Chen HY, Chang GC et al. MicroRNA Signature Predicts Survival and Relapse in Lung Cancer. Cancer Cell 13:48–57. 10.1016/j.ccr.2007.12.008

41. Spahn M, Kneitz S, Scholz CJ, Stenger N, Rüdiger T, Ströbel P, Riedmiller H, Kneitz B. Expression of microRNA-221 is progressively reduced in aggressive prostate cancer and metastasis and predicts clinical recurrence. Int J Cancer 127:394–403. 10.1002/ijc.24715

42. Schetter AJ, Leung SY, Sohn JJ, Zanetti KA, Bowman ED, Yanaihara N, Yuen ST, Chan TL, Kwong DL, Au GK, Liu CG, Calin GA, Croce CM, Harris CC. MicroRNA expression profiles associated with prognosis and therapeutic outcome in colon adenocarcinoma. JAMA 299:425–436. 10.1001/jama.299.4.425

43. Pérez-Rivas LG, Jerez JM, Carmona R, de Luque V, Vicioso L, Claros MG, Viguera E, Pajares B, Sánchez , Ribelles N, Alba E, Lozano J. A microRNA Signature Associated with Early Recurrence in Breast Cancer. PLoS One 14:e91884. 10.1371/journal.pone.0091884

44. Amit M, Binenbaum Y, Trejo–Leider L, Sharma K, Ramer N, Ramer I, Agbetoba A, Miles B, Xang X, Lei D, Bjørndal K, Godballe C, Mücke T, Wolff KD, Eckardt AM, Copelli C,

23

62

Sesenna E, Palmer F, Ganly I, Patel S, Gil Z. International collaborative validation of intraneural invasion as a prognostic marker in adenoid cystic carcinoma of the head and neck. Head Neck 37:1038–1045. 10.1002/hed.23710

45. Barrett AW, Speight PM. Perineural invasion in adenoid cystic carcinoma of the salivary glands: A valid prognostic indicator? Oral Oncol 45:936–940. 10.1016/j.oraloncology.2009.07.001

46. Ma W, Kang Y, Ning L, Tan J, Wang H, Ying Y. Identification of microRNAs involved in gefitinib resistance of non-small-cell lung cancer through the insulin-like growth factor receptor 1 signaling pathway. Exp Ther Med 14:2853–2862. 10.3892/etm.2017.4847

47. Andersson MK, Afshari MK, Andre Y, Wick MJ, Stenman G. Targeting the Oncogenic Transcriptional Regulator MYB in Adenoid Cystic Carcinoma by Inhibition of IGF1R/AKT Signaling. J Natl Cancer Inst 10.1093/jnci/djx017

48. Jang JS, Simon VA, Feddersen RM, Rakhshan F, Schultz DA, Zschunke MA, Lingle WL, Kolbert CP, Jen J. Quantitative miRNA Expression Analysis Using Fluidigm Microfluidics Dynamic Arrays. BMC Genomics 12:144. 10.1186/1471-2164-12-144

49. Chen Y, Gelfond JA, McManus LM, Shireman PK. Reproducibility of quantitative RT-PCR array in miRNA expression profiling and comparison with microarray analysis. BMC Genomics. 10:407. 10.1186/1471-2164-10-407

50. Mestdagh P, Feys T, Bernard N, Guenther S, Chen C, Speleman F, Vandesomplete J. High-throughput stem-loop RT-qPCR miRNA expression profiling using minute amounts of input RNA. Nucleic Acids Res 36:e143. 10.1093/nar/gkn725

24

63

Figure legends

Figure 1

Comparison of clinical outcome of patients with adenoid cystic carcinoma in the training cohort and

the validation cohort.

(A) Overall survival and (B) recurrence-free survival was similar in the training and validation

cohorts (log-rank, p=0.11 and 0.17, respectively).

Figure 2

MicroRNA with independent prognostic value in the training cohort and validation cohort of

adenoid cystic carcinoma.

In the training cohort, (A) high expression of hsa-mir-4676 is associated with reduced overall

survival (OS) (p=0.04) and (B) low expression of hsa-miR-1180 is associated with reduced

recurrence-free survival (RFS) (p=0.03). In the validation cohort, high expression of (C) hsa-mir-

21, (D) hsa-mir-181a-2, and (E) hsa-mir-152 is associated with reduced OS (p=0.04, <0.01, and

0.03, respectively) whereas low expression of hsa-miR-374c is associated with reduced RFS

(p=0.01).

Figure 3

Clustering of adenoid cystic carcinoma according to miRNA expression.

(A) Unsupervised hierarchical clustering separated adenoid cystic carcinoma in two separate

clusters, a small group 1 and large group 2. Note that clusters formed irrespective of solid

histological growth pattern and involvement of *MYB, MYBL1*, or either of these genes. One case

placed separately from these groups, a parotid gland tumor in a 14-year-old female with *MYB-NFIB*

fusion. (B) Supervised hierarchical clustering of group 1 and 2 carcinomas identified 1,658

differentially expressed miRNAs. Note that several clusters formed within group 2 especially.

Figure 4

Comparison of overall survival between group 1 and 2.

Comparison of group 1 and 2 did not identify a difference in overall survival (log-rank, p=0.17).

Figure 5

Principal component analysis (PCA) of adenoid cystic carcinoma according to miRNA signature.

PCA demonstrating a complete overlap of adenoid cystic carcinoma in microRNA expression

irrespective of gene status. Note that the non-rearranged carcinomas are similar to those with *MYB*

and *MYBL1* involvement. The *MYB*-rearranged case in the upper left corner is the outlier described

in Figure 2A.

26

Table 1

Baseline clinicopathological characteristics of the training cohort and validation

cohort characterized for prognostic microRNAs.

		Training cohort (*n*=64)		Validation cohort (*n*=120)	
Age at diagnosis	Median (range, years)	55 (14–83)		61 (22–88)	
Follow-up	Median (IQR, months)	92 (117)		71 (85)	
		n	*%*	*n*	*%*
Site	Parotid gland	13	20.3	29	24.2
	Submandibular gland	28	43.7	35	29.2
	Sublingual gland	3	4.7	7	5.8
	Sinonasal tract	9	14.1	16	13.3
	Oral minor salivary glands*	8	12.5	25	20.8
	Other^	3	4.7	8	6.7
Sex	Female	33	51.6	52	43.3
	Male	31	48.4	68	56.7
Stage	I/II	41	64.1	72	60
	III/IV	23	35.9	48	40
	Missing	0	0	0	0
Tumor margins	Free	14	21.9	25	20.8
	Close#/Involved	48	75	92	76.7
	Missing	2	3.1	3	2.5
Histological growth pattern	Solid	7	10.9	24	20
	Tubulocribriform	55	85.9	94	78.3
	Missing	2	3.2	2	1.7
Radiotherapy	Yes	60	93.8	103	85.9
	No	4	6.2	16	13.3
	Missing	0	0	1	0.8
Vascular invasion	Yes	11	17.2	18	15
	No	45	70.3	77	64.2
	Missing	12	18.75	25	20.8
Perineural invasion	Yes	54	84.4	97	80.8
	No	7	10.9	15	12.5
	Missing	3	4.7	8	6.7

IQR= Interquartile range. *Training cohort: three from the palate, three from buccal mucosa, two from oral tongue; validation cohort: eighteen from the palate, seven from buccal mucosa. ^Training cohort: one larynx, two base of tongue; validation cohort: three larynx, five base of tongue. #Close defined as <5mm.

Table 2

Prognostic value of clinicopathological parameters in overall and recurrence-free survival in salivary gland adenoid cystic carcinoma.

	Training cohort (n=64)		Validation cohort (n=120)	
	HR (95% CI)	p-value	HR (95% CI)	p-value
	Overall survival			
Stage: III or IV vs I or II[a]	3.00 (1.37–6.56)	0.006	2.21 (1.32–3.69)	0.002
Tumor margins: Close or involved vs free[a]	1.71 (0.64–4.59)	0.290	1.20 (0.64–2.21)	0.575
Histological growth pattern: Solid vs tubulocribriform[a]	2.42 (0.89–6.54)	0.072	2.61 (1.47–4.63)	0.001
Vascular invasion: No vs yes[a]	0.32 (0.13–0.82)	0.017	0.29 (0.16–0.74)	<0.001
Radiotherapy No vs yes[a]	1.03 (0.24–4.37)	0.970	1.14 (0.57–2.27)	0.718
Perineural invasion No vs yes[a]	0.83 (0.26–5.33)	0.141	0.84 (0.34–4.94)	0.100
	Recurrence-free survival			
Stage: III or IV vs I or II[a]	3.30 (1.45–7.52)	0.005	3.70 (2.05–6.67)	<0.001
Tumor margins: Close or involved vs free[a]	4.87 (1.14–8.60)	0.033	2.33 (1.06–5.13)	0.036
Histological growth pattern: Solid vs tubulocribriform[a]	2.91 (1.05–8.06)	0.040	3.60 (1.99–6.53)	<0.001
Vascular invasion: No vs yes[a]	0.30 (0.11–0.81)	0.020	0.26 (0.17–0.76)	0.001
Radiotherapy No vs yes[a]	1.75 (0.52–5.89)	0.369	1.16 (0.54–2.50)	0.709
Perineural invasion No vs yes[a]	0.72 (0.20–4.71)	0.119	0.65 (0.20–4.34)	0.943

[a]Reference group.

Table 3

Correlation between miRNA expression and overall and recurrence-free survival in salivary gland

adenoid cystic carcinoma as measured with qPCR.

| Overall survival | | | | | | Recurrence-free survival | | | | | |
| Training cohort | | | Validation cohort | | | Training cohort | | | Validation cohort | | |
miRNA	HR (95%CI)	p-value	miRNA	HR (95%CI)	p-value	ID miRNA	HR (95%CI)	p-value	miRNA	HR (95%CI)	p-value
hsa-miR-4676	4.25 (1.06–16.96)	0.04	hsa-mir-21	1.26 (1.01–1.57)	0.04	hsa-mir-1180	0.53 (0.29–0.95)	0.03	hsa-miR-374c	0.64 (0.46–0.90)	0.01
			hsa-mir-181a-2	1.78 (1.21–2.60)	<0.01						
			hsa-mir-152	1.60 (1.05–2.43)	0.03						

Figure 1

Figure 2

Figure 3 Click here to download Figure Fig 3.tif
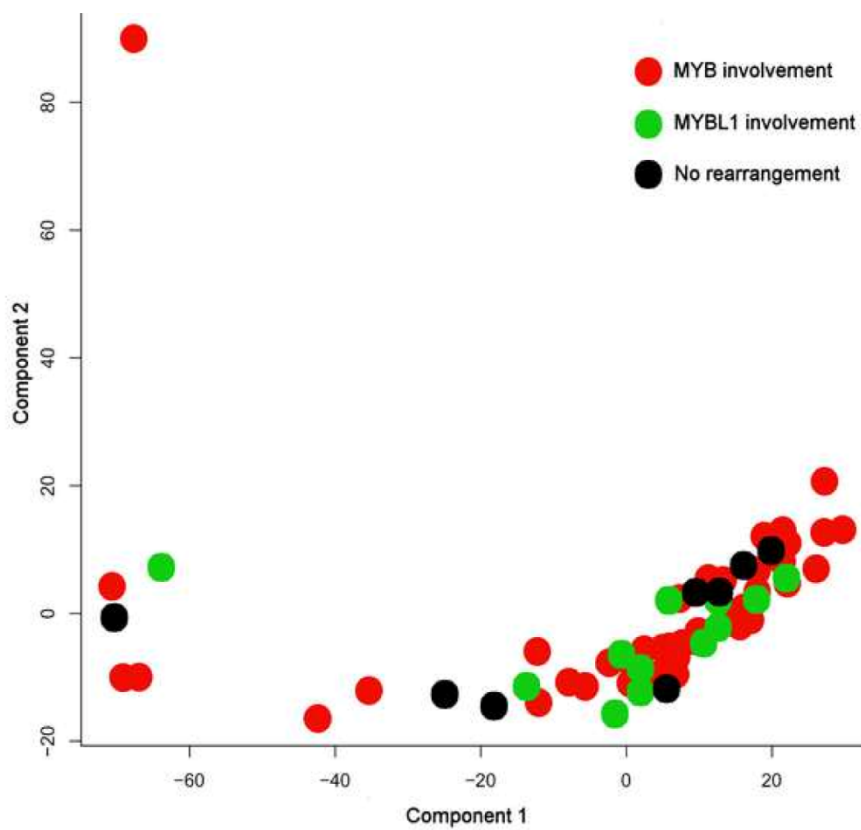
Figure 4

72

Figure 5

73

ORIGINAL ARTICLE

CrossMark

Prognostic significance of 1p36 locus deletion in adenoid cystic carcinoma of the salivary glands

Petr Šteiner [1,2] · Simon Andreasen [3,4] · Petr Grossmann [2] · Lukáš Hauer [5] · Tomáš Vaněček [1,2] · Markéta Miesbauerová [1] · Thalita Santana [6] · Katalin Kiss [7] · David Slouka [8] · Alena Skálová [1]

Abstract

Adenoid cystic carcinoma (AdCC) of the salivary glands is characterized by *MYB-NFIB* or *MYBL1-NFIB* fusion, prolonged but relentlessly progressive clinical course with frequent recurrences, and development of distant metastasis resulting in high long-term mortality. Currently, no effective therapy is available for patients with advanced non-resectable and/or metastatic disease. Complicating the clinical management of this patient group is the lack of prognostic markers. The purpose of this study is to investigate the prognostic value of 1p36 loss in patients with AdCC. The presence of 1p36 deletion and gene fusions involving the *MYB*, *NFIB*, and *MYBL1* genes in a cohort of 93 salivary gland AdCCs was studied using fluorescence in situ hybridization. These results were statistically correlated with clinical data and outcome. Deletion of 1p36 in AdCC was identified in 13 of 85 analyzable cases (15.29%). *MYB-NFIB* fusion was detected in 57/85 (67.1%), *MYBL1-NFIB* fusion in 12/85 (14.1%), *MYB-X* fusion in 4/85 (4.7%), *MYBL1-X* in 4/85 (4.7%), and *NFIB-X* in 2/85 (2.4%) of AdCC cases. None of the 1p36-deleted samples showed *MYBL1* rearrangement. Statistical analysis demonstrated a significant correlation between 1p36 deletion and advanced tumor stage and solid histology ($p = 0.0061$ and 0.0007, respectively). Kaplan-Meier survival curves showed statistically significant correlations between 1p36 deletion and decreased overall survival, disease-specific survival, recurrence-free interval, and recurrence-free survival, all of which were maintained in multivariate analysis. We demonstrate that 1p36 deletion can serve as an indicator of unfavorable outcome of patients with salivary gland AdCC.

Keywords Salivary gland · Adenoid cystic carcinoma · 1p36 locus deletion · *MYB-NFIB* · Prognosis

Introduction

Salivary gland carcinomas are rare and constitute a morphologically heterogeneous group of lesions that are often diagnostically challenging [1]. In recent years, the taxonomy of salivary gland carcinomas has improved dramatically by the discovery of type-specific fusion oncogenes generated by chromosomal translocations [2].

The preliminary results of the study were presented as a poster at USCAP Meeting 2018, Vancouver, Canada.

✉ Petr Šteiner
  steiner@biopticka.cz

1   Department of Pathology, Faculty of Medicine in Plzen, Charles University, Plzen, Czech Republic

2   Bioptic Laboratory, Ltd, Molecular Pathology Laboratory, Mikulášské náměstí 4, 326 00 Plzen, Czech Republic

3   Department of Otorhinolaryngology Head and Neck Surgery and Audiology, Rigshospitalet, Copenhagen University Hospital, Copenhagen, Denmark

4   Department of Otorhinolaryngology and Maxillofacial Surgery, Zealand University Hospital, Køge, Denmark

5   Department of Maxillofacial Surgery, Faculty of Medicine in Plzen, Clinic of Dentistry, Charles University, Plzen, Czech Republic

6   Department of Oral Pathology, Faculty of Dentistry, University of São Paulo, São Paulo, Brazil

7   Department of Pathology, Rigshospitalet, Copenhagen University Hospital, Copenhagen, Denmark

8   Department of Otorhinolaryngology, Faculty of Medicine in Plzen, Charles University, Plzen, Czech Republic

🌀 Springer

Adenoid cystic carcinoma (AdCC) is among the most frequent carcinomas of the salivary gland and sinonasal tract [1]. Following surgical resection, AdCC is characterized by a slow but relentlessly progressive clinical course due to frequent local and distant recurrences and fatal outcome in 40% of patients after 10 years [3]. This ranks AdCC as one of the most-aggressive and least-predictable malignancy among head and neck cancers [4]. Histologically, AdCC is a highly infiltrative and morphologically bland biphasic tumor composed of abluminal myoepithelial and luminal ductal cells arranged in tubular, cribriform, and solid growth patterns. The carcinoma cells tend to have scant cytoplasm and angulated hyperchromatic nuclei. Perineural invasion is almost invariably present [5].

The discovery of the *MYB-NFIB* gene fusion is the most significant advance in understanding the molecular pathology of AdCC [6]. The *MYB-NFIB* fusion is unique for AdCC among salivary gland malignancies and can be detected in up to 86% of cases, making it an important diagnostic tool in histopathologically equivocal cases [7–10]. Recently, a subset of *MYB-NFIB*-negative cases was shown to harbor an alternative *MYBL1-NFIB* gene fusion along with more rare variants including *MYBL1* fusions with *YTHDF3* and *RAD51B* and *NFIB* fusions with *XRCC4*, *NKAIN2*, *PTPRD*, and *AIG1* [11, 12].

Several studies of the mutational landscape in AdCC have shown a heterogeneous repertoire of somatic mutations, with solid variants showing a higher number of copy number alterations, including chromosomal losses involving 1p and 6q [13–21]. The 1p36 locus contains several tumor suppressor genes (e.g., *TP73*, *CHD5*, *SPEN*), and its deletion has been reported in various types of cancer, including breast, cervical, pancreatic, pheochromocytoma, hepatocellular, lung, colorectal, and melanoma [22–28]. In addition, 1p36 deletion has been shown to have prognostic value in patients with oligodendrogliomas, where concurrent deletion of 19q13 predicts for better treatment response [29].

Although deletions including 1p36 has been studied and identified in various proportions of AdCC cases [13–16], only one study has shown some evidence suggesting that 1p36 deletion correlates with poor prognosis [30]. Therefore, the aim of the present study was to investigate the prognostic value of 1p36 deletion in a large cohort of AdCCs.

Materials and methods

Material

The consultation files of the Salivary Gland Tumor Registry, at the Department of Pathology, Faculty of Medicine in Plzen, Biopticka Laborator, Ltd., Plzen, Czech Republic (AS), and Copenhagen University Hospital (KK and SA)

harvested 93 cases of AdCC of major and minor salivary glands, for which complete clinical follow-up data were available. Five cases were excluded from the further analysis because of poor tissue quality and three due to incomplete follow-up.

The histopathological features of all tumors and the immunohistochemical stains, when available, were reviewed by two experienced head and neck pathologists (AS and KK). Sinonasal AdCCs were investigated for HPV in order to exclude HPV-related multiphenotypic carcinoma as previously described [31]. Grading and staging of AdCCs were performed based on criteria published recently by WHO Classification of Head and Neck Tumors [1].

Immunohistochemistry

For conventional microscopy, the excised tissues were fixed in formalin, routinely processed, embedded in paraffin (FFPE), cut, and stained with hematoxylin and eosin. For immunohistochemical studies, 4-μm-thick sections were cut from paraffin blocks and mounted on positively charged slides (TOMO, Matsunami Glass IND, Japan). Sections were processed on a BenchMark ULTRA (Ventana Medical System, Tucson, AZ), deparaffinized, and then subjected to heat-induced epitope retrieval by immersion in a CC1 solution at pH 8.6 at 95 °C.

Primary antibodies used are summarized in Table 1. The bound antibodies were visualized using the ultraView Universal DAB Detection Kit (Roche) and ultraView Universal Alkaline Phosphatase Red Detection Kit (Roche). The slides were counterstained with Mayer's hematoxylin. Appropriate positive and negative controls were employed. Cut-off value for MYB positivity was defined as 5% of positive carcinoma cells.

Fish

Four-micrometer-thick FFPE sections were placed onto positively charged slides. The unstained slides were routinely deparaffinized and incubated in 1× Target Retrieval Solution Citrate at pH 6 (Dako, Glostrup, Denmark) at 95 °C for 40 min and subsequently cooled for 20 min at room temperature in the same solution. Slides were washed in deionized water for 5 min and digested in protease solution with pepsin (0.5 mg/ml, Sigma Aldrich, St. Louis, MO, USA) in 0.01 M HCl at 37 °C for 25 to 60 min, according to the sample conditions. Slides were then placed into deionized water for 5 min, dehydrated in a series of ethanol solution (70, 85, and 96% for 2 min each), and air dried.

For detection of rearrangement of *MYB*, *MYBL1*, and *NFIB*, ZytoLight SPEC *MYB* Dual Color Break Apart Probe (ZytoVision GmbH, Bremerhaven, Germany), custom-designed SureFish *NFIB* Break Apart probe, SureFish

Table 1 Antibodies used for immunohistochemical study

Antibody specificity	Clone	Dilution	Antigen retrieval (time)	Source
S-100 protein	Polyclonal	RTU	CC1 (20 min)	Ventana
CK7	OV-TL 12/30	1:200	CC1 (36 min)	Dako Cytomation
MYB	EP769Y	1:100	CC1 (64 min)	Abcam
Ki-67	30-9	RTU	CC1 (64 min)	Ventana
P63	4A4	RTU	CC1 (64 min)	Ventana
SOX10	Polyclonal	1:100	CC1 (64 min)	Cell Marque

RTU, ready to use (prediluted); CC1, EDTA buffer (pH 8.6)

MYBL1 Break Apart probe, and SureFish *MYB-NFIB* Dual Fusion probe (Agilent Technologies, Santa Clara, California, USA) were used. Chromosomal locations (build Human Genome version 19) used for custom *NFIB* break-apart probe oligos were chr9:13740671-14140560 and chr9:14340306-14740560, for *MYBL1* break-apart probe were chr8:67076230-67474559 and chr8:67526335-68426199, and for custom-designed *MYB-NFIB* dual-fusion probe were chr6:135271234-135771043 and chr9:13990266-14490285. For the detection of 1p36 locus deletion by FISH, Zyto*Light*® SPEC 1p36/1q25 Dual Color Probe (ZytoVision Gmbh) was used. For the SureFish custom designed probe, 0.5 µl of both green and orange probe 0.5 µl of deionized water and 3.5 µl of LSI Buffer (Vysis/Abbott Molecular, IL, USA) were mixed before applying onto specimen. *MYB* Dual Color Break Apart and 1p36/1q25 probes were factory premixed.

Probe was applied onto the specimen, covered with a glass coverslip, and sealed with rubber cement. Slides were incubated in the ThermoBrite instrument (StatSpin/Iris Sample Processing, Westwood, MA, USA) with co-denaturation at 85 °C for 8 min and hybridization at 37 °C for 16 h. Rubber-cemented coverslip was then removed, and the slide was placed in post-hybridization wash solution (2xSSC + 0.3% NP-40) at 72 °C for 2 min. The slides were air dried in the dark, counterstained with 4′,6′-diamidino-2-phenylindole (DAPI; Vysis/Abbott Molecular, IL, USA), coverslipped, and immediately examined. Appropriate positive and negative controls for each FISH probe were employed.

FISH interpretation

The sections were examined with an Olympus BX51 fluorescence microscope (Olympus Corporation, Tokyo, Japan) using a ×100 objective and filter sets triple-band pass (DAPI/SpectrumGreen/SpectrumOrange), dual-band pass (SpectrumGreen/SpectrumOrange), and single-band pass (SpectrumGreen or SpectrumOrange).

A minimum of 100 randomly selected, non-overlapping tumor cell nuclei were evaluated for the presence of yellow, orange, and green fluorescent signals. For break-apart probes, yellow signals were considered negative, whereas separate

orange and green signals were considered positive. For the fusion probe, yellow signals were considered positive, while separate orange and green signals were considered negative. Cut-off values were set to more than 10 and 20% of the nuclei for break-apart and fusion probes, respectively, showing split or break fused signals (mean + 3 standard deviation in normal non-neoplastic control tissues). For 1p36, sample was considered positive when the ratio between orange and green signal sums was equal/bellow 0.7 [32]. Nuclei presenting only one color were excluded from the analysis.

Statistical analysis

Statistical analysis was performed using SW SAS (SAS Institute Inc., Cary, NC, USA). The descriptive statistics such as mean, standard deviation, variance, median, Q1, Q3, minimum, and maximum were calculated for each group and subgroup. Categorical variables were described using frequency tables (age variable cut-off value = 55Y). Box & Whisker plot diagrams and Pie Charts were performed to get a view on the data. Non-parametric tests (Wilcoxon two-sample test or Kruskal-Wallis test) were used for the comparison of differences between investigated parameters. The statistical significance of observed differences in proportions was tested using the χ^2 test and Fisher's exact test when data were sparse. Relations between variables were analyzed using Spearman correlation coefficients.

Overall survival (OS), disease-specific survival (DSS), recurrence-free interval (RFI), and recurrence-free survival (RFS) were estimated using the Kaplan-Meier survival method. Univariate analyses to evaluate differences in survival between investigated groups were performed using the Log-Rank Test and Gehan Wilcoxon Test. The Cox proportional hazard model was used to specify the role of the independent prognostic value of individual parameters (1p36 deletion, age, stage, histological grade, and sex) for OS, DSS, RFI, and RFS. The multivariate analyses were performed using Cox stepwise regression and Cox hazard model "score procedure" (best achieved score of prognostic factor combinations). Level of statistical significance was set to $p = 0.05$.

Table 2 Summary of clinical and follow-up data in 1p36-positive/negative groups, part 1

Variables	Age	Follow-up	Follow-up—DOD1	Recurrence	Recurrence—DOD1
Total					
Min	14	0	0	1	1
Max	85	322	155	182	127
Mean	56.54	92.73	50.33	51.33	28.25
Median	56	77.5	36	32	19
1p36 positive					
Min	44	0	0	7	7
Max	84	192	64	172	38
Mean	63.23	51.83	27.75	47.88	21.67
Median	57	31	17	32	22
1p36 negative					
Min	14	3	4	1	1
Max	85	322	155	182	127
Mean	55.33	99.54	64.23	52.59	32.20
Median	55.1	92	58	32	19

DOD1, died of disease

Results

Clinical characteristics of the study group

From 93 cases, 85 were analyzable with complete follow-up (46 females and 39 males). Age ranged from 14 to 85 years, with mean of 56.54 years. The most frequent site was the submandibular gland (36 cases), followed by parotid gland (17 cases), minor salivary glands of oral cavity (15 cases), sinonasal tract (12 cases), sublingual gland (4 cases), and larynx (1 case). Thirty-five patients (41.18%) had stage 3 or 4 disease.

Follow-up data

Follow-up data was available for all patients and ranged from 2 to 322 months (mean 93 months). Recurrences occurred in 30/85 (35.29%) patients. Interval to recurrence ranged from 1 to 182 months (mean 52 mo).

Eighty patients underwent surgical resection of the primary tumor, in the remaining five cases, one patient underwent surgery after the study closure, two patients had inoperable disease, for two patients the information on surgery was not available. In the resected specimens, 16 patients (18.82%) had clear surgical margin whereas the remaining 64 cases (75.29%) had close/positive margins. Five cases did not have available data on margin status. Seventy-six patients (89.41%) received adjuvant radiotherapy. Thirty patients (35.29%) died during the follow-up period and 21 (24.71%) died of AdCC (Tables 2 and 3).

Molecular genetic findings

Thirteen of 85 analyzed tumors (15.29%) showed 1p36 loss (Fig. 1; Tables 2 and 3). Sixty of 85 analyzable tumors (70.59%) had were positive for break in *MYB* gene (Fig. 2a), 69/85 (81.18%) for *NFIB* gene break, 57/79 (72.15%) for the

Table 3 Summary of clinical and follow-up data in 1p36-positive/negative groups, part 2

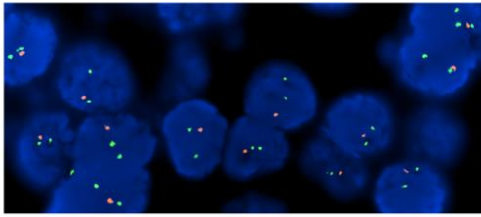|	Stage 3 or 4	Clear Margins	Received radiotherapy	Death	DOD1
Total	35	16	76	30	21
Number of 1p36 positive	10	1	11	9	8
Number of 1p36 negative	25	15	65	21	13
Uninformative results	0	5	3	0	55
Uninformative in 1p36-positive group	0	2	1	0	4
Uninformative in 1p36-negative group	0	3	2	0	51

DOD1, died of disease

Fig. 1 Pictures showing example of FISH analysis of 1p36 locus deletion. Positivity of 1p36 locus deletion is represented by loss of one locus-specific (orange) signal with two control (green) signals

MYB-NFIB dual fusion (Fig. 2b) and 16/28 (57.14%) for *MYBL1* gene break (Tables 4 and 5).

Histological findings

All cases showed the histological hallmarks of AdCC (Fig. 3). AdCC is typically composed of all growth patterns in variable proportions and is graded based on the extent of any solid growth component; more than 30% of solid component constitutes grade 3 [33, 34]. In the present series, 27/85 cases (31.76%) were mostly solid and represented grade 3 AdCC, 40/85 cases (47.06%) had a predominantly cribriform pattern (grade 2), and 18/85 cases (21.18%) were predominantly tubular (grade 1).

Among the 13 cases that showed 1p36 deletion, 9 (69.23%) were classified as grade 3, while 4 (30.77%) were grade 1.

Immunohistochemical findings

All examined AdCCs were strongly and diffusely positive for CK7 in both the ductal and the modified myoepithelial cells. Staining for S100 protein and SOX10 showed variable, patchy positivity. The outer myoepithelial cells were decorated by p63 immunoexpression. Proliferative activity was generally low to moderate, with a mean MIB1 index of 25% (range 5–60%).

Table 4 Results of FISH testing of adenoid cystic carcinomas

Used FISH probe	Positive/all tested	Positive in percent (%)
MYB ba	60/85	70.59
NFIB ba	69/85	81.18
MYB-NFIB DF	57/79	72.15
MYBL1 ba	16/28	57.14
1p36/1q25	13/85	15.29

ba, break apart; DF, dual fusion

MYB immunohistochemical staining was performed on all cases, of which 45 cases (51.14%) were positive. Most cases exhibited focal nuclear MYB expression in tumor cells, predominantly in abluminal myoepithelial cells. Only six cases showed diffuse nuclear expression in 70–90% of tumor cells, including abluminal and luminal cells. Forty-three cases (48.86%) were negative for MYB.

Survival analysis

Using univariate analysis, 1p36 deletion was significantly associated with tumor stage 3/4 (p value = 0.0061) and histological grade 3 (p value = 0.0007) and negatively correlated with *MYBL1* break (p value = 0.0349) as no 1p36-deleted sample had *MYBL1* break. Break of *MYBL1* was associated with tumor stage 1/2 (p value = 0.0219) and *MYB-NFIB* dual-fusion with grade 2 (p value = 0.0280). Immunohistochemical MYB expression correlated with 1p36 deletion (p value = 0.0141), clear surgical margins (p value = 0.0482) and grade 2 (p value = 0.0238). All cases that showed *MYBL1* break (16/85) were negative for MYB IHC (p value < 0.0001).

Kaplan-Meier analysis identified decreased overall survival, disease-specific survival, recurrence-free interval, and recurrence-free survival with higher age, tumor stage (stage 3 or 4), grade 3, solid component, and 1p36 deletion (Fig. 4). Decreased OS and DSS correlated with *MYB* break. Decreased DSS correlated with MYB immunohistochemical positivity (p value = 0.0238). Lower RFI value correlated with

Fig. 2 Pictures showing examples of (MYB) break apart (BA) probes and (MYB-NFIB) dual-fusion (DF) probes. Positive BA probe is represented by one orange-yellow-green complex signal from normal allele and one separated orange and one green signal from allele with break (**a**). Positive DF probe is represented by one separated orange and one green signal from normal alleles and one or two orange-yellow-green fused signals (**b**)
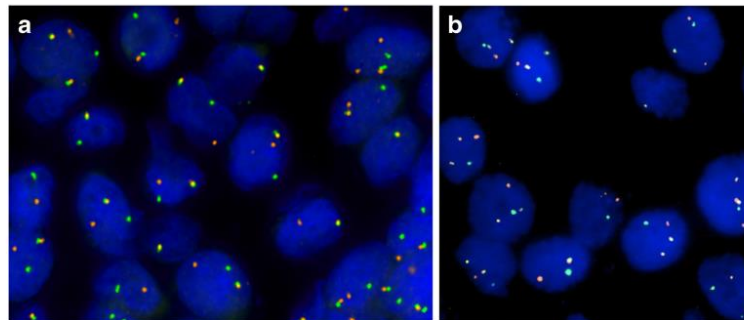
78

Table 5 Predicted fusion based on FISH testing results

Predicted fusion	Frequency	Predicted fusion	Frequency
MYB-NFIB	57 (67.06%)	NFIB-X	2 (2.35%)
MYBL1-NFIB	12 (14.12%)	Negative	3 (3.53%)
MYB-X	4 (4.71%)	Incomplete results	3 (3.53%)
MYBL1-X	4 (4.71%)	Fusions together	79 (92.94%)

X, unknown fusion partner

closed/involved surgical margins. All data with respective p-values are presented in Table 6.

Multivariate analysis (MA) demonstrated decreased OS with increased age, male sex, higher tumor stage, and 1p36 deletion (p values = 0.0005, 0.0239, 0.0422, and 0.0054, respectively). Decreased DSS and RFI both correlated with higher age, high tumor stage, and 1p36 deletion (p values = 0.0294, 0.0154, and 0.0100 and p value = 0.0037, 0.0123, and 0.0055, respectively). Recurrence-free survival correlated negatively with age, male sex, high tumor stage, and 1p36 deletion (p values < 0.0001, 0.0359, 0.0532, and 0.049, respectively). The results are summarized in Fig. 5.

Univariate statistical analysis did not show significant correlation between 1p36 deletion and age (p value = 0.1866), gender (p value = 0.7636), site of origin (p value = 0.4830), surgical margins (p value = 0.4480), MYB break (p value = 0.0630), NFIB break (p value = 0.6744), and MYB-NFIB dual fusion (p value = 0.6793).

Discussion

The discovery of the t(6;9)(q22-23;p23-24) translocation in AdCC and its characterization by Persson et al. in 2009 was one of the most significant events in understanding of
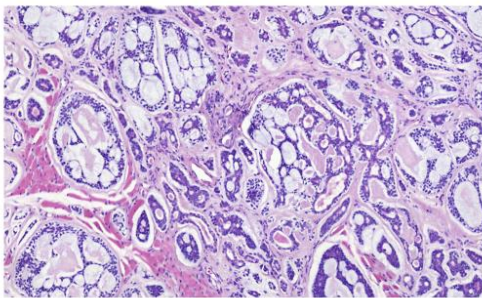

Fig. 3 Adenoid cystic carcinoma is biphasic invasive carcinoma composed of abluminal myoepithelial and luminal ductal cells arranged in tubular, cribriform, and solid growth patterns. The cells tend to have scant cytoplasm and angulated hyperchromatic nuclei. Perineural invasion is a common finding

molecular pathology of AdCC, and is present in AdCC irrespective of site of origin [6, 35–39]. MYB-NFIB drives proliferation in AdCC through activation of downstream targets involved in cell cycle control, DNA replication and repair, and RNA processing [35]. Activation of the transcription factor MYB by gene fusion, mutation, or other mechanisms (e.g., deletion of the 3′ UTR of the MYB gene) has been shown in up to 80% of AdCCs [7–9, 40]. Interestingly, in the MYB-NFIB-negative subset of AdCC, another gene fusion between NFIB and MYBL1, a gene closely related to MYB, was recently described [11, 12].

We identified gene fusions involving MYB, NFIB, and MYBL1 genes in 79/85 (92.94%) of AdCCs. This confirms the fusion of MYB-NFIB, MYBL1-NFIB, and their variants as involved in the vast majority of AdCC, although involvement of NFIB has been reported in other types of salivary gland tumors [41, 42]. Despite their apparently fundamental role in AdCC biology, the value of these gene fusions as prognostic markers has been a topic of debate [9, 11, 43–46]. Herein, we demonstrate the presence of MYB rearrangement to correlate with decreased OS and DSS. Moreover, we provide the evidence that MYBL1 rearrangement correlates with lower stage.

Studies using array comparative genome hybridization has identified various copy number alteration in AdCC, e.g., chromosomal losses involving 1p32-36, 6q, 22q13, and 8p and gains of chromosome 8, 6p, 22q13, and 16p [13–16, 30]. 1p36 locus is non-randomly deleted in various human malignancies, supporting its important role in carcinogenesis [24–26, 28]. Moreover, 1p36 deletion seems to serve as a favorable prognostic factor in oligodendrogliomas [29]. 1p36 locus deletion has been found in various proportions (0–44%) of AdCC by comparative genome hybridization or loss of heterozygosity methods [15, 16, 18, 20, 21, 30, 47]. In our study, we identified heterozygous loss of 1p36 in 13/85 (15.29%) AdCC. This is a relatively low number as compared with results of Rao et al. [30], who found 1p32-36 locus deletions in 23/53 (44%) of cases and correlated the deletion with clinical data. Rao et al. found that deletion of 1p32-36 correlated with reduced OS and solid histology, which we were able to confirm in an even larger cohort. In addition, in our cohort, the 1p36 deletion also correlated with lower DSS, RFI, RFS, high tumor stage, solid histology, and absence of MYBL1 break.

Absence of MYBL1 break in all 1p36-deleted samples was another interesting finding. Hence, as 1p36 deletion correlates with advanced tumor stage and solid histology while MYBL1 rearrangement correlated with low tumor stage, these two genetic alterations in AdCC could be mutually exclusive and indicators of the biological potential of AdCC.

Many genes, including several tumor suppressors, have been identified at the 1p36 locus [23]. Probably the most important gene located in 1p36 region, associated with
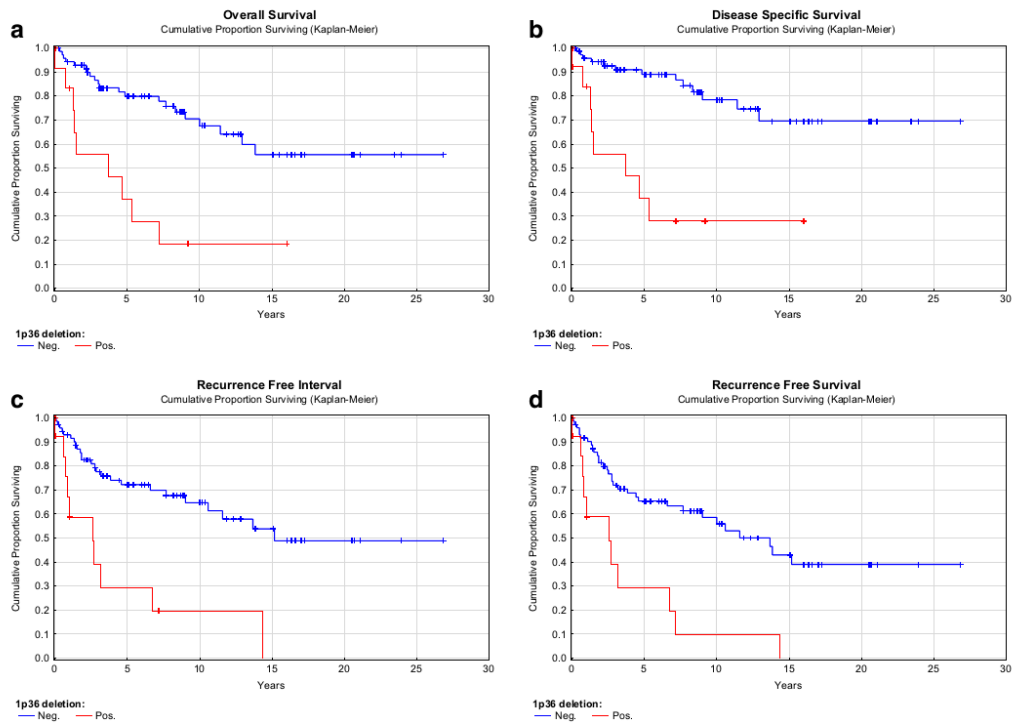
Fig. 4 Graphs representing correlation of 1p36 locus deletion with overall survival (**a**), disease-specific survival (**b**), recurrence-free interval (**c**), and recurrence-free survival (**d**)

Table 6 Kaplan-Meier analysis summarization in our cohort

Variable	OS (*p* value)	DSS (*p* value)	RFI (*p* value)	RFS (*p* value)
Age	Neg. (< 0.0001)	Neg. (0.0082)	Neg. (0.0004)	Neg. (< 0.0001)
Sex	NO (0.1126)	NO (0.3623)	NO (0.4052)	NO (0.1923)
Site	NO (0.0626)	NO (0.3657)	NO (0.4352)	NO (0.2164)
Stage	Neg. (0.0011)	Neg. (0.0002)	Neg. (0.0004)	Neg. (0.0020)
Margins	NO (0.6055)	NO (0.1299)	Neg. (0.0172)	NO (0.1241)
Radiotherapy	NO (0.8774)	NO (0.7891)	NO (0.1849)	NO (0.3516)
Histological grade	Neg. (0.0348)	Neg. (0.0110)	Neg. (0.0101)	Neg. (0.0163)
Solid component	Neg. (0.0215)	Neg. (0.0032)	Neg. (0.0025)	Neg. (0.0067)
MYB IHC	NO (0.1237)	Neg. (0.0238)	NO (0.0903)	NO (0.1487)
MYB ba	Neg. (0.0168)	Neg. (0.0189)	NO (0.0983)	NO (0.0709)
NFIB ba	NO (0.5104)	NO (0.8355)	NO (0.6603)	NO (0.4931)
MYB-NFIB DF	NO (0.3490)	NO (0.1582)	NO (0.2820)	NO (0.4207)
MYBL1 ba	NO (0.3189)	NO (0.3262)	NO (0.8559)	NO (0.8266)
1p36 deletion	Neg. (0.0001)	Neg. (< 0.0001)	Neg. (< 0.0001)	Neg. (0.0001)

OS, overall survival; DSS, disease-specific survival; RFI, recurrence-free interval; RFS, recurrence-free survival; NO, no statistical significant correlation; Neg, decreased survival with higher clinical value
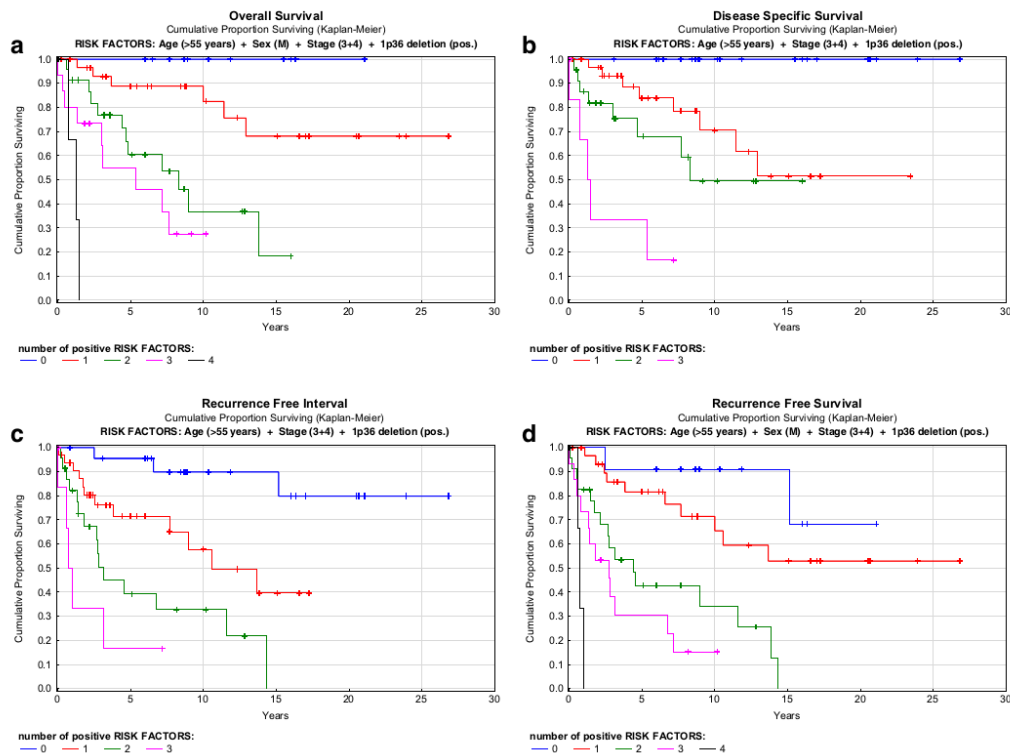
⚫ Springer

80

Fig. 5 Multivariate analysis: overall survival (**a**), disease-specific survival (**b**), recurrence-free interval (**c**), and recurrence-free survival (**d**) with cumulative proportion surviving

AdCC is *SPEN*, whose truncating mutations have been found in 20.8% of analyzed AdCC patients [19]. Interestingly, some evidence suggests that the *SPEN* mutations correlate with solid histology and therefore poor prognosis [19]. *SPEN* functions as a negative regulator of the NOTCH pathway, one of the main signaling pathways to be affected in AdCC [17, 19, 38]. Activation of the NOTCH pathway in AdCCs can also occur through *NOTCH1* gene mutations. These mutations correlate with solid histology, advanced stage, higher propensity to bone and liver metastasis, and significantly decreased OS and RFS [48, 49]. In our study, we found significant correlation of 1p36 deletion with solid histology. Our data support that 1p36 deletion, possibly due to loss of *SPEN*, is involved in especially AdCC with solid histology.

In conclusion, we confirm that 1p36 deletion is an independent predictor of adverse outcome in salivary gland AdCC. Interestingly, 1p36 deletion correlated with advanced tumor stage and solid histology and negatively correlated with

MYBL1 break. To the best of our knowledge, this study represents the largest cohort of AdCC in which 1p36 aberrations are correlated with clinical outcomes. Further molecular characterization of specific aberrations in genes at 1p36 could be useful for better understanding of AdCC and to identify potential therapeutic targets.

Compliance with ethical standards

Study design has been approved by Danish Regional Ethics Committee (H-6-2014-086), the Danish Data Protection Agency (REG-94-2014), and local ethical committee of Charles University, Faculty of Medicine Plzen.

Conflicts of interest The authors declare that they have no conflict of interest.

References

1. Stenman G, Licitra L, Said-Al-Naief N, van Zante A, Yarborough W. Adenoid cystic carcinoma. In: El-Naggar A, Chan J, 2017 Grandis J, Takata T, Slootweg P (eds) World Health Organization classification of tumours. IARC Press, Lyon, 164–165

2. Skálová A, Stenman G, Simpson RHW, Hellquist H, Slouka D, Svoboda T, Bishop JA, Hunt JL, Nibu KI, Rinaldo A, Vander Poorten V, Devaney KO, Steiner P, Ferlito A (2017) The role of molecular testing in the differential diagnosis of salivary gland carcinomas. Am J Surg Pathol. https://doi.org/10.1097/PAS.0000000000000980

3. Bjørndal K, Krogdahl A, Therkildsen MH, Charabi B, Kristensen CA, Andersen E, Schytte S, Primdahl H, Johansen J, Pedersen HB, Andersen LJ, Godballe C (2015) Salivary adenoid cystic carcinoma in Denmark 1990-2005: outcome and independent prognostic factors including the benefit of radiotherapy. Results of the Danish Head and Neck Cancer Group (DAHANCA). Oral Oncol 51:1138–1142. https://doi.org/10.1016/j.oraloncology.2015.10.002

4. Godge P, Sharma S, Yadav M (2012) Adenoid cystic carcinoma of the parotid gland. Contemp Clin Dent 3:223–226. https://doi.org/10.4103/0976-237X.96838

5. Coca-Pelaz A, Rodrigo JP, Bradley PJ, Vander Poorten V, Triantafyllou A, Hunt JL, Strojan P, Rinaldo A, Haigentz M, Takes RP, Mondin V, Teymoortash A, Thompson LD, Ferlito A (2015) Adenoid cystic carcinoma of the head and neck—an update. Oral Oncol 51:652–661. https://doi.org/10.1016/j.oraloncology.2015.04.005

6. Persson M, Andrén Y, Mark J, Horlings HM, Persson F, Stenman G (2009) Recurrent fusion of MYB and NFIB transcription factor genes in carcinomas of the breast and head and neck. Proc Natl Acad Sci U S A 106:18740–18744. https://doi.org/10.1073/pnas.0909114106

7. Brill LB, Kanner WA, Fehr A, Andrén Y, Moskaluk CA, Löning T, Stenman G, Frierson HF (2011) Analysis of MYB expression and MYB-NFIB gene fusions in adenoid cystic carcinoma and other salivary neoplasms. Mod Pathol 24:1169–1176. https://doi.org/10.1038/modpathol.2011.86

8. Mitani Y, Li J, Rao PH, Zhao YJ, Bell D, Lippman SM, Weber RS, Caulin C, El-Naggar AK (2010) Comprehensive analysis of the MYB-NFIB gene fusion in salivary adenoid cystic carcinoma: incidence, variability, and clinicopathologic significance. Clin Cancer Res 16:4722–4731. https://doi.org/10.1158/1078-0432.CCR-10-0463

9. West RB, Kong C, Clarke N, Gilks T, Lipsick JS, Cao H, Kwok S, Montgomery KD, Varma S, Le QT (2011) MYB expression and translocation in adenoid cystic carcinomas and other salivary gland tumors with clinicopathologic correlation. Am J Surg Pathol 35:92–99. https://doi.org/10.1097/PAS.0b013e3182002777

10. Xu B, Drill E, Ho A, Dunn L, Prieto-Granada CN, Chan T, Ganly I, Ghossein R, Katabi N (2017) Predictors of outcome in adenoid cystic carcinoma of salivary glands: a clinicopathologic study with correlation between MYB fusion and protein expression. Am J Surg Pathol 41:1422–1432. https://doi.org/10.1097/PAS.0000000000000918

11. Brayer KJ, Frerich CA, Kang H, Ness SA (2016) Recurrent fusions in MYB and MYBL1 define a common, transcription factor-driven oncogenic pathway in salivary gland adenoid cystic carcinoma. Cancer Discov 6:176–187. https://doi.org/10.1158/2159-8290.CD-15-0859

12. Mitani Y, Liu B, Rao PH, Borra VJ, Zafereo M, Weber RS, Kies M, Lozano G, Futreal PA, Caulin C, El-Naggar AK (2016) Novel MYBL1 gene rearrangements with recurrent MYBL1-NFIB fusions in salivary adenoid cystic carcinomas lacking t(6;9)

13. translocations. Clin Cancer Res 22:725–733. https://doi.org/10.1158/1078-0432.CCR-15-2867-T

14. Bernheim A, Toujani S, Saulnier P, Robert T, Casiraghi O, Validire P, Temam S, Menard P, Dessen P, Fouret P (2008) High-resolution array comparative genomic hybridization analysis of human bronchial and salivary adenoid cystic carcinoma. Lab Invest 88:464–473. https://doi.org/10.1038/labinvest.2008.18

15. Freier K, Flechtenmacher C, Walch A, Ohl S, Devens F, Burke B, Hassfeld S, Lichter P, Joos S, Hofele C (2005) Copy number gains on 22q13 in adenoid cystic carcinoma of the salivary gland revealed by comparative genomic hybridization and tissue microarray analysis. Cancer Genet Cytogenet 159:89–95. https://doi.org/10.1016/j.cancergencyto.2004.09.007

16. Oga A, Uchida K, Nakao M, Kawauchi S, Furuya T, Chochi Y, Ikemoto K, Okada T, Ueyama Y, Sasaki K, Yousefpour F (2011) Loss of 6q or 8p23 is associated with the total number of DNA copy number aberrations in adenoid cystic carcinoma. Oncol Rep 26:1393–1398. https://doi.org/10.3892/or.2011.1446

17. Persson M, Andrén Y, Moskaluk CA, Frierson HF, Cooke SL, Futreal PA, Kling T, Nelander S, Nordkvist A, Persson F, Stenman G (2012) Clinically significant copy number alterations and complex rearrangements of MYB and NFIB in head and neck adenoid cystic carcinoma. Genes Chromosom Cancer 51:805–817. https://doi.org/10.1002/gcc.21965

18. Rettig EM, Talbot CC, Sausen M, Jones S, Bishop JA, Wood LD, Tokheim C, Niknafs N, Karchin R, Fertig EJ, Wheelan SJ, Marchionni L, Considine M, Fakhry C, Papadopoulos N, Kinzler KW, Vogelstein B, Ha PK, Agrawal N (2016) Whole-genome sequencing of salivary gland adenoid cystic carcinoma. Cancer Prev Res (Phila) 9:265–274. https://doi.org/10.1158/1940-6207.CAPR-15-0316

19. Seethala RR, Cieply K, Barnes EL, Dacic S (2011) Progressive genetic alterations of adenoid cystic carcinoma with high-grade transformation. Arch Pathol Lab Med 135:123–130. https://doi.org/10.1043/2010-0048-OAR.1

20. Stephens PJ, Davies HR, Mitani Y, Van Loo P, Shlien A, Tarpey PS, Papaemmanuil E, Cheverton A, Bignell GR, Butler AP, Gamble J, Gamble S, Hardy C, Hinton J, Jia M, Jayakumar A, Jones D, Latimer C, McLaren S, McBride DJ, Menzies A, Mudie L, Maddison M, Raine K, Nik-Zainal S, O'Meara S, Teague JW, Varela I, Wedge DC, Whitmore I, Lippman SM, McDermott U, Stratton MR, Campbell PJ, El-Naggar AK, Futreal PA (2013) Whole exome sequencing of adenoid cystic carcinoma. J Clin Invest 123:2965–2968. https://doi.org/10.1172/JCI67201

21. Tse DT, Finkelstein SD, Benedetto P, Dubovy S, Schiffman J, Feuer WJ (2006) Microdissection genotyping analysis of the effect of intraarterial cytoreductive chemotherapy in the treatment of lacrimal gland adenoid cystic carcinoma. Am J Ophthalmol 141:54–61. https://doi.org/10.1016/j.ajo.2005.09.002

22. Zhang L, Mitani Y, Caulin C, Rao PH, Kies MS, Saintigny P, Zhang N, Weber RS, Lippman SM, El-Naggar AK (2013) Detailed genome-wide SNP analysis of major salivary carcinomas localizes subtype-specific chromosome sites and oncogenes of potential clinical significance. Am J Pathol 182:2048–2057. https://doi.org/10.1016/j.ajpath.2013.02.020

23. Bagchi A, Mills AA (2008) The quest for the 1p36 tumor suppressor. Cancer Res 68:2551–2556. https://doi.org/10.1158/0008-5472.CAN-07-2095

24. Henrich KO, Schwab M, Westermann F (2012) 1p36 tumor suppression—a matter of dosage? Cancer Res 72:6079–6088. https://doi.org/10.1158/0008-5472.CAN-12-2230

25. Koshikawa K, Nomoto S, Yamashita K, Ishigure K, Takeda S, Nakao A (2004) Allelic imbalance at 1p36 in the pathogenesis of human hepatocellular carcinoma. Hepato-Gastroenterology 51:186–191

Springer

82

25. Kuroda N, Toi M, Hiroi M, Shuin T, Enzan H (2003) Review of renal oncocytoma with focus on clinical and pathobiological aspects. Histol Histopathol 18:935–942. https://doi.org/10.14670/HH-18.935

26. Lefeuvre M, Gunduz M, Nagatsuka H, Gunduz E, Al Sheikh Ali M, Beder L, Fukushima K, Yamanaka N, Shimizu K, Nagai N (2009) Fine deletion analysis of 1p36 chromosomal region in oral squamous cell carcinomas. J Oral Pathol Med 38:94–98. https://doi.org/10.1111/j.1600-0714.2008.00666.x

27. Leonard JH, Cook AL, Nancarrow D, Hayward N, Van Gele M, Van Roy N, Speleman F (2000) Deletion mapping on the short arm of chromosome 1 in Merkel cell carcinoma. Cancer Detect Prev 24: 620–627

28. Midorikawa Y, Yamamoto S, Tsuji S, Kamimura N, Ishikawa S, Igarashi H, Makuuchi M, Kokudo N, Sugimura H, Aburatani H (2009) Allelic imbalances and homozygous deletion on 8p23.2 for stepwise progression of hepatocarcinogenesis. Hepatology 49: 513–522. https://doi.org/10.1002/hep.22698

29. van den Bent MJ (2000) Chemotherapy of oligodendroglial tumours: current developments. Forum (Genova) 10:108–118

30. Rao PH, Roberts D, Zhao YJ, Bell D, Harris CP, Weber RS, El-Naggar AK (2008) Deletion of 1p32-p36 is the most frequent genetic change and poor prognostic marker in adenoid cystic carcinoma of the salivary glands. Clin Cancer Res 14:5181–5187. https://doi.org/10.1158/1078-0432.CCR-08-0158

31. Andreasen S, Bishop JA, Hansen TV, Westra WH, Bilde A, von Buchwald C, Kiss K (2017) Human papillomavirus-related carcinoma with adenoid cystic-like features of the sinonasal tract: clinical and morphological characterization of six new cases. Histopathology 70:880–888. https://doi.org/10.1111/his.13162

32. Mohapatra G, Betensky RA, Miller ER, Carey B, Gaumont LD, Engler DA, Louis DN (2006) Glioma test array for use with formalin-fixed, paraffin-embedded tissue: array comparative genomic hybridization correlates with loss of heterozygosity and fluorescence in situ hybridization. J Mol Diagn 8:268–276. https://doi.org/10.2353/jmoldx.2006.050109

33. Perzin KH, Gullane P, Clairmont AC (1978) Adenoid cystic carcinomas arising in salivary-glands - correlation of histologic features and clinical course. Cancer 42:265–282. https://doi.org/10.1002/1097-0142(197807)42:1<265::aid-cncr2820420141>3.0.co;2-z

34. Szanto PA, Luna MA, Tortoledo ME, White RA (1984) Histologic grading of adenoid cystic carcinoma of the salivary glands. Cancer 54:1062–1069

35. Andersson MK, Afshari MK, Andrén Y, Wick MJ, Stenman G (2017) Targeting the oncogenic transcriptional regulator MYB in adenoid cystic carcinoma by inhibition of IGF1R/AKT signaling. J Natl Cancer Inst 109. https://doi.org/10.1093/jnci/djx017

36. Andersson MK, Stenman G (2016) The landscape of gene fusions and somatic mutations in salivary gland neoplasms—implications for diagnosis and therapy. Oral Oncol 57:63–69. https://doi.org/10.1016/j.oraloncology.2016.04.002

37. Andreasen S, Tan Q, Agander TK, Steiner P, Bjørndal K, Høgdall E, Larsen SR, Erentaite D, Olsen CH, Ulhøi BP, von Holstein SL, Wessel I, Heegaard S, Homøe P (2018) Adenoid cystic carcinomas of the salivary gland, lacrimal gland, and breast are morphologically and genetically similar but have distinct microRNA expression profiles. Mod Pathol. https://doi.org/10.1038/s41379-018-0005-y

38. Ho AS, Kannan K, Roy DM, Morris LG, Ganly I, Katabi N, Ramaswami D, Walsh LA, Eng S, Huse JT, Zhang J, Dolgalev I, Huberman K, Heguy A, Viale A, Drobnjak M, Leversha MA, Rice CE, Singh B, Iyer NG, Leemans CR, Bloemena E, Ferris RL, Seethala RR, Gross BE, Liang Y, Sinha R, Peng L, Raphael BJ, Turcan S, Gong Y, Schultz N, Kim S, Chiosea S, Shah JP, Sander C, Lee W, Chan TA (2013) The mutational landscape of adenoid cystic carcinoma. Nat Genet 45:791–798. https://doi.org/10.1038/ng.2643

39. Nordkvist A, Mark J, Gustafsson H, Bang G, Stenman G (1994) Non-random chromosome rearrangements in adenoid cystic carcinoma of the salivary glands. Genes Chromosom Cancer 10:115–121

40. Stenman G (2013) Fusion oncogenes in salivary gland tumors: molecular and clinical consequences. Head Neck Pathol 7(Suppl 1):S12–S19. https://doi.org/10.1007/s12105-013-0462-z

41. Andreasen S, Persson M, Kiss K, Homøe P, Heegaard S, Stenman G (2016) Genomic profiling of a combined large cell neuroendocrine carcinoma of the submandibular gland. Oncol Rep 35:2177–2182. https://doi.org/10.3892/or.2016.4621

42. Geurts JM, Schoenmakers EF, Röijer E, Aström AK, Stenman G, van de Ven WJ (1998) Identification of NFIB as recurrent translocation partner gene of HMGIC in pleomorphic adenomas. Oncogene 16:865–872. https://doi.org/10.1038/sj.onc.1201609

43. Chen TY, Keeney MG, Chintakuntlawar AV, Knutson DL, Kloft-Nelson S, Greipp PT, Garrity JA, Salomao DR, Garcia JJ (2017) Adenoid cystic carcinoma of the lacrimal gland is frequently characterized by MYB rearrangement. Eye (Lond) 31:720–725. https://doi.org/10.1038/eye.2016.307

44. D'Alfonso TM, Mosquera JM, MacDonald TY, Padilla J, Liu YF, Rubin MA, Shin SJ (2014) MYB-NFIB gene fusion in adenoid cystic carcinoma of the breast with special focus paid to the solid variant with basaloid features. Hum Pathol 45:2270–2280. https://doi.org/10.1016/j.humpath.2014.07.013

45. Mitani Y, Rao PH, Futreal PA, Roberts DB, Stephens PJ, Zhao YJ, Zhang L, Mitani M, Weber RS, Lippman SM, Caulin C, El-Naggar AK (2011) Novel chromosomal rearrangements and break points at the t(6;9) in salivary adenoid cystic carcinoma: association with MYB-NFIB chimeric fusion, MYB expression, and clinical outcome. Clin Cancer Res 17:7003–7014. https://doi.org/10.1158/1078-0432.CCR-11-1870

46. Roden AC, Greipp PT, Knutson DL, Kloft-Nelson SM, Jenkins SM, Marks RS, Aubry MC, García JJ (2015) Histopathologic and cytogenetic features of pulmonary adenoid cystic carcinoma. J Thorac Oncol 10:1570–1575. https://doi.org/10.1097/JTO.0000000000000656

47. Costa AF, Altemani A, Vékony H, Bloemena E, Fresno F, Suárez C, Llorente JL, Hermsen M (2010) Genetic profile of adenoid cystic carcinomas (ACC) with high-grade transformation versus solid type. Anal Cell Pathol (Amst) 33:217–228. https://doi.org/10.3233/ACP-CLO-2010-0547

48. Ferrarotto R, Mitani Y, Diao L, Guijarro I, Wang J, Zweidler-McKay P, Bell D, William WN, Glisson BS, Wick MJ, Kapoun AM, Patnaik A, Eckhardt G, Munster P, Faoro L, Dupont J, Lee JJ, Futreal A, El-Naggar AK, Heymach JV (2017) Activating NOTCH1 mutations define a distinct subgroup of patients with adenoid cystic carcinoma who have poor prognosis, propensity to bone and liver metastasis, and potential responsiveness to Notch1 inhibitors. J Clin Oncol 35:352–360. https://doi.org/10.1200/JCO.2016.67.5264

49. Sajed DP, Faquin WC, Carey C, Severson EA, Afrogheh A, Johnson CA, Blacklow SC, Chau NG, Lin DT, Krane JF, Jo VY, Garcia JJ, Sholl LM, Aster JC (2017) Diffuse staining for activated notch1 correlates with notch1 mutation status and is associated with worse outcome in adenoid cystic carcinoma. Am J Surg Pathol 41: 1473–1482. https://doi.org/10.1097/PAS.0000000000000945

AU1

Small Subset of Adenoid Cystic Carcinoma of the Skin Is Associated With Alterations of the *MYBL1* Gene Similar to Their Extracutaneous Counterparts

Liubov Kyrpychova, MD,* Tomas Vanecek, PhD,*† Petr Grossmann, PhD,*† Petr Martinek, PhD,*†
Petr Steiner,*† Ladislav Hadravsky, MD, PhD,‡ Irena E. Belousova, MD, PhD,§
Ksenya V. Shelekhova, MD, PhD,¶‖ Marian Svajdler,*† Pavol Dubinsky, PhD, MHA,**
AU2
Michal Michal, MD,*† and Dmitry V. Kazakov, MD, PhD*†

Abstract: Adenoid cystic carcinoma (ACC) of the skin is a rare malignant neoplasm histologically identical to homonymous tumors in other organs. Cutaneous ACC has been found to harbor *MYB* gene activations, either through *MYB* chromosomal abnormalities or by generation of the *MYB–NFIB* fusion. In salivary gland ACC, in addition to the *MYB* gene, alterations in *MYBL1*, the gene closely related to *MYB*, have been reported. We studied 10 cases of cutaneous ACC (6 women, 4 men; and age range 41–83 years) for alterations in the *MYB*, *NFIB*, and *MYBL1* genes, using FISH and PCR. *MYB* break-apart and *NFIB* break-apart tests were positive in 4 and 5 cases, respectively. *MYB–NFIB* fusions were found in 4 cases. The break of *MYBL1* was found in 2 cases, and in one of them, the *NFIB* break-apart probe was positive, strongly indicating a *MYBL1–NFIB* fusion. In 2 cases, the *MYB* break-apart test was positive, whereas no *MYB–NFIB* was detected, strongly suggesting another fusion partner. It is concluded that *MYBL1* alterations are detected in primary cutaneous ACC but are apparently less common compared with *MYB* and *NFIB* alterations.

Key Words: adenoid cystic carcinoma, skin, adnexal neoplasms, MYB, MYBL1, NFIB

(Am J Dermatopathol 2017;00:1–6)

INTRODUCTION

AU5   Adenoid cystic carcinoma (ACC) of the skin is a rare malignant neoplasm histologically identical to homonymous tumors in other organs, including salivary glands, respiratory

tract, ear, lacrimal gland, ceruminous gland, Bartholin gland, and breast.[1–9] Approximately 60% of the studied cases of cutaneous ACC have been found to harbor *MYB* gene activations, either through *MYB* chromosomal abnormalities or by generation of the *MYB–NFIB* fusion.[10,11] In the latter case, a recurrent t(6, 9) translocation fuses the myeloblastosis (MYB) proto-oncogene on chromosome 6q22-23 to the NFIB gene on chromosome 9p23-24.[12] The *MYB–NFIB* fusion oncogene activates transcription of genes involved in cell cycle control, DNA repair, and apoptosis. The translocation t(6, 9) appears a tumor-type specific because it has been detected in ACC in different organs and anatomical structures, including salivary glands, lacrimal glands, breast, upper respiratory tract, ear, and Bartholin glands.[3,4,8,13,14] In addition to the *MYB* gene, alterations in *MYBL1*, the gene closely related to *MYB*, have been reported in salivary gland ACC.[15–17] Reciprocal *MYB* and *MYBL1* expression was consistently found in ACC.[16] Because we are not aware of any studies on cutaneous ACC studying alterations in *MYBL1*, our main goal was to find out whether this gene is involved in cutaneous ACC.

MATERIAL AND METHODS

Case Selection

    Ten cases of cutaneous ACC with available paraffin blocks were randomly selected from our consultation files. The HE slides were reviewed together with the clinical information to confirm the diagnosis. Clinical data and follow-up information were obtained from the attending clinicians. In all cases, MYB immunostaining (clone EP769Y, diluation 1:100, ABCAM) was performed either at the time of the diagnosis or retrospectively.   AU6

Detection of *MYB–NFIB* Fusions and *MYBL1* Rearrangements by FISH

    Four micrometre thick formalin-fixed paraffin-embedded (FFPE) sections were placed onto positively charged slides. Corresponding HE-stained slides were examined to determine the areas for cell counting. The unstained slides were routinely deparaffinized and incubated in the 1× Target Retrieval Solution Citrate pH 6

(Dako, Glostrup, Denmark) at 95°C/40 minutes and subsequently cooled for 20 minutes at room temperature in the same solution. The slides were washed in deionized water for 5 minutes and digested in a protease solution with Pepsin (0.5 mg/mL) (Sigma Aldrich, St. Louis, MO) in 0.01 M HCl at 37°C/25–60 minutes according to the sample conditions. The slides were then placed into deionized water for 5 minutes, dehydrated in a series of an ethanol solution (70%, 85%, 96% for 2 minutes each), and air-dried.

The *MYB–NFIB* fusions were detected by FISH using one commercial probe, ZytoLight SPEC *MYB* Dual Color Break-Apart Probe (ZytoVision GmbH, Bremerhaven, Germany) and custom-designed SureFish probes, namely a NFIB Break-Apart probe, a MYB–NFIB dual-fusion probe, and a MYBL2 break-apart probe (Agilent Technologies, Santa Clara, CA). Chromosomal regions for the NFIB break-apart probe oligos are chr9:13740671-14140560 and chr9:14340306-14740560, for the MYB–NFIB fusion probe chr6:135271234-135771043 and chr9:13990266-14490285, and for the MYBL1 probe chr8:67076230-67474559 and chr8:67526335-68426199.

AU7

For the SureFish designed probes, 0.5 μL of each probe (each color was delivered in a separated well), 0.5 μL of deionized water, and 3.5 μL of LSI buffer (Vysis/
AU8 Abbott Molecular, IL) were mixed before applying onto the specimen, whereas the *MYB* Dual Color Break-Apart Probe was factory premixed. An appropriate amount of the premixed probe was applied on the specimen, covered with a glass coverslip and sealed with rubber cement. The slides were incubated in the ThermoBrite instrument (StatSpin/Iris Sample Processing, Westwood, MA) with codenaturation at 85°C/8 minutes and hybridization at 37°C/16 hours. The rubber-cemented coverslip was then removed, and the slide was placed in a posthybridization wash solution (2× SSC/0.3% NP-40) at 72°C for 2 minutes. The slide was air-dried in the dark, counterstained with 4′, 6′ -diamidino-2-phenylindole (DAPI) (Vysis/Abbott Molecular), coverslipped, and immediately examined.

FISH Interpretation

The sections were examined with an Olympus BX51 fluorescence microscope (Olympus Corporation, Tokyo, Japan) using a 100× objective and filter sets triple band pass (DAPI/SpectrumGreen/SpectrumOrange), dual band pass (SpectrumGreen/SpectrumOrange), and single band pass (SpectrumGreen or SpectrumOrange). For each probe, 100 randomly selected nonoverlapping tumor cell nuclei were examined for the presence of yellow or green and orange fluorescent signals. Regarding break-apart probes, the yellow signals were considered negative, whereas the

separate orange and green signals were considered positive. Conversely, for the fusion probe, the yellow signals were considered positive, whereas the separate orange and green signals were considered negative. The cut off values were set to more than 10% and 20% of the nuclei (break-apart and fusion probes, respectively) with chromosomal breakpoint/fusion signals (mean + 3 SD in normal non-neoplastic control tissues).

Detection of *MYB–NFIB* Fusions by RT-PCR

RNA from FFPE tissue samples was extracted using   AU9
a QIASymphony RNA Kit (QIAGEN, Hilden, Germany) on the QIASymphony SP instrument (QIAGEN). RNA quantity and quality were measured using a Nanodrop 1000 Spectrophotometer (Thermo Scientific, Waltham, MA) and reverse transcribed using a Transcriptor First Strand cDNA Synthesis Kit (Roche, Basel, Switzerland) according to the manufacturer instructions. RNA integrity was determined by a control PCR comprising 2 μL of cDNA, 12.5 μL of HotStar Taq PCR Master Mix (QIAGEN), 10 pM of each primer, and distilled water up to 25 μL. The primers are showed in Table   T1
1. The amplification program comprised 95°C/14 minutes, then 40 cycles of denaturation at 95°C/1 minute, annealing at 60°C/0.5 minutes, extension at 72°C/1 minute, and final extension at 72°C/7 minutes. Samples with RNA integrity below 133 bp were excluded from further analysis.

For the own fusion detection, 2 μL of cDNA was added to the reaction consisting of 12.5 μL of HotStar Taq PCR Master Mix (QIAGEN), 10 pM of each primer, and distilled water up to 25 μL. The amplification program comprises initial denaturation at 95°C/14 minutes, then 40 cycles of denaturation at 95°C/1 minute, annealing at 55°C/1 minute, and extension at 72°C/1.5 minutes. The program was finished by incubation at 72°C/7 minutes. The primers used for the PCR were described elsewhere.[18]

Successfully amplified PCR products of the *MYB–NFIB* fusion gene were purified, using a Montage PCR Centrifugal Filter Devices (Millipore, Billerica, MA). Then, the PCR products were both sides sequenced using a Big Dye Terminator Sequencing kit (Applied Biosystems, Carlsbad, CA), run on an automated genetic analyzer ABI Prism 3130xl (Applied Biosystems) at a constant voltage of 13.2 kV for 20 minutes and compared with the GenBank sequence.

RESULTS

Clinical Data

There were 6 female and 4 male patients, ranging in age at the diagnosis from 51 to 83 years (mean 68.5 years and median 67 years). Locations included the head (n = 4), thigh (n = 2), back (n = 2), and vulva (n = 2). All patients presented

---

TABLE 1. Primer Sequences With Respective Amplicon Lengths Used for RNA Integrity Testing

Primer Name	Amplicon Length, bp	Forward Primer Sequence	Reverse Primer Sequence
B2M	105	GAAAAAGATGAGTATGCCTG	ATCTTCAAACCTCCATGATG
B2M—133	133	CTCGCGCTACTCTCTCTTTCT	TGTCGGATTGATGAAACCCAG
PGK	247	CAGTTTGGAGCTCCTGGAAG	TGCAAATCCAGGGTGCAGTG

with a solitary neoplasm, varying in size from 5 to 50 mm in largest dimension (mean 18.6 mm). Two patients (case 7 and 9) presented with a recurrent tumor. In case 7, a small ACC had been removed at the same site 2 years earlier, whereas in case 9, the recurrence of vulvar ACC occurred 12 years after initial surgery. One patient (case 3) had been diagnosed with polycythemia 2 years before the occurrence of cutaneous ACC.

In 7 cases, the lesions were surgically removed, whereas in both patients with vulvar neoplasms, a vulvectomy with unilateral lymphadenectomy was performed, and in the remaining patient, surgery was combined with radiation therapy. Follow-up was available for 9 patients. In 7 patients, there was no evidence of disease at 6, 9, 37, 39, 40, 42, and 82 months. Two of them (cases 6, 10) later died, one of an unknown cause and the other patient because of an ovarian carcinoma. The patient (case 9) with the recurrent vulvar neoplasm developed pulmonary metastasis 1 year after the vulvectomy and then she was lost to follow-up. In the remaining patient (case 5), the tumor recurred within the scar 7 years after the initial diagnosis, and a year later, multiple pulmonary, rib, and liver metastases were detected; the patient died (Table 2).

Histopathologic and Immunohistochemical Features

In all but one case, there was a mixture of cribriform, tubular, and solid patterns forming variably shaped nodules in the dermis. In the remaining case, solid areas were lacking. The cribriform and tubular patterns dominated in 5 and 3 neoplasms, respectively, whereas in the remaining 2 cases, the solid pattern prevailed (>50% of the tumor volume). In all cases, both true small bilayered ducts and pseudocysts were recognized. The true ductal structures had small round lumina and were composed of inner epithelial cells with uniform round nuclei an outer layer of basal/myoepithelial cells. The pseudocystic structures were larger than the ducts and contained abundant basophilic mucinous material positive for Alcian blue at pH 2.5 and/or hyalinized PAS-positive eosinophilic material. The solid areas were composed of small basaloid cells with hyperchromatic, slightly angulated nucleus, and scant cytoplasm. Mitotic activity was low. Perineural invasion was seen in 4 cases. The stroma varied from hyalinized and paucicellular to focally fibrotic and myxoid. Of the 10 tumors studied, 5 neoplasms exhibited immunopositivity for MYB (>50% cells) (Fig. 1).

FISH Findings

MYB break-apart and *NFIB* break-apart tests were positive in 4 and 5 cases, respectively (Figs. 2 and 3). *MYB–NFIB* fusions were found in 4 cases (Fig. 4). The break of *MYBL1* was found in 2 cases, and in one of them, the *NFIB* break-apart probe was positive, strongly indicating a *MYBL1–NFIB* fusion (Fig. 5). In 2 cases, the *MYB* break-apart test was

TABLE 2. Main Clinicopathologic and Molecular Biologic Features

Case N	Sex/Age	Location/Size	Predominent Pattern/Perineural Invasion	IHC (MYB)	*MYB* ba	*NFIB* ba
1	F/58	Scalp	Cribriform/no	−	Neg	+
2	M/65	Thigh	Tubular/no	−	Neg	+
3	F/83	Scalp	Tubular/yes	+	Neg	Neg
4	M/51	Back	Cribriform/no	+	+	Neg
5	M/74	Shin	Solid/no	+	NA	NA
6	F/78	Head	Cribroform/yes	−	Neg	+
7	M/62	Face	Cribriform/no	−	Neg	Neg
8	F/69	Vulva	Tubular/yes	+	+	+
9	F/65	Vulva	Cribriform/yes	−	+	+
10	F/80	Sacral	Solid/no	+	+	Neg

Case N	*MYB–NFIB* Fusion	*MYBL1*	*MYB–NFIB* RT-PCR	Treatment	Follow-up
1	+	Neg	NA	Excision	Lost to follow-up
2	Neg	+	Neg	Excision	NED at 37 mo
3	Neg	Neg	NA	Excision	NED at 39 mo
4	Neg	Neg	Neg	Excision	NED at 40 mo
5	NA	Neg	Neg	Excision	Local recurrence in 87 mo, then pulmonary, liver and rib metastases 13 mo later and DOD
6	+	Neg	Neg	Excision	DUC at 82 mo
7	Neg	+	Neg	Excision	NED at 9 mo
8	+	Neg	+	Vulvectomy with lymphadenectomy	NED at 6 mo
9	+	Neg	Neg	Vulvectomy with lymphadenectomy	Pulmonary metastases in 1 y, then lost to follow-up
10	Neg	Neg	Neg	Excision + RT (51GY)	NED at 42 mo, then DUC 2 y later

DOD, death of disease; DUC, death of unknown or unrelated course; NA, not analyzable; NED, no evidence of disease; RT, radiation therapy.
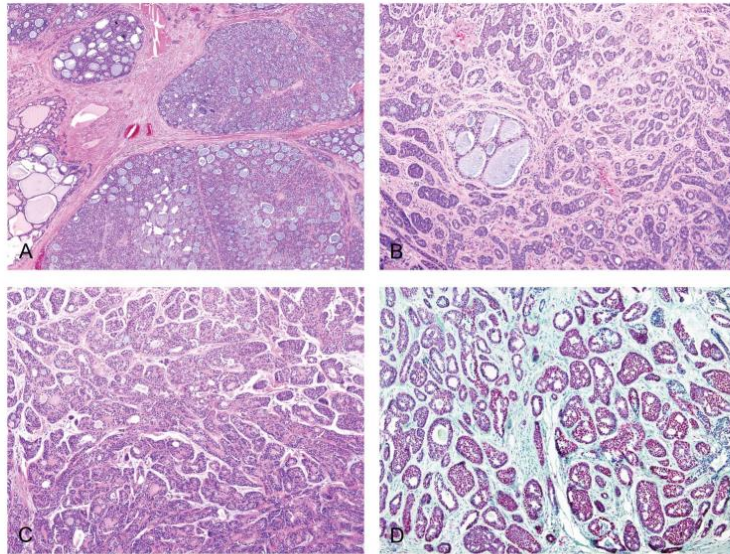
FIGURE 1. Adenoid cystic carcinoma of the skin with a predominant cribriform (A), tubular (B), and solid (C) patterns. Positive immunohistochemical staining for MYB protein (D).

positive, whereas no *MYB–NFIB* was detected, strongly suggesting another fusion partner. In case 3, all 4 FISH tests were negative, and in the remaining case, both *MYB* and *NFIB* break-apart samples were nonanalyzable, as were samples for *MYB–NFIB* fusions.

RT-PCR Findings

Of the 8 cases analyzed, *MYB–NFIB* fusions were detected in one neoplasm.

DISCUSSION

MYB is one of the earliest identified proto-oncogenes discovered as a cellular homologue of the viral oncogene (v-MYB) carried by 2 different avian leukemia retroviruses and plays a vital functional role in the establishment of definitive hematopoiesis. The MYB protein is a founding member of c-MYB transcription factor family that also encompasses MYBL1 (AMYB) and MYBL2 (BMYB) proteins. MYB plays a key role in the control of cell proliferation, survival,
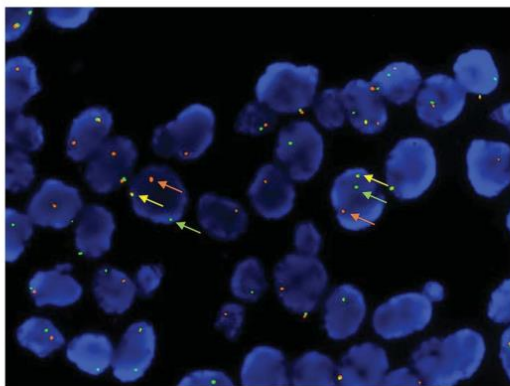

FIGURE 2. Interphase FISH analysis using break-apart probe ZytoLight SPEC *MYB* dual color break-apart probe (6q23.3). Positive nuclei contains separate (split) orange and (or) green signals indicating a rearrangement (break) of one copy of the *MYB* gene region and also one orange-yellow-green fusion signal representing one normal (intact) copy of the homolog *MYB* locus.
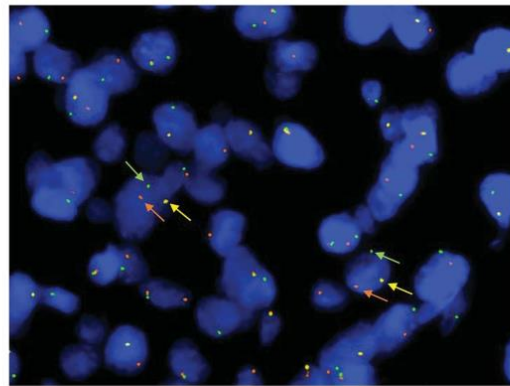

FIGURE 3. Interphase FISH analysis using custom-designed SureFISH *NFIB* break-apart probe (9p22.3). Positive nuclei contains separate (split) orange and (or) green signals indicating a rearrangement (break) of one copy of the *NFIB* gene region and also one orange-yellow-green fusion signal representing one normal (intact) copy of the homolog *NFIB* locus.
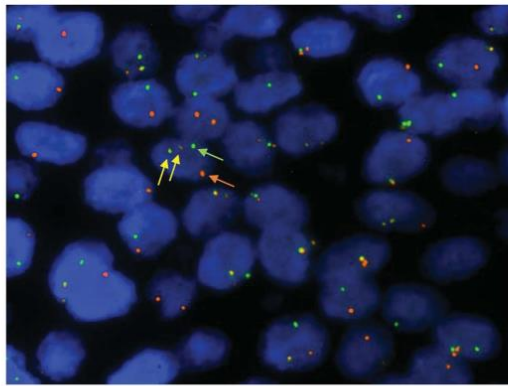
FIGURE 4. Interphase FISH analysis using custom-designed SureFISH *MYB–NFIB* dual fusion probe. Positive nuclei shows orange-yellow-green fusion signals representing reciprocal translocation t(6, 9) (q22-23; p23-24) and also separate orange and green signals showing the normal homolog.

differentiation, and angiogenesis.[19,20] MYB expression has been found a potent driver of some animal and human neoplasms. In humans, MYB overexpression is detected in most myeloid and acute lymphoid leukemia.[19,20] Recent evidence showed that *MYB* alterations are common in ACC, as are changes involving *NFIB*.[1–7] NFIB, located on chromosome 9, is one of the 4 genes comprising the Nuclear Factor One family of transcription factors (NFIA, NFIB, NFIC, and NFIX). NFIB is essential for the development of various organ system, including salivary glands.[21] Involvement of MYB and/or NFIB in ACC in a variety of organs has been well documented, often as MYB–NFIB fusions.[1–7]
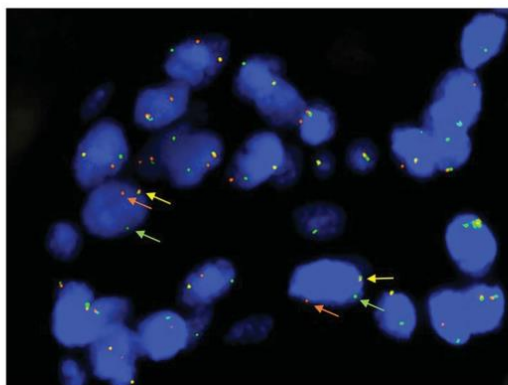

FIGURE 5. Interphase FISH analysis using custom–designed SureFISH MYBL1 (8q13.1) break-apart probe positive nuclei contains separate (split) orange and (or) green signals indicating a rearrangement (break) of one copy of the *MYBL1* gene region and also one orange-yellow-green fusion signal representing one normal (intact) copy of the *MYBL1* locus.

Apart from *MYB–NFIB* gene fusions, alterations involving *MYBL1* have recently been identified in a subset of salivary gland ACC. Mitani et al described a novel *MYBL1–NFIB* gene fusion as a result of t(8, 9) translocation and multiple rearrangements in the *MYBL1* gene in 35% of ACC (12 cases) negative for the t(6, 9). All *MYBL1* alterations involved deletion of the C-terminal negative regulatory domain and were associated with high *MYBL1* expression. The authors also found reciprocal *MYB* and *MYBL1* expression. In addition, the authors identified 2 t(8, 9) negative cases that were characterized by *MYBL1–YTHDF3* fusions. In addition, there were 2 cases negative for t(8, 9) and showing no fusion of *MYBL1* but exhibiting *MYBL1* truncation. Lastly, in one case, a MYBL1–RAD51B fusion was found.[16] A case showing a similar fusion of MYBL1 to an intron of the RAD51B gene on chromosome 14q23-q24.2, leading to antisense transcription of part of the RAD51B intron was found by Brayer et al.[17] The authors showed that the A-MYB protein is truncated, but no part of the RAD51B protein is included in the predicted fusion protein[17] Among 33 of ACC, Drier et al[7] found a case with *MYB* translocation to the *TGFBR3* locus. Among 33 cases of salivary gland ACC studied by Fujii et al,[15] *MYBL1–NFIB* fusions were seen in 2 cases, and in one case, the fusion partner for MYBL1 remained unknown (labeled *MYBL1-X*), as for 4 and 6 cases with *MYB* and *NFIB*, respectively (labeled *MYB-X* and *NFIB-X*). MYBL1–NFIB fusions were also detected by Rettig et al who additionally identified t(6, 9) (q23.3; p22.3) fusions involving MAP3K5-NFIB 5. They also demonstrated that NFIB also recombined with 3 other genes on chromosome 6q, namely RPS6KA2, MYO6, and RIMS1. By contrast, MYB recombined with only one gene other than NFIB.[22]

In our series of cutaneous ACC, *MYB–NFIB* fusions were found in 4 cases. Remarkably, in 2 of these cases (cases 1 and 6), the *MYB* break-apart probe was negative. The discrepancies between break-apart and fusion probes in these cases be explained by several mechanisms including (1) an insertion of an *NFIB* gene segment immediately centromeric to the *MYB* gene outside the target region of the *MYB* break-apart probe, (2) breakpoints distal to the *MYB* gene (both reviewed in detail in Ref. 1), and (3) or by another yet undescribed mechanism. A similar pattern has been found in one of 9 vulvar ACC in a recent study.[8]

The break of *MYBL1* was found in our cohort in 2 cases (cases 2 and 7). In one of them (case 2), the *NFIB* break-apart probe was positive, strongly indicating a *MYBL1–NFIB* fusion, whereas in the second case (case 7), the fusion partner remained unknown.

In 2 cases (cases 4 and 10), the *MYB* break-apart test was positive, whereas no *MYB–NFIB* was detected, strongly suggesting another fusion partner. In one case (case 3), all 4 FISH tests were negative. In the remaining case (case 5), both *MYB* and *NFIB* break-apart samples were nonanalyzable, as were samples for *MYB–NFIB* fusions, whereas the remaining 2 investigations proved negative (Table 2).

Noteworthy is also the discrepancy between the results of FISH and RT-PCR for *MYB–NFIB* fusions. Of the 4 cases (cases 1, 6, 8, 9) where *MYB–NFIB* fusions were detected by FISH, only in one case was the fusion detected by RT-PCR.

Similar findings have previously been reported by North et al. In their series, *MYB–NFIB* fusion transcripts were identified in 2 of the 9 studied cases. All RT-PCR negative cases were immunohistochemically positive for MYB, and 4 showed various *MYB* rearrangements by FISH. The discrepancy can probably be explained by use of FFPE samples with degraded RNA and/or incapability of RT-PCR primes to detect all fusion transcript variants.

In our series, only 5 tumors manifested positivity for MYB (>50% cells), which is lower than previously reported. Among the 5 MYB-negative cases, there were 2 cases with *MYBL1* alterations, which is a likely explanation for the immunonegativity. For the remaining 3 cases, the immunonegative reaction for MYB oncoprotein is unclear. For comparison, in the series of North, 8 of the 9 cases stained for MYB were positive, but the authors used a different antibody.[10] It has recently been shown that MYB labeling by immunohistochemistry is more sensitive and more specific for mammary ACC than *MYB* labeling by FISH.[23] Obviously, this statement cannot be applied to primary ACC of the skin, nonetheless larger more studies are needed.

In conclusion, *MYBL1* alterations are detected in primary cutaneous ACC but are apparently less common compared with *MYB* and *NFIB* alterations. Our study suggests the occurrence of *MYBL1–NFIB* fusions but also existence of another fusion partner.

REFERENCES

1. von Holstein SL, Fehr A, Persson M, et al. Adenoid cystic carcinoma of the lacrimal gland: MYB gene activation, genomic imbalances, and clinical characteristics. *Ophthalmology.* 2013;120:2130–2138.
2. Ho AS, Kannan K, Roy DM, et al. The mutational landscape of adenoid cystic carcinoma. *Nat Genet.* 2013;45:791–798.
3. Persson M, Andren Y, Mark J, et al. Recurrent fusion of MYB and NFIB transcription factor genes in carcinomas of the breast and head and neck. *Proc Natl Acad Sci U S A.* 2009;106:18740–18744.
4. West RB, Kong C, Clarke N, et al. MYB expression and translocation in adenoid cystic carcinomas and other salivary gland tumors with clinicopathologic correlation. *Am J Surg Pathol.* 2011;35:92–99.
5. D'Alfonso TM, Mosquera JM, MacDonald TY, et al. MYB-NFIB gene fusion in adenoid cystic carcinoma of the breast with special focus paid to the solid variant with basaloid features. *Hum Pathol.* 2014;45:2270–2280.
6. Martelotto LG, De Filippo MR, Ng CK, et al. Genomic landscape of adenoid cystic carcinoma of the breast. *J Pathol.* 2015;237:179–189.
7. Drier Y, Cotton MJ, Williamson KE, et al. An oncogenic MYB feedback loop drives alternate cell fates in adenoid cystic carcinoma. *Nat Genet.* 2016;48:265–272.
8. Xing D, Bakhsh S, Melnyk N, et al. Frequent NFIB-associated gene rearrangement in adenoid cystic carcinoma of the vulva. *Int J Gynecol Pathol.* 2017;36:289–293.
9. Ramakrishnan R, Chaudhry IH, Ramdial P, et al. Primary cutaneous adenoid cystic carcinoma: a clinicopathologic and immunohistochemical study of 27 cases. *Am J Surg Pathol.* 2013;37:1603–1611.
10. North JP, McCalmont TH, Fehr A, et al. Detection of MYB alterations and other immunohistochemical markers in primary cutaneous adenoid cystic carcinoma. *Am J Surg Pathol.* 2015;39:1347–1356.
11. Prieto-Granada CN, Zhang L, Antonescu CR, et al. Primary cutaneous adenoid cystic carcinoma with MYB aberrations: report of three cases and comprehensive review of the literature. *J Cutan Pathol.* 2017;44:201–209.
12. Brill LB II, Kanner WA, Fehr A, et al. Analysis of MYB expression and MYB-NFIB gene fusions in adenoid cystic carcinoma and other salivary neoplasms. *Mod Pathol.* 2011;24:1169–1176.
13. Chen TY, Keeney MG, Chintakuntlawar AV, et al. Adenoid cystic carcinoma of the lacrimal gland is frequently characterized by MYB rearrangement. *Eye (Lond).* 2017;31:720–725.
14. Di Palma S, Fehr A, Danford M, et al. Primary sinonasal adenoid cystic carcinoma presenting with skin metastases–genomic profile and expression of the MYB-NFIB fusion biomarker. *Histopathology.* 2014;64:453–455.
15. Fujii K, Murase T, Beppu S, et al. MYB, MYBL1, MYBL2, and NFIB gene alterations and MYC overexpression in salivary gland adenoid cystic carcinoma. *Histopathology.* 2017;71:823–834.
16. Mitani Y, Liu B, Rao PH, et al. Novel MYBL1 gene rearrangements with recurrent MYBL1-NFIB fusions in salivary adenoid cystic carcinomas lacking t(6;9) translocations. *Clin Cancer Res.* 2016;22:725–733.
17. Brayer KJ, Frerich CA, Kang H, et al. Recurrent fusions in MYB and MYBL1 define a common, transcription factor-driven oncogenic pathway in salivary gland adenoid cystic carcinoma. *Cancer Discov.* 2016;6:176–187.
18. Fehr A, Kovacs A, Loning T, et al. The MYB-NFIB gene fusion-a novel genetic link between adenoid cystic carcinoma and dermal cylindroma. *J Pathol.* 2011;224:322–327.
19. Ramsay RG, Gonda TJ. MYB function in normal and cancer cells. *Nat Rev Cancer.* 2008;8:523–534.
20. Drabsch Y, Robert RG, Gonda TJ. MYB suppresses differentiation and apoptosis of human breast cancer cells. *Breast Cancer Res.* 2010;12:R55.
21. Mellas RE, Kim H, Osinski J, et al. NFIB regulates embryonic development of submandibular glands. *J Dent Res.* 2015;94:312–319.
22. Rettig EM, Talbot CC Jr, Sausen M, et al. Whole-genome sequencing of salivary gland adenoid cystic carcinoma. *Cancer Prev Res (Phila).* 2016;9:265–274.
23. Poling JS, Yonescu R, Subhawong AP, et al. MYB labeling by immunohistochemistry is more sensitive and specific for breast adenoid cystic carcinoma than MYB labeling by FISH. *Am J Surg Pathol.* 2017;41:973–979.

　　　　　　　　　　Copyright © 2017 Wolters Kluwer Health, Inc. All rights reserved.

The incidence of MYB gene breaks in adenoid cystic carcinoma of the salivary glands and its prognostic significance

Martin Broz[a], Petr Steiner[b], Richard Salzman[a], Lukas Hauer[c], Ivo Starek[a]

Aims. To detect MYB gene breaks in adenoid cystic carcinoma (ACC) of the salivary glands and its correlation with prognosis and selected clinical parameters

Methods. MYB gene break was detected by FISH assay in 23 adenoid cystic carcinomas using formalin-fixed paraffin-embedded blocks. The Kaplan-Meier survival analysis was used to estimate prognosis.

Results. Fifteen of 23 evaluated tumours were MYB positive and 8 MYB negative. The 10-year cumulative survival, respectively disease free interval, was 60.0%, respectively 59.3%, in MYB positive patients and 88.5%, respectively 80.0%, in MYB negative patients (long rank test, P=0.23). There were no significant differences in age, gender, perineural invasion, the presence of hematogenic or nodal metastases or degree of histopathological grading between MYB positive and MYB negative patients.

Conclusion. A tendency to differences in the survival of patients with ACC, depending on their MYB status. MYB negative patients were predisposed to better prognosis.

[a]Department of Otorhinolaryngology, University Hospital Olomouc and Faculty of Medicine and Dentistry, Palacky University Olomouc, Czech Republic
[b]Bioptic Laboratory Ltd, Molecular Pathology Laboratory, Pilsen and Department of Pathology, Faculty of Medicine in Plzen, Charles University in Prague, Pilsen, Czech Republic
[c]Department of Maxillofacial Surgery, Faculty of Medicine in Pilsen, Charles University in Prague, Pilsen, Czech Republic
Corresponding author: Martin Broz, e-mail: Martin.Broz@fnol.cz

INTRODUCTION

Salivary gland tumours only account for about 1% of all human tumours. However, they represent a very specific cancer group characterized by great histomorphological diversity and variability of biological behavior, even within the same pathological entity, causing difficulties in determining prognosis. The severity of some salivary gland tumours is primarily given by their histopathologic diagnosis which is suggested by their grading (e.g. highly malignant small cell carcinoma vs. low-malignant acinic cell carcinoma). For other tumours (e.g. adenoid cystic carcinoma and mucoepidermoid carcinoma), special criteria were developed to determine their differentiation. For rare tumours without clinical-histopathologic correlations, there are no grading classifications established yet. In individual cases, however, the clinical course of the disease often does not match the specified histopathologic grade of malignancy. Therefore there is a tendency to divide salivary carcinomas into tumours with low- and high-risk rather than into lesions of low and high grade of malignancy. To predict local or regional recurrences of parotid carcinomas only, a score has been developed based solely on clinical data, without regard to histological type of tumour[1].

However, this is complex and time-consuming and thus not used in routine practice.

Adenoid cystic carcinoma (ACC), the second or third most common cancer of major salivary glands and the prevailing malignancy of minor salivary glands[2,3], is a lesion with poorly predictable prognosis. It affects patients of any age, but mostly those in their fifth or sixth decade of life[3]. The poor prognosis results from often very difficult, and sometimes even impossible, resection of the entire tumour. Perineural spread is commonly responsible for difficulties in surgical removal. Incomplete resection frequently leads to a pronounced tendency to local, regional or distant recurrences. Moreover, a chronic course is typical with development of late hematogenic metastases, primarily affecting the lungs, liver or skeleton. These sometimes act indolently and patients often live for long time with confirmed recurrence[4]. In pathomorphological terms, this tumour is characterized by the presence of tubular, cribriform and solid structures. The relative proportion of the latter component has become a basis for the later modified histopathological grading[5,6]. Seethala[7] points out, however, that its prognostic importance has not been clearly demonstrated and clinical stage continues to be the decisive prognostic factor for ACC (as with other cancers of the salivary glands). ACC that have undergone high-grade transformation are characterized by a rapid fatal course[8].

Difficulties in predicting the clinical course of salivary cancers led to intensive search for new prognostic

and predictive molecular markers. This mainly concerns identification of genes, or their products, responsible for the initiation, progression and metastasizing of various types of tumours. In addition, it is expected that their targeted biological blockade could improve the survival in prognostically severe, high-risk salivary tumours.

Genetic abnormalities in salivary tumours

Oncogenic alterations are caused by a variety of mechanisms. One of these is fusion translocation, leading to a generation of new genes. Genetic changes are assumed to be responsible for the development of up to 20% of all human neoplasms[9]. Of the broad histopathological spectrum of salivary tumours, genetic alterations have only been identified in 5 tumours.

Pleomorphic adenoma is initiated by a unique (and therefore important for histopathological differential diagnosis) fusion translocation of genes PLAG1 and HMGA2 (ref.[10]). Cancerization of this tumour is caused by amplification of MDM2, HMGA2-WIF1 and HER2 genes[9]. Translocation of CRTC1 and MAML2 genes is typical for mucoepidermoid carcinoma[11]. It has also prognostic importance, since it has been associated with longer survival time, fewer local recurrences, and a decreased tendency to metastasize[12]. Detection of the fusion genes ETV6 and NTRK3 (ref.[13]) has enabled the identification of mammary analogue secretory carcinoma (MASC) of the salivary glands, which was previously incorrectly diagnosed as biologically more favorable acinic cell carcinoma. Hyalising clear cell carcinoma is characterized by translocation between the ESWR1 and ATF1 genes[14].

Adenoid cystic carcinoma is a salivary tumour in which genetic abnormalities were studied. Jian Fen He[15] and Sasahira[16] found a negative correlation between the expression of the RUNX3 suppressor gene and its prognosis. This tumour, like some other salivary carcinomas, is associated with increased but prognostically irrelevant expression of the c-kit oncoprotein and EGFR (ref.[17-19]).

Recent studies confirm that most ACCs are associated with an alteration of the MYB gene. The MYB gene is located in the g22-q23 region of chromosome 6. Its protein product is a key transcription factor for the physiological regulation of stem cells in the bone marrow and in the intestinal crypts. Deregulation and aberrant function of this gene leads to the development of several malignant diseases. For instance in pediatric acute basophilic and lymphocytic leukemia, MYB-GATA1 translocation[9,20,29] and recurrent chromosomal translocations and duplications in the MYB locus[21] were identified.

The MYB gene alteration (MYB-NFIB translocation) is specific for ACC and has not been found in other salivary tumours or normal salivary glands[22-25]. It is noteworthy that opinions on the prognostic importance of this gene, and its expression, remain inconsistent. While Mitani[25] and West[23] found a significant relationship to the survival and certain clinical parameters, other authors refute these relationships[22]. Therefore, we analyzed the presence of MYB gene breaks using FISH technique and evaluated their prognostic importance.

MATERIALS AND METHODS

Clinical features of patients

In the salivary gland tumour archive at the Šikl's Institute of Pathology in Pilsen, archived materials of 31 patients treated for ACC in the period from 1989 through 2014 were retrieved. Samples where relevant clinical data were not available or those where FISH assay was not interpretable were excluded from study. A total of 23 samples were analyzed.

The group included 9 males and 14 females. The age of the patients ranged from 24 to 84 (mean 55.7±16.1) years. In total, 7 carcinomas were localized in parotid glands, 7 in submandibular glands, 2 in sublingual glands and 7 in minor salivary glands.

At the time of diagnosis, seven patients were at stage T1, 5 at stage T2, 6 at stage T3 and 5 at stage T4. Cervical lymph nodes were involved as follows: stage N1 metastases were found in 3, and stage N2b metastases in two patients. Distant metastases were found in 1 patient. Two tumours were found to be well, 12 cases moderately, and 9 poorly differentiated. Clinical characteristics are shown in Table 1.

Six submandibular and 2 sublingual tumours were completely removed with the glands. Of the 7 parotid tumours, 6 were removed by total, and 1 by conservative parotidectomy. Two tumours of the 7 minor salivary glands were completely removed. In 10, respectively 4, out of 17 patients, the surgery was followed by adjuvant radiation therapy and/or chemoradiotherapy. Three patients were treated by surgery only. Of the remaining 5 patients, 2 were indicated for chemoradiotherapy, one for curative radiotherapy, one for palliative radiotherapy, and one patient received symptomatic treatment only.

The follow up interval ranged from 5.0 to 286.1 (mean 71.4 ± 64.1) months. Of the total 23 patients, 21 achieved complete remission. Sixteen patients were alive at the conclusion of the study. One of them lived with signs of the disease. Six patients died. . The last died from cardiovascular disease.

Detection of MYB break by FISH

Four μm thick section was placed onto positively charged slide. Hematoxylin and eosin stained slides were examined for determination of areas for cell counting. The unstained slide was routinely deparaffinized and incubated in 1x Target Retrieval Solution Citrate pH 6 (Dako, Glostrup, Denmark) for 40 min at 95°C and subsequently cooled for 20 min at room temperature in the same solution. The slide was washed in deionized water for 5 min and digested in protease solution with Pepsin (0.5 mg/mL) (Sigma Aldrich, St. Louis, MO, USA) in 0.01 M HCl at 37 °C for 30 min. The slide was then placed in deionized water for 5 min, dehydrated in a series of ethanol solution (70%, 85%, 96% for 2 min each) and air-dried. Detection of the rearrangement of the MYB gene was performed using ZytoLight® SPEC MYB Dual Color Break Apart Probe (ZytoVision GmbH, Bremerhaven, Germany). An appropriate amount of factory premixed

Table 1. Clinical characteristics of patients with ACC and their MYB status.

Patient	Age	Primary tumour site	Sex	Stage	Grade	OAS	DFI	Death	Recurrence	MYB (FISH)
1.	32	submandibular	m	1	2	33.5	32.2	0	0	1
2.	84	minor	m	4	3	9.1	x	1	0	1
3.	58	minor	f	2	2	97.4	95.4	0	0	1
4.	60	minor	f	1	2	59.8	20.1	0	1	1
5.	48	minor	f	2	3	85.2	80.1	0	0	1
6.	48	submandibular	f	3	2	141.1	42.6	1	1	1
7.	47	submandibular	f	1	3	38.6	31.0	1	1	1
8.	65	sublingual	m	1	2	81.2	79.2	0	0	1
9.	45	parotid	m	3	2	46.7	41.6	0	0	0
10.	79	minor	f	4	2	5.1	x	1	0	1
11.	77	parotid	f	2	3	22.4	21.1	0	0	1
12.	49	submandibular	f	3	2	164.3	163.6	0	0	0
13.	76	sublingual	f	3	3	5.0	3.5	0	0	0
14.	51	minor	m	4	2	87.3	83.7	0	0	0
15.	24	submandibular	m	1	2	286.1	285.8	0	0	1
16.	65	parotid	f	3	1	73.2	70.2	0	0	0
17.	33	submandibular	m	1	2	65.3	65.1	0	0	0
18.	61	submandibular	f	2	3	27.4	26.8	0	0	1
19.	57	minor	m	4	3	23.9	7	1	1	1
20.	54	parotid	f	3	1	66.9	50.1	0	1	0
21.	34	parotid	m	3	2	39.6	36.5	0	0	1
22.	71	parotid	f	4	3	152	79.3	1	1	1
23.	64	parotid	f	1	3	34.8	32.2	1	0	0

x- remission not achieved, DFI - disease free interval, OAS - overall survival.

probe was applied to the specimen, covered with a glass coverslip and sealed with rubber cement. The slide was incubated in the ThermoBrite™ instrument (StatSpin/Iris Sample Processing, Westwood, MA, USA) with co-denaturation parameters 85 °C for 8 min and hybridization parameters 37 °C for 16 h. The rubber cemented coverslip was then removed and the slide was placed in post-hybridization wash solution (2xSSC/0.3% NP-40) at 72 °C for 2 min. The slide was air-dried in the dark, counterstained with 4′,6′-diamidino-2-phenylindole DAPI (Vysis/Abbott Molecular, IL, USA), coverslipped and immediately examined.

The section was examined with an Olympus BX51 fluorescence microscope (Olympus Corporation, Tokyo, Japan) using a 100x objective and filter sets Triple Band Pass (DAPI / SpectrumGreen / SpectrumOrange), Dual Band Pass (SpectrumGreen / SpectrumOrange) and Single Band Pass (SpectrumGreen or SpectrumOrange). One hundred randomly selected nonoverlapping tumour cell nuclei were examined for yellow (normal) or green and orange (chromosomal breakpoint) fluorescent signals (Fig. 1). The cut off value was set to more than 10% of nuclei with chromosomal breakpoint signals (mean + 3 standard deviation in normal non-neoplastic control tissues).

Statistical methods of assessment

Kaplan-Meier survival analysis was performed. Survivors were referred to as "censored". The difference between the overall survival and disease free interval in patients with MYB-positive and MYB-negative tumours was evaluated using the log-rank test. The status of this gene was correlated with age and gender of patients, the presence of nodal or distant metastases, perineural invasion and histopathological grading using the chi square test. The statistical significance was set at $P = 0.05$.

RESULTS

Of the total of 23 examined patients with ACC, MYB gene breaks were identified in 15 (i.e. 65%) of patients.

The study showed no statistically significant differences between MYB positive and MYB negative patients for age, gender, tumour extent, presence of nodal or hematogenic metastases, histopathological grading, perineural invasion ($P > 0.05$, chi square test, see Table 2).

The overall survival ranged from 5.1 to 286.1 (mean 73.5±74.1, median 39.6) months in MYB-positive patients, and from 5.0 to 164.3 (mean 67.9±46.6, median 66.1) in MYB negative patients. The 10-year cumulative overall survival rate was 60.0% for MYB-positive and 88.5% for MYB-negative patients (log rank test, $P = 0.23$, Fig. 2).

The disease free interval ranged from 7.0 to 285.8 (mean 64.4±72.2, median 36.5) months in MYB-positive patients, and from 3.5 to 163.6 (mean 63.7±47.7, median 57.6) in MYB negative patients. The 10-year cumulative overall survival rate was 59.3% for MYB-positive (and 80.0% for MYB-negative patients (log rank test, $P = 0.21$, Fig. 3).

Table 2. Correlation of the MYB status with selected clinical and histopathological parameters of ACC.

	MYB+	MYB –	*P*
Age			
under 50	9	5	0.63
up 50	6	3	
Sex			
males	6	3	0.63
females	9	5	
Primary site			
minor	6	1	0.18
major	9	7	
Stage			
1+2	2	6	0.12
3+4	9	6	
Nodal status			
positive	2	3	0.28
negative	12	6	
Distant spread			
yes	1	0	0.65
no	14	8	
Grade			
I+II	8	6	0.29
III	7	2	
PNI			
yes	3	1	0.60
no	1	1	

PNI - perineural invasion.

Fig. 1. FISH MYB positive reactions in ACC patients.

Fig. 2. The overall survival and MYB status in patients with ACC.

Fig. 3. Disease free interval and MYB status in patients with ACC.

DISCUSSION

In ACC, an alteration of the MYB was first described in 2009 by Persson[26] in 6 patients in whom tumours originated in major and minor salivary glands, lacrimal glands and breast. All these cases involved a translocation of the MYB gene and its fusion with a small portion NFIB gene which is located on chromosome 9 in the p23-p24 region. The author therefore believed that this fusion translocation, which is known to increase the MYB transcription activity of tumour cells[27], is the sole mechanism of ACC.

Other studies[23,24,28], examining MYB-NFIB fusion and the immunohistochemical expression of this fusion gene, demonstrated that the immunohistochemical expression is not always increased. Thus, it is assumed that the MYB gene is also activated by other, not yet completely explained mechanisms[24]. Using the FISH technique, West[23] found abnormal condition of the MYB gene in 16% of cases in his group of patients with ACC. The authors believed a duplication was involved, which was not associated with the NFIB gene. Similar findings were observed in patients with acute T cell lymphocytic leukemia[21]. Another possibility of the MYB gene alteration is the break demonstrated by us, which occurred in 65% of the analyzed samples. Such gene anomaly has not been described to date.

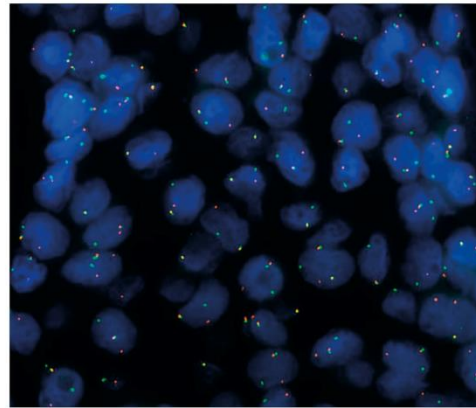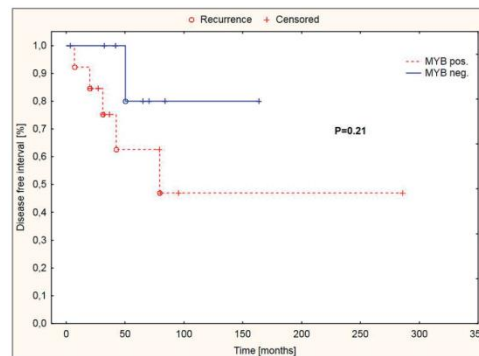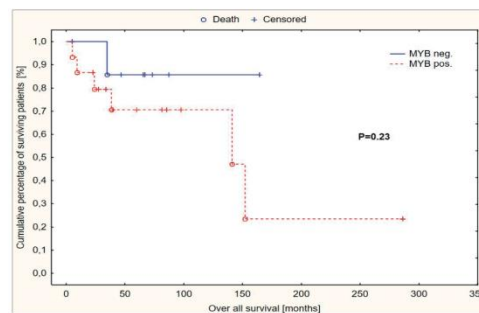Our study suggests the prognostic relevance of the MYB gene break. A tendency to prolonged survival was seen in MYB-negative patients. A larger cohort might provide a statistically significant difference. West[23] and Mitani[24,25] examined the prognostic importance of the MYB-NFIB fusion . In their group of ACC patients, this occurred in 49 % and 28% of the examined samples, respectively. The first author found a lower survival rate

420

93

in patients with this alteration. However, the result did not reach the statistical significance possibly due to small sample. The second author studied the prognostic impact of the presence of the MYB-NFIB fusion translocation in ACC patients in two consecutive trials. The first study involving 72 subjects showed a noticeable, however insignificant difference[24] in OAS between patients with MYB-NFIB positive and negative tumours. Statistical relevance[25] was achieved in the second study involving 103 cases.

Distant metastases were found only in one out of 23 patients. In this patient, we demonstrated break of the MYB gene. On the other hand, 14 patients with this alteration remained free of any evidence of tumour generalization. In the West's group[23], hematogenous metastasis occurred only in two out of 37 patients with ACC. No MYB/NFIB fusion was demonstrated in either of the two above-mentioned patients, but it was present in 24 out of 35 metastasis-free patients.

Nodal metastases were detected in 5 of our patients, of whom 2 were MYB FISH positive. Of the total of 15 patients with this alteration, carcinoma was detected in the nodes only in 2 cases. West's study[23] included 7 patients with nodular involvement, 4 of whom were MYB/NFIB positive. Four out of 18 patients in his cohort had nodal metastases. The results of both studies suggest that neither of these gene alterations is related to the lymphogenic or hematogenous spread of the tumour.

In this study, 3 out of 4 patients with perineural invasion (PNI) were MYB FISH positive. These 3 patients accounted for 20% of the total number of 15 patients with positive MYB gene break. In contrast, West[23] reported on PNI invasion in 15 of 18 patients in his group i.e. 83% of MYB FISH positive patients. Our study, unlike the West's study, suggests a trend to perineural invasion in patients with the reported changes in this gene.

Our study revealed that 6 patients with minor salivary gland tumours were MYB positive. These six patients accounted for 84% of the total 7 tumours originating in minor salivary glands. Similarly in his study, West[23] reported on 17 MYB-NFIB positive out of the total 24 patients with ACC of minor salivary glands.

NFIB is still the only identified partner for the MYB gene. We can therefore assume that the MYB positive patients have NFIB fusion at the same time. However, we cannot rule out that the MYB gene has yet unknown additional fusion partners, which may have a significant prognostic or predictive relevance.

CONCLUSION

The study showed a MYB gene break in 65% of ACC cases. MYB status very likely plays a role in the biological nature of ACC. A tendency to different prognosis (both over all survival and disease free interval) was apparent, unfortunately, without significant possibly due to low figures resulting from scarcity of this pathological entity. The MYB gene appears not to effect traditional prognostic factors such as TNM classification or tumour differen-

tiation. Subsequent studies are required to elucidate its involvement in ACC.

ABBREVIATIONS

ACC, adenoid cystic carcinoma; PNI, perineural invasion.

REFERENCES

1. Vander Poorten VL, Balm AJ, Hilgers FJ, Tan IB, Loftus Coll BM, Keus RB, Hart AA. The development of a prognostic score for patients with parotid carcinoma. Cancer 1999;85(9):2057-67.
2. Milano A, Longo,F, Basile M, Iaffaioli RV, Caponigro, F. Recent advances in the treatment of salivary gland cancers: emphasis on molecular targeted therapy. Oral oncology 2007;43(8):729-34.
3. Gondivkar SM, Gadbail AR, Chole R, Parikh RV. Adenoid cystic carcinoma: a rare clinical entity and literature review. Oral oncol 2011;47(4):231-6.
4. Speight PM, & Barrett AW. Salivary gland tumours. Oral diseases 2002;8(5):229-40.
5. Szanto PA, Luna MA, Tortoledo ME, White RA. Histologic grading of adenoid cystic carcinoma of the salivary glands. Cancer 1984;54(6):1062-9.
6. Spiro RH, Huvos AG. Stage means more than grade in adenoid cystic carcinoma. Am J Surg 1992;164(6):623-8.
7. Seethala R.R. An update on grading of salivary gland carcinomas. Head Neck Pathol 2009;3(1):69-77.
8. Seethala RR, Hunt JL, Baloch ZW, LiVolsi VA, Barnes EL. Adenoid cystic carcinoma with high-grade transformation: a report of 11 cases and a review of the literature. Am J Surg Pathol 2007;31(11):1683-94.
9. Weinreb I. Translocation-associated salivary gland tumours: a review and update. Adv Anat Pathol 2013;20(6):367-77.
10. Geurts JM, Schoenmakers EF, Röijer E, Aström AK, Stenman G, van de Ven WJ. Identification of NFIB as recurrent translocation partner gene of HMGIC in pleomorphic adenomas. Oncogene 1998;16(7):865-72.
11. Behboudi A, Enlund F, Winnes M, Nordkvist A, Leivo I, Flaberg E, Szekely L, Mäkitie A, Grenman R, Mark J, Stenman G. Molecular classification of mucoepidermoid carcinomas-Prognostic significance of the fusion oncogene. Genes Chromosomes Cancer 2006;45(5):470-81.
12. Hellquist H, Skalova A. Histopathology of the salivary glands. In: miscellaneous. Springer 2014; p 430-431.
13. Skálová A, Vanecek T, Sima R, Laco J, Weinreb I, Perez-Ordonez B, Michal, M. Mammary analogue secretory carcinoma of salivary glands, containing the ETV6-NTRK3 fusion gene: a hitherto undescribed salivary gland tumour entity. Am J Surg Pathol 2010;34(5):599-608.
14. Antonescu CR, Zhang L, Chang NE, Pawel BR, Travis W, Katabi N, Fletcher CD. EWSR1-POU5F1 fusion in soft tissue myoepithelial tumours. A molecular analysis of sixty-six cases, including soft tissue, bone, and visceral lesions, showing common involvement of the EWSR1 gene. Genes Chromosomes Cancer 2010;49(12):1114-24.
15. Sasahira T, Kurihara M, Yamamoto K, Bhawal UK, Kirita T,Kuniyasu H. Downregulation of runt-related transcription factor 3 associated with poor prognosis of adenoid cystic and mucoepidermoid carcinomas of the salivary gland. Cancer Sci 2011;102(2):492-7.

16. He JF, Ge MH., Zhu X., Chen C, Tan, Z, Li YN, Gu ZY. Expression of RUNX3 in salivary adenoid cystic carcinoma: implications for tumour progression and prognosis. Cancer Sci 2008; 99(7):1334-40.

17. Stárek I, Kučerová L, Skálová A, Brož M, Bakaj T, Langová K. Imunohistochemická exprese C-kit onkoproteinu u karcinomů slinných žláz (pilotní studie). Otorinolaryngologie a foniatrie 2010;(3):129-35.

18. Stárek I, Kučerová L, Skálová A, Brož M, Bakaj T, Zapletalová A, Hostička L. Imunohistochemická exprese onkoproteinu EGFR a její prognostický význam u karcinomů slinných žláz. Otorinolaryngologie a foniatrie 2011;2:78-84.

19. Lee SK, Kwon MS, Lee YS, Choi, SH, Kim, SY, Cho KJ, Nam, SY. Prognostic value of expression of molecular markers in adenoid cystic cancer of the salivary glands compared with lymph node metastasis: a retrospective study. World J Surg Oncol 2012;10:266.

20. Pattabiraman DR, Gonda TJ. Role and potential for therapeutic targeting of MYB in leukemia. Leukemia 2013;27(2):269-77.

21. Clappier E, Cuccuini W, Kalota A, Crinquette A, Cayuela JM, Dik WA, Soulier J. The C-MYB locus is involved in chromosomal translocation and genomic duplications in human T-cell acute leukemia (T-ALL), the translocation defining a new T-ALL subtype in very young children. Blood 2007;110(4):1251-61.

22. Bell D, Roberts D, Karpowicz M, Hanna EY, Weber RS, El-Naggar AK. Clinical significance of Myb protein and downstream target genes in salivary adenoid cystic carcinoma. Cancer Biol Ther 2011;12(7):569-73.

23. West RB, Kong C, Clarke N, Gilks T, Lipsick J, Cao H, Le,QT. MYB expression and translocation in adenoid cystic carcinomas and other salivary gland tumours with clinicopathologic correlation. Am J Surg Pathol 2011;35(1):92.

24. MitaniY, Li J, Rao PH, ZhaoYJ, Bell D, Lippman SM, El-Naggar AK. Comprehensive analysis of the MYB-NFIB gene fusion in salivary adenoid cystic carcinoma: Incidence, variability, and clinicopathologic significance. Clin Cancer Res 2010;16(19):4722-31.

25. Mitani Y, Rao PH, Futreal PA, Roberts DB, Stephens PJ, Zhao YJ, El-Naggar AK. Novel chromosomal rearrangements and break points at the t (6; 9) in salivary adenoid cystic carcinoma: association with MYB–NFIB chimeric fusion, MYB expression, and clinical outcome. Clin Cancer Res 2011;17(22):7003-14.

26. Persson M, Andrén Y, Mark J, Horlings, HM, Persson F, Stenman,G. Recurrent fusion of MYB and NFIB transcription factor genes in carcinomas of the breast and head and neck. Proceedings of the National Academy of Sciences 2009;106(44):18740-4.

27. Moskaluk CA. Adenoid cystic carcinoma: clinical and molecular features. Head Neck Pathol 2013;7(1):17-22.

28. Brill LB, Kanner WA, Fehr A, Andrén Y, Moskaluk, CA, Löning, T, Frierson HF. Analysis of MYB expression and MYB-NFIB gene fusions in adenoid cystic carcinoma and other salivary neoplazma. Mod Pathol 2011;24(9):1169-76.

29. Belloni E, Shing D, Tapinassi C, Viale A, Mancuso P, Malazzi O, Pelicci PG. In vivo expression of an aberrant MYB-GATA1 fusion induces leukemia in the presence of GATA1 reduced levels. Leukemia 2011;25(4):733.

95

2. část - Sekreční karcinom mamárního typu (MASC)

Nově popsaný sekreční karcinom slinných žláz mamárního typu (mammary analogue secretory carcinoma - MASC) byl definován na základě detekce translokace t(12;15)(p13;q25), která vede ke vzniku fúzního genu *ETV6-NTRK3* [3]. Identický fúzní transkript *ETV6-NTRK3* byl sice již dávno před objevem MASC identifikován v řadě mesenchymálních [47-51], hematologických [52] a epiteliálních malignit [4, 53], ale v onkologii slinných žláz je specifický pro MASC a nebyl nalezen v žádné jiné nádorové jednotce slinných žláz.

V přiložené studii „*Mammary analogue secretory carcinoma of salivary glands: a new entity associated with ETV6 gene rearrangement*" [26] bylo zrevidováno 183 primárních karcinomů velkých a malých slinných žláz pro výskyt histologických a imunohistochemických znaků typických pro MASC. V retrospektivním souboru salivárních karcinomů bylo identifikováno 7 (3,83 %) případů, které splňovaly kritéria MASC. Následně bylo těchto 7 vzorků testováno metodou FISH na průkaz zlomu genu *ETV6* a metodou RT-PCR na průkaz fúzního transkriptu *ETV6-NTRK3*. Tyto nádory byly původně hodnoceny jako adenokarcinom/cystadenokarcinom (3 případy), acinický karcinom (2 případy), a mukoepidermoidní a salivární duktální karcinom (každý v jednom případě).

Imunohistochemicky všechny MASC vykazovaly expresi CK7, CK8, S100, mammaglobinu, STAT5a a vimentinu, a byly negativní na p63 a DOG1 protein. Molekulárně-geneticky bylo 6 ze 7 (85,71 %) studovaných případů pozitivních na zlom *ETV6*, sedmý případ byl neanalyzovatelný pro nedostatek materiálu. Fúzní transkript *ETV6-NTRK3* byl detekován u 3 ze 7 (42,86 %) případů.

V retrospektivní studii „*Mammary Analogue Secretory Carcinoma of Salivary Glands: Molecular Analysis of 25 ETV6 Rearranged Tumors With Lack of Detection of Classical ETV6-NTRK3 Fusion Transcript by Standard PCR: Report of 4 Cases Harboring ETV6-X gene fusion*" [27] bylo identifikováno 25 případů MASC se zlomem genu *ETV6* prokázaným pomocí FISH, kde však RT-PCR neprokázala přítomnost fúzního transkriptu *ETV6-NTRK3*. RT-PCR detekující klasické spojení mezi exony 5-15 u *ETV6* a *NTRK3* byla doplněna o citlivější nested RT-PCR, jak pro klasické spojení 5-15, tak i pro atypické spojení exonů 4 a 14 a jejich kombinace. FISH vyšetření bylo doplněno o vyšetření zlomu *NTRK3* genu. Tímto postupem bylo identifikováno 16 případů nesoucích klasickou variantu s *ETV6-NTRK3* fúzí a vzácnou a neznámou variantu MASC s fúzí *ETV6* s neznámým fúzním partnerem. MASC s fúzí *ETV6-X* při korelaci výsledků s dostupnými klinickými údaji vykazovaly agresivnější chování.

Identifikovat fúzního partnera u *ETV6-X* případů se nám podařilo později využitím NGS s Archer DX kitem. Výsledky studie byly publikovány v poslední přiložené práci této části „*Molecular profiling of mammary analogue secretory carcinoma revealed a subset of tumors harboring a novel ETV6-RET translocation: report of 10 cases*" [9]. V této studii byla celkem v 10 případech MASC nalezena nová fúze *ETV6-RET* a následně potvrzena metodami RT-PCR se specifickými primery a FISH pro identifikaci zlomu *RET* a fúze *ETV6-RET*. Správná identifikace *ETV6-RET* nebo *ETV6-NTRK3* fúze u MASC je potenciálně důležitá pro možnou biologickou léčbu pacientů s recidivujícími nebo metastazujícími nádory, protože pacienti pozitivní na *ETV6-RET* by mohli profitovat z jiné cílené léčby (RXDX105 a LOXO292) [20, 21, 54, 55] než pacienti s *ETV6-NTRK3* (entrectinib) [22, 56].

V poslední práci této části, „*Mammary analogue secretory carcinoma of the sinonasal tract*" [30] jako první popisujeme dva případy MASC vznikající v nosní sliznici. Diagnóza MASC byla potvrzena průkazem *ETV6-NTRK3* translokace pomocí FISH i RT-PCR v obou případech.

ORIGINAL ARTICLE

Mammary analogue secretory carcinoma of salivary glands: a new entity associated with *ETV6* gene rearrangement

**Hanna Majewska · Alena Skálová · Dominik Stodulski ·
Adéla Klimková · Petr Steiner · Czesław Stankiewicz ·
Wojciech Biernat**

Abstract Mammary analogue secretory carcinoma (MASC) is a recently described salivary gland tumour that harbours the recurrent *ETV6-NTRK3* translocation. This is the first series of MASC cases identified in the historic cohort of carcinomas of salivary glands with clinical/pathological correlation and follow-up data. We reviewed 183 primary carcinomas of major and minor salivary glands resected at the Medical University of Gdańsk, Poland, between 1992 and 2012. Based on morphology and immunohistochemistry, cases suspicious for MASC were selected, and the diagnosis was confirmed by fluorescence in situ hybridization (FISH) for *ETV6* rearrangement and by RT-PCR for the *ETV6-NTRK3* fusion transcript. Seven carcinomas met the criteria of MASC, as they exhibited a typical appearance with solid/microcystic and papillary architecture and intraluminal secretions, and cells completely devoid of basophilic cytoplasmic zymogen granules indicative of true acinar differentiation. The only paediatric case was an unencapsulated tumour composed of macrocystic structures covered by a mostly single but, focally, double layer of cells with apocrine morphology. In all cases, the neoplastic cells revealed immunoreactivity for S100, mammaglobin, cytokeratin CK7, CK8, STAT5a and vimentin. FISH for *ETV6* gene rearrangement was positive in six out of seven cases, and RT-PCR was positive in three cases. MASC is a new entity of malignant epithelial salivary gland tumours not included in the 2005 WHO Classification of Head and Neck Tumours. There is a growing body of evidence that it is not as rare as was assumed, as is also indicated by our series (3.8 %). In most cases, MASC shares some microscopic features with AciCC, adenocarcinoma/cystadenocarcinoma NOS and low-grade MEC. In rare cases, MASC with high-grade transformation may mimic the morphological appearances of high-grade salivary gland malignancies, such as salivary duct carcinoma.

H. Majewska · W. Biernat
Department of Pathomorphology, Medical University of Gdańsk,
Gdańsk, Poland

A. Skálová
Department of Pathology, Faculty of Medicine in Plzen, Charles
University in Prague, Prague, Czech Republic

D. Stodulski · C. Stankiewicz
Department of Otolaryngology, Medical University of Gdańsk,
Gdańsk, Poland

A. Klimková · P. Steiner
Bioptic Laboratory, Ltd., Molecular Pathology Laboratory, Plzen,
Czech Republic

H. Majewska (✉)
Department of Pathology, Medical University of Gdansk,
ul.Smoluchowskiego, 80-211 Gdańsk, Poland
e-mail: hania.majewska@gumed.edu.pl

Introduction

Mammary analogue secretory carcinoma (MASC) is a new tumour entity described by Skálová et al. in 2010 [26] that harbours the recurrent translocation t(12;15)(p13;q25) resulting in the *ETV6-NTRK3* gene fusion, the same cytogenetic abnormality is described earlier in secretory breast carcinoma [26, 27]. The fusion gene *ETV6-NTRK3* encodes a chimeric tyrosine kinase, which has potential transforming activity and plays a major role in oncogenesis [8]. Conceivably, a small molecular tyrosine kinase inhibitor might be a potential treatment for patients of whom the tumour carries this fusion gene [8]. The resultant fusion protein *ETV6-NTRK3* has transforming activity, not only in epithelial but

 Springer

98

also in mesenchymal and blood cell lineages. Earlier, the *ETV6-NTRK3* translocation has been described in infantile fibrosarcoma [16], congenital mesoblastic nephroma and acute myelogenous leukaemia [8, 16]. *ETV6* is genetically unstable and fuses not only with *NTRK3* but also with other genes such as *ABL1*, *EGFR3*, *PAX5*, *SYK* and *JAK2* in leukaemia, myelodysplastic syndromes and sarcomas [8, 27].

Since the seminal paper of Skálová et al. [26], a number of retrospective studies and case reports have been published. They further characterized the tumour in terms of histopathology and immunohistochemistries [3, 9, 13, 15, 18, 22] as well as cytology [6, 14, 19]. However, the number of large clinicopathological studies with long follow-up data describing the full spectrum of salivary gland tumours that may mimic MASC is very limited. Single studies have re-evaluated historical files of acinic cell carcinomas (AciCC) [13, 18] or other classical mimickers in the light of this newly emerging entity [10]. Only a single study of a historical retrospective cohort of the whole spectrum of salivary gland tumours has been published so far [15].

Histomorphologically, MASC is a distinctive entity [26], and histology in conjunction with an appropriate immunohistochemical profile is sufficient for a diagnosis in most cases. However, several histomorphological features of MASC overlap with those of other salivary gland tumours [24, 26, 29]. AciCC and adenocarcinomas/cystadenocarcinomas NOS are the most frequent MASC mimics, followed by low-grade mucoepidermoid carcinoma [3, 24]. The aim of our study is to describe the morphological and clinical features of MASC in seven patients identified retrospectively from a variety of low- and high-grade malignant epithelial salivary gland tumours.

Materials and methods

We reviewed all the primary carcinomas of major and minor salivary glands (183) resected at the Medical University of Gdańsk (Departments of Otolaryngology and Maxillofacial Surgery) between 1992 and 2012 and reclassified them according to the criteria published by WHO 2005 (HM and AS) [2] based on histomorphology and immunohistochemistry. In cases suspicious for MASC, fluorescence in situ hybridization (FISH) for detection of *ETV6* rearrangement was performed.

The salivary gland tumour material included adenoid cystic carcinoma, (AdCC, *n*=61), mucoepidermoid carcinoma (MEC, *n*=25), carcinoma ex pleomorphic adenoma (CXPA, *n*=24), acinic cell carcinoma (AciCC, *n*=17), adenocarcinoma (*n*=14), salivary duct carcinoma (SDC, *n*=11), polymorphous low-grade adenocarcinoma (PLGA, *n*=7), epithelial-myoepithelial carcinoma (*n*=6), basal cell carcinoma (*n*=4), undifferentiated carcinoma (*n*=3), squamous cell carcinoma (*n*=3), myoepithelial carcinoma (*n*=2), neuroendocrine

carcinoma (*n*=2), papillary cystadenocarcinoma (*n*=2), lymphoepithelial carcinoma (*n*=1) and one case of newly recognized entity of cribriform adenocarcinoma of the tongue and other minor salivary glands (CATS). Based on histomorphology and expression of immunohistochemical markers, seven cases of mammary analogue secretory carcinoma (MASC) were retrieved. The original diagnoses in these cases include AciCC (two cases), adenocarcinoma (two cases), cystadenocarcinoma, MEC and SDC (one case each).

Paraffin blocks and recuts were available for histological and immunohistochemical analysis for all the studied cases. Clinical data and follow-up were obtained from the patients or their physicians (DS, CS).

Immunohistochemical study

For conventional microscopy, resected tissues were cut and stained with haematoxylin and eosin. For immunohistochemistry, 4-μm-thick sections were cut from paraffin blocks, mounted on silanized slides, deparaffinized in xylene and rehydrated in descending grades (100–70 %) of ethanol. Sections were then subjected to heat-induced epitope retrieval by immersion in a 0.01 citrate buffer at pH 6 at 95 °C in a microwave oven (Micromed TTmega) for 20 min. Endogenous peroxidase was blocked by a 5-min treatment with 3 % hydrogen peroxide in absolute methanol. The slides were then stained by immunostainer BenchMark ULTRA (Roche). The primary antibodies employed in the study are listed in Table 1. The bound antibodies were visualized using the Histofine Simple Stain MAX PO (Multi) Universal Immunoperoxidase Polymer, Anti-Mouse and Rabbit (Nichirei Biosciences inc., Tokyo, Japan), and 3-3′-diaminobenzidine (Sigma) as chromogen. The slides were counterstained with Mayer's haematoxylin. Appropriate positive and negative controls were employed.

Table 1 Antibodies used and sources

Antibody	Clone	Dilution	Source
CK7	OV-TL 12/30	1:200	Dako
CK8	35 βH11	RTU	Dako
S-100 protein	Polyclonal	1:2000	Dako
Mammaglobin	304-1A5	RTU	Dako
STAT5	Polyclonal	1:400	Assay designs
P63	4A4	RTU	Ventana
P40	N/A	RTU	Roche
Vimentin	V9	RTU	Dako
DOG1	Polyclonal	RTU	Roche

VENTANA at pH 8 and at 95 °C

RTU ready to use

Molecular genetic study

Detection of the ETV6-NTRK3 fusion transcript by RT-PCR

RNA from all cases of MASCs was extracted using the RecoverAll Total Nucleic Acid Isolation Kit (Ambion, Austin, TX, USA). Synthesis of complementary DNA (cDNA) was performed using the Transcriptor First Strand cDNA Synthesis Kit (RNA input 1 μg) (Roche Diagnostics, Mannheim, Germany). All procedures were performed according to the manufacturer's protocols. Amplification of the 105 and 133 bp product of the two-microglobulin gene and the 247-bp product of the *PGK* gene was used to test the quality of the extracted RNA, as previously described [1, 11, 28].

Detection of 110 bp fragments of *ETV6-NTRK3* fusion transcripts was performed by RT-PCR, as follows [7]. Two microliters of cDNA was added to a reaction mixture containing 12.5 μl of Hot Star Taq PCR Master Mix (QIAgen, Hilden, Germany), 10 pmol of each primer TRKC1059 complementary to *NTRK3* with sequence (5′-CAGTTCTCGCTT CAGCACGATG-3′) and TEL971 complementary to *ETV6* with sequence (5′-ACCACATCATGGTCTCTGTCTCCC-3′) and distilled water up to 25 μl. The amplification program comprised of denaturation at 95 °C for 14 min and 45 cycles of denaturation at 95 °C for 1 min, annealing at 65 °C for 1 min and extension at 72 °C for 1 min. The program was finished by incubation at 72 °C for 7 min.

Successfully amplified PCR products were purified with magnetic beads Agencourt® AMPure® (Agencourt Bioscience Corporation, A Beckman Coulter Company, Beverly, MA, USA). The products were then bi-directionally sequenced using the Big Dye Terminator Sequencing kit (PE/Applied Biosystems, Foster City, CA, USA) purified with magnetic particles Agencourt® CleanSEQ® (Agencourt Bioscience Corporation), all according to the manufacturer's protocol and run on an automated sequencer ABI Prism 3130xl (Applied Biosystems, Foster City, CA, USA) at a constant voltage of 13.2 kV for 11 min.

Detection of ETV6-NTRK3 gene break by FISH

FISH method

For the FISH study, the LSI ETV6 (TEL) Dual Color, Break Apart Rearrangement Probe (VYSIS/Abott, Abott Park, IL) was used. The specimen, a 4-μm-thick FFPE section, was placed onto a positively charged slide. Tissues were deparaffinized in xylene three times for 5 min and then washed twice in 100 % ethanol once in 95 % ethanol and once in deionized water for 5 min. The slides were then heated in the 1× Target Retrieval Solution (pH 6) (DAKO, Glostrup,

Denmark) for 40 min at 95 °C and subsequently cooled for 20 min at room temperature in the same solution. The slides were washed in deionized water for 5 min and covered with the Proteinase K (20 mg/ml) (SERVA, Heidelberg, Germany) for 10 min at room temperature. The slides were then placed into deionized water for 5 min, dehydrated in a series of ethanol solution (70, 85 and 96 % for 2 min each) and air-dried. An appropriate amount of FISH probe was applied onto each specimen, which was then covered with a glass cover slip and sealed with rubber cement. The slides were incubated in the ThermoBrite™ instrument (StatSpin/Iris Sample Processing, Westwood, MA, USA) with co-denaturation parameters at 85 °C for 8 min and hybridization parameters 37 °C for 16 h. The rubber cemented cover slips were then removed, and the slides were placed in a post-hybridization wash solution (2xSSC/0.3 % NP-40) at 72 °C for 2 min. The slides were air-dried in the dark, counterstained with DAPI II (VYSIS/Abbott), cover slipped and immediately examined.

FISH interpretation

Hybridized slides were examined with an Olympus BX51 fluorescence microscope using a ×100 objective and as filter sets triple band pass (DAPI/Spectrum Green/Spectrum Orange), dual band pass (FITC/Texas Red) and single band pass (Spectrum Green or Spectrum Orange) filters. One hundred randomly selected non-overlapping tumour cell nuclei were examined for the presence of yellow (normal) or green and red (chromosomal breakpoint) fluorescent signals. The sample was considered positive if more than 10 % of nuclei showed a breakpoint signal. Molecular genetic analysis (RT-PCR and FISH) was performed in Biopticka Laboratory in Plzen, Czech Republic (AK, PS).

Results

Clinical and follow-up data

The seven patients with MASC concerned two females and five males ranging in age between 17 and 73 years (median 51.4 years). One tumour was located in the hard palate; the other six were in the parotid gland. The duration of symptoms was known for five of seven patients, on the average 16.2 months (range 3–38 months). For four patients, the clinical course was indolent with a non-tender slowly growing mass covered by intact skin (three tumours in the parotid gland) or mucous membrane (one tumour in the palate). The other three patients presented with symptoms suggesting malignancy, such as accelerated growth, pain, skin infiltration, neck lymphadenopathy or ulceration of the skin or a mucous membrane. Four patients presented in early

clinical stage (I or II), and three patients were in stages III and IVa. The clinical features are summarized in Table 2.

Fine needle aspiration biopsy (FNAB) results are summarized in Table 3. In two cases, the tumours were preoperatively diagnosed as benign lesions (cyst and adenoma) and in three cases as malignancy. All patients underwent surgical treatment: partial conservative parotidectomy (PCP, with facial nerve preservation) was performed in five patients and semi-conservative (PSCP, with preservation of some facial nerve branches) in one patient. In one case, partial resection of the hard palate was performed. In two cases, the neck lymph nodes were dissected. In three of seven cases, patients received supplementary radiotherapy due to metastases to the regional lymph nodes and/or positive or uncertain surgical resection margins. One patient was treated by chemotherapy (no. 5).

Four of seven patients (cases 1–4) remained without evidence of disease during 67–120 months follow-up (median 93 months). In one case (no. 7), loco-regional recurrence occurred 48 months after excision of the hard palate tumour. This patient remained disease-free after combined treatment (lateral rhinotomy with neck dissection and radiation therapy) for 31 months. Two patients (cases five and six), who were also described elsewhere [25], died of disease progression 20 and 79 months after diagnosis.

Histopathological and immunohistochemical findings

On low power magnification, MASC displayed three major growth patterns. Firstly, some tumours were well circumscribed and surrounded by a thick, uninterrupted fibrous capsule (cases 1 and 3) with predominating papillary and microcystic structures (Fig. 1a). In the second pattern, the tumour revealed a solid and lobular growth pattern characterized by a multilobular structure divided by hyalinized or fibrous septa with local infiltrative borders, unencapsulated or only partially encapsulated (cases 2 and 5–7). These cases were predominantly composed of microcystic and slightly dilated glandular spaces filled with an eosinophilic homogenous secretory material (Fig. 1b). A minor component was represented by some papillary structures (Fig. 1c). The third pattern in the only paediatric case (no. 4) was macrocystic (Fig. 1d). The tumour appeared unencapsulated and was composed of cystic structures lined mostly by a single and focally a double layer of cells with focal apocrine differentiation (Fig. 1e). The cysts contained abundant protein-like eosinophilic material. The tumour cells revealed abundant pale pink vacuolated and foamy cytoplasm with vesicular, bland-looking nuclei and prominent nucleoli (Fig. 1 f).

In two cases (cases 5 and 6), the tumours were composed of two distinct carcinomatous components (Fig. 2). One component was a conventional MASC composed of uniform neoplastic cells arranged in solid, tubular and microcystic

structures divided by fibrous septa that were partly hyalinized. The tumour cells had typical low-grade morphology with vesicular round to oval nuclei with finely granular chromatin and distinct centrally located nucleoli (Fig. 2a). The other component, sharply delineated from the conventional MASC, was of high grade (HG) and composed of anaplastic cells with abundant cytoplasm and large pleomorphic nuclei. Solid tumour islands revealed areas of large geographical comedo-like necrosis (Fig. 2b). Desmoplastic stroma was indicative of invasion. Tumour cells of the HG component had high mitotic activity and nuclear polymorphism and failed to produce secretory material in contrast to the low-grade component of MASC. Perineural invasion was observed in both cases.

Immunohistochemically, all MASCs showed diffuse and strong staining for CK7, CK8, S100, mammaglobin (secretory material was also positive), STAT5a (signal transducer and activator of transcription 5a) and vimentin (Fig. 2 g, h). Stains for p63 protein and DOG1 were negative in all cases.

Molecular genetic findings

The samples of all seven cases of MASC were analyzed by FISH, and six of seven cases showed ETV6 rearrangement (Fig. 3). In case 1, the cellular material was very limited (cystic tumour with delicate cellular lining) and insufficient for analysis. However, the tumour revealed morphological and immunohistochemical features typical of MASC, and hence, it was finally included in the study. Five AciCC served as negative controls and did not show ETV6 gene rearrangement (data not shown). The positive control, breast secretory carcinoma, demonstrated ETV6 gene rearrangement (data not shown).

In all seven cases of MASC, RT-PCR was performed, and in three cases, as well as in the positive control (breast secretory carcinoma, data not shown), ETV6-NTRK3 fusion transcripts were found (Fig. 3).

Discussion

According to the 2005 WHO Classification of Head and Neck Tumours [2], the group of malignant epithelial salivary gland tumours contains many heterogeneous entities. The histomorphological classification of these tumours is complex, and their clinical behaviour is not completely elucidated, partly because they are so rare. Some entities, such as adenocarcinoma/cystadenocarcinoma NOS, might encompass subtypes still to be discovered by molecular analysis. Careful histomorphological examination of cases that did not entirely fulfil the criteria of one given entity, in conjunction with a typical pattern of expression of immunohistochemical markers, enabled Skálová et al. [26] to define mammary

Table 2 Clinico-pathological features of patients with mammary analogue of secretory carcinoma

	Sex/ age	Localization	Tumour size (cm)	Clinical course	TNM/Stage (2002)	Treatment	Surgical margins/LN metastases	Status/months
1	F/42	Parotid	2.2×1.3	Mild (3 months), asymptomatic cystic mass	T2N0/II	PCP	Negative	NED/96
2	M/63	Parotid	2.3×2.0	Aggressive (12 months) mass with rapid growth, pain, skin infiltration, neck lymphadenopathy	T3N1/III	PCP, MRND RT	Close LN metastases (−)	NED/90
3	F/51	Parotid	2.5×1.2	Mild (24 months) asymptomatic cystic mass	T2N0/II	PCP	Close	NED/67
4	M/17	Parotid	$4 \times 3.5 \times 2.5$	Mild, multinodular tumour	T2N0/II		Negative	NED/120
5	M/73	Parotid	$3 \times 1.5 \times 1.4$	Aggressive, neck lymphadenopathy, skin infiltration, facial nerve paralysis, 6× reoperated due to lymph node meta or local recurrences	T2N2b/IVa	RT, ChT	Positive/multiple LN metastasis	DOD/79
6	M/60	Parotid	$4 \times 3.5 \times 2.5$	Aggressive (6 months) mass with rapid growth, skin infiltration, neck lymphadenopathy	T4aN2b/IVa	TSCP, SND RT	Positive LN metastases (+) 7/7 ECS	Local recurrence/4–excision distant metastases (lungs, bones)/16 DOD/20
7	M/54	Hard palate	2.0×1.0	Mild (36 months) mass smooth>aggressive (2 months) mass smooth>ulcerated mucous membrane	T1N0/I	HP resection	Close	Loco-regional recurrence/48 lateral rhinotomy, SND, RT LN metastases (+) 1/11; Surgical margins (+) NED/31 (overall survival/79)

FNAB fine needle aspiration biopsy, *PCP* partial conservative parotidectomy, *TSCP* total semi-conservative parotidectomy, *SND* selective neck dissection, *MRND* modified radical neck dissection, *RT* radiation therapy, *HP* hard palate, *AciCC* acinic cell carcinoma, *MEC* mucoepidermoid carcinoma, *NED* no evidence of disease, *DOD* died on disease

102

Table 3 Results of fine needle aspiration biopsy, original histological diagnosis of patients, RT-PCR and FISH results

	Sex/age	Original cytopathologic diagnosis	Original histologic diagnosis	RT-PCR	FISH	Final diagnosis
1	F/42	Cyst	Low-grade cystadenocarcinoma NOS	Negative	Not diagnostic	MASC
2	M/62	Adenocarcinoma	Adenocarcinoma NOS, grade 2	Negative	Positive [38/100]	MASC
3	F/51	Adenoma	AciCC /papillary cystic variant	Positive	Positive [81/100]	MASC
4	M/17	–	AciCC	Negative	Positive [39/100]	MASC
5	M/73	–	SDC grade 2	Positive	Positive [80/100]	MASC with high-grade transformation
6	M/60	Adenocarcinoma	MEC grade 2	Negative	Positive [89/100]	MASC with high-grade transformation
7	M/54	LG carcinoma of salivary gland	Adenocarcinoma NOS, grade 2	Positive	Positive [74/100]	MASC

secretory analogue carcinoma (MASC) as a new entity. As a consequence, the recognition and differentiation of MASC from other primary salivary gland tumours are essential in order to clarify its histomorphological features and biological behaviour.

Inspired by the original report and reports from other groups [9, 13, 15, 18, 26], we reviewed primary salivary gland tumours diagnosed in our department and identified seven tumours which met the criteria for MASC. We collected all available clinico-pathological and follow-up data. All cases diagnosed upon revision as MASCs had been diagnosed histologically as malignancy, as adenocarcinoma/cystadenocarcinoma NOS (in three cases), AciCC (two cases) and MEC and SDC (one case each). Fine needle aspiration biopsy (FNAB) results were available in five of seven cases. Two cases had been diagnosed as benign (cyst and adenoma) and in three as malignant lesion.

On cytological smears, MASCs have been reported as variably cellular and with two different architectural patterns: 1) tissue fragments with isomorphic cells arranged in a sheet-like or papillary configuration and 2) dispersed and dissociated cells. Cells contained abundant vacuolated granular and sometimes vacuolated cytoplasm [6, 14, 22, 23]. Nuclear atypia was mild to moderate. Mucin was present, sometimes abundant or absent. MASC cytology represents considerable overlap with other tumours such as AciCC, MEC, SDC and oncocytoma [14] and in the differential diagnosis of low-grade salivary gland neoplasms MASC should be included.

The differential diagnosis of MASC should include AciCC, adenocarcinoma NOS, cystadenocarcinoma and low-grade mucoepidermoid carcinoma. One of our cases (no. 5) was originally diagnosed as salivary duct carcinoma (SDC) due to high-grade transformation prevalent in its morphology [25]. SDC as MASC mimic has not been reported before. Morphologically, the HG component of MASC in both our cases was composed of anaplastic cells with abundant cytoplasm and large polymorphous nuclei arranged in solid structures with
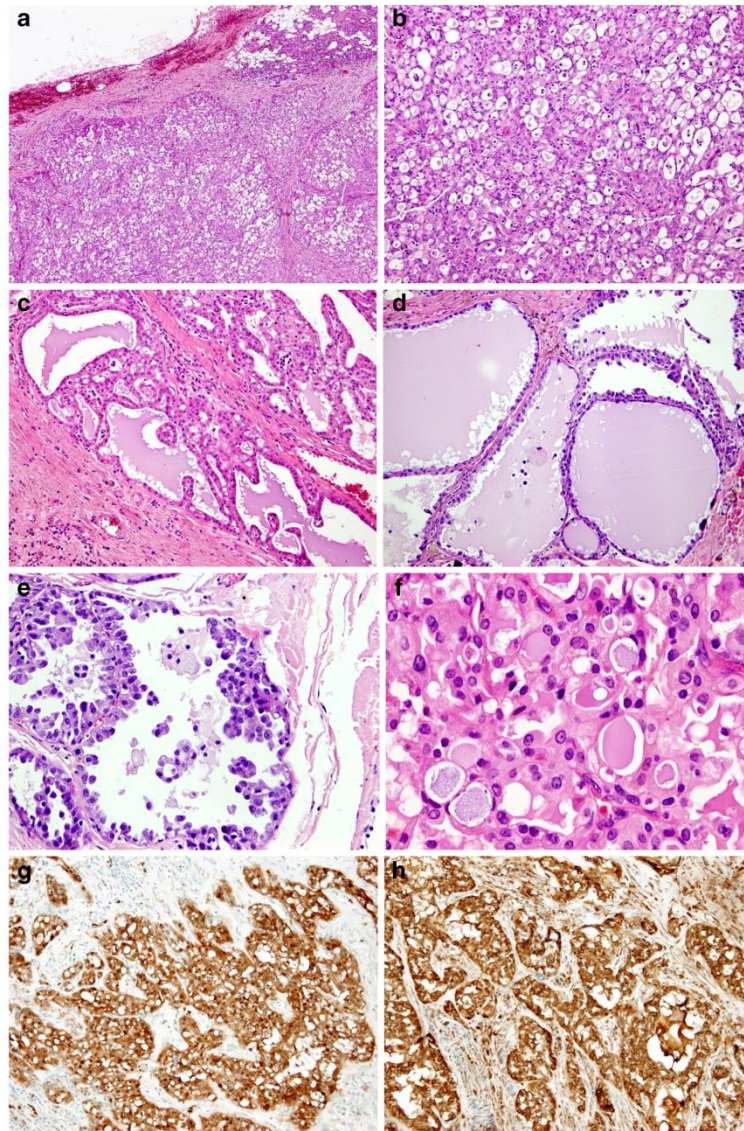
focal comedo-like necrosis. In addition, the tumours showed high mitotic activity and invasion of stroma and of peripheral nerves. The high-grade component did not contain colloid- or protein-like material, but the presence of ETV6 rearrangement was confirmed. Immunohistochemistry may be useful to differentiate MASC with high-grade transformation from SDC, which, in contrast to MASC, typically shows expression of androgen receptor or HER-2/neu but not of S100 protein.

The other MASC case was previously diagnosed as mucoepidermoid carcinoma (MEC) with intermediate differentiation, mostly due to focal but unequivocal PAS-positive mucinous differentiation. This feature and variable expression of myoepithelial markers (HMWCK, p63 and CD10) make MEC an important differential diagnosis from MASC [10, 17]. However, the basal/myoepithelial markers (calponin, p63 and CD10) are usually diffusely and strongly expressed in MEC, while weak and focal in MASC [17]. Additionally, lack of squamoid areas with intercellular bridges and/or basal-like intermediate cells supports a diagnosis of MASC. Moreover, MEC often (in 38 to 81 % of cases) harbours a t(11;19) translocation resulting in CRTC1-MAML2 fusion transcript [12, 20]. This differs from MASC, which tends to have the t(12;15)(p13;q25) translocation resulting in the ETV6-NTRK3 fusion transcript.

The most common mimic of MASC is zymogen granule-poor AciCC [13, 18]. We also found two cases (out of 17, 12 %) formerly diagnosed as AciCC: one with papillary cystic (case 3) and the other with macrocystic (case 4) growth pattern. AciCC is characterized by a wide variety of architectural patterns, some of which (microcystic, follicular and papillary cystic) need to be differentiated from MASC. Strong and diffuse S100 protein expression and positive mammaglobin staining should favour a diagnosis of MASC [4, 21].

Adenocarcinoma/cystadenocarcinoma not otherwise specified (ANOS) is a poorly defined entity of otherwise unclassifiable salivary gland carcinoma. Its diagnosis should be

made by exclusion of other salivary gland carcinoma types. The differentiation from MASC requires evidence of the *ETV6-NTRK3* translocation through which many cases diagnosed as ANOS were reclassified as MASC [3, 5, 9, 13, 15, 24, 29]. Our series contained 14 cases of ANOS, three of which (21 %) were reclassified as MASC.

We performed both FISH and RT-PCR for molecular genetic analysis. In our study, on FISH, all but one case (6/7) was positive for ETV6 gene rearrangement. In the cystic tumour with delicate cellular lining (case 1), the neoplastic material was very limited and, thus, insufficient for analysis. By RT-PCR, only three out of seven cases
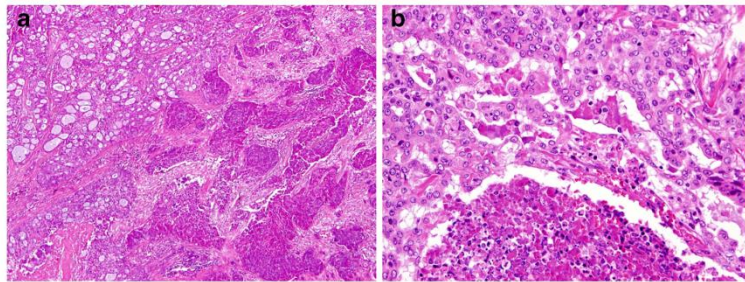
Fig. 2 MASC with high-grade (HG) transformation: **a** The tumour contains two distinct carcinomatous components. One represents conventional MASC composed of uniform neoplastic cells arranged in solid, tubular and microcystic growth structures divided by fibrous septa that were partly hyalinized. The tumour cells show typical low-grade morphology: vesicular round to oval nuclei with finely granular chromatin and distinct centrally located nucleoli (*left*). The HG component is composed of anaplastic cells with abundant cytoplasm and large pleomorphic nuclei (*right*) (H&E; ×40); **b** solid tumour islands of MASC high-grade component with areas of large geographical comedo-like necrosis (H&E; ×200)

were positive for the t(12,15) (*ETV6-NTRK3*) fusion transcript. Petersson et al. proposed as possible explanation for negative RT-PCR results a different fusion partner for the *ETV6* gene [22]. In haematopoietic malignant disorders, *ETV6* fusions other than with *NTRK3* have been described with *ABL1*, *RUNX1* or *FLT3* [9]. Moreover, the *ETV6-NTRK3* fusion is not found in 100 % of secretory carcinomas of the breast [22].
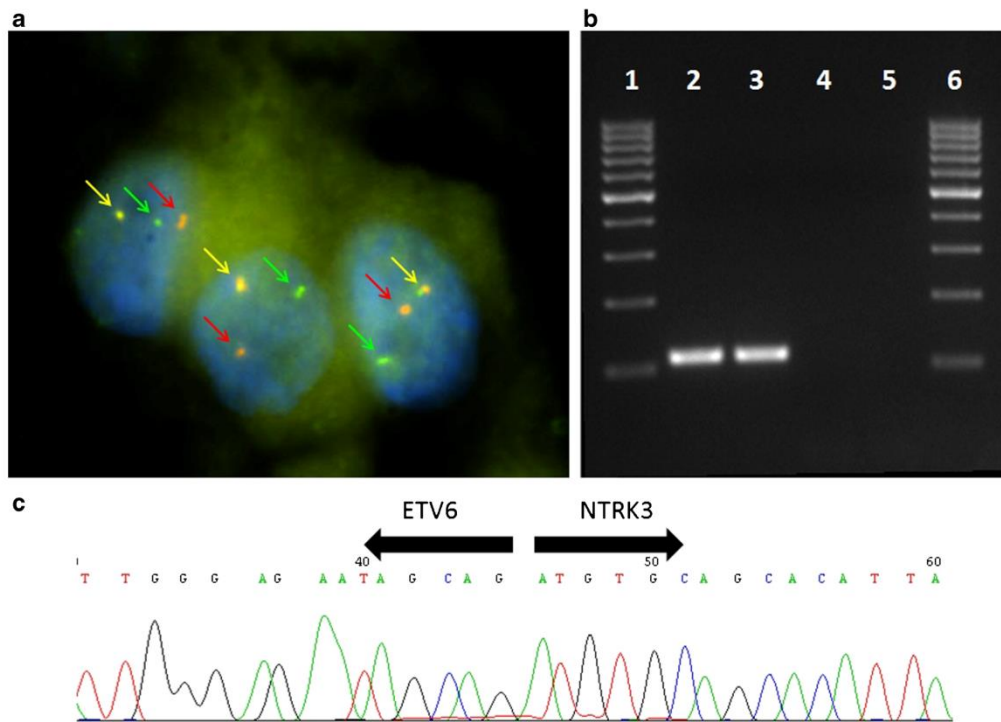

Fig. 3 **a** Fluorescent in situ hybridization with ETV6 (12p13) break apart probe. Nuclei with split *red and green signals* indicate ETV6 break. Chromosomes with normal ETV6 gene show *yellow signal* (*overlapping green and red*); **b** expression of the ETV6-NTRK3 fusion transcript by reverse transcription PCR; **c** sequence analysis of the ETV6-NTRK3 fusion transcript. *Arrows* indicate translocation break point

105

The majority of MASC arose in the parotid gland, followed by the oral cavity (lip, soft palate and buccal mucosa) and submandibular gland [5, 26]. Of our cases, all but one (85 %) developed in the parotid gland. The remaining tumour arose in a small salivary gland of the hard palate. The male predominance in our series (2.5:1) is more prominent than in other reports which found MASC to be only slightly more common in males (53 %) [3]. Age varied widely in our cases from 17 to 73 years (median 51.4) corresponding to earlier data (range from 14 to 78 years) [3]. The size of MASC ranged from 0.2 to 5.5 cm [3, 6, 9, 13–15, 18, 19, 22, 26, 29]. In our series, the smallest tumour (2.0 cm) was located in the hard palate (case 7), whereas others ranged from 2.2 to 4 cm. This is consistent with data from the literature in that MASC in the oral cavity tends to be smaller (mean 0,9 cm) than in the parotid gland (mean 2, 2 cm) [3].

The limited number of cases of MASC with full clinical correlation and follow-up data precludes assessment of its prognosis and response to treatment. Although MASC is currently treated as a low-grade carcinoma with overall favourable prognosis, it has potential for regional lymph node metastasis. In cases with positive surgical margins [9, 26], the tumour often recurs locally, and therefore, adjuvant radiotherapy is recommended. Two of our patients with MASC with high-grade transformation (cases 5 and 6) died of neoplastic disease, one with distant metastasis 20 and 79 months after primary surgery. MASC has a capacity for an aggressive course, and the *ETV6-NTRK3* translocation might provide a potential therapeutic target [9].

In conclusion, MASC is a morphologically and molecularly well-defined salivary gland neoplasm. MASC may share microscopic features with AciCC, adenocarcinoma/cystadenocarcinoma NOS and low-grade MEC. In rare cases, MASC with high-grade transformation may morphologically mimic high-grade salivary gland malignancies, such as salivary duct carcinoma.

References

1. Antonescu CR, Kawai A, Leung DH, Lonardo F, Woodruff JM, Healey JH, Ladanyi M (2000) Strong association of SYT-SSX fusion type and morphologic epithelial differentiation in synovial sarcoma. Diagn Mol Pathol 9:1–8. doi:10.1097/00019606-200003000-00001

2. Barnes L, Eveson J, Reichard P, Sidransky D (eds) (2005) WHO organization classification of tumors. Pathology and genetics of head and neck tumors. IARC Press, Lyon France

3. Bishop JA (2013) Unmasking MASC: bringing to light the unique morphologic, immunohistochemical and genetic features of the newly recognized mammary analogue secretory carcinoma of salivary glands. Head Neck Pathol 7:35–39. doi:10.1007/s12105-013-0429-0

4. Bishop JA, Yonescu R, Batista D, Begum S, Eisele DW, Westra WH (2013) Utility of mammaglobin immunohistochemistry as a proxy marker for the ETV6-NTRK3 translocation in the diagnosis of salivary mammary analogue secretory carcinoma. Hum Pathol 44:1982–1988. doi:10.1016/j.humpath.2013.03.017

5. Bishop JA, Yonescu R, Batista D, Westra WH, Eisele DW (2013) Most nonparotid 'acinic cell carcinomas' represent mammary analog secretory carcinomas. Am J Surg Pathol 37:1053–1057. doi:10.1097/PAS.0b013e3182841554

6. Bishop JA, Yonescu R, Batista DA, Westra WH, Ali SZ (2013) Cytopathologic features of mammary analogue secretory carcinoma. Cancer Cytopathol 121:228–233. doi:10.1002/cncy.21245

7. Bourgeois JM, Knezevich SR, Mathers JA, Sorensen PHB (2000) Molecular detection of the ETV6-NTRK3 gene fusion differentiates congenital fibrosarcoma from other childhood spindle cell tumors. Am J Surg Pathol 24:937–946. doi:10.1097/00000478-200007000-00005

8. Chi HT, Ly BTK, Watanabe T, Kano Y, Tojo A, Sato Y (2012) ETV6-NTRK3 as a therapeutic target of small molecule inhibitor PKC412. Biochem Biophys Res Commun 429:87–92. doi:10.1016/j.bbrc.2012.10.087

9. Chiosea SI, Griffith C, Assaad A, Seethala RR (2012) Clinicopathological characterization of mammary analogue secretory carcinoma of salivary glands. Histopathology 61:387–394. doi:10.1111/j.1365-2559.2012.04232.x

10. Connor A, Perez-Ordonez B, Shago M, Skalova A, Weinreb I (2012) Mammary analog secretory carcinoma of salivary gland origin with the ETV6 gene rearrangement by fish: expanded morphologic and immunohistochemical spectrum of a recently described entity. Am J Surg Pathol 36:27–34

11. Gaffney R, Chakerian A, O'Connell JX, Mathers J, Garner K, Joste N, Viswanatha DS (2003) Novel fluorescent ligase detection reaction and flow cytometric analysis of SYT-SSX fusions in synovial sarcoma. J Mol Diagn 5:127–135. doi:10.1016/s1525-1578(10)60462-x

12. García JJ, Hunt JL, Weinreb I, McHugh JB, Barnes EL, Cieply K, Dacic S, Seethala RR (2011) Fluorescence in situ hybridization for detection of MAML2 rearrangements in oncocytic mucoepidermoid carcinomas: utility as a diagnostic test. Hum Pathol 42:2001–2009. doi:10.1016/j.humpath.2011.02.028

13. Griffith C, Seethala R, Chiosea SI (2011) Mammary analogue secretory carcinoma: a new twist to the diagnostic dilemma of zymogen granule poor acinic cell carcinoma. Virchows Arch 459:117–118. doi:10.1007/s00428-011-1098-6

14. Griffith CC, Stelow EB, Saqi A, Khalbuss WE, Schneider F, Chiosea SI, Seethala RR (2013) The cytological features of mammary analogue secretory carcinoma: a series of 6 molecularly confirmed cases. Cancer Cytopathol 121:234–241. doi:10.1002/cncy.21249

15. Jung MJ, Song JS, Kim SY, Nam SY, Roh JL, Choi SH, Kim SB, Cho KJ (2013) Finding and characterizing mammary analogue secretory carcinoma of the salivary gland. Korean J Pathol 47:36–43. doi:10.4132/KoreanJPathol.2013.47.1.36

16. Knezevich SR, Garnett MJ, Sorensen PHB, Pysher TJ, Beckwith JB, Grundy PE (1998) ETV6-NTRK3 gene fusions and trisomy 11 establish a histogenetic link between mesoblastic nephroma and congenital fibrosarcoma. Cancer Res 58:5046–5048

17. Laco J, Ryška A, Svajdler M Jr, Andrejs J, Hrubala D, Hácová M, Vaněček T, Skálová A (2013) Mammary analog secretory carcinoma of salivary glands: a report of 2 cases with expression of basal/myoepithelial markers (calponin, CD10 and p63 protein). Pathol Res Pract. doi:10.1016/j.prp.2012.12.005

18. Lei Y, Chiosea SI (2012) Re-evaluating historic cohort of salivary acinic cell carcinoma with new diagnostic tools. Head Neck Pathol 6:166–170. doi:10.1007/s12105-011-0312-9

19. Levine P, Fried K, Krevitt LD, Wang B, Wenig BM (2014) Aspiration biopsy of mammary analogue secretory carcinoma of accessory parotid gland: another diagnostic dilemma in matrix-containing tumors of the salivary glands. Diagn Cytopathol 42:49–53. doi:10.1002/dc.22886

20. O'Neill ID (2009) t(11;19) translocation and CRTC1-MAML2 fusion oncogene in mucoepidermoid carcinoma. Oral Oncol 45:2–9. doi:10.1016/j.oraloncology.2008.03.012

21. Patel KR, Solomon IH, El-Mofty SK, Lewis JS, Chernock RD (2013) Mammaglobin and S-100 immunoreactivity in salivary gland carcinomas other than mammary analogue secretory carcinoma. Hum Pathol 44:2501–2508. doi:10.1016/j.humpath.2013.06.010

22. Petersson F, Lian D, Chau YP, Yan B (2012) Mammary analogue secretory carcinoma: the first submandibular case reported including findings on fine needle aspiration cytology. Head Neck Pathol 6:135–139. doi:10.1007/s12105-011-0283-x

23. Pisharodi L (2013) Mammary analog secretory carcinoma of salivary gland: cytologic diagnosis and differential diagnosis of an unreported entity. Diagn Cytopathol 41:239–241. doi:10.1002/dc.21766

24. Skalova A (2013) Mammary analogue secretory carcinoma of salivary gland origin: an update and expanded morphologic and immunohistochemical spectrum of recently described entity. Head Neck Pathol 7(Suppl 1):S30–S36. doi:10.1007/s12105-013-0455-y

25. Skálová A, Vanecek T, Majewska H, Laco J, Grossmann P, Simpson RH, Hauer L, Andrle P, Hosticka L, Branžovský J, Michal M (2014) Mammary analogue secretory carcinoma of salivary glands with high-grade transformation: report of 3 cases with the ETV6-NTRK3 gene fusion and analysis of TP53, β-catenin, EGFR, and CCND1 genes. Am J Surg Pathol 38:23–33. doi:10.1097/PAS.0000000000000088

26. Skálová A, Vanecek T, Sima R, Laco J, Weinreb I, Perez-Ordonez B, Starek I, Geierova M, Simpson RH, Passador-Santos F, Ryska A, Leivo I, Kinkor Z, Michal M (2010) Mammary analogue secretory carcinoma of salivary glands, containing the ETV6-NTRK3 fusion gene: a hitherto undescribed salivary gland tumor entity. Am J Surg Pathol 34:599–608. doi:10.1097/PAS.0b013e3181d9efcc

27. Tognon C, Knezevich SR, Melnyk N, Mathers JA, Sorensen PHB, Huntsman D, Roskelley CD, Becker L, Carneiro F, MacPherson N, Horsman D, Poremba C (2002) Expression of the ETV6-NTRK3 gene fusion as a primary event in human secretory breast carcinoma. Cancer Cell 2:367–376. doi:10.1016/S1535-6108(02)00180-0

28. Tsuji S, Hisaoka M, Morimitsu Y, Hashimoto H, Shimajiri S, Komiya S, Ushijima M, Nakamura T (1998) Detection of SYT-SSX fusion transcripts in synovial sarcoma by reverse transcription polymerase chain reaction using archival paraffin-embedded tissues. Am J Pathol 153:1807–1812. doi:10.1016/s0002-9440(10)65695-7

29. Wang L, Liu Y, Lin X, Zhang D, Li Q, Qiu X, Wang EH (2013) Low-grade cribriform cystadenocarcinoma of salivary glands: report of two cases and review of the literature. Diagn Pathol 8:28. doi:10.1186/1746-1596-8-28

107

Mammary Analogue Secretory Carcinoma of Salivary Glands

Molecular Analysis of 25 ETV6 Gene Rearranged Tumors With Lack of Detection of Classical ETV6-NTRK3 Fusion Transcript by Standard RT-PCR: Report of 4 Cases Harboring ETV6-X Gene Fusion

Alena Skálová, MD, PhD,*† Tomas Vanecek, PhD,*‡
Roderick H.W. Simpson, MB, ChB, FRCPath,§ Jan Laco, MD, PhD,‖
Hanna Majewska, MD, PhD,¶ Martina Baneckova, MUC,* Petr Steiner, MSc,*‡
and Michal Michal, MD*

Abstract: *ETV6* gene abnormalities are well described in tumor pathology. Many fusion partners of *ETV6* have been reported in a variety of epithelial and hematological malignancies. In salivary gland tumor pathology, however, the *ETV6-NTRK3* translocation is specific for mammary analogue secretory carcinoma (MASC), and has not been documented in any other salivary tumor type. The present study comprised a clinical and molecular analysis of 25 cases morphologically and immunohistochemically typical of MASC. They all also displayed the *ETV6* rearrangement as visualized by fluorescent in situ hybridization but lacked the classical *ETV6-NTRK3* fusion transcript by standard reverse-transcriptase-polymerase chain reaction. In 4 cases, the classical fusion transcript was found by more sensitive, nested reverse-transcription-polymerase chain reaction. Five other cases harbored atypical fusion transcripts as detected by both standard and nested reverse-transcription-polymerase chain reaction. In addition, fluorescent in situ hybridization with an *NTRK3* break-apart probe was also performed; rearrangement of *NTRK3* gene was detected in 16 of 25 cases. In 3 other cases, the tissue was not analyzable, and in 2 further cases analysis could not be performed because of a lack of appropriate tissue material. Finally, in the 4 remaining cases whose profile was *NTRK3* split-negative and *ETV6* split-positive, unknown (non-*NTRK*) genes appeared to fuse with *ETV6* (*ETV6-X* fusion). In looking for possible fusion partners, analysis of rearrangement of other kinase genes known to fuse with *ETV6* was also performed, but without positive results. Although numbers were small, correlating the clinico-pathologic features of the 4 *ETV6-X* fusion tumors and 5 MASC cases with atypical fusion transcripts raises the possibility of that they may behave more aggressively.

Key Words: mammary analogue secretory carcinoma, MASC, *ETV6-NTRK3*, *ETV6-X* fusion transcript, clinicopathologic analysis

(*Am J Surg Pathol* 2016;40:3–13)

Mammary analogue secretory carcinoma (MASC) of salivary gland origin is a recently described tumor that harbors a characteristic balanced chromosomal translocation, t(12;15) (p13;q25) resulting in an *ETV6-NTRK3* fusion[1] identical to that in secretory carcinoma of the breast.[2] Histologically, MASC is composed of uniform cells with bland-looking vesicular nuclei and eosinophilic vacuolated cytoplasm, arranged in tubular, microcystic and solid growth patterns with abundant periodic acid-Schiff –positive secretions. MASC may histologically resemble zymogen granule-poor acinic cell carcinoma, low-grade cribriform cystadenocarcinoma, and adenocarcinoma not otherwise specified.[1] However, the diagnosis of MASC in most cases is not difficult based on histologic, immunohistochemical, and molecular features. Detection of *ETV6* by fluorescent in situ hybridization (FISH) is technically feasible and more than 150 cases of MASC have been published in the last 4 years since its original description in 2010.[1]

There have been several studies extending the description of the clinical, histologic, and immunohistochemical features of MASC[3–12] and the number of

reported MASCs has grown considerably.[13–15] However, the molecular genetic and epigenetic background of MASC has not been completely studied, except for the *ETV6-NTRK3* fusion. Therefore, a recent paper by Ito et al[16] describing 2 MASC cases with *ETV6* fused with an unknown gene partner immediately attracted our attention; the authors hypothesized that such tumors may have unique clinicopathologic features.

Up until then, in all cases of MASC where the fusion was known, this was *ETV6* with *NTRK3*, and no other fusion partners have been reported so far. Nevertheless, for several years, we have been aware of a number of MASC cases positive for the *ETV6* gene split as visualized by FISH, but in which the classical *ETV6-NTRK3* fusion transcript (exon 5-exon 15 junction) was not detected by standard reverse-transcriptase polymerase chain reaction (RT-PCR). Twenty-five such MASC cases were retrieved from our consultation files and further analyzed.

MATERIALS AND METHODS

Among more than 4300 cases of primary salivary gland tumors, 121 cases of the newly recognized entity MASCs were retrieved from the consultation files of the Salivary Gland Tumor Registry, at the Department of Pathology, Faculty of Medicine in Plzen, Czech Republic (AS). The histopathologic features of all tumors and the immunohistochemical stains when available were reviewed by 2 pathologists (A.S. and M.B.). A diagnosis of MASC was confirmed in cases that displayed, if at least focally, histologic features consistent with original description[1] in conjunction with appropriate immunohistochemical profile, that is coexpression of S-100 protein, cytokeratin CK7, and mammaglobin with absence of p63 and DOG1 staining. For the purpose of this particular study, we have included only unequivocal cases of MASC positive for *ETV6* rearrangement by FISH. Twenty-five tumors harboring *ETV6* gene rearrangement as visualized by FISH but without detection of the classical *ETV6-NTRK3* fusion transcript by standard RT-PCR were further analyzed.

For conventional microscopy, the excised tissues were fixed in formalin, routinely processed, embedded in paraffin, cut, and stained with hematoxylin-eosin. In most cases, additional stains were also performed, including periodic acid-Schiff with and without diastase, mucicarmin, and alcian blue at pH 2.5.

For immunohistochemical studies, 4-μm-thick sections were cut from paraffin blocks, mounted on slides coated with 3-aminopropyltriethoxy-silane (Sigma, St. Louis), deparaffinized in xylene, and rehydrated in descending grades (100% to 70%) of ethanol. Sections were then subjected to heat-induced epitope retrieval by immersion in a CC1 solution at pH 8, at 95°C. Endogenous peroxidase was blocked by a 5-minute treatment with 3% hydrogen peroxide in absolute methanol. The slides were then stained by immunostainer BenchMark ULTRA (Roche). The primary antibodies used are summarized

in Table 1. The bound antibodies were visualized using the Histofine Simple Stain MAX PO (Multi) Universal Immuno-peroxidase Polymer, anti-mouse and rabbit (Nichirei Biosciences Inc., Tokyo, Japan), and 3-3′-diaminobenzidine (Sigma) as chromogen. The slides were counterstained with Mayer hematoxylin. Appropriate positive and negative controls were employed.

Clinical follow-up was obtained from the patients, their physicians, or from referring pathologists.

Molecular Genetic Study

Detection of *ETV6-NTRK3* Fusion Transcript by RT-PCR

RNA was extracted using the RecoverAll Total Nucleic Acid Isolation Kit (Ambion, Austin, TX). cDNA was synthesized using the Transcriptor First Strand cDNA Synthesis Kit (RNA input 500 ng) (Roche Diagnostics, Mannheim, Germany). All procedures were performed according to the manufacturer's protocols. Amplification of a 105 and 133 bp product of the β2-microglobulin gene and 247 bp product of *PGK* gene was used to test the quality of the extracted RNA as previously described.[17–19] A detection of classical, exon 5 of *ETV6* gene and exon 15 of *NTRK3* gene,[20] as well as atypical, exon 4 of the *ETV6* gene and exon 14 of the *NTRK3* gene (and their combinatorial variants), fusion transcript was performed by RT-PCR. In addition, more sensitive, nested RT-PCR was performed for detection classical[16] as well as selected atypical junction of transcripts.

For single-round PCR, 2 μL of cDNA was added to reaction consisted of 12.5 μL of HotStar Taq PCR Master Mix (Qiagen, Hilden, Germany), 10 pmol of each primer (Table 2) and distilled water up to 25 μL. The amplification program comprised denaturation at 95°C for 14 minutes and then 45 cycles of denaturation at 95°C for 1 minute, annealing at temperature seen in Table 2 for 1 minute, and extension at 72°C for 1 minute. The program was finished by incubation at 72°C for 7 minutes. For nested PCR, the same reaction conditions were set. One microliter of PCR product from the first round was used as a template.

Successfully amplified PCR products were purified with magnetic particles Agencourt AMPure (Agencourt Bioscience Corporation, A Beckman Coulter Company, Beverly, MA). Products were then bidirectionally sequenced using Big Dye Terminator Sequencing kit (PE/Applied Biosystems, Foster City, CA), purified with magnetic particles Agencourt CleanSEQ (Agencourt Bioscience Corporation), all according to the manufacturer's protocol and run on an automated sequencer ABI Prism 3130xl (Applied Biosystems) at a constant voltage of 13.2 kV for 11 minutes.

Detection of *ETV6, NTRK3,* and Other 13 Genes Break by FISH Method

From each tumor, 4-μm-thick sections were cut from formalin-fixed paraffin-embedded blocks and placed

TABLE 1. Antibodies Used for Immunohistochemical Study

Antibody Specificity	Clone	Dilution	Antigen Retrieval/Time	Source
S-100 protein	Polyclonal	1:2000	CC1/20 min	DakoCytomation
CK7	OV-TL 12/30	1:200	CC1/36 min	DakoCytomation
GCDFP-15	EP1582y	RTU	CC1/64 min	Cell Marque
Mammaglobin	304-1A5	RTU	CC1/36 min	DakoCytomation
STAT 5a	Polyclonal	1:400	CC1/36 min	Assay Designs Inc.
Ki-67	30-9	RTU	CC1/64 min	Ventana
P63	4A4	RTU	CC1/64 min	Ventana
DOG1	K9	RTU	CC1/36 min	Leica
GATA3	L50-823	1:250	CC1/52 min	BioCare Medical
SOX10	Polyclonal	1:50	CC1/64 min	Cell Marque

CC1 indicates EDTA buffer, pH 8.6; RTU, ready to use.

on positively charged slides. The slides were routinely deparaffinized in xylen 3 times for 5 minutes and then washed twice in 100% ethanol, once in 95% ethanol and once in deionized water for 5 minutes. Then, the slides were heated in the 1× Target Retrieval Solution (pH 6) (Dako, Glostrup, Denmark) for 40 minutes at 95°C and subsequently cooled for 20 minutes at room temperature in the same solution. The slides were washed in deionized water for 5 minutes and tissues were covered with the Proteinase K (20 mg/mL) (SERVA, Heidelberg, Germany) for 10 minutes at room temperature. The slides were then placed into deionized water for 5 minutes, dehydrated in a series of ethanol solution (70%, 85%, 96% for 2 min each) and air-dried.

An appropriate amount of mixed break-apart probe (Table 3) was applied on each specimen and was incubated in the ThermoBrite instrument (StatSpin/Iris Sample Processing, Westwood, MA) at 85°C for 8 minutes and then at 37°C for 16 hours. Subsequently, the slide was washed in 2× SSC/0.3% NP-40 solution at 72°C for 2 minutes and counterstained with DAPI.

FISH Interpretation

Each specimen was examined with an Olympus BX51 fluorescence microscope using a 100× objective and filter sets Triple Band Pass (DAPI/SpectrumGreen/SpectrumOrange), Dual Band Pass (FITC/Texas Red), and Single Band Pass (SpectrumGreen or SpectrumOrange). Scoring was performed by counting the number of fluorescent signals in 100 randomly selected nonoverlapping tumor cell nuclei. The slides were independently enumerated by 2 observers (T.V. and P.S.). The cut-off value for gene break was set at 10%.[1]

TABLE 2. Primers for Detection of *ETV6-NTRK3* Fusion Transcripts

Original Primer Name	Sequence	Localization
ETV6-ex4-F3	AGCCGGAGGTCATACTGCAT	ETV6 exon 4 inner
ETV6-ex4-F4	CATTCTTCCACCCTGGAAAC	ETV6 exon 4 outer
ETV6B*	ACATCATGGTCTCTGTCTCCCCGC	ETV6 exon 5 inner
TEL971† (ETV6A*)	ACCACATCATGGTCTCTGTCTCCC	ETV6 exon 5 outer
NTRK3-ex14-R1	GTGATGCCGTGGTTGATGT	NTRK3 exon 14 inner
NTRK3 ex14-R2	AGTCATGCCAATGACCACAG	NTRK3 exon 14 outer
NTRK3B*	TTCTCGCTTCAGCACGATGTCT	NTRK3 exon 15 inner
TRKC1059† (NTRK3A*)	CAGTTCTCGCTTCAGCACGATG	NTRK3 exon 15 outer

*Ito et al.[16]
†Bourgeois et al.[20]

RESULTS

Molecular Genetic Findings

After making the histologic diagnosis of MASC and confirming the *ETV6* split, 25 cases with the absence of classical, exon 5-exon 15, *ETV6-NTRK3* fusion transcript as detected by standard RT-PCR were analyzed in greater detail (Table 4). The classical fusion transcript was analyzed by potentially more sensitive nested RT-PCR.[14] In addition, atypical, exon 4-exon 14, *ETV6-NTRK3* fusion transcript, and also possible combinations of exons involved in classical and atypical junction were analyzed by nested RT-PCR and/or RT-PCR. In 4 cases, the classical fusion transcript was found by nested RT-PCR. Five other cases harbored atypical, exon 4-exon 14 or exon 5-exon 14, *ETV6-NTRK3* fusion transcript as detected by both, nested and/or standard RT-PCR (Fig. 1). The rest of the cases remained negative on RT-PCR. In addition to RT-PCR studies, FISH with *NTRK3* break-apart probe was performed. The *NTRK3* gene split was detected in 16 of 25 cases. In 3 cases, the tissue was not analyzable, and in 2 other cases analysis could not be performed because of lack of formalin-fixed paraffin-embedded tissue material.

TABLE 3. Probes Used in Study

Gene Name	BAC Clone/Localization of Probe	Producer	Reaction Mixture (Probe-Probe:Water:Buffer)
ETV6	Commercial	Abbott/Vysis	1:2:7[+]
NTRK3	RP11-97O12	BlueGnome	1-1:1:7[++]
	RP11-96B23		
NTRK1	chr1:156188056-156785595	Agilent	1-1:1:7[++]
	chr1:156851496-157451790		
NTRK2	chr9:86361009-87360838	Agilent	1-1:1:7[++]
	chr9:87560839-88561053		
ABL1	RP11-17L7	BlueGnome	1-1:1:7[++]
	RP11-143H20		
ABL2	chr1:178664366-179063610	Agilent	1-1:1:7[++]
	chr1:179203866-180203965		
FGFR3	RP11-386I15	BlueGnome	1-1:1:7[++]
	RP11-262P20		
FLT3	RP11-438F9	BlueGnome	1-1:1:7[++]
	RP11-502P18		
FRK	chr6:115762599-116262838	Agilent	1-1:1:7[++]
	chr6:116381774-116882068		
JAK2	Commercial	KREATECH Diagnostics	Ready to use
LYN	chr8:56192225-56792519	Agilent	1-1:1:7[++]
	chr8:56925305-57525154		
PDGFRA	RP11-367N1	BlueGnome	1-1:1:7[++]
	RP11-116G9		
PDGFRB	Commercial	CYTOCELL Technologie	Ready to use
PER1	RP11-298H4	BlueGnome	1-1:1:7[++]
	RP11-89A15		
SYK	RP11-61N16	BlueGnome	1-1:1:7[++]
	RP11-367F23		

TABLE 4. Results of Molecular Genetic Analysis of ETV6 and NTRK3 Genes Rearrangement and ETV6-NTRK3 Fusion Transcripts

Case Number	FISH		RT-PCR Classical 5-15	Nested RT-PCR Classical 5-15	RT-PCR Atypical 4-14[1] or 5-14[2]	Nested RT-PCR Atypical 4-14[1]	RT-PCR Control Genes 105/133/247
	ETV6 Break	NTRK3 Break					
Case 1	+	NA	−	−	−	−	+/+/−
Case 2	+	+	−	−	−	−	+/+/−
Case 3	+	+	−	+	−	−	+/+/+
Case 4	+	NA	−	−	−	−	+/−/−
Case 5	+	NP	−	−	−	−	+/+/+
Case 6	+	−	−	−	−	−	+/+/+
Case 7	+	NP	−	−	−	−	+/−/−
Case 8	+	+	−	+	−	−	+/+/−
Case 9	+	+	−	−	−	+[1]	+/+/+
Case 10	+	+	−	−	−	−	+/+/+
Case 11	+	NA	−	−	−	−	+/+/+
Case 12	+	+	−	+	−	−	+/+/+
Case 13	+	+	−	−	+[2]	−*	+/+/+
Case 14	+	+	−	−	+[1]	+[1]	+/+/+
Case 15	+	−	−	−	−	−	+/+/+
Case 16	+	+	−	−	−	−	+/+/−
Case 17	+	−	−	−	−	−	+/+/+
Case 18	+	+	−	+	−	−	+/+/−
Case 19	+	+	−	−	+[1]	+[1]	+/−/−
Case 20	+	−	−	−	−	−	+/+/+
Case 21	+	+	−	−	−	−	+/+/−
Case 22	+	+	−	−	−	−	+/+/−
Case 23	+	+	−	−	−	−	+/+/+
Case 24	+	+	−	−	−	−	+/+/+
Case 25	+	+	−	−	+[1]	+[1]	+/+/+

4, 5—numbers of exons of ETV6 gene; 14, 15—numbers of exons of NTRK3 gene.
*Only 4-14 junction was analyzed by nested RT-PCR.
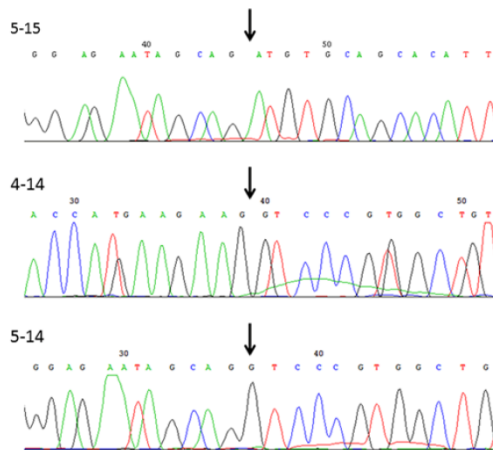NA indicates not analyzable; NP, not performed.

FIGURE 1. Sequence analysis of *ETV6-NTRK3* fusion transcripts. The most common exon 5-exon 15 (5-15) as well as 2 other atypical (4-14 and 5-14) fusions are shown. Arrows show point of fusion.

In the 4 remaining cases with the profile of *NTRK3* split-negative and *ETV6* split-positive, the fusion of *ETV6* gene to a non-*NTRK3* gene was suggested. To pursue possible fusion partners in these cases, we examined involvement of *NTRK1* and *NTRK2* genes, both members of the NTRK family. However, neither an *NTRK1* nor *NTRK2* gene split was detected (Fig. 2). Other kinase genes known to be possible partners of *ETV6*, such as *ABL1, ABL2, FGFR3, FLT3, FRK, JAK2, LYN, PDGFRA, PDGFRB, PER1*, and SYK were analyzed in cases, in which a sufficient formalin-fixed paraffin-embedded tissue was available (cases 17, 20). In case 17, no break of these genes was detected. In case 20, all genes except unanalyzable *FLT3, PDGFRA*, and *SYK* were negative, too.

Clinical and Histologic Characteristics of the Study Group

The clinical and follow-up data are summarized in Table 5. There were 9 female and 16 male patients. The median patient age was 47 years, with a range between 15 and 77 years. The most common anatomic site of involvement was the parotid gland, occurring in 12 patients (48%). Other sites of origin were the submandibular gland in 6 patients (24%), minor salivary gland of buccal mucosa, and retromolar gingiva in 2 patients each (8%) and 3 tumors arose in the upper lip (12%).

Follow-up Data

Clinical follow-up data were obtained from 22 patients, and ranged from 9 months to 19 years (mean 3 y and 11 mo), 3 patients were lost to follow-up. Detailed clinical, follow-up, and histologic findings in 25 patients with MASC are summarized in Table 6.

Five of the 22 patients experienced locally recurrent tumor 1 month to 19 years after the primary diagnosis (mean 55 mo). Cervical lymph node metastases developed in 6 patients, one of whom died of disseminated cancer 20 months after diagnosis with nodal (4 mo after diagnosis of primary tumor) and multiple distant metastases to lungs, liver, and bones at 10 months (case 9). Fourteen of 22 patients were alive with no evidence of recurrent or metastatic disease at last follow-up.

All tumors were treated by surgical excision; in 9 cases the excision was radical with clear surgical margins, but in 11 cases the surgical margins were positive and in 4 cases the tumor infiltration was close (< 0.5 mm) to the surgical margins. One patient underwent subtotal conservative parotidectomy in combination with radiotherapy (case 5). Recurrences were treated by radical re-excision with clear surgical margins in all 5 patients, radiotherapy was used in 4 of these 5 patients with recurrent disease.

Macroscopic Features

The median tumor size was 2.1 cm, with a range of 0.5 to 5.0 cm. Grossly, most tumors were variably invasive: 4 were entirely circumscribed, 6 had focally infiltrative edges, and 15 were predominantly infiltrative.

Microscopic and Immunohistochemical Features

On low-power magnification, 3 major growth patterns of MASC were identified in our material. Firstly, some tumors were well circumscribed and surrounded by a thick, focally uninterrupted, fibrous capsule enclosing predominantly papillary and macrocystic structures (Fig. 3). The second pattern was characterized by solid and lobular growth with a multilobular structure divided by thick hyalinized or thin fibrous septa (Fig. 4). These tumors either lacked a capsule or were only partially encapsulated with prominent infiltrative borders. These cases were predominantly composed of microcystic and slightly dilated glandular spaces filled with variable amount of eosinophilic homogenous secretory material. A prominent fibrosclerotic stroma with isolated tumor cells in small islands or trabeculae were seen in central part of the tumor in 12/25 (48%) cases (Fig. 5). The third pattern comprised a macrocystic growth pattern, in which larger cystic structures were lined mostly by a single, and focally a double layer of cells with prominent or focal apocrine differentiation including hobnail cells (Fig. 6). The cysts contained abundant proteinaceous eosinophilic material. However, most tumors demonstrated 2 or more architectural patterns with microcystic, tubular, solid, and papillary patterns often occurring together.

Regardless of the growth pattern of MASC, the tumor cells were often bland looking with abundant pale pink vacuolated and foamy cytoplasm and with vesicular oval nuclei with a single small but prominent nucleolus. The cytologic features were similar from cases to case. Range of nuclear atypia was assessed as grades 1 to 3. Mitotic figures were rare and necrosis was absent.
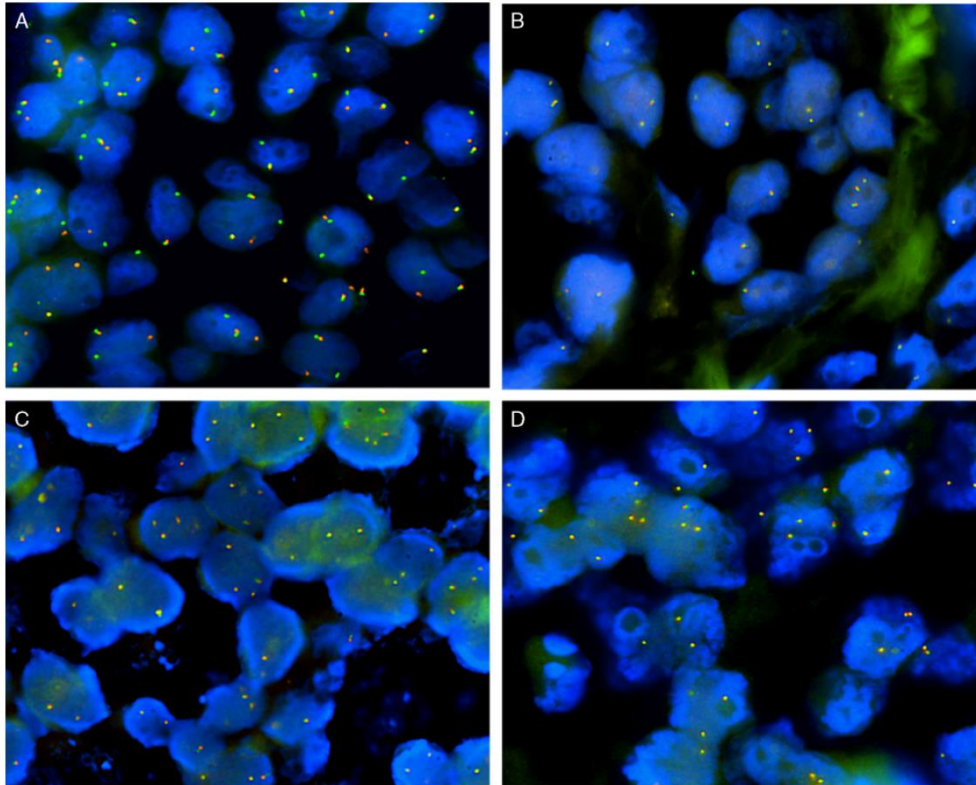
FIGURE 2. FISH analysis reveal rearranged *ETV6* gene (A), and intact genes *NTRK1* (B), *NTRK2* (C), and *NTRK3* (D) respectively, using break-apart probes. Yellow (red/green fusion) signal demonstrates intact chromosome, separated red and green signals mean gene break.

Lymphovascular invasion was present in 2 cases (8%), and perineural invasion was seen in 12 tumors (48%) (Table 5).

Histologic Findings in 4 MASC Cases *NTRK3* Split-negative *ETV6* Split-positive (*ETV6-X* Fusion)

Invasive growth into fibroadipose tissue adjacent to salivary glands was seen in 3 of the 4 (cases 15, 17, 20), and the remaining tumor was received as multiple fragments, and thus invasion could not be assessed (case 6). In detail: skeletal muscle was involved in 1 case (case 15), lymphovascular invasion in 1 (case 15), and perineural invasion seen in 2 (cases 17, 15). A capsule was not present in any of these tumors. The fibrosclerotic stroma and thick hyalinized fibrous septa were particularly prominent in 2 of 4 cases. Nuclei were assessed as grade 1 in 3 tumors, and nuclear grade 2 in the remaining 1 (case 20) (Tables 4 and 6).

Histologic Findings in 5 MASC Cases With Atypical Profile of *ETV6-NTRK3* Fusion Transcript

Except for 1 patient (case 25), all the other 4 tumors were invasive and nonencapsulated with infiltration of periglandular tissue and positive surgical margins. Perineural (2/5) and lymphovascular (1/5) invasion were observed. Four cases showed thick fibrous septa with focal hyalinization, and in each of 3 cases, trabeculae and nests of neoplastic cells were embedded in a completely hyalinized central part of the tumor (Fig. 7). Nuclei were assessed as grade 1 in 3 tumors (cases 14, 19, 25), and nuclear grade 3 in the remaining 1 (case 9) (Tables 4 and 6).

High-grade morphology was seen in 1 patient (case 9). The tumor was composed of 2 distinct carcinomatous components (Fig. 8). One component was a conventional MASC made of uniform neoplastic cells arranged in solid, tubular, and microcystic growth structures, divided by fibrous septa that were thick and partly hyalinized. The tumor cells had typical low-grade morphology;

TABLE 5. Clinical and Histologic Findings in 25 MASC Cases With *ETV6*-Split and Absence of *ETV6-NTRK3* Fusion Transcript by Standard RT-PCR

	N/Total (%)
Age	
Median age (y)	47
Range (y)	15-77
Sex	
Female	9/25 (36)
Male	16/25 (64)
Anatomic location	
Parotid gland	12/25 (48)
Submandibular gland	6/25 (24)
Minor gland	7/25 (28)
Size (cm)	
Median	2.1
Range	0.5-5.0
Follow-up data available	22/25 (88)
Median follow-up period	3 y 11 mo
Range	9-228 mo
Metastatic disease	
Cervical LN metastasis	6/22 (28)
Distant metastasis	1/22 (4)
Local recurrent disease	5/22 (23)
Histologic findings	
Invasive growth	15/25 (60)
Perineural invasion	12/25 (48)
LVI	2/25 (8)
Prominent hyalinized stroma	12/25 (48)

LN indicates lymph node; LVI, lymphovascular invasion.

vesicular round to oval nuclei with finely granular chromatin and distinct centrally located nucleoli. The other component was sharply delineated from the conventional MASC. It was composed of anaplastic cells with abundant cytoplasm and large pleomorphic nuclei. Solid tumor islands revealed large areas of large geographical comedo-like necrosis and desmoplastic stroma indicated invasion. The tumor cells of the high-grade component had significantly increased mitotic activity and nuclear polymorphism and failed to produce secretory material, in contrast to the low-grade component.

Immunohistochemical Findings

By immunohistochemistry, all examined MASC cases were positive for S100 protein (25/25), mammaglobin (17/17), typically in strong and diffuse fashion (secretory material was also positive), and cytokeratin CK7 (17/17). GATA-3, SOX-10, and STAT5a staining was detected in most analyzed cases, respectively (17/17), (5/10), and (5/5). P63 protein was completely negative in most cases, with limited areas of positive peripheral myoepithelial cell staining suggestive of a focal intraductal component in 3 cases. DOG1 was negative in all cases (16/16). Proliferative activity was generally low, with mean MIB1 index 17% (range 5% to 40%).

DISCUSSION

MASC is a relatively newly described neoplasm of minor and major salivary glands characterized in most cases by a distinctive molecular alteration: a balanced t(12;15) (p13;q25) chromosomal rearrangement resulting in the fusion of the *ETV6* and *NTRK3* genes.[1] Interestingly, the same translocation, *ETV6-NTRK3*, can be seen not only in secretory carcinoma of breast,[2] but also in infantile fibrosarcoma,[21] congenital mesoblastic nephroma,[22] some hematopoietic malignancies,[23] ALK-negative inflammatory myofibroblastic tumors,[24] and in radiation-induced papillary thyroid carcinoma.[25]

The *ETV6-NTRK3* fusion gene encodes a chimeric oncoprotein tyrosine kinase that activates the Ras-MAP kinase and phosphatidylinositol-3-kinase–Akt pathways. An *ETV6* rearrangement may be detected from paraffin-embedded tissue by break-apart FISH or alternatively, the fusion transcript can be identified by RT-PCR. Detection of *ETV6* rearrangement from paraffin-embedded tissue is technically feasible, relatively widely available and is considered the gold standard for the diagnosis of MASC. However, in some of our MASC cases previously reported, RT-PCR failed to demonstrate the *ETV6-NTRK3* fusion transcript, even though they were FISH positive.[1,11,26]

Recently, Ito et al[16] reported 2 cases of MASC with the *ETV6* gene split detected by FISH but in which the *ETV6* gene appeared to be fused with a gene partner other than *NTRK3*. They further demonstrated that neither *NTRK1* nor *NTRK2* genes were involved.[16] In hematopoietic malignancies, >30 *ETV6* partner genes have been molecularly characterized,[27] but in MASC *ETV6* usually fuses with *NTRK3*, and no other fusion partners have been reported so far.[1,16] However, the 2 cases reported by Ito et al[16] plus several examples of MASC in our previous studies[1,11,26] that failed to demonstrate *ETV6-NTRK3* fusion transcript by classical RT-PCR together suggested that *ETV6* may on occasions fuse with an unknown non-*NTRK* gene partner (*ETV6-X* fusion). Therefore, we retrieved from our consultation files 25 such MASC cases all *ETV6* split by FISH but negative for *ETV6-NTRK3* fusion transcript as detected by standard RT-PCR.[20] This reaction analyzes the most common fusion in MASC, which is the junction of exon 5 of *ETV6* and exon 15 of *NTRK3* genes by single-round RT-PCR. In the present study, we used the more sensitive, nested RT-PCR,[16] and consequently we revealed the presence of the classical transcript in another 4 cases. In addition, we found 5 cases with atypical junctions. These junctions have not been described in MASC but are relatively common in radiation-induced papillary thyroid carcinoma.[25]

Simultaneously with the RT-PCR study, we performed FISH analysis of our tumors with various break-apart probes. Firstly, we investigated splits in the *NTRK3* gene. This analysis revealed, as in the study of Ito et al,[16] the presence of *ETV6*-positive/*NTRK3*-negative cases. On 2 available samples, we then performed analysis for rearrangement of *NTRK3* homologs *NTRK1* and *NTRK2* but these were negative, similar to the findings of Ito et al[16] In addition to these *NTRK* homologs, we analyzed several kinase genes commonly fused with *ETV6* in hematological malignancies,[27] but we were unable to

TABLE 6. Clinical and Histologic Findings of 25 MASC Cases

Case Number	Age/Sex	Primary Site	Tumor Size (mm)	Capsule	Invasion (LVI, PN)	Septa	Hyalinized Sclerosis
1	31/F	Buccal mucosa	10	Complete	No	No	No
2	24/F	Buccal mucosa	10	Invasive	No	No	No
3	38/F	Parotid	30	Invasive	PN+	+ +	+
4	48/M	Upper lip	10	Invasive	No	+ +	+
5	28/M	Parotid, deep lobe	$50 \times 30 \times 15$	Invasive	PN+	+ +	+ +
6	50/M	Lip	15	Invasive	No	No	No
7	66/F	Parotid	8	Complete	No	No	No
8	17/M	Parotid	$40 \times 35 \times 25$	Invasive	No	No	No
9	60/M	Parotid	$40 \times 35 \times 25$	Invasive	PN+LVI+	+ +	+ + +
10	39/M	Parotid	14	Incomplete	PN+	+	+
11	69/F	Retromolar gingiva	6	Complete	No	No	No
12	35/F	Parotid	$27 \times 15 \times 10$	Incomplete	PN+	+ +	No
13	15/M	Submandibular	18	Invasive	PN+	+ +	+
14	44/M	Submandibular	15	Incomplete	PN+	+ +	+
15	29/M	Parotid	23	Invasive	PN+LVI+	+	+ +
16	74/M	Parotid	$30 \times 30 \times 25$	Invasive	PN+	+	No
17	31/M	Submandibular	30	Invasive	PN+	+ +	+ +
18	73/M	Retromolar gingiva	$15 \times 20 \times 25$	Invasive	No	+	No
19	35/M	Submandibular	25	Invasive	No	+	No
20	77/F	Submandibular	25	Invasive	No	+ +	+ +
21	62/F	Lip	10	Complete	PN+	+	+
22	25/M	Parotid	13	Incomplete	No	+	No
23	62/M	Parotid	$23 \times 20 \times 20$	Incomplete	No	+	No
24	52/M	Submandibular	20	Invasive	No	+	No
25	48/F	Parotid	10	Incomplete	PN+	+ +	+

*PE—subtotal conservative parotidectomy.
†Close margins means distance from tumor < 0,5 mm.
CHT indicates chemotherapy; LN, lymph node; LVI, lymphovascular invasion; NA, not available; NED, no evidence of disease; PN, perineural invasion; RD, residual disease; RT, radiotherapy; SP, superficial parotidectomy.

identify any possible *ETV6* fusion partner. The remainder of our cases fell either firstly into a group with a different exon junction to that tested, or secondly into a group with expression below the detection limit of the methods used, or thirdly into a group with low quality of RNA.

The novel finding in our study is the identification of 5 MASC cases with atypical junctions, exon 4 of *ETV6* with exon 14 of *NTRK3* and exon 5 of *ETV6* with exon 14 of *NTRK3* that have not been described in MASC so far. Moreover, we confirmed the observation of Ito et al[16] that a subset of MASC cases very likely harbors *ETV6* fused with non-*NTRK* genes (*ETV6-X* fusion).

What was a particularly interesting finding of our study is that in both these groups of MASC with atypical junctions and *ETV6-X* fusion, we observed a more aggressive invasive growth pattern in 6/9 (67%) together with more frequent perineural invasion in 5/9 (55%), and lymphovascular invasion in 2/9 (22%) than in the cases with classical *ETV6-NTRK3* fusion. In addition, lymph node metastases were seen in 2 patients, and 1 patient even died of disseminated disease with multiple distant metastases. This is in accordance with recent observation of Ito et al,[16] who published 2 cases of *ETV6-X* fusion MASC with invasive histologic features including perineural or vascular involvement—this is in contrast with

the generally low-grade behavior of MASC. Nevertheless, in our series, even MASC cases with the classical *ETV6-NTRK3* fusion often displayed an invasive growth pattern (12/16) as well as perineural invasion (6/16) but lymphovascular invasion was not seen.

Ito et al[16] have also suggested that MASC cases with *ETV6-X* fusion may have distinctive histomorphology, in particular, thick fibrous septa and abundant hyalinized stroma. We have found extensive hyalinized stromal fibrosis in 4/16 cases of MASC with classical *ETV6-NTRK3* fusion transcript, remaining 12 cases were devoid of extensive central fibrosclerotic foci. Thick fibrous septa were observed in most cases of MASC with classical fusion (11/16). The MASC cases with atypical exon junctions *ETV6-NRTK3* and *ETV6-X* fusions displayed more often central hyalinized fibrosis in 6/9 (66%) and thick fibrous septa in 7/9 (77%) than MASC with classical *ETV6-NTRK3* fusion.

In conclusion, the present study indicates that *ETV6* may fuse with genes other than *NTRK3*, or a subset of MASC cases may display atypical exon junctions *ETV6-NTRK3*. Our preliminary results also suggest that these atypical molecular features may be associated with more infiltrative histologic features of MASC, and less favorable clinical outcomes in patients, though the

TABLE 6. (*Continued*)

Surgical Margins	TNM	Metastasis (y, mo)	Local Recurrence (y, mo)	Treatment	Follow-up (y,mo)	Outcome
Clear	T1N0M0	No	No	Excision	11 mo	NED
Positive	T1N1M0	LN 2 y	Multiple 2 y	Excision	2 y, 4 mo	RD
Positive	pT2/cN0/cM0		rpT3 (19 y)	Excision, RT	19 y	NED
Positive	T1N0M0	No	rpT2 (2 mo)	Excision, re-excision margins clear	9 mo	NED
Positive	T3N0M0	No	No	*PE, RT	11 mo	NED
Positive	NA	NA	NA	NA	NA	NA
Clear	T1N0M0	No	No	Excision, SP	1 y, 6 mo	NED
Clear	T2N0M0	No (0/0)	No	Excision	12 y	NED
Positive	T4aN2bM1	LN 4 mo lung, liver, bones 10 mo	4 mo excision	Excision, RT	1 y, 8 mo	DOD
Close†	T2N0M0	No	No	SP	3 y, 1 mo	NED
Clear	T1N0M0	No	No	Excision	2 y	NED
Clear	pT2NxMx	No	No	Excision	4 y	NED
Close†	T3N2bM0	LN +	No	Excision, RT	4 y	NED
Positive	T1N0M0	No	No	Resection	4 y, 11 mo	NED
Positive	T2N1M0	LN+	No	Local excision, RT no neck dissection	2 y, 10 mo	NED
Positive	T2N0M0	No	No	Excision RT, CHT	8 y	NED
Positive	pT3pN0M0	No	Residual tumor	Excision, radical resection (1 mo)	2 y	NED
Positive	T2N2M0	LN+	NA	NA	NA	NA
Clear	T2N2M0	LN + (3/36)	No	Excision, RT	4 y, 2 mo	NED
Clear	T2N0M0	No	No	Excision	1 y, 6 mo	NED
Clear	T1N0M0	No	No	Wide local excision	3 y	NED
Clear	T1N0M0	No	No	Excision	1 y, 3 mo	NED
Close†	T3N1M0	No (0/2)	No	Excision	7 y, 6 mo	NED
	T1N0M0	NA	NA	Excision	NA	NA
Close†	pT1N0M0	No	No	Excision	1 y, 3 mo	NED

numbers of published cases are low so far. Currently, molecular confirmation is considered the gold standard for the diagnosis of MASC, but there is growing body of evidence that the majority of tumors (up to 95%) can be accurately classified as MASC based solely on morphology and immunohistochemistry.[28] Recognizing MASC and testing for *ETV6* rearrangement may be, however, of potential value in patient treatment, because the presence of the *ETV6-NTRK3* translocation may represent a therapeutic target in MASC. Recent studies suggested

that the inhibition of *ETV6-NTRK3* activation could serve as a therapeutic target for the treatment of patients with this fusion at other sites.[29,30]
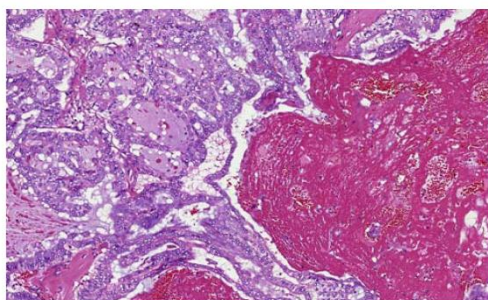

FIGURE 3. MASC (case 20, *ETV6-X* fusion) was composed of predominantly papillary and macrocystic structures.
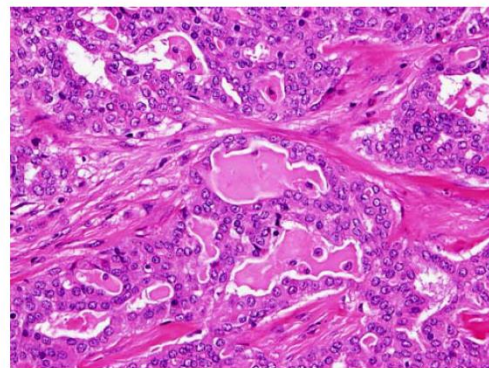

FIGURE 4. MASC composed of multilobular structure divided by thick hyalinized fibrous septa with microcystic and slightly dilated glandular spaces filled with variable amount of eosinophilic homogenous secretory material.
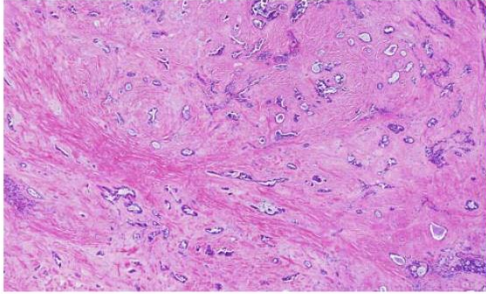
116

FIGURE 5. MASC (case 15, *ETV6-X* fusion) shows a prominent fibrosclerotic stroma with isolated tumor cells in small islands or trabeculae.
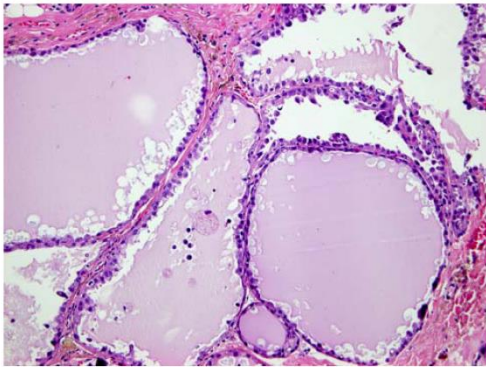

FIGURE 6. MASC with macrocystic growth pattern, in which larger cystic structures were lined mostly by a single, and focally a double layer of cells with prominent or focal apocrine differentiation including hobnail cells.
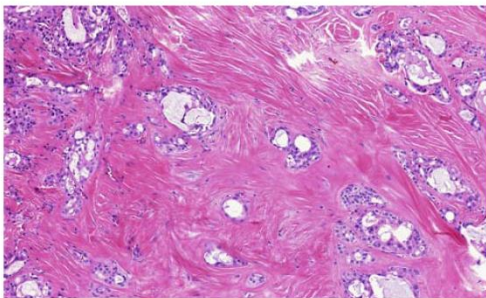

FIGURE 7. Thick fibrous septa with prominent hyalinization and trabeculae of neoplastic cells embedded in a completely hyalinized central part of the tumor were typical for *ETV6-X* fusion (case 17).
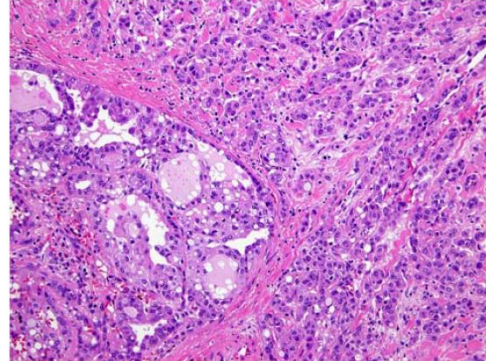
FIGURE 8. MASC with high-grade transformation was seen in 1 patient (case 9, atypical *ETV6/NTRK3* fusion). The tumor was composed of 2 distinct carcinomatous components.

REFERENCES

1. Skalova A, Vanecek T, Sima R, et al. Mammary analogue secretory carcinoma of salivary glands, containing the *ETV6-NTRK3* fusion gene: a hitherto undescribed salivary gland tumor entity. *Am J Surg Pathol.* 2010;34:599–608.
2. Tognon C, Knezevich SR, Huntsman D, et al. Expression of the *ETV6-NTRK3* gene fusion as a primary event in human secretory breast carcinoma. *Cancer Cell.* 2002;2:367–376.
3. Griffith C, Seethala R, Chiosea SI. Mammary analogue secretory carcinoma: a new twist to the diagnostic dilemma of zymogen granule poor acinic cell carcinoma. *Virchows Arch.* 2011;459:117–118.
4. Connor A, Perez-Ordoñez B, Shago M, et al. Mammary analog secretory carcinoma of salivary gland origin with the *ETV6* gene rearrangement by FISH: expanded morphologic and immunohistochemical spectrum of a recently described entity. *Am J Surg Pathol.* 2012;36:27–34.
5. Chiosea SI, Griffith C, Assad A, et al. The profile of acinic cell carcinoma after recognition of mammary analog secretory carcinoma. *Am J Surg Pathol.* 2012;36:343–350.
6. Chiosea SI, Griffith C, Assad A, et al. Clinicopathological characterization of mammary analogue carcinoma of salivary glands. *Histopathology.* 2012;61:387–394.
7. Laco J, Švajdler M Jr, Andrejs J, et al. Mammary analogue secretory carcinoma of salivary glands: a report of 2 cases with

expression of basal/myoepithelial markers (calponin, CD10 and p63 protein). *Pathol Res Pract.* 2013;209:167–172.

8. Bishop JA, Yonescu R, Batista D, et al. Utility of mammaglobin immunohistochemistry as a proxy marker for the ETV6-NTRK3 translocation in the diagnosis of salivary mammary analogue secretory carcinoma. *Hum Pathol.* 2013;44:1982–1988.

9. Bishop JA. Unmasking MASC: bringing to light the unique morphologic, immunohistochemical and genetic features of the newly recognized mammary analogue secretory carcinoma of salivary glands. *Head Neck Pathol.* 2013;7:35–39.

10. Patel KR, Solomon IH, El-Mofty SK, et al. Mammaglobin and S-100 immunoreactivity in salivary carcinomas other than mammary analogue secretory carcinoma. *Hum Pathol.* 2013;44:2501–2508.

11. Majewska H, Skálová A, Stodulski D, et al. Mammary analogue secretory carcinoma of salivary glands: first retrospective study of a new entity in Poland with special reference to *ETV6* gene rearrangement. *Virchows Arch.* 2015;466:245–254.

12. Urano M, Nagao T, Miyabe S, et al. Characterization of mammary analogue secretory carcinoma of salivary gland: discrimination from its mimics by the presence of the *ETV6-NTRK3* translocation and novel surrogate marker. *Hum Pathol.* 2015;46:94–103.

13. Bishop JA. Mammary analog secretory carcinoma of salivary glands: review of new entity with emphasis on differential diagnosis. *Pathol Case Rev.* 2015;20:7–12.

14. Bishop JA, Yonescu R, Batista D, et al. Most nonparotid "acinic cell carcinomas" represent mammary analog secretory carcinomas. *Am J Surg Pathol.* 2013;37:1053–1057.

15. Luo W, Lindley SW, Lindley PH, et al. Mammary analog secretory carcinoma of salivary gland with high-grade histology arising in palate, report of a case and review of literature. *Int J Clin Exp Pathol.* 2014;7:9008–9022.

16. Ito Y, Ishibashi K, Masaki A, et al. Mammary analogue secretory carcinoma of salivary glands: a clinicopathological and molecular study including 2 cases harboring *ETV6-X* fusion. *Am J Surg Pathol.* 2015;39:602–610.

17. Viswanatha DS, Foucar K, Berry BR, et al. Blastic mantle cell leukemia: an unusual presentation of blastic mantle cell lymphoma. *Mod Pathol.* 2000;13:825–833.

18. Gaffney R, Chakerian A, O'Connell JX, et al. Novel fluorescent ligase detection reaction and flow cytometric analysis of SYT-SSX fusions in synovial sarcoma. *J Mol Diagn.* 2003;5:127–135.

19. Antonescu CR, Kawai A, Leung DH, et al. Strong association of SYT-SSX fusion type and morphologic epithelial differentiation in synovial sarcoma. *Diagn Mol Pathol.* 2000;9:1–8.

20. Bourgeois JM, Knezevich SR, Mathers JA, et al. Molecular detection of the ETV6-NTRK3 gene fusion differentiates congenital fibrosarcoma from other childhood spindle cell tumors. *Am J Surg Pathol.* 2000;24:937–946.

21. Knezevich SR, McFadden DE, Tao W, et al. A novel ETV6-NTRK3 gene fusion in congenital fibrosarcoma. *Nat Genet.* 1998;18:184–187.

22. Rubin BP, Chen CJ, Morgan TW, et al. Congenital mesoblastic nephroma t(12;15) is associated with ETV6-NTRK3 gene fusion: cytogenetic and molecular relationship to congenital (infantile) fibrosarcoma. *Am J Pathol.* 1998;153:1451–1458.

23. Kralik JM, Kranewitter W, Boesmueller H, et al. Characterization of a newly identified ETV6 NTRK3 fusion transcript in acute myeloid leukemia. *Diagn Pathol.* 2011;6:19.

24. Alassiri A, Lum A, Goytain A, et al. *ETV6-NTRK3* is expressed in a subset of ALK-negative inflammatory myofibroblastic tumors: case series of 20 patients. *Mod Pathol.* 2015;28:36.

25. Leeman-Neill RJ, Kelly LM, Liu P, et al. *ETV6-NTRK3* is a common chromosomal rearrangement in radiation-associated thyroid cancer. *Cancer.* 2014;120:799–807.

26. Skálová A, Vanecek T, Majewska H, et al. Mammary analogue secretory carcinoma of salivary glands with high-grade transformation: report of 3 cases with the *ETV6-NTRK3* gene fusion and analysis of TP53, beta-catenin, EGFR, and CCND1 genes. *Am J Surg Pathol.* 2014;38:23–33.

27. De Braekeleer E, Douet-Guilbert N, Morel F, et al. ETV6 fusion genes in hematological malignancies: a review. *Leuk Res.* 2012; 36:945–961.

28. Shah AA, Wenig BM, LeGallo RD, et al. Morphology in conjunction with immunohistochemistry is sufficient for the diagnosis of mammary analogue secretory carcinoma. *Head Neck Pathol.* 2015;9:85–95.

29. Chi HT, Ly BT, Kano Y, et al. *ETV6-NTRK3* as a therapuetic target of small molecule inhibitor PKC412. *Biochem Biophys Res Commun.* 2012;429:87–92.

30. Tognon CE, Somasiri AM, Evdokimova VE, et al. *ETV6-NTRK3*-mediated breast epithelial cell transformation is blocked by targeting the IGF1R signaling pathway. *Cancer Res.* 2011;71:1060–1070.

Molecular Profiling of Mammary Analog Secretory Carcinoma Revealed a Subset of Tumors Harboring a Novel *ETV6-RET* Translocation

Report of 10 Cases

Alena Skalova, MD, PhD,*† Tomas Vanecek, PhD,‡ Petr Martinek, PhD,‡ Ilan Weinreb, MD,§
Todd M. Stevens, PhD,‖ Roderick H.W. Simpson, MD, MB, ChB, FRCPath,¶
Martin Hyrcza, MD, PhD,# Niels J. Rupp, MD,** Martina Baneckova, MD,*†
Michael Michal, Jr, MD,*†† David Slouka, MD, MBA, PhD,‡‡ Tomas Svoboda, MD, PhD,§§
Alena Metelkova, MD, PhD,‖‖ Arghavan Etebarian, DDS, OMP,¶¶
Jaroslav Pavelka, PhD,‡## Steven J. Potts, PhD,*** Jason Christiansen, PhD,***
Petr Steiner, MSc,*‡ and Michal Michal, MD*

Abstract: *ETV6* gene abnormalities are well described in tumor pathology. Many fusion partners of *ETV6* have been reported in a variety of epithelial, mesenchymal, and hematological malignancies. In salivary gland tumor pathology, however, the *ETV6-NTRK3* translocation is specific for (mammary analog) secretory carcinoma, and has not been documented in any other salivary tumor type. The present study comprised a clinical, histologic, and molecular analysis of 10 cases of secretory carcinoma, with typical morphology and immunoprofile harboring a novel *ETV6-RET* translocation.

(M)ammary analog) secretory carcinoma of salivary gland origin is a recently described tumor that harbors a characteristic balanced t(12;15)(p13;q25) chromosomal translocation resulting in an *ETV6-NTRK3* fusion[1] identical to that commonly found in secretory carcinoma (SC) of the breast.[2] The *ETV6-NTRK3* fusion gene encodes a chimeric tyrosine kinase with transforming activity in epithelial and myoepithelial cells in the mouse mammary gland.[3]

Over many years, Skalova et al[1] began to identify a distinctive, hitherto unrecognized neoplasm arising in the salivary glands characterized by morphologic and immunohistochemical features strongly reminiscent of those of SC of the breast. These salivary carcinomas are composed of microcystic and solid areas with abundant vacuolated colloid-like periodic acid-Schiff-positive secretory material within the microcystic spaces. These tumors had previously been categorized as either unusual variants of salivary acinic cell carcinoma (AciCC) or adenocarcinoma not otherwise specified.[1]

Salivary SC was initially recognized as an entity different from AciCC on the basis of 3 major findings.[1] First, SC showed no basophilia in the cytoplasm of any of the constituent cells, which is the hallmark of the serous acinar cells of AciCC resulting from the presence of cytoplasmic zymogen granules. Second, these neoplasms had a completely different immunohistochemical profile, almost always expressing S100 protein, mammaglobin, vimentin, STAT5, and MUC4, all of which are rarely expressed in AciCC. Finally, SCs were found to harbor an

TABLE 1. Antibodies Used for Immunohistochemical Study

Antibody Specificity	Clone	Dilution	Antigen Retrieval/Time (min)	Source
S100 protein	Polyclonal	RTU	CC1/20	Ventana
CK7	OV-TL 12/30	1:200	CC1/36	Dako Cytomation
GCDFP-15	EP1582y	RTU	CC1/64	Cell Marque
Mammaglobin	304-1A5	RTU	CC1/36	Dako Cytomation
STAT 5a	Polyclonal	1:400	CC1/36	Assay Designs Inc.
Ki-67	30-9	RTU	CC1/64	Ventana
P63	4A4	RTU	CC1/64	Ventana
DOG1	SP31	RTU	CC1/36	Cell Marque
GATA3	L50-823	1:200	CC1/52	BioCare Medical
SOX10	Polyclonal	1:100	CC1/64	Cell Marque

CC1 indicates EDTA buffer, pH 8.6; RTU, ready to use (prediluted).

ETV6-NTRK3 fusion gene due to a t(12; 15)(p13,q25) translocation, a finding identical to SC of the breast[2] and absent in AciCCs.[1] Because of the morphologic similarities and identical *ETV6-NTRK3* fusion transcripts, the designation "mammary analog secretory carcinoma of salivary gland" has been proposed,[1] and the name was widely accepted and used in the literature. The most recent version of the World Health Organization Classification of Head and Neck Tumors, however, utilizes the terminology "secretory carcinoma"[4] for consistency, and because SCs have been recently described at other extrasalivary and extramammary sites, such as thyroid gland,[5–8] skin,[9,10] and sinonasal mucosa.[11]

The presence of the *ETV6-NTRK3* fusion gene has not been demonstrated in any other salivary gland tumor, but the same translocation can be seen not only in SC of breast,[2] but also in infantile fibrosarcoma,[12] congenital mesoblastic nephroma,[13] certain hematopoietic malignancies,[14] ALK-negative inflammatory myofibroblastic tumors,[15] a small subset of gastrointestinal stromal tumors,[16] and in radiation-induced papillary thyroid carcinomas.[17] Moreover, *ETV6-NTRK3* translocated papillary thyroid cancers have been recently described in adult patients with no history of radiation exposure.[18]

The near 100% rate of *ETV6* gene rearrangement in SC has been subsequently confirmed by many other studies.[19–25] Detection of *ETV6* rearrangements by fluorescent in situ hybridization (FISH) or the *ETV6-NTRK3* fusion by reverse-transcriptase polymerase chain reaction (RT-PCR) in formalin-fixed paraffin-embedded (FFPE) material is technically relatively straightforward and >300 cases of SC have been published since its original description.

Up until now, in all published cases of SC where the fusion partner is identified, *ETV6* is fused with *NTRK3*, and no other fusion partners have been reported so far. Nevertheless, for several years, we have been aware of several SC cases positive for the *ETV6* gene split as visualized by FISH, but in which the classic *ETV6-NTRK3* fusion transcript (exon 5-exon 15 junction) was not detected by standard RT-PCR. A subset of SCs showing *ETV6* rearrangements with so far unknown partners have been recently reported and provisionally called *ETV6-X* translocated SCs,[26] in agreement with a study of Ito et al,[27] who found 2 such cases. In the present study using the next-generation sequencing (NGS) as a diagnostic platform, we describe 10 cases morphologically and immunohistochemically typical of SC, harboring a novel *ETV6-RET* translocation.

MATERIALS AND METHODS

Among >4500 cases of primary salivary gland tumors, 194 cases of SCs were retrieved from the consultation files of the Salivary Gland Tumor Registry, at

TABLE 2. Primers for Detection of *ETV6-NTRK3* Fusion Transcripts

Original Primer Name	Sequence	Annealing Temperature (°C)	Localization
ETV6-ex4-F3	AGCCGGAGGTCATACTGCAT	55	ETV6 exon 4 inner
ETV6-ex4-F4	CATTCTTCCACCCTGGAAAC	55	ETV6 exon 4 outer
ETV6B†	ACATCATGGTCTCTGTCTCCCCGC	55	ETV6 exon 5 inner
TEL971* (ETV6A†)	ACCACATCATGGTCTCTGTCTCCC	65	ETV6 exon 5 outer
NTRK3-ex14-R1	GTGATGCCGTGGTTGATGT	55	NTRK3 exon 14 inner
NTRK3 ex14-R2	AGTCATGCCAATGACCACAG	55	NTRK3 exon 14 outer
NTRK3B†	TTCTCGCTTCAGCACGATGCT	55	NTRK3 exon 15 inner
TRKC1059* (NTRK3A†)	CAGTTCTCGCTTCAGCACGATG	65	NTRK3 exon 15 outer
ETV6-Archer1-F1	CGATGGGAGGACAAAGAATC	55	ETV6 exon 6
RET-Archer1-R1	AACCAAGTTCTTCCGAGGGA	55	RET exon 12
ETV6-Archer1-F2	CAACGGACTGGCTCGACTG	55	ETV6 exon 6
RET-Archer1-R2	GACCACTTTTCCAAATTCGCCT	55	RET exon 12

*Bourgeois et al[32]
†Ito et al,[27] Skalova et al.[26]

FIGURE 1. A, The result of analysis by NGS with custom-designed ArcherDX Kit of case 3 (case 17 in Skalova et al[26]). Analysis revealed the presence of fusion transcript *ETV6-RET* joining exons 6 and 12, respectively. The red arrows represent position of primers. B, The confirmation of the presence of *ETV6-RET* fusion transcript by RT-PCR followed by Sanger sequencing. The black arrow indicates area of fusion.

the Department of Pathology, Faculty of Medicine in Plzen, and Biopticka Laborator Ltd, Plzen, Czech Republic (A.S. and M.M.).

The histopathologic features of all tumors and the immunohistochemical stains, when available, were reviewed by 2 pathologists (A.S. and M.B.). A diagnosis of SC was confirmed in cases that displayed, at least focally, histologic features consistent with original description[1] in conjunction with the appropriate immunohistochemical profile, that is, coexpression of S100 protein, cytokeratin CK7, and mammaglobin with the absence of p63 and DOG1 staining. For the purpose of this particular study, we have included 4 cases of SC with *ETV6-X* profile from study Skalova et al[26] and 26 cases of SC with *ETV6* gene break found by FISH or with morphologic and immunohistochemical pattern of SC but without analyzable *ETV6* gene break by FISH due to low quality or lack of material. Thus, a total of 30 SC cases were studied by NGS using ArcherDX Fusion Plex Kit.

For conventional microscopy, the excised tissues were fixed in formalin, routinely processed, embedded in paraffin (FFPE), cut, and stained with hematoxylin and eosin. In most cases, additional stains were also performed, including periodic acid-Schiff with and without diastase, mucicarmine, and alcian blue at pH 2.5.

For immunohistochemical studies, 4 μm thick sections were cut from paraffin blocks and mounted on positively charged slides (TOMO, Matsunami Glass Ind., Japan). Sections were processed on a BenchMark ULTRA (Ventana Medical System, Tucson, AZ), deparaffinized, and then subjected to heat-induced epitope retrieval by immersion in a CC1 solution at pH 8.6 at 95°C. After antigen retrieval, sections were stained with a pan-RTK antibody cocktail consisting of rabbit monoclonal

antibodies, all obtained from Cell Signaling (Danvers, MA), targeting pan-Trk (A7H6R, active against TrkA, TrkB, and TrkC, 1:50 dilution), ROS1 (D4D6, 1:50), and ALK (D5F3, 1:50), as described previously.[28]

All other primary antibodies used are summarized in Table 1. The bound antibodies were visualized using the ultraView Universal DAB Detection Kit (Roche) and ultraView Universal Alkaline Phosphatase Red Detection Kit (Roche). The slides were counterstained with the Mayer hematoxylin. Appropriate positive and negative controls were used.

Clinical follow-up was obtained from the patients, their physicians, or from referring pathologists.

Molecular Genetic Study

Detection of ETV6-NTRK3 and ETV6-RET Fusion Transcripts by RT-PCR

RNA was extracted using the RecoverAll Total Nucleic Acid Isolation Kit (Ambion, Austin, TX). cDNA was synthesized using the Transcriptor First Strand cDNA Synthesis Kit (RNA input 500 ng; Roche Diagnostics, Mannheim, Germany). All procedures were performed according to the manufacturer's protocols. Amplification of a 105 and 133 bp product of the μ2-microglobulin gene and 247 bp product of the *PGK* gene was used to test the quality of the extracted RNA as previously described.[29–31] A detection of classic exon 5 of *ETV6* gene and exon 15 of *NTRK3* gene,[32] as well as atypical exon 4 of the *ETV6* gene and exon 14 of the *NTRK3* gene (and their combinatorial variants) fusion transcript was performed by RT-PCR. In addition, more sensitive, nested RT-PCR was performed for the detection of classic[26,27] as well as selected atypical junction of transcripts. Except that,
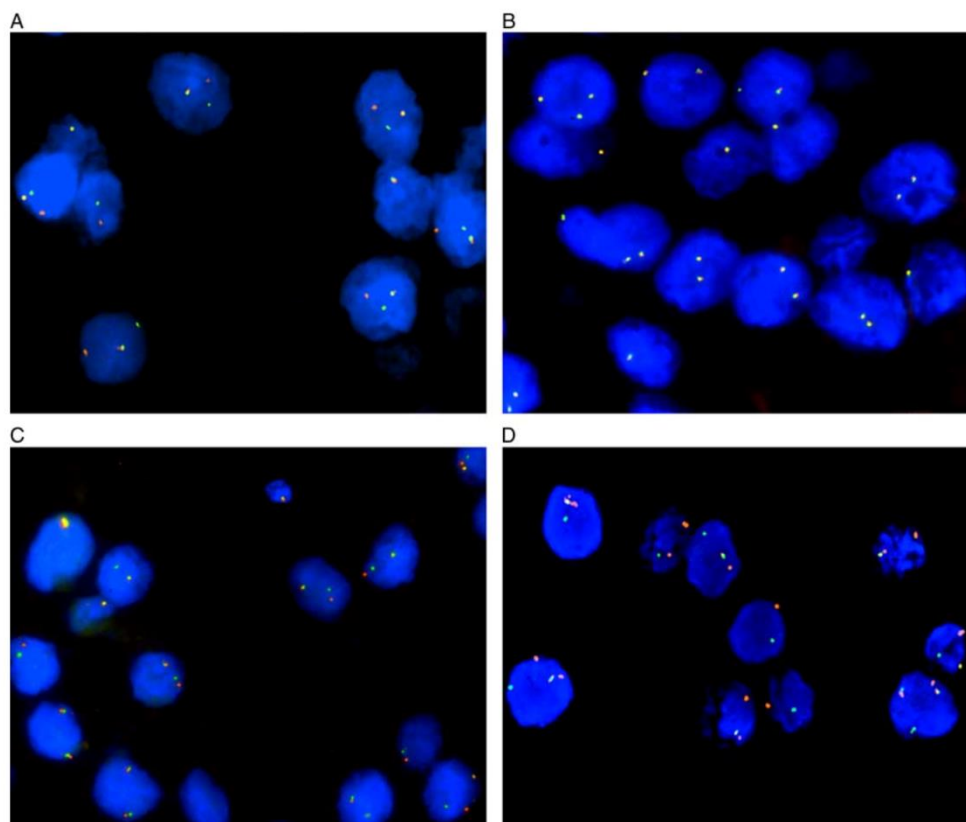
FIGURE 2. Interphase FISH analysis using break-apart probes (A–C) and dual-fusion probe (D). Positive cells with break-apart *ETV6* (A) and *RET* (C) probes contain nucleus with separate (split) orange and (or) green signals indicating a rearrangement (break) of 1 copy of the gene region and also 1 orange/green (yellow) fusion signal representing 1 normal (intact) copy of homolog locus. Negative cells with break-apart *NTRK3* (B) probe contain only normal (not split) yellow signal. Positive cells using fusion probe *ETV6-RET* (D) show orange/green (yellow) fusion signals representing translocation *ETV6-RET* and also separate orange and green signals showing the intact genes.

RT-PCR for *ETV6-RET* fusion transcript detection was also carried out after receiving of the NGS results.

For single-round PCR, 2 L of cDNA was added to reaction consisting of 12.5 μL of HotStar Taq PCR Master Mix (QIAgen, Hilden, Germany), 10 pmol of each primer (Table 2), and distilled water up to 25 μL. The amplification program comprised denaturation at 95°C for 14 minutes and then 45 cycles of denaturation at 95°C for 1 minute, annealing at temperature seen in Table 2 for 1 minute and extension at 72°C for 1 minute. The program was finished by incubation at 72°C for 7 minutes. For nested PCR, the same reaction conditions were utilized. One microliter of PCR product from the first round was used as a template.

Successfully amplified PCR products were purified with magnetic particles of Agencourt AMPure (Agencourt

Bioscience Corporation, A Beckman Coulter Company, Beverly, MA). Products were then bidirectionally sequenced using Big Dye Terminator Sequencing Kit (Applied Biosystems, Foster City, CA), and purified with magnetic particles of Agencourt CleanSEQ (Agencourt Bioscience Corporation), all according to the manufacturer's protocol, and run on an automated sequencer ABI Prism 3130xl (Applied Biosystems) at a constant voltage of 13.2 kV for 11 minutes.

Detection of Alteration of ETV6, NTRK3, and RET Genes by FISH Method

Four-micrometer-thick FFPE sections were placed onto positively charged slides. Hematoxylin and eosin–stained slides were examined for determination of areas for cell counting.

122

TABLE 3. Molecular Genetics Findings in 10 Cases of SC With *ETV6-RET* Fusion

Case #	Case #	NGS Results	Fusion	FISH ETV6ba	FISH NTRK3ba	RT-PCR ETV6-NTRK3	FISH RETba	FISH ETV6-RET	RT-PCR ETV6-RET
1	6*	+	*ETV6-RET*	+	−	−	+	+	+
2	15*	+	*ETV6-RET*	+	−	−	+	ND	+
3	17*	+	*ETV6-RET*	+	−	−	+	+	+
4	20*	+	*ETV6-RET*	+	−	−	+	+	−
5		+	*ETV6-RET*	+	−	−	+	+	+
6		+	*ETV6-RET*	ND	ND	−	ND	+	+
7		+	*ETV6-RET*	+	−	−	+	+	+
8		+	*ETV6-RET*	NA	NA	−	NA	+	+
9		+	*ETV6-RET*	ND	ND	−	ND	ND	−
10	12†	+	*ETV6-RET*	+	−	−	+	+	+

*Skalova et al[26] (Table 6).
†Stevens et al[8] (Table 2).
NA indicates not analyzable; ND, not done due to lack of material.

The unstained slides were routinely deparaffinized and incubated in the ×1 Target Retrieval Solution Citrate pH 6 (Dako, Glostrup, Denmark) at 95°C for 40 minutes and subsequently cooled for 20 minutes at room temperature in the same solution. Slides were washed in deionized water for 5 minutes and digested in protease solution with Pepsin (0.5 mg/mL; Sigma Aldrich, St Louis, MO) in 0.01 M HCl at 37°C for 25 to 60 minutes, according to the sample conditions. Slides were then placed into deionized water for 5 minutes, dehydrated in a series of ethanol solutions (70%, 85%, 96% for 2 min each), and air dried.

Two commercial probes were used for the detection of rearrangement of *ETV6* and *RET* genes, Vysis ETV6 Break Apart FISH Probe Kit (Vysis/Abbott Molecular, IL) and ZytoLight SPEC RET Dual Color Break Apart Probe (ZytoVision GmbH, Bremerhaven, Germany). ETV6 probe was mixed with water and LSI/WCP (Locus-Specific Identifier/Whole Chromosome Painting) Hybridization buffer (Vysis/Abbott Molecular) in a 1:2:7 ratio, respectively. RET probe was factory premixed.

Probes for detection of rearrangement of *NTRK3* gene region and *ETV6-RET* genes fusion were mixed from custom designed SureFISH probes (Agilent Technologies Inc., Santa Clara, CA). Chromosomal regions for *NTRK3* break-apart probe oligos are chr15:87501469-88501628 and chr15:88701444-89700343; for *ETV6-RET* fusion probe, chr12:11675872-12175711 and chr10:43354893-43849282. Probe mixture was prepared from corresponding probes (each color was delivered in a separate well), deionized water, and LSI Buffer (Vysis/Abbott Molecular) in a 1:1:1:7 ratio, respectively.

An appropriate amount of mixed and premixed probes was applied on specimens, covered with a glass coverslip, and sealed with rubber cement. Slides were incubated in the ThermoBrite instrument (StatSpin/Iris Sample Processing, Westwood, MA) with codenaturation at 85°C for minutes and hybridization at 37°C for hours. Rubber cemented coverslip was then removed and the slide was placed in posthybridization wash solution (2×SSC/0.3% NP-40) at 72°C for 2 minutes. The slide was air dried in the dark, counterstained with 4′,6′-diamidino-2-phenylindole DAPI (Vysis/Abbott Molecular), coverslipped, and immediately examined.

FISH Interpretation

The sections were examined with an Olympus BX51 fluorescence microscope (Olympus Corporation, Tokyo, Japan) using a ×100 objective and filter sets Triple Band Pass (DAPI/SpectrumGreen/SpectrumOrange), Dual Band Pass (SpectrumGreen/SpectrumOrange), and Single Band Pass (SpectrumGreen or SpectrumOrange).

TABLE 4. Details of NGS Analysis by the Archer Platform in 10 Cases of SC With *ETV6-RET* Translocation

Case #	Case #	NGS Results	Fusion	Exons Included in Fusion	No. Valid Fusion Read	% of Reads Supporting Fusion	No. Unique Start Sites
1	Case 6*	+	ETV6-RET	6-12	51	100	17
2	Case 15*	+	ETV6-RET	6-12	84	20.1	33
3	Case 17*	+	ETV6-RET	6-12	1126	23.5	183
4	Case 20*	+	ETV6-RET	6-12	15	1.8	10
5		+	ETV6-RET	6-12	163	11.4	63
6		+	ETV6-RET	6-12	21	100	11
7		+	ETV6-RET	6-12	49	14	32
8		+	ETV6-RET	6-12	100	86.2	51
9		+	ETV6-RET	6-12	41	60.3	14
10	Case 12†	+	ETV6-RET	6-12	24	14.8	17

*Skalova et al[26] (Table 6).
†Stevens et al[8] (Table 2).

TABLE 5. Clinical Findings in 10 SCs With *ETV6-RET* Fusion Transcript

Case #	Age/ Sex	Case #	Stadium TNM	Local Recurrence	Length of Symptoms	Metastasis (y, mo)	Treatment	Follow-up	Outcome
1	50/M	Case 6*	NA	NA		NA	NA	NA	NA
2	29/M	Case 15*	pT2pN1M0	No	6 y	LN+	SP and RT, no neck dissection	4 y 6 mo	Alive NED
3	31/M	Case 17*	pT3pN0M0	Residual tumor	7 y	No	Excision radical resection (1 mo)	4 y	Alive NED
4	77/F	Case 20*	pT2N0M0	No	1 y	No	Excision, RT	3 y	DOC
5	51/M		pT3N0M0	Residual tumor	15 mo	No	Excision SP after 3 mo	8 mo	Alive NED
6	20/F		pT3N0M0	No	NA	No	PE	NA	NA
7	55/M		pT3N0M3	No	3 y	Multiple bone meta (pelvic, scapula) at 15 mo	PP, RT, and CHT	2 y	DOD
8	28/F		pT1N0M0	No	1 mo	No	Parotid resection and lymphadenectomy level II: 12 lymph nodes negative	2 y	Alive NED
9	33/M		pT1pN0 (0/2)	No	6 mo	No	PP	3 y 9 mo	Alive NED
10	34/M	Case 12†	pT2N0M0 (0/1)	No	Several months, very slow enlargement	No	SP	4 y 2 mo	Alive NED

*Skalova et al[26] (Table 6).
†Stevens et al[8] (Table 2).
CHT indicates chemotherapy; DOC, dead of other causes; DOD, dead of disease; LN, lymph nodes; NA, not available; NED, no evidence of disease; PE, parotidectomy; PP, partial parotidectomy; RT, radiotherapy; SP, superficial parotidectomy.

For each probe, 100 randomly selected nonoverlapping tumor cell nuclei were examined for the presence of yellow or green and orange fluorescent signals. Regarding break-apart probes, yellow signals were considered negative, and separate orange and green signals were considered positive; conversely, for fusion probe, yellow signals were considered positive, and separate orange and green signals were considered negative.

Cutoff values were set to > 10% and 20% of nuclei (break-apart and fusion probes, respectively) with chromosomal breakpoint signals (mean, +3 SD rounded up in normal non-neoplastic control tissues).

Sample Preparation for NGS

For NGS studies, 2 to 3 FFPE sections (10 µm thick) were macrodissected to isolate tumor-rich regions. Samples were extracted for total nucleic acid using Agencourt FormaPure Kit (Beckman Coulter, Brea, CA) following the corresponding protocol with an overnight digest and an additional 80°C incubation as described in modification of the protocol by ArcherDX (ArcherDX Inc., Boulder, CO). Total nucleic acid was quantified using the Qubit Broad Range RNA Assay Kit (Thermo Fisher Scientific) and 2 µL of sample.

RNA Integrity Assessment and Library Preparation for NGS

Unless otherwise indicated, 250 ng of FFPE RNA was used as input for NGS studies. To assess RNA quality, the PreSeq RNA QC Assay using iTaq Universal SYBR Green Supermix (Biorad, Hercules, CA) was performed on all samples during library preparation to generate a measure of the integrity of RNA (in the form of a cycle threshold value). Library preparation and RNA QC were performed following the Archer Fusion Plex Protocol for Illumina (ArcherDX Inc.). A custom primer set with 28 primers spanning regions on 3 specific genes of interest, including all 8 exons of *ETV6* gene in 3′ direction, was designed and used. Final libraries were diluted 1:100,000 and quantified in a 10 µL reaction following the Library Quantification for Illumina Libraries protocol and assuming a 200 bp fragment length (KAPA, Wilmington, MA). The concentration of final libraries was around 200 nM. The threshold representing the minimum molar concentration for which sequencing can be robustly performed was set at 50 nM.

NGS and Analysis

Libraries were sequenced on a MiSeq sequencer (Illumina, San Diego, CA). They were diluted to 4 nM and equal amounts of up to 16 libraries were pooled per run. The optimal number of raw reads per sample was set to 500,000. Library pools were diluted to 16 pM library stock with 5% 12.5 pM PhiX and loaded into the MiSeq cartridge. Analysis of sequencing results was performed using the Archer Analysis software (v5; ArcherDX Inc.). Fusion parameters were set to a minimum of 5 valid fusion reads with a minimum of 3 unique start sites within the valid fusion reads.

RESULTS

Molecular Genetic Findings

Selected 30 cases of SC (as described earlier) were analyzed by NGS using the ArcherDX analysis platform.

124

TABLE 6. Clinical and Histologic Findings in 10 SCs With *ETV6-RET* Fusion Transcript

Case #	Age/ Sex	Case #	Location	Tumor Size (mm)	Capsule	Surgical Margins	Thick Fibrous Septa	Hyalinized Sclerosis	Invasion (LVI, PN)	Cystic Pattern	Necrosis	Comments
1	50/M	Case 6*	Lip	15	NA	2	No	No	NA	No	−	Fragmented tissue
2	29/M	Case 15*	Parotid	23	No	1	+	++	PN+, LVI +Extraglandular, muscle invasion	No	−	Hyalinized, multilobular, microcystic, and solid growth pattern
3	31/M	Case 17*	Submand	30	No	2	++	++	PN+	No	−	Hyalinized, multilobular, microcystic
4	77/F	Case 20*	Submand	70	Focal		+	+	No	+	−	Multicystic, papillary with apocrine cells
5	51/M		Parotid	10	No	1	++	++	PN+	No	+	Central hyalinized sclerosis, invasive growth pattern
6	20/F		Parotid	40	No	2	+	+	Extraglandular	No	−	Lobular, microcystic
7	55/M		Parotid	70	No	2	+	+	PN+, perivascular	+	+	High grade component
8	28/F		Parotid	12	No	1	+	+	Intraglandular	No	−	Predominantly solid and microcystic
9	33/M		Parotid	17	+	1	No	No	No	+	−	Predominantly cystic
10	34/M	Case 12†	Parotid	19	+	0	No	No	No	+	−	Multicystic with mural nodules

*Skalova et al[26] (Table 6).
†Stevens et al[8] (Table 2).
Surgical margins: free-0; close (means distance from the tumor <0.5 mm) -1; positive-2.
F indicates female; LVI, lymphovascular invasion; M, male; NA, not available; PN, perineural invasion.

This analysis detected a novel *ETV6-RET* fusion transcript joining exon 6 of *ETV6* gene and exon 12 of *RET* gene in 10 cases of salivary gland tumors displaying histologic and immunohistochemical features typical of SC (Fig. 1). All but 1 *ETV6-RET* positive SC case were then tested by at least 1 FISH probe for the presence of *ETV6-RET* rearrangements (Fig. 2). In case 9, there was no residual tissue material for confirmation of the NGS analysis by FISH tests. In addition, RT-PCR for the confirmation of the presence of *ETV6-RET* fusion transcript followed by Sanger sequencing on positive samples was performed in all 10 cases (Fig. 1). The results of the NGS tests, details of the analysis, and results of confirmatory genetic tests are summarized in Tables 3 and 4. In addition, NGS analysis resulted in detection of the *ETV6-NTRK3* fusion in 15 SC cases. In 4 cases, NGS revealed negative results, and 1 case was unanalyzable (detailed data not shown). No other fusion transcripts different from *ETV6-NTRK3* or *ETV6-RET* were found by NGS in any analyzable case of SC.

Clinical and Histologic Characteristics of the Study Group

The clinical and follow-up data of 10 patients with *ETV6-RET* translocated SC of salivary glands are summarized in Table 5. There were 3 female and 7 male patients. The median patient age was 40.8 years, with a range between 20 and 77 years. The most common anatomic site of involvement was the parotid gland, occurring in 7 patients. Other primary sites of the origin included the submandibular gland and minor salivary gland of the upper lip in 2 patients and 1 patient, respectively.

Follow-up Data

Clinical follow-up data were obtained from 8 patients, and ranged from 6 to 50 months (mean, 36 mo); 2 patients were lost to follow-up. Detailed clinical, follow-up, and histologic findings in 10 patients with *ETV6-RET* translocated SC are summarized in Table 5.

All tumors were treated by surgical excision; in 1 patient the excision was radical with clear surgical margins, in 4 cases the surgical margins were positive, and in 4 additional patients, the tumor infiltration was close (<0.5 mm) to the surgical margins. Five patients underwent subtotal conservative parotidectomy, in 3 of them in combination with radiotherapy (cases 2, 4, and 7). Residual tumors were treated by radical reexcision with clear surgical margins in 2 patients. Concomitant chemotherapy and radiotherapy was used in 1 patient with high-grade transformed SC complicated by metastatic
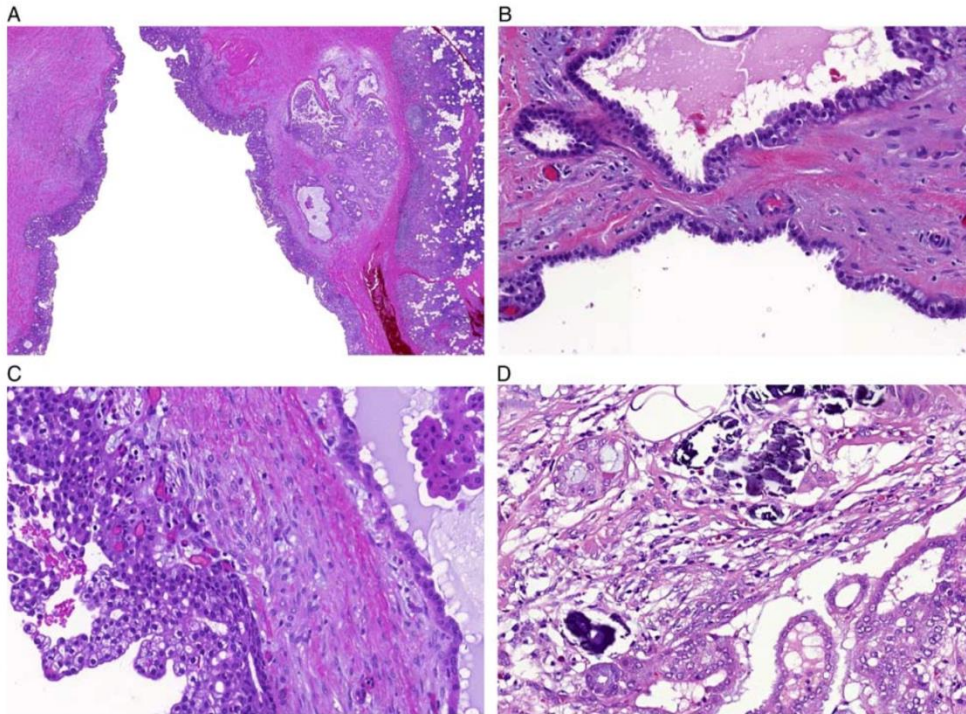
FIGURE 3. A, SC is well circumscribed and surrounded by a thick fibrous capsule enclosing predominantly multicystic growth pattern with multiple mural nodules. The cysts were lined mostly by a single or focally by a double layer of cells with prominent apocrine differentiation including hobnail (B) and vacuolated foamy cells (C). The fibrous capsule and septa comprised psammoma bodies in places (D).

disease at 15 months after surgery (case 7). Clinical and follow-up findings are summarized in Table 5.

Macroscopic Features

Detailed clinical and morphologic findings in 10 patients with *ETV6-RET* translocated SC are summarized in Table 6. The median tumor size was 3.6 cm, with a range of 1.0 to 7.0 cm. Grossly, most tumors were variably invasive: 2 were entirely circumscribed and encapsulated, 1 had focally infiltrative edges, and 7 were predominantly infiltrative.

Microscopic and Immunohistochemical Features

On low power magnification, 3 major growth patterns of SC were identified in our material. First, 3 tumors were well circumscribed and surrounded by a thick, focally uninterrupted, fibrous capsule enclosing a predominantly multicystic growth pattern with multiple mural nodules (Fig. 3A). The cysts were lined mostly by a single or focally by a double layer of cells with prominent apocrine differentiation including hobnail and vacuolated foamy cells (Figs. 3B, C), and contained abundant

proteinaceous eosinophilic material. The fibrous capsule and septa comprised psammomatoid calcifications in some places (Fig. 3D). The second pattern was characterized by solid and microcystic growth with a multilobular structure divided by thin fibrous septa (Fig. 4A). The tumors either lacked a capsule or were only partially encapsulated with prominent infiltrative borders (Fig. 4B). These cases were predominantly composed of microcystic and slightly dilated glandular spaces filled with a variable amount of eosinophilic homogenous secretory material (Fig. 4C). The third pattern, prevailing in 3 cases, comprised a prominent fibrosclerotic stroma with isolated tumor cells in small islands or trabeculae, which were seen in the central part of the tumor (Fig. 5A). In case 7, 2 different growth patterns were seen, in particular low-grade components arranged in multiple macrocystic and microcystic lobules with comedo-like necroses, and high-grade components with limited secretory material and high proliferative activity (Fig. 5B).

However, most tumors demonstrated 2 or more architectural patterns, with microcystic, tubular, solid, and papillary patterns often occurring together. Regardless of
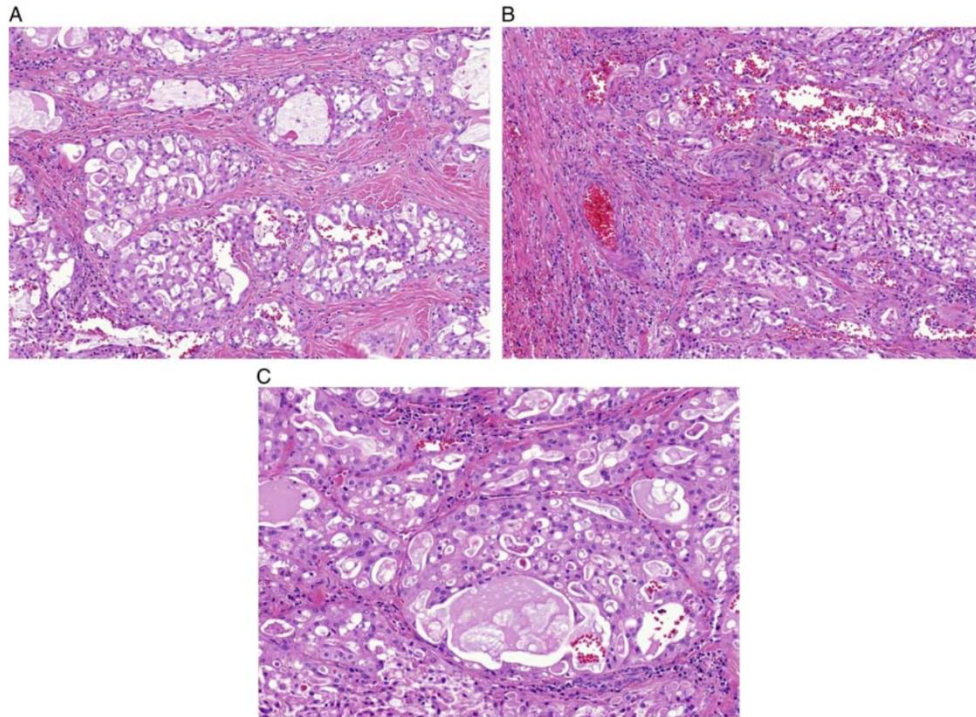
126

FIGURE 4. A, SC is characterized by solid and microcystic growth with a multilobular structure divided by thin fibrous septa. B, The tumor has a prominent infiltrative border. C, The tumor is predominantly composed of microcystic and slightly dilated glandular spaces filled with a variable amount of eosinophilic homogenous secretory material.

the growth pattern of SC, the tumor cells were often bland looking, with abundant pale pink vacuolated and foamy cytoplasm and with vesicular oval nuclei with a single small but prominent nucleolus. The cytologic features were similar from case to case. The range of nuclear atypia was assessed as grades 1 to 3. Mitotic figures were rare and necrosis was absent. Prominent perineural and intraneural invasion was seen in case 7 (Fig. 5C). Only 1 patient (case 2) presented with a single periparotideal lymph node metastasis at the time of diagnosis.

Immunohistochemical Findings

By immunohistochemistry, all examined SC cases were positive for S100 protein (Fig. 6A), mammaglobin (Fig. 6B), typically in strong and diffuse fashion (secretory material was also positive), and cytokeratin CK7 (Fig. 6C). GATA-3, SOX-10 (Fig. 6D), and STAT5a expression was detected in 3/6, 5/6, and 2/3 cases, respectively. P63 protein was completely negative in most cases, with limited areas of positive peripheral myoepithelial cell staining suggestive of a focal intraductal component in 3 cases. DOG1 was negative in all examined cases.

Proliferative activity was generally low, with a mean MIB1 index of 15% (range, 5% to 40%).

DISCUSSION

Salivary gland tumors are increasingly being found to have characteristic chromosomal rearrangements. SC is a salivary gland tumor that recapitulates the histology and genetics of a rare malignancy of the breast SC. These tumors are defined by the t(12;15)(q13;q15) translocation, a fusion of the *ETV6* gene from chromosome 12 and the *NTRK3* gene from chromosome 15. The same translocation has been detected in most cases of the infantile fibrosarcomas, congenital mesoblastic nephromas,[13] chronic eosinophilic leukemias,[33] acute myeloid leukemia,[14] and some papillary carcinomas of the thyroid with and without previous irradiation.[18] These groups of tumors are the focus of interest, because tumors with *ETV6-NTRK3* fusion translocation respond well to treatment by entrectinib, which is a potent inhibitor of tyrosine kinases TRKA/B/C, ROS1, and ALK. The drug entrectinib is administered orally, is safe and well tolerated, and can cross the blood-brain barrier,
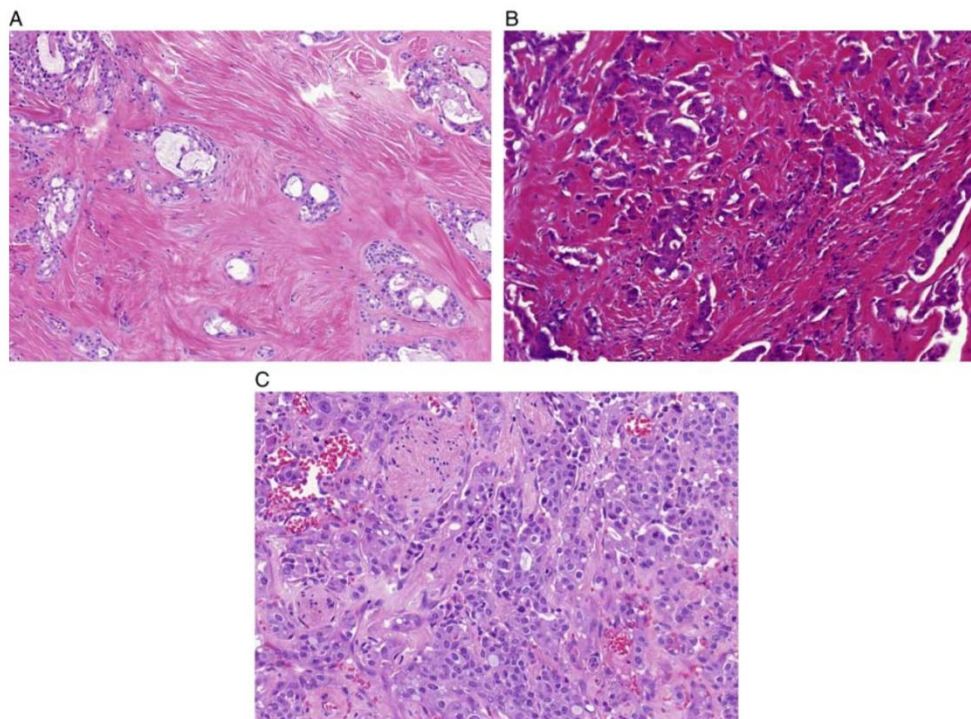
FIGURE 5. A, The third pattern of SC has a prominent fibrosclerotic stroma with isolated tumor cells in small islands or trabeculae were seen in the central part of the tumor. B, High-grade component of SC with limited secretory material and high proliferative activity. C, Prominent perineural and intraneural invasion was seen in 1 tumor.

so that it can be effective for treatment of brain metastases.[34,35]

Originally it appeared that all cases of SC share the same *ETV6-NTRK3* fusion translocation. However, in recent years Ito et al[27] and Skalova et al[26] described altogether 6 cases of SC with the *ETV6* gene split detected by FISH, but in which the *ETV6* gene appeared to be fused with a gene different to *NTRK3*. These cases were marked as SCs with *ETV6-X* fusion.

Herein, we describe a novel *ETV6-RET* fusion in 10 cases of salivary gland carcinomas with histologic features and IHC profile typical of SC, including the 4 *ETV6-X* SC cases published previously.[26] The presence of *ETV6-RET* fusion in SC was proven by at least 3 independent tests (NGS, FISH, RT-PCR), in all but 2 cases (Table 3, cases 4 and 9). In case 4, NGS and FISH confirmed *ETV6-RET* fusion but RT-PCR was negative, probably due to low or focal expression of fusion transcript (Table 4). Case 9 was the only sample unconfirmed by independent analysis. There was a lack of material for FISH analysis and RT-PCR for *ETV6-RET* fusion transcript detection was

negative. In this case, low quality of RNA rather than low or focal expression is responsible for this result.

The alternative *ETV6-RET* transcription will be important for treatment of those SCs with uncontrolled regional growth or SCs with metastatic foci, as treatment with entrectinib and similar drugs with the same target specificity will probably be ineffective in these SCs with alternative fusion transcript different from *ETV6-NTRK3*. The alternative fusion partner different from *ETV6-NTRK3* in SC should not be of great surprise, because infantile fibrosarcoma with *ETV6-NTRK3* translocation may have alternative *EML4-NTRK3* translocation,[36] and there are descriptions of acute myeloid leukemias in which the *ETV6* gene fuses with many alternative fusion partners, including *ETV6-ABL1*,[37] *ETV6-LPXN*,[38] *ETV6-RUNX1*,[39] *ETV6-NCOA2*,[40] and many others.

To our knowledge, *ETV6-RET* fusions have not been reported in salivary gland tumors so far. Notably, however, recent studies using RNA sequencing have revealed that salivary duct carcinoma (SDC) may also be added to the growing list of gene fusion-positive salivary
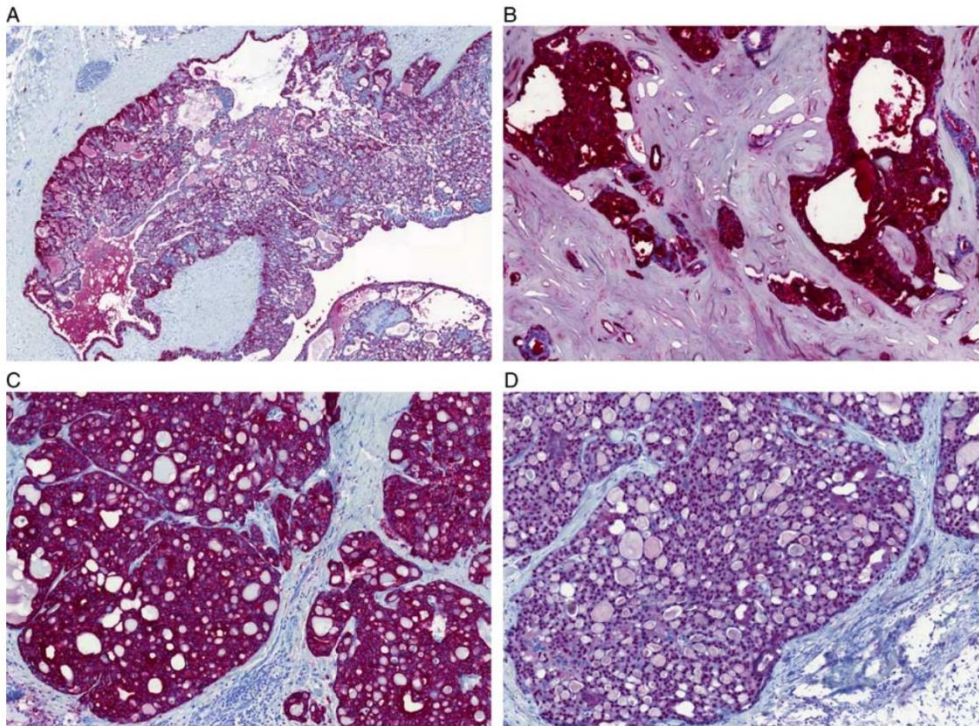
FIGURE 6. SC cases were all positive for S100 protein (A), mammaglobin (B), typically in strong and diffuse fashion (secretory material was also positive), and cytokeratin CK7 (C). SOX-10 positive nuclear expression is present (D).

carcinomas. *NCOA4-RET* fusions have been found in 2 SDCs.[41] Both *NCOA4-RET* translocated SDCs were positive for androgen receptors, and the tumors progressed in spite of undergoing concurrent chemoradiation, combination chemotherapy, and dual androgen deprivation therapy. Both patients with *NCOA4-RET* translocation, however, benefited from *RET*-targeted therapy.[41]

The treatment of SC has varied, ranging from simple excision to radical resection, neck dissection, adjuvant radiotherapy, and/or adjuvant systemic chemotherapy.[1,42,43] For patients presenting with a locally advanced, recurrent, or metastatic disease, the treatment options are currently limited and mainly palliative.[42,43] Therefore, SCs with *ETV6-RET* fusion translocation must be clearly distinguished from SCs with *ETV6-NTRK3* translocation, because the drugs RXDX105 and LOXO 292, effective with various tumors driven with *RET* gene alterations, are being tested for the treatment. SCs with *ETV6-RET* translocation might respond much better to these drugs, whereas entrectinib and similar inhibitors of tyrosine kinases TRKA/B/C will probably be ineffective.[44–47]

In summary, a novel finding in our study has been the discovery of a subset of SC patients with *ETV6-RET* fusions who may benefit from *RET*-targeted therapy. Many salivary gland malignancies are still included in the group of adenocarcinomas not otherwise specified. We believe that detailed genomic profiling and NGS of a large cohort of these unspecified neoplasms may lead to the identification of novel gene fusions and driver mutations characterizing new clinically relevant subgroups of salivary gland carcinomas. This study highlights that further molecular analyses of salivary gland tumors are warranted and deserve special attention to identify new tumor types with possible therapeutic implications.

REFERENCES

1. Skalova A, Vanecek T, Sima R, et al. Mammary analogue secretory carcinoma of salivary glands, containing the *ETV6-NTRK3* fusion gene: a hitherto undescribed salivary gland tumor entity. *Am J Surg Pathol.* 2010;34:599–608.
2. Tognon C, Knezevich SR, Huntsman D, et al. Expression of the *ETV6-NTRK3* gene fusion as a primary event in human secretory breast carcinoma. *Cancer Cell.* 2002;2:367–376.
3. Li Z, Tognon CE, Godinho FJ, et al. *ETV6-NTRK3* fusion oncogene initiates breast cancer from committed mammary progenitors via activation of AP1 complex. *Cancer Cell.* 2007;12:542–558.
4. Skálová A, Bell D, Bishop JA, et al. Secretory carcinoma. In: El-Naggar A, Chan JKC, Grandis JR, Takata T, Slootweg PJ, eds. *World Health Organization (WHO) Classification of Head and Neck Tumours*, 4th ed. Lyon, France: IARC Press; 2017:177–178.
5. Dogan S, Wang L, Ptashkin RN, et al. Mammary analog secretory carcinoma of the thyroid gland: a primary thyroid adenocarcinoma harboring *ETV6-NTRK3* fusion. *Mod Pathol.* 2016;29:985–995.
6. Reynolds S, Shaheen M, Olson G, et al. A case of primary mammary analog secretory carcinoma (MASC) of the thyroid masquerading as papillary thyroid carcinoma: potentially more than a one off. *Head Neck Pathol.* 2016;10:405–413.
7. Dettloff J, Seethala RR, Stevens TM, et al. Mammary analog secretory carcinoma (MASC) involving the thyroid gland: a report of the first 3 cases. *Head Neck Pathol.* 2007;11:266–267.
8. Stevens TM, Kovalovsky AO, Velosa C, et al. Mammary analog secretory carcinoma, low-grade salivary duct carcinoma, and mimickers: a comparative study. *Mod Pathol.* 2015;28:1084–1100.
9. Hyrcza MD, Ng T, Crawford RI. Detection of the *ETV6-NTRK3* translocation in cutaneous mammary-analogue secretory carcinoma. *Diagn Histopathol.* 2015;21:481–484.
10. Bishop JA, Taube JM, Su A, et al. Secretory carcinoma of the skin harboring *ETV6* gene fusions. A cutaneous analogue to secretory carcinomas of the breast and salivary glands. *Am J Surg Pathol.* 2017;41:62–66.
11. Lurquin E, Jorissen M, Debiec-Rychter M, et al. Mammary analogue secretory carcinoma of the sinus ethmoidalis. *Histopathology.* 2015;67:749–751.
12. Rubin BP, Chen CJ, Morgan TW, et al. Congenital mesoblastic nephroma t(12;15) is associated with ETV6-NTRK3 gene fusion: cytogenetic and molecular relationship to congenital (infantile) fibrosarcoma. *Am J Pathol.* 1998;153:1451–1458.
13. Knezevich SR, Garnett MJ, Pysher TJ, et al. *ETV6- NTRK3* gene fusions and trisomy 11 establish a histogenetic link between mesoblastic nephroma and congenital fibrosarcoma. *Cancer Res.* 1998;15:5046–5048.
14. Kralik JM, Kranewitter W, Boesmueller H, et al. Characterization of a newly identified ETV6-NTRK3 fusion transcript in acute myeloid leukemia. *Diagn Pathol.* 2011;6:19.
15. Alassiri AH, Ali RH, Shen Y, et al. *ETV6-NTRK3* is expressed in a subset of ALK-negative inflammatory myofibroblastic tumor. *Am J Surg Pathol.* 2016;40:1051–1061.
16. Brenca M, Rossi S, Polano M, et al. Transcriptome sequencing identifies *ETV6–NTRK3* as a gene fusion involved in GIST. *J Pathol.* 2016;238:543–549.
17. Leeman-Neill RJ, Kelly LM, Liu P, et al. *ETV6-NTRK3* is a common chromosomal rearrangement in radiation-associated thyroid cancer. *Cancer.* 2014;120:799–807.
18. Seethala RR, Chiosea SI, Liu CZ, et al. Clinical and morphological features of *ETV6-NTRK3* translocated papillary thyroid carcinoma in an adult population without radiation exposure. *Am J Surg Pathol.* 2017;41:446–457.
19. Griffith C, Seethala R, Chiosea SI. Mammary analogue secretory carcinoma: a new twist to the diagnostic dilemma of zymogen granule poor acinic cell carcinoma. *Virchows Arch.* 2011;459:117–118.
20. Fehr A, Loning T, Stenman G. Mammary analogue secretory carcinoma of the salivary glands with *ETV6-NTRK3* gene fusion. Letter to the editor. *Am J Surg Pathol.* 2011;35:1600–1602.
21. Connor A, Perez-Ordoñez B, Shago M, et al. Mammary analog secretory carcinoma of salivary gland origin with the *ETV6* gene rearrangement by FISH: expanded morphologic and immunohistochemical spectrum of a recently described entity. *Am J Surg Pathol.* 2012;36:27–34.
22. Chiosea SI, Griffith C, Assad A, et al. The profile of acinic cell carcinoma after recognition of mammary analog secretory carcinoma. *Am J Surg Pathol.* 2012;36:343–350.
23. Majewska H, Skálová A, Stodulski D, et al. Mammary analogue secretory carcinoma of salivary glands: first retrospective study of a new entity in Poland with special reference to *ETV6* gene rearrangement. *Virchows Arch.* 2015;466:245–254.
24. Pinto A, Nosé V, Rojas C, et al. Searching for mammary analogue secretory carcinoma among their mimicks. *Mod Pathol.* 2014;27:30–37.
25. Bishop JA. Unmasking MASC: bringing to light the unique morphologic, immunohistochemical and genetic features of the newly recognized mammary analogue secretory carcinoma of salivary glands. *Head Neck Pathol.* 2013;7:35–39.
26. Skalova A, Vanecek T, Simpson RHW, et al. Mammary analogue secretory carcinoma of salivary glands. Molecular analysis of 25 *ETV6* gene rearranged tumors with lack of detection of classical *ETV6-NTRK3* fusion transcript by standard rt-pcr: report of 4 cases harboring *ETV6-X* gene fusion. *Am J Surg Pathol.* 2016;40:3–13.
27. Ito Y, Ishibashi K, Masaki A, et al. Mammary analogue secretory carcinoma of salivary glands: a clinicopathological and molecular study including 2 cases harboring *ETV6-X* fusion. *Am J Surg Pathol.* 2015;39:602–610.
28. Murphy DA, Ely HA, Shoemaker R, et al. Detecting gene rearrangements in patient populations through a 2-step diagnostic test comprised of rapid IHC enrichment followed by sensitive next-generation sequencing. *Appl Immunohistochem Mol Morphol.* 2017;25:513–523.
29. Viswanatha DS, Foucar K, Berry BR, et al. Blastic mantle cell leukemia: an unusual presentation of blastic mantle cell lymphoma. *Mod Pathol.* 2000;13:825–833.
30. Gaffney R, Chakerian A, O'Connell JX, et al. Novel fluorescent ligase detection reaction and flow cytometric analysis of SYT-SSX fusions in synovial sarcoma. *J Mol Diagn.* 2003;5:127–135.
31. Antonescu CR, Kawai A, Leung DH, et al. Strong association of SYT-SSX fusion type and morphologic epithelial differentiation in synovial sarcoma. *Diagn Mol Pathol.* 2000;9:1–8.
32. Bourgeois JM, Knezevich SR, Mathers JA, et al. Molecular detection of the ETV6-NTRK3 gene fusion differentiates congenital fibrosarcoma from other childhood spindle cell tumors. *Am J Surg Pathol.* 2000;24:937–946.
33. Su RJ, Jonas BA, Welborn J, et al. Chronic eosinophilic leukemia, NOS with t(5;12)(q31;p13)/ETV6-ACSL6 gene fusion: a novel variant of myeloid proliferative neoplasm with eosinophilia. *Hum Pathol.* 2016;5:6–9.
34. Drilon A, Siena S, Ou SI, et al. Safety and antitumor activity of the multitargeted Pan-TRK, ROS1, and ALK inhibitor Entrectinib: Combined results from two phase I trials ALKA-372-001 and STARTRK-1. *Cancer Discov.* 2017;7:400–407.
35. Drilon A, Li G, Dogan S, et al. What hides behind the MASC: clinical response and acquired resistance to entrectinib after *ETV6-NTRK3* identification in a mammary analogue secretory carcinoma (MASC). *Ann Oncol.* 2016;27:920–926.
36. Tannenbaum-Dvir S, Glade Bender JL, Church AJ, et al. Characterization of a novel fusion gene *EML4-NTRK3* in a case of recurrent congenital fibrosarcoma. *Cold Spring Harb Mol Case Stud.* 2015;1:a000471.
37. Tirado CA, Siangchin K, Shabsovich DS, et al. A novel three-way rearrangement involving *ETV6* (12p13) and *ABL1* (9q34) with an unknown partner on 3p25 resulting in a possible *ETV6-ABL1* fusion in a patient with acute myeloid leukemia: a case report and a review of the literature. *Biomark Research.* 2016;4:16.
38. Abe A, Yamamoto Y, Iba S, et al. *ETV6-LPXN* fusion transcript generated by t(11;12)(q12.1;p13) in a patient with relapsing acute myeloid leukemia with NUP98-HOXA9. *Genes Chromosomes Cancer.* 2016;55:242–250.
39. Garcia DR, Arancibia AM, Ribeiro RC, et al. Intrachromosomal amplification of chromosome 21 (iAMP21) detected by *ETV6/RUNX1* FISH screening in childhood acute lymphoblastic leukemia: a case report. *Rev Bras Hematol Hemoter.* 2013;35:369–371.

40. Strehl S, Nebral K, König M, et al. *ETV6-NCOA2*: a novel fusion gene in acute leukemia associated with coexpression of T-lymphoid and myeloid markers and frequent NOTCH1 mutations. *Clin Cancer Res*. 2008;14:977–983.
41. Wang K, Russell JS, McDermott JD, et al. Profiling of 149 salivary duct carcinomas, carcinoma ex pleomorphic adenomas, and adenocarcinomas, not otherwise specified reveals actionable genomic alterations. *Clin Cancer Res*. 2016;22:6061–6068.
42. Skálová A, Vanecek T, Majewska H, et al. Mammary analogue secretory carcinoma of salivary glands with high-grade transformation: report of 3 cases with the *ETV6-NTRK3* gene fusion and analysis of TP53, beta-catenin, EGFR, and CCND1 genes. *Am J Surg Pathol*. 2014;38:23–33.
43. Luo W, Lindley SW, Lindley PH, et al. Mammary analog secretory carcinoma of salivary gland with high-grade histology arising in palate, report of a case and review of literature. *Int J Clin Exp Pathol*. 2014;7:9008–9022.
44. Li GG, Somwar R, Joseph J, et al. Antitumor activity of RXDX-105 in multiple cancer types with RET rearrangements or mutations. *Clin Cancer Res*. 2017;23:2981–2990.
45. Sabari JK, Siau ED, Drilon A. Targeting RET-rearranged lung cancers with multikinase inhibitors. *Oncoscience*. 2017;4:23–24.
46. Chi HT, Ly BT, Kano Y, et al. *ETV6-NTRK3* as a therapeutic target of small molecule inhibitor PKC412. *Biochem Biophys Res Commun*. 2012;429:87–92.
47. Tognon CE, Somasiri AM, Evdokimova VE, et al. *ETV6-NTRK3*-mediated breast epithelial cell transformation is blocked by targeting the IGF1R signaling pathway. *Cancer Res*. 2011;71: 1060–1070.

131

Mammary Analog Secretory Carcinoma of the Nasal Cavity

Characterization of 2 Cases and Their Distinction From Other Low-grade Sinonasal Adenocarcinomas

Martina Baneckova, MD,*† Abbas Agaimy, MD,‡ Simon Andreasen, MD,§‖
Tomas Vanecek, PhD,¶ Petr Steiner, Mgr,*¶ David Slouka, MD, MBA, PhD,#
Tomas Svoboda, MD, PhD,** Marketa Miesbauerova, MD,*† Michael Michal Jr, MD,*†
and Alena Skálová, MD, PhD*†

Abstract: Secretory carcinoma, originally described as mammary analog secretory carcinoma (MASC), is a low-grade salivary gland tumor characterized by a t(12;15)(p13;q25) translocation, resulting in an *ETV6-NTRK3* gene fusion. Most MASCs are localized to the parotid gland and intraoral minor salivary glands. Moreover, *ETV6*-rearranged carcinomas with secretory features have been reported recently in the thyroid (with and without a history of radiation exposure), skin, and in very rare instances in the sinonasal tract. Here, we describe 2 cases of primary MASC in the sinonasal tract and provide a detailed clinical and histopathologic characterization of their morphology, immunohistochemical profile, and genetic background and highlight features allowing for its separation from its recently described molecular mimicker, *ETV6*-rearranged low-grade sinonasal adenocarcinoma.

Key Words: nasal cavity, mammary analog secretory carcinoma, MASC, low-grade sinonasal adenocarcinoma, *ETV6-NTRK3*

(*Am J Surg Pathol* 2018;00:000–000)

Secretory carcinoma (SC), originally described as mammary analog secretory carcinoma (MASC), is a low-grade salivary gland tumor characterized by a t(12;15)(p13;q25) translocation, resulting in an *ETV6-NTRK3* gene fusion.[1] In addition to having identical genetics with SC, MASC expresses S100 and mammaglobin while being negative for DOG-1 and p63, thus highly resembling SC of the breast.[2] However, these features are unique among tumors of the salivary gland.

Most MASCs are localized in the parotid gland, submandibular gland, and minor salivary glands of the oral cavity, such as soft palate, lips, base of the tongue, and buccal mucosa. Since its description in the major and minor salivary glands,[1] MASC has been described in several other locations, such as skin,[3–5] thyroid,[6–8] and the sinonasal tract.[9,10] The first case of MASC of the sinonasal tract was reported by Lurquin et al,[9] and, very recently, another case with high-grade transformation was reported in the maxillary sinus.[10]

Primary sinonasal adenocarcinomas (SNACs) are uncommon and morphologically heterogenous.[11] These tumors are divided into nonsalivary and salivary types. Non–salivary-type SNACs are further classified into 2 broad categories: intestinal-type adenocarcinoma (ITAC) and the non–intestinal-type adenocarcinoma (non-ITAC).[12] The non–intestinal-type SNAC is of presumed surface epithelium/seromucinous gland origin and accounts for <1% of head and neck cancers.[11–13] It is morphologically a very diverse group, as it can show high-grade or low-grade features, as determined by the proliferative activity and pattern of growth.[14–17] An increasing number of distinct types of non-ITAC has been recognized recently, including a subset with rearrangement of the *ETV6* gene, the so-called *ETV6* gene–rearranged sinonasal low-grade SNAC.[18]

By screening a series of low-grade SNACs with fluorescence in situ hybridization (FISH) and/or reverse transcription polymerase chain reaction (RT-PCR), we identified 2 cases of primary MASC arising in the nasal cavity, and herein we provide a detailed clinical, histopathologic, and molecular characterization. Recognizing MASC in the sinonasal tract among other SNACs of the salivary type, as well as *ETV6*-rearranged low-grade SNAC, is important, as the correct diagnosis is prognostically relevant, and *ETV6*-related fusions serve as therapeutic targets.[19,20]

MATERIALS AND METHODS

Patient Material

Fifteen cases of low-grade non–intestinal-type SNAC with secretory features resembling MASC were identified in a review of the Salivary Gland Tumor Registry, at the

TABLE 1. Antibodies Used for Immunohistochemical Study

Antibody Specificity	Clone	Dilution	Antigen Retrieval/Time (min)	Source
S100 protein	Polyclonal	RTU	CC1/20	Ventana Medical Systems
Mammaglobin	304-1A5	RTU	CC1/36	DakoCytomation
CK7	OV-TL 12/30	1:200	CC1/36	DakoCytomation
CK20	Ks20.8	1:100	CC1/36	DakoCytomation
CDX2	EPR2764Y	RTU	CC1/64	Cell Marque
GCDFP-15	EP1582y	RTU	CC1/64	Cell Marque
p63	4A4	RTU	CC1/64	Ventana Medical Systems
DOG-1	SP31	RTU	CC1/36	Cell Marque
GATA-3	L50-823	1:200	CC1/52	BioCareMedical
SOX10	Polyclonal	1:100	CC1/64	Cell Marque
Pan-TRK	A7H6R	1:20	CC1/64	Cell Signaling
SATB2	Polyclonal	1:100	CC2/68	Sigma Aldrich
STAT5a	Polyclonal	1:400	CC1/36	AssayDesigns Inc.
MIB1	30-9	RTU	CC1/64	Ventana Medical Systems

CC1 indicates EDTA buffer, pH 8.6; RTU, ready to use.

Department of Pathology, Faculty of Medicine in Plzen, and Biopticka Laboratory Ltd, Plzen, Czech Republic. Two additional cases with features mimicking MASC were retrieved from the files of the Institute of Pathology, Friedrich-Alexander University, Erlangen, Germany, thus amounting to a total of 17 cases. Clinical follow-up was obtained from the patients, their physicians, or from referring pathologists.

Histology and Immunohistochemistry

For conventional microscopy, tissues were fixed in formalin, routinely processed, embedded in paraffin (FFPE), cut, and stained with hematoxylin and eosin. In most cases, additional stains were also performed, including periodic acid-Schiff with and without diastase, mucicarmine, and alcian blue at pH 2.5.

For immunohistochemistry, 4-μm-thick sections were cut from paraffin blocks and mounted on positively charged slides (TOMO; Matsunami Glass Ind., Japan). Sections were processed on a BenchMark ULTRA (Ventana Medical Systems, Tucson, AZ), deparaffinized, and subjected to heat-induced epitope retrieval by immersion in a CC1 solution (pH 8.6) at 95°C. Following antigen retrieval, sections were stained with a pan-TRK antibody cocktail consisting of rabbit monoclonal antibodies, all obtained from Cell Signaling (Danvers, MA), targeting pan-TRK (clone A7H6R, active against TrkA, TrkB, and TrkC, 1:50 dilution), ROS1 (clone D4D6, 1:50), and ALK (clone D5F3, 1:50), as described elsewhere.[21]

All other primary antibodies used are summarized in Table 1. Visualization was performed using the ultraView Universal DAB Detection Kit (Roche Diagnostics, Mannheim, Germany) and ultraView Universal Alkaline Phosphatase Red Detection Kit (Roche Diagnostics). The slides were counterstained with Mayer hematoxylin. Appropriate positive and negative controls were used.

Molecular Genetic Study

Detection of *ETV6-NTRK3* Fusion Transcript by RT-PCR

RNA was extracted using the RecoverAll Total Nucleic Acid Isolation Kit (Ambion, Austin, TX). cDNA was synthesized using the Transcriptor First Strand cDNA Synthesis Kit (RNA input 500 ng) (Roche Diagnostics). All procedures were performed according to the manufacturer's protocols. Amplification of a 105 bp product and a 133 bp product of the β2-microglobulin gene, and a 247 bp product of the *PGK* gene was used to test the quality of the extracted RNA, as previously described.[22–24] This resulted in the detection of the classic fusion transcript of exon 5 of the *ETV6* gene and exon 15 of the *NTRK3* gene.[25]

For PCR, 2 μL of cDNA was added to the reaction, which consisted of 12.5 μL of HotStar Taq PCR Master Mix (Qiagen, Hilden, Germany), 10 pmol of each primer (Table 2), and distilled water up to 25 μL.[26,27] The amplification program comprised denaturation at 95°C for 14 minutes followed by 45 cycles of denaturation at 95°C for 1 minute; annealing at temperatures shown in Table 2 was carried out for 1 minute and extension at 72°C for 1 minute. The procedure was completed by incubation at 72°C for 7 minutes.

Successfully amplified PCR product was purified with magnetic particles using Agencourt AMPure (Agencourt

TABLE 2. Primers for Detection of *ETV6-NTRK3* Fusion Transcripts

Original Primer Name	Sequence	Annealing Temperature (°C)	Localization
TEL971* (ETV6A†)	ACCACATCATGGTCTCTGTCTCCC	65	*ETV6* exon 5 outer
TRKC1059* (NTRK3A†)	CAGTTCTCGCTTCAGCACGATG	65	*NTRK3* exon 15 outer

*Bourgeois et al.[25]
†Ito et al,[26] Skalova et al.[27]

Bioscience Corporation, A Beckman Coulter Company, Beverly, MA). The product was then bidirectionally sequenced using Big Dye Terminator Sequencing Kit (PE/Applied Biosystems, Foster City, CA) and purified with magnetic particles using Agencourt CleanSEQ (Agencourt Bioscience Corporation); all this was carried out according to the manufacturer's protocols and run on an automated sequencer ABI Prism 3130xl (Applied Biosystems) at a constant voltage of 13.2 kV for 11 minutes.

Detection of *ETV6* and *NTRK3* by FISH Method

Four-μm-thick FFPE sections were placed onto positively charged slides. Hematoxylin and eosin–stained slides were examined for determination of areas for cell counting.

The unstained slides were routinely deparaffinized and incubated in the 1× Target Retrieval Solution Citrate pH 6 (Dako, Glostrup, Denmark) at 95°C/40 minutes and subsequently cooled for 20 minutes at room temperature in the same solution. The slides were washed in deionized water for 5 minutes and digested in protease solution with Pepsin (0.5 mg/mL) (Sigma Aldrich, St Louis, MO) in 0.01 M HCl at 37°C/25 to 60 minutes according to the sample conditions. The slides were then placed in deionized water for 5 minutes, dehydrated in a series of ethanol solution (70%, 85%, 96% for 2 min each), and air-dried.

For the detection of *ETV6* rearrangement, a commercial probe, Vysis *ETV6* Break Apart FISH Probe Kit (Vysis/Abbott Molecular, Illinois), was used. The *ETV6* probe was mixed with water and LSI/WCP (Locus-Specific Identifier/Whole Chromosome Painting) Hybridization buffer (Vysis/Abbott Molecular) in a 1:2:7 ratio, respectively.

The probe for the detection of the rearrangement of the *NTRK3* gene region was mixed from custom-designed SureFISH probes (Agilent Technologies Inc., Santa Clara, CA). Chromosomal regions for *NTRK3* break-apart probe oligos are chr15:87501469-88501628 and chr15:88701444-89700343. The probe mixture was prepared from corresponding probes (each color was delivered in a separated well), deionized water, and LSI Buffer (Vysis/Abbott Molecular) in a 1:1:1:7 ratio, respectively.

An appropriate amount of mixed probe was applied on specimens, covered with a glass coverslip, and sealed with rubber cement. The slides were incubated in the ThermoBrite instrument (StatSpin/Iris Sample Processing, Westwood, MA) with codenaturation at 85°C/8 minutes and hybridization at 37°C/16 hours. The rubber-cemented coverslip was then removed, and the slide was placed in posthybridization wash solution (2× SSC/0.3% NP-40) at 72°C/2 minutes. The slide was air-dried in the dark, counterstained with 4′, 6′-diamidino-2-phenylindole (DAPI; Vysis/Abbott Molecular), coverslipped, and immediately examined.

FISH Interpretation

The sections were examined with an Olympus BX51 fluorescence microscope (Olympus Corporation, Tokyo, Japan) using a ×100 objective and filter sets Triple Band Pass (DAPI/SpectrumGreen/SpectrumOrange), Dual Band Pass (SpectrumGreen/SpectrumOrange), and Single Band Pass (SpectrumGreen or SpectrumOrange).

For each probe, 100 randomly selected non-overlapping tumor cell nuclei were examined for the presence of yellow or green and orange fluorescent signals. Yellow signals were considered negative, and separate orange and green signals were considered as positive.

Cutoff values were set to > 10% of nuclei with chromosomal breakpoint signals (mean, +3 SD in normal non-neoplastic control tissues).

Sample Preparation for Next-generation Sequencing

For next-generation sequencing (NGS) studies, 2-3 FFPE sections (10 μm thick) were macrodissected to isolate tumor-rich regions. The samples were extracted for total nucleic acid using Agencourt FormaPure Kit (Beckman Coulter, Brea, CA), following the corresponding protocol with overnight digestion and an additional 80°C incubation, as described in the modification of the protocol by ArcherDX (ArcherDX Inc., Boulder, CO). Total nucleic acid was quantified using the Qubit Broad Range RNA Assay Kit (Thermo Fisher Scientific) and 2 μL of sample.

RNA Integrity Assessment and Library Preparation for NGS

Unless otherwise indicated, 250 ng of FFPE RNA was used as an input for NGS studies. To assess RNA quality, the PreSeq RNA QC Assay using iTaq Universal SYBR Green Supermix (Biorad, Hercules, CA) was performed on all samples during library preparation to generate a measure for the integrity of RNA (in the form of a cycle threshold value). Library preparation and RNA QC were performed following the Archer Fusion Plex Protocol for Illumina (ArcherDX Inc.). A custom primer set with 28 primers spanning regions on 3 specific genes of interest including *ETV6* was used. Final libraries were diluted 1:100,000 and quantified in a 10 μL reaction following the Library Quantification for Illumina Libraries protocol and assuming a 200 bp fragment length (KAPA, Wilmington, MA). The concentration of the final libraries was around 200 n. The threshold representing the minimum molar concentration for which sequencing can be robustly performed was set at 50 nM.

NGS and Analysis (Archer)

The libraries were sequenced on an MiSeq sequencer (Illumina, San Diego, CA). The libraries were diluted to 4 nM, and equal amounts of up to 16 libraries were pooled per run. The recommended number of raw reads per sample was set to 500,000. Library pools were diluted to 16 pM library stock with 10% 12.5 pM PhiX and loaded in the MiSeq cartridge. Analysis of sequencing results was performed using the Archer Analysis software (version 5; ArcherDX Inc.). Fusion parameters were set to a minimum of 5 valid fusion reads with a minimum of 3 unique start sites within the valid fusion reads.
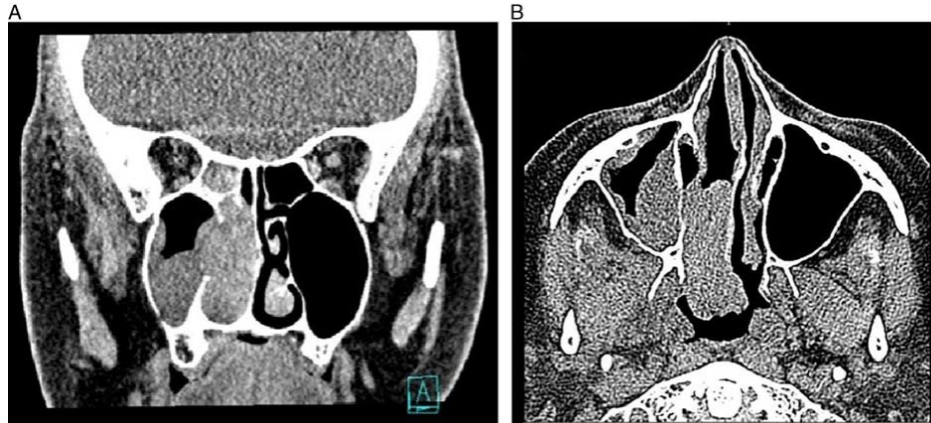
FIGURE 1. Representative imaging of case 2. A, Coronal computed tomography of case 2 demonstrating a right-sided nasal mass. B, The mass extends into the nasopharynx. There was no involvement of the maxillary sinus.

RESULTS

Case Histories

Case 1

A 51-year-old woman, nonsmoker without a prior history of breast cancer, presented with intermittent tenderness or pain behind the right eye and occasional forehead discomfort. A mass was identified on the right side of the nasal septum, and the patient was referred to surgical resection. The resected specimen measured 1.5×1.5×0.4 cm, and the patient was staged as T1N0M0. The patient was alive and showed no evidence of recurrent disease after > 10 years of follow-up.

Case 2

A 65-year-old woman, nonsmoker without prior history of breast cancer, presented with right-sided nasal obstruction, nasopharyngeal secretion, and occasional retrobulbar pain. Past medical history was unremarkable except for a pleomorphic adenoma of the palate 5 years previously. Computed tomography identified a mass in the right nasal cavity extending into the nasopharynx. The patient underwent surgical excision of the mass including the middle turbinate along with maxillary sinus antrostomy, right ethmoidectomy, and partial resection of the nasal septum. The tumor measured 4×4×1.5 cm, and the patient was staged as T2NxM0. The patient received adjuvant radiotherapy and is alive with no evidence of disease after 4 years of follow-up (Figs. 1A, B).

Detailed clinicopathologic findings in these 2 patients are presented in Table 3.

Histopathology and Immunohistochemical Findings

Cases 1 and 2 had histologic features and immunoprofiles identical to salivary gland MASC. The tumors were unencapsulated and composed of tubular, papillary, and microcystic growth patterns with invasive margins (Fig. 2A). The tumor cells had low-grade vesicular and round to oval nuclei with fine, granular chromatin. Abundant eosinophilic homogenous extracellular periodic acid-Schiff with diastase–positive material (Fig. 2B) was present in both cases. The tumors were composed of solid microcystic growth patterns, in places divided by thick hyalinized fibrous septa (Fig. 2C). Focal necrotic areas were present in case 2 (Fig. 2D). In contrast to acinic cell carcinoma (AciCC), both tumors lacked cytoplasmic periodic acid-Schiff with diastase–positive zymogen granules. Mitoses were few, and there was no lymphovascular invasion or perineural growth.

In contrast, cases 3 to 17 displayed histologic features of low-grade tubulopapillary adenocarcinomas or

TABLE 3. Clinical Findings in 2 MASCs of the Nasal Cavity

Cases	Age (y)/Sex	Site	Size (cm)	Stage (TNM)	Local Recurrence	Duration of Symptoms (y)	Treatment	Follow-up (y)	Outcome
1	51/F	Right nasal septum	1.5×1.5×0.4	T1N0M0	No	1-2	Surgery	14	Alive NED
2	65/F	Right nasal cavity	4×4×1.5	pT2pNxM0	No	1	Surgery+RT	4	Alive NED

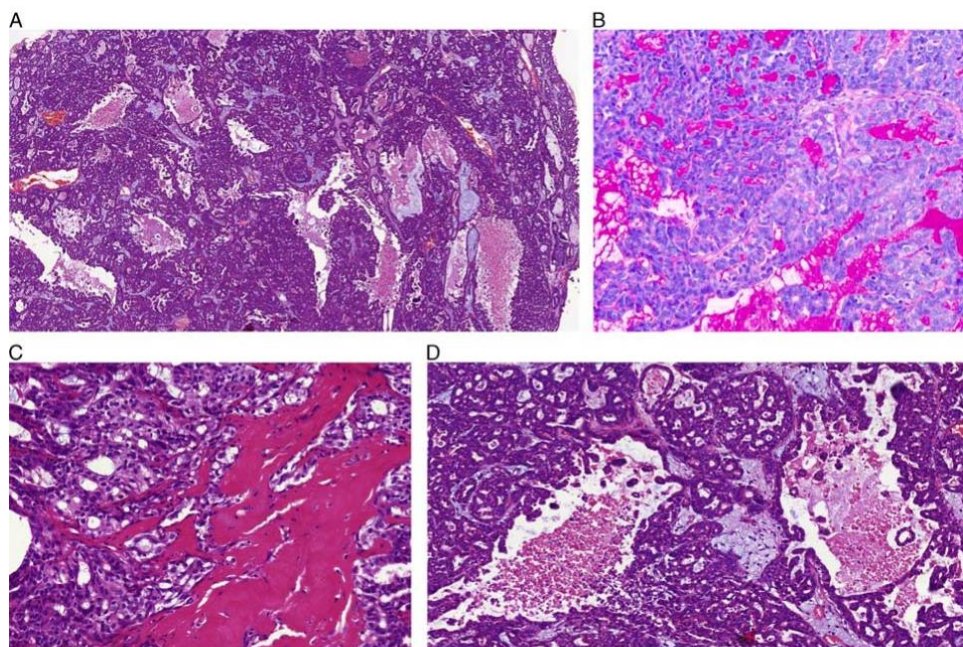F indicates female; NED, no evidence of disease; RT, radiotherapy.

FIGURE 2. Histologic findings of sinonasal MASC. A, MASC shows admixed tubular, papillary, and microcystic growth patterns. B, Abundant periodic acid-Schiff with diastase–positive extracellular material within tubular and cystic spaces. C, The tumors were composed of solid, microcystic growth patterns, occasionally divided by thick hyalinized fibrous septa. D, Focal necrosis was present in case 2.

low-grade non–intestinal-type SNAC, not otherwise specified.[13,16,17]

The immunohistochemical findings are summarized in Tables 4 and 5. Both MASCs were positive for CK7,

TABLE 4. Immunohistochemical Results of 2 Cases of MASC in the Nasal Cavity

Antibody	Case 1	Case 2
CK7	+(D)	+(D)
S100	+(D)	+(F)
Mammaglobin	+(D)	+(F)
GATA3	+(D)	+(D)
SOX10	+(D)	+(D)
Pan-TRK	+	+
Stat5	+	+
p63	Neg	Neg
CK20	Neg	Neg
CDX2	Neg	Neg
DOG-1	Neg	Neg
GCDFP*	+(F)*	+(E)*
MIB1	5%	40%

*Immunochemistry performed at Department of Otorhinolaryngology and Maxillofacial Surgery, Køge University Hospital, and Department of Otolaryngology Head & Neck Surgery Rigshospitalet.
D indicates diffuse staining; E, staining of extracellular material; F, focal staining.

SOX10, GATA3, STAT5, and S100 (diffuse and strong staining in all tumor cells). Immunohistochemical staining for mammaglobin was diffusely positive in case 1 and focally positive in case 2 (Figs. 3A–D). Both cases were negative for p63 protein, CK20, CDX2, SATB2, and DOG-1 (Table 4). The remaining 15 cases, except for case 13, were negative for mammaglobin. Case 13 was S100 protein/SOX10/GATA3-positive with focal staining for mammaglobin in <5% of the tumor cells. Data from all 17 cases are summarized in Table 5.

Genetic Findings

After histologic and immunohistochemical characterization, all 17 cases were characterized for the presence of the *ETV6-NTRK3* fusion transcript and/or rearrangement of *ETV6*. These findings are summarized in Table 6. Two cases, cases 1 and 2, showed *ETV6* gene rearrangement by FISH. Case 1 was negative with RT-PCR, but a product was identified with RT-PCR in case 2, and sequencing confirmed an exon 5 to 15 junction. In case 1, NGS identified an atypical exon 5-13 fusion. Cases 3 to 17 were negative or not analyzable with either RT-PCR or FISH, or were negative for both methods (Table 6 and Figs. 4A–C).

136

TABLE 5. Immunohistochemical Results of All 17 Cases

Case No.	Final Diagnosis	CK7	CK20	DOG-1	GATA3	SOX10	S100	MGA	p63	STAT5	MIB1	CDX2	SATB2
1	MASC	+	Neg	Neg	+	+	+	+	Neg	+	5%	Neg	Neg
2	MASC	+	Neg	Neg	+	+	+	+	Neg	+	40%	Neg	Neg
3	LG SNAC	+	Neg	Neg	+	+	+	Neg	Neg	ND	ND	Neg	ND
4	LG SNAC	Neg	Neg	Neg	+	+	+	Neg	Neg	ND	ND	Neg	ND
5	LG SNAC	+	Neg	Neg	Neg	Neg	Neg	Neg	Neg	ND	20%	Neg	Neg
6	LG SNAC	+	Neg	Neg	Neg	Neg	Neg	Neg	Neg	+	3%	Neg	Neg
7	LG SNAC	+	Neg	Neg	+	+	Neg	Neg	Neg	+	3%	Neg	Neg
8	LG SNAC	+	Neg	Neg	ND	+	+	Neg	Neg	ND	5%	Neg	ND
9	LG SNAC	+	Neg	Neg	Neg	+	+	Neg	Neg	+	3%	Neg	Neg
10	LG SNAC	+	Neg	NA	NA	NA	Neg	NA	NA	NA	NA	NA	NA
11	LG SNAC	+	Neg	Neg	Neg	Neg	Neg	Neg	Neg	ND	90%	Neg	ND
12	LG SNAC	+	Neg	Neg	Neg	Neg	+	Neg	+	+	5%	Neg	ND
13	LG SNAC	+	Neg	Neg	+	+	+	+(F) 5%	Neg	+	10%	Neg	ND
14	LG SNAC	+	Neg	Neg	Neg	Neg	+(F)	Neg	+	+(F)	2%	Neg	Neg
15	LG SNAC	+	Neg	Neg	Neg	Neg	+	Neg	Neg	Neg	2%	Neg	Neg
16	LG SNAC	+	Neg	Neg	ND	+(F)	+	Neg	Neg	ND	2%	Neg	Neg
17	LG SNAC	+	Neg	Neg	+	Neg	Neg	Neg	Neg	ND	0%	ND	Neg

F indicates focally; LG, low grade; NA, not analyzable; ND, not done; Neg, negative.

DISCUSSION

In contrast to the sinonasal tract, diagnosing MASC in the major salivary glands as well as the oral minor glands is not difficult in most cases. MASC is well characterized not only by histologic and immunohistochemical features but also by the *ETV6-NTRK3* gene fusion.[1] However, if MASC is present in unexpected locations, the differential diagnosis is more challenging. MASC can be confused with other salivary gland tumors, including AciCC and adenocarcinoma not otherwise specified.[28]

More than half of cases previously diagnosed as zymogen granule–poor AciCC were positive for *ETV6* translocation on rereview and therefore classified as MASC, and most tumors previously diagnosed as AciCC of the minor salivary glands also represent MASC.[29,30] In contrast to AciCC, MASC shows no basophilic granularity in the cytoplasm of any of the constituent cells, this being the hallmark of the serous acinar cells of AciCC. Moreover, MASC has a completely different immunohistochemical profile than AciCC, almost always strongly expressing
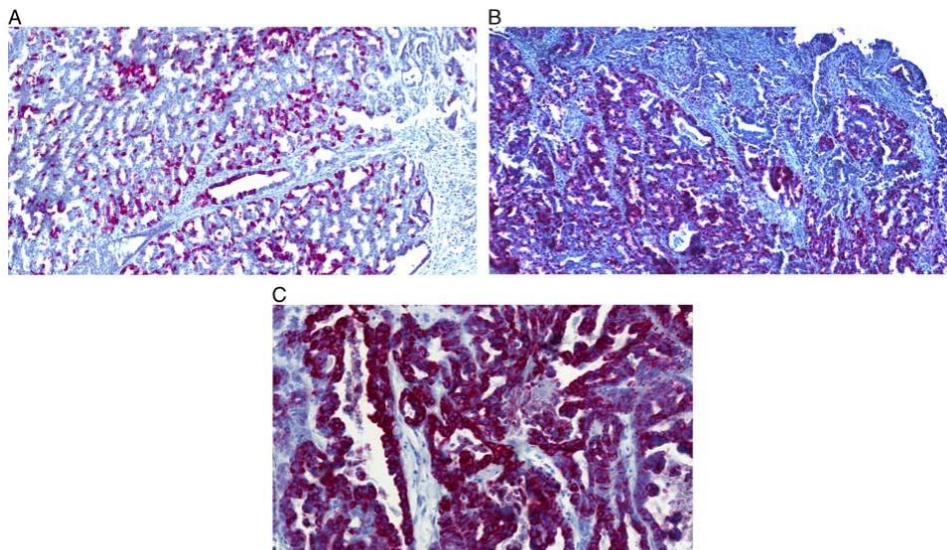

FIGURE 3. Immunohistochemical characteristics of MASC in the sinonasal tract. In both MASCs, tumor cells were intensely and diffusely positive for mammaglobin (A), S100 (B), and CK7 (C).

TABLE 6. Results of Molecular Analysis of 17 Cases of Sinonasal Carcinomas

		FISH		RT-PCR		
Cases	Final Diagnosis	*ETV6*	*NTRK3*	Exons 5-15 Fusion Transcript	Archer NGS	Gene Status
1	MASC	Break	NA	Neg	*ETV6-NTRK3* exons 5-13	*ETV6-NTRK3*
2	MASC	Break	Break	+	ND	*ETV6-NTRK3*
3	LG SNAC	NA	Intact	NA	ND	Neg
4	LG SNAC	Intact	Intact	Neg	ND	Neg
5	LG SNAC	Intact	ND	Neg	ND	Neg
6	LG SNAC	Intact	ND	Neg	ND	Neg
7	LG SNAC	Intact	ND	Neg	ND	Neg
8	LG SNAC	NA	ND	Neg	ND	Neg
9	LG SNAC	Intact	ND	ND	ND	Neg
10	LG SNAC	Intact	ND	ND	ND	Neg
11	LG SNAC	Intact	ND	Neg	ND	Neg
12	LG SNAC	NA	ND	NA	ND	NA
13	LG SNAC	NA	ND	Neg	ND	Neg
14	LG SNAC	Intact	ND	Neg	ND	Neg
15	LG SNAC	Intact	ND	Neg	ND	Neg
16	LG SNAC	NA	ND	NA	ND	NA
17	LG SNAC	Intact	ND	Neg	ND	Neg

LG indicates low grade; NA, not analyzable; ND, not done.

S100 protein and mammaglobin,[1,31,32] and lacking DOG-1 expression.[33]

Low-grade SNACs represent a histologically heterogenous group of tumors, including non-ITAC and ITAC subtypes.[13] In recent years, an increasing number of distinct types of SNACs have been recognized, including HPV-related multiphenotypic sinonasal carcinoma, SMARCB1-deficient sinonasal carcinoma, and tubulopapillary low-grade SNAC.[16,34–37] Recently, Andreasen et al[18] reviewed a series of low-grade SNACs of non-ITAC type with tubulopapillary growth pattern and found a subset of tumors harboring *ETV6* rearrangements and the *ETV6-NTRK3* fusion in 2 of 3 cases. From a strictly genetic perspective, *ETV6*-rearranged low-grade SNAC represents a pitfall for identifying true sinonasal MASC. However, despite the identical genetic features of sinonasal MASC and *ETV6*-rearranged low-grade SNAC, the following features allow for accurate separation. First, all 3 *ETV6*-rearranged low-grade SNACs reported were predominantly tubular, composed of cylindrical to cuboidal
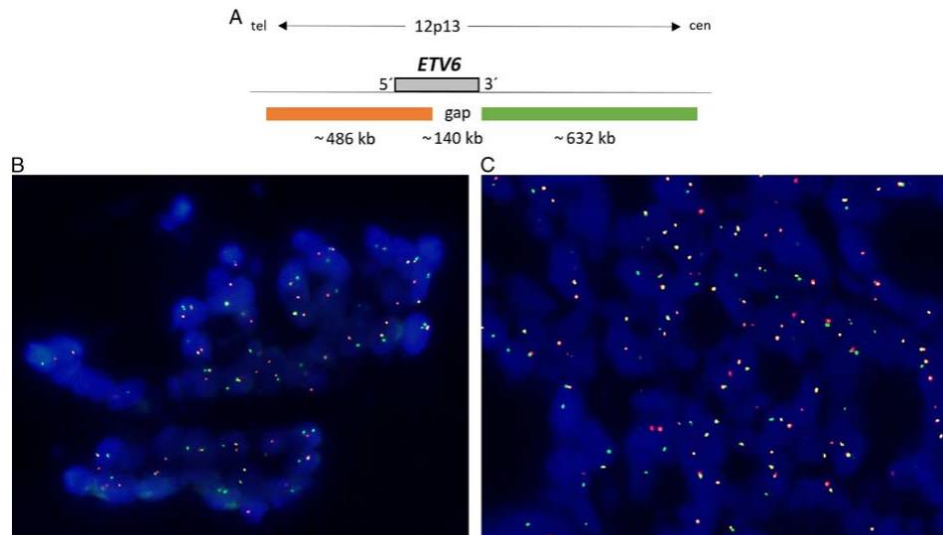

FIGURE 4. FISH. A, Design of the *ETV6* break-apart probe. B, Case 1 showing separate green and orange signals for *ETV6*. C, *NTRK3* indicating concomitant rearrangement of both genes.
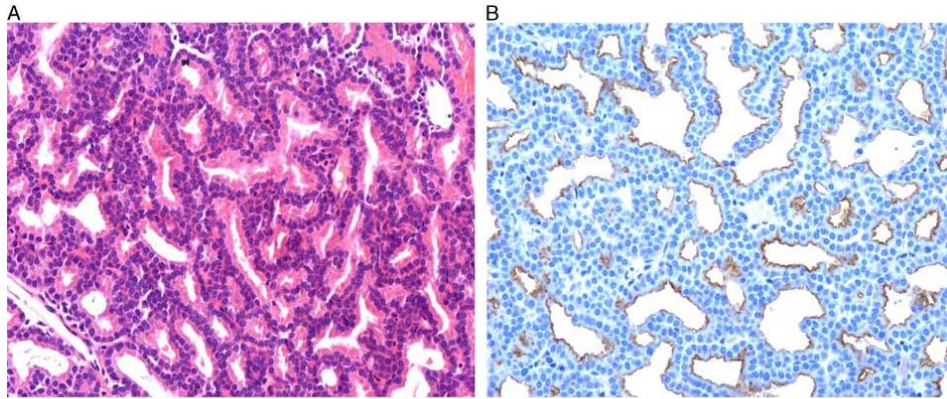
FIGURE 5. Histologic and immunohistochemical findings in *ETV6*-rearranged low-grade SNACs. A, *ETV6*-rearranged low-grade SNACs are composed of glands arranged back-to-back with little intervening stroma and minimal to absent secretory features. B, Tumors are focally DOG-1 positive.

tumor cells with occasional apocrine features and focal trabecular areas, which were not prominent features of sinonasal MASC. Second, tumor cells in *ETV6*-rearranged low-grade SNAC were arranged back-to-back with little intervening stroma with minimal or absent secretory features (Fig. 5A).[18] In contrast, both our MASCs showed abundant hyalinized septae and pronounced secretory features. Third, *ETV6*-rearranged low-grade SNAC is positive for DOG-1, negative for mammaglobin, and negative or patchy positive for S100, with the opposite being the case in MASC (Fig. 5B). Fourth, both MASCs presented here were invasive, whereas this was not seen in *ETV6*-rearranged low-grade SNAC.

The most important reason for separating these 2 entities is the difference in clinical behavior. While low-grade non-ITAC, including *ETV6*-rearranged low-grade SNAC, behaves in an essentially benign manner, MASC is a bona fide malignancy. Awareness of the existence of MASC within this anatomic region is important not only for separating these from the recently described *ETV6*-rearranged low-grade SNAC but also for separating MASC from more aggressive SNACs of non-ITAC and ITAC types.

In conclusion, we report 2 cases of sinonasal MASC and describe its unique features, which are valuable in its separation from *ETV6*-rearranged low-grade SNAC and other low-grade SNACs. Importantly, this separation is merited not only for academic reasons, as the more aggressive nature of MASC could necessitate treatment with TRK inhibitors.[19,20]

REFERENCES

1. Skalova A, Vanecek T, Sima R, et al. Mammary analogue secretory carcinoma of salivary glands, containing the *ETV6-NTRK3* fusion gene: a hitherto undescribed salivary gland tumor entity. *Am J Surg Pathol.* 2010;34:599–608.
2. Tognon C, Knezevich SR, Huntsman D, et al. Expression of the *ETV6-NTRK3* gene fusion as a primary event in human secretory breast carcinoma. *Cancer Cell.* 2002;2:367–376.
3. Amin SM, Beattie A, Ling X, et al. Primary cutaneous mammary analog secretory carcinoma with *ETV6-NTRK3* translocation. *Am J Dermatopathol.* 2016;38:842–845.
4. Bishop JA, Taube JM, Su A, et al. Secretory carcinoma of the skin harboring *ETV6* gene fusions: a cutaneous analogue to secretory carcinomas of the breast and salivary glands. *Am J Surg Pathol.* 2017;41:62–66.
5. Hyrcza MD, Ng T, Crawford RI. Detection of the *ETV6-NTRK3* translocation in cutaneous mammary-analogue secretory carcinoma. *Diagn Histopathol.* 2015;21:481–484.
6. Dogan S, Wang L, Ptashkin RN, et al. Mammary analog secretory carcinoma of the thyroid gland: a primary thyroid adenocarcinoma harboring *ETV6–NTRK3* fusion. *Modern Pathol.* 2016;29:985–995.
7. Dettloff J, Seethala RR, Stevens TM, et al. Mammary analog secretory carcinoma (MASC) involving the thyroid gland: a report of the first 3 cases. *Head Neck Pathol.* 2017;11:124–130.
8. Stevens TM, Kovalovsky AO, Velosa C, et al. Mammary analog secretory carcinoma, low-grade salivary duct carcinoma, and mimickers: a comparative study. *Mod Pathol.* 2015;28:1084–1100.
9. Lurquin E, Jorissen M, Debiec-Rychter M, et al. Mammary analogue secretory carcinoma of the sinus ethmoidalis. *Histopathology.* 2015; 67:749–751.
10. Xu B, Aryeequaye R, Wang L, et al. Sinonasal secretory carcinoma of salivary gland with high grade transformation: a case report of this under-recognized diagnostic entity with prognostic and therapeutic implications. *Head Neck Pathol.* 2017; DOI:10.1007/s12105-017-0855-5.
11. Slootweg PJ, Chan JKC, Stelow EB, et al. Tumours of the nasal cavity, paranasal sinuses and skull base. In: El-Naggar AK, Chan JKC, Grandis JR, Takata T, Slootweg PJ, eds. *WHO Classification of Head and Neck Tumours*, 4th ed. Lyon: IARC Press; 2017:11–76.
12. Leivo I. Sinonasal adenocarcinoma: update on classification, immunophenotype and molecular features. *Head Neck Pathol.* 2016;10:68–74.
13. Skalova A, Bell D, Bishop JA, et al. Secretory carcinoma. In: El-Naggar AK, Chan JKC, Grandis JR, Takata T, Slootweg PJ, eds. *WHO Classification of Head and Neck Tumours*, 4th ed. Lyon: IARC Press; 2017:177–178.
14. Heffner DK, Hyams VJ, Hauck KW, et al. Low-grade adenocarcinoma of the nasal cavity and paranasal sinuses. *Cancer.* 1982;50:312–322.
15. Wenig B, Hyams VJ, Heffner DK. Nasopharyngeal papillary adenocarcinoma. A clinicopathologic study of a low-grade carcinoma. *Am J Surg Pathol.* 1988;12:946–953.

16. Skálová A, Cardesa A, Leivo I, et al. Sinonasal tubulopapillary low-grade adenocarcinoma. Histopathological, immunohistochemical and ultrastructural features of poorly recognised entity. *Virchows Arch*. 2003;443:152–158.

17. Luna MA. Sinonasal tubulopapillary low-grade adenocarcinoma. A specific diagnosis or just another seromucous adenocarcinoma? *Adv Anat Pathol*. 2015;12:109–115.

18. Andreasen S, Skálová A, Agaimy A, et al. *ETV6* Gene rearrangements characterize a morphologically distinct subset of sinonasal low-grade non–intestinal-type adenocarcinoma. A novel translocation-associated carcinoma restricted to the sinonasal tract. *Am J Surg Pathol*. 2017;41:1552–1560.

19. Drilon A, Li G, Dogan S, et al. What hides behind the MASC: clinical response and acquired resistance to entrectinib after ETV6-NTRK3 identification in a mammary analogue secretory carcinoma (MASC). *Ann Oncol*. 2016;27:920–926.

20. Skalova A, Stenman G, Simpson RHW, et al. The role of molecular testing in the differential diagnosis of salivary gland carcinomas. *Am J Surg Pathol*. 2018;42:e11–e27.

21. Murphy DA, Ely HA, Shoemaker R, et al. Detecting gene rearrangements in patient populations through a 2-step diagnostic test comprised of rapid ihc enrichment followed by sensitive next-generation sequencing. *Appl Immunohistochem Mol Morphol*. 2017;25:513–523.

22. Viswanatha DS, Foucar K, Berry BR, et al. Blastic mantle cell leukemia: an unusual presentation of blastic mantle cell lymphoma. *Mod Pathol*. 2000;13:825–833.

23. Gaffney R, Chakerian A, O'Connell JX, et al. Novel fluorescent ligase detection reaction and flow cytometric analysis of SYT-SSX fusions in synovial sarcoma. *J Mol Diagn*. 2003;5:127–135.

24. Antonescu CR, Kawai A, Leung DH, et al. Strong association of SYT-SSX fusion type and morphologic epithelial differentiation in synovial sarcoma. *Diagn Mol Pathol*. 2000;9:1–8.

25. Bourgeois JM, Knezevich SR, Mathers JA, et al. Molecular detection of the ETV6-NTRK3 gene fusion differentiates congenital fibrosarcoma from other childhood spindle cell tumors. *Am J Surg Pathol*. 2000;24:937–946.

26. Ito Y, Ishibashi K, Masaki A, et al. Mammary analogue secretory carcinoma of salivary glands: a clinicopathological and molecular study including 2 cases harboring *ETV6-X* fusion. *Am J Surg Pathol*. 2015;39:602–610.

27. Skalova A, Vanecek T, Simpson RHW, et al. Mammary Analogue Secretory Carcinoma of Salivary Glands. Molecular Analysis of 25 *ETV6* Gene Rearranged Tumors With Lack of Detection of Classical *ETV6-NTRK3* Fusion Transcript by Standard RT-PCR: Report of 4 Cases Harboring *ETV6-X* Gene Fusion. *Am J Surg Pathol*. 2016; 40:3–13.

28. Chiosea SI, Griffith C, Assaad A, et al. Clinicopathological characterization of mammary analogue secretory carcinoma of salivary glands. *Histopathology*. 2012;61:387–394.

29. Chiosea SI, Griffith C, Assaad A, et al. The profile of acinic cell carcinoma after recognition of mammary analog secretory carcinoma. *Am J Surg Pathol*. 2012;36:343–350.

30. Bishop JA, Yonescu R, Batista D, et al. Most nonparotid "acinic cell carcinomas" represent mammary analog secretory carcinomas. *Am J Surg Pathol*. 2013;37:1053–1057.

31. Skálová A. Mammary analogue secretory carcinoma of salivary gland origin: an update and expanded morphologic and immunohistochemical spectrum of recently described entity. *Head Neck Pathol*. 2013;7: S30–S36.

32. Bishop JA. Unmasking MASC: bringing to light the unique morphologic, immunohistochemical and genetic features of the newly recognized mammary analogue secretory carcinoma of salivary glands. *Head Neck Pathol*. 2013;7:35–39.

33. Chenevert J, Duvvuri U, Chiosea S, et al. DOG1: a novel marker of salivary acinar and intercalated duct differentiation. *Mod Pathol*. 2012;25:919–929.

34. Bishop JA. Newly described tumor entities in sinonasal tract pathology. *Head Neck Pathol*. 2016;10:23–31.

35. Bishop JA, Andreasen S, Hang JF, et al. HPV-related multiphenotypic sinonasal carcinoma: an expanded series of 49 Cases of the tumor formerly known as HPV-related carcinoma with adenoid cystic carcinoma-like features. *Am J Surg Pathol*. 2017;41:1690–1701.

36. Andreasen S, Bishop JA, Hansen TV, et al. Human papillomavirus-related carcinoma with adenoid cystic-like features of the sinonasal tract: clinical and morphological characterization of six new cases. *Histopathology*. 2017;70:880–888.

37. Agaimy A, Hartmann A, Antonescu CR, et al. SMARCB1 (INI-1)-deficient sinonasal carcinoma: a series of 39 cases expanding the morphologic and clinicopathologic spectrum of a recently described entity. *Am J Surg Pathol*. 2017;41:458–471.

140

3. část - Přehledové články

Přehledový článek „*The role of molecular testing in the differencial diagnosis of Salivary Gland Carcinomas*" [25] obsáhle komentuje translokační salivární karcinomy spolu s nejagresivnějším salivárním duktálním karcinomem a polymorfním a kribriformním adenokarcinomem. Karcinomy jsou detailně histologicky popsány, včetně diferenciální diagnózy, prognózy onemocnění a poznatků z molekulární genetiky.

Druhý článek „*Novinky v molekulární diagnostice karcinomů slinných žláz: „translokační karcinomy"*" [35] pojednává o translokacích diagnostického či prognostického významu nalezených u salivárních karcinomů. Konkrétně se jedná o t(11;19)(q21;p13) a t(11;15)(q21;q26) neboli *CRTC1-MAML2* a *CRTC3-MAML2* vyskytující se u převážně low-grade mukoepidermoidního karcinomu, dále t(6;9)(q22-23;p23-24) neboli *MYB-NFIB* u adenoidně cystického karcinomu, t(12;15)(p13;q25) neboli *ETV6-NTRK3* u sekrečního karcinomu mamárního typu a konečně t(12;22)(q13;q12) neboli *EWSR1-ATF1* u hyalinizujícího světlobuněčného karcinomu malých slinných žláz.

Poslední přehledový článek „*Metody detekce molekulárních prognostických a prediktivních markerů v diagnostice adenoidně cystického karcinomu slinných žláz*" [23] se zaobírá především popisem principů molekulárně-genetických metodik a poznatků, jež bylo využitím daných metodik dosaženo u adenoidně cystického karcinomu slinných žláz. Mezi tyto metodiky patří reverzně-transkripční PCR, fluorescenční in-situ hybridizace, komparativní genomová hybridizace, expresní čipová analýza, sekvenování nové generace, epigenetické metody pro detekci metylace promotorů genů a imunohistochemie.

The Role of Molecular Testing in the Differential Diagnosis of Salivary Gland Carcinomas

Alena Skálová, MD, PhD,* Göran Stenman, MD, PhD,†‡
Roderick H.W. Simpson, MD, ChB, FRCPath,§ Henrik Hellquist, MD, PhD, FRCPath,∥
David Slouka, MD, PhD,¶ Tomas Svoboda, MD, PhD,# Justin A. Bishop, MD,**
Jennifer L. Hunt, MD, MEd,†† Ken-Ichi Nibu, MD, PhD,‡‡
Alessandra Rinaldo, MD, FRCSEd ad hominem, FRCS (Eng, Ir) ad eundem, F,§§
Vincent Vander Poorten, MD, MSc, PhD,§∥∥¶¶
Kenneth O. Devaney, MD, JD, FCAP,## Petr Steiner, Mgr,****
and Alfio Ferlito, MD, DLO, DPath, FRCSEd ad hominem, FRCS (Eng, Glas)†††

Abstract: Salivary gland neoplasms are a morphologically heterogenous group of lesions that are often diagnostically challenging. In recent years, considerable progress in salivary gland taxonomy has been reached by the discovery of tumor type-specific fusion oncogenes generated by chromosome translocations. This review describes the clinicopathologic features of a selected group of salivary gland carcinomas with a focus on their distinctive genomic characteristics. Mammary analog secretory carcinoma is a recently described entity characterized by a t(12;15)(p13;q25) translocation resulting in an *ETV6-NTRK3* fusion. Hyalinizing clear cell carcinoma is a low-grade tumor with infrequent nodal and distant metastasis, recently shown to harbor an *EWSR1-ATF1* gene fusion. The *CRTC1-MAML2* fusion gene resulting from a t(11;19)(q21;p13)

translocation, is now known to be a feature of both low-grade and high-grade mucoepidermoid carcinomas associated with improved survival. A t(6;9)(q22-23;p23-34) translocation resulting in a *MYB-NFIB* gene fusion has been identified in the majority of adenoid cystic carcinomas. Polymorphous (low-grade) adenocarcinoma and cribriform adenocarcinoma of (minor) salivary gland origin are related entities with partly differing clinicopathologic and genomic profiles; they are the subject of an ongoing taxonomic debate. Polymorphous (low-grade) adenocarcinomas are characterized by hot spot point E710D mutations in the *PRKD1* gene, whereas cribriform adenocarcinoma of (minor) salivary glands origin are characterized by translocations involving the *PRKD1-3* genes. Salivary duct carcinoma (SDC) is a high-grade adenocarcinoma with morphologic and molecular features akin to invasive ductal carcinoma of the breast, including *HER2* gene amplification, mutations of *TP53*, *PIK3CA*, and *HRAS* and loss or mutation of *PTEN*. Notably, a recurrent *NCOA4-RET* fusion has also been found in SDC. A subset of SDC with apocrine morphology is associated with overexpression of androgen receptors. As these genetic aberrations are recurrent they serve as powerful diagnostic tools in salivary gland tumor diagnosis, and therefore also in refinement of salivary gland cancer classification. Moreover, they are promising as prognostic biomarkers and targets of therapy.

Key Words: salivary gland carcinoma, mammary analog secretory carcinoma, mucoepidermoid carcinoma, hyalinizing clear cell carcinoma, adenoid cystic carcinoma, salivary duct carcinoma, polymorphous adenocarcinoma, cribriform adenocarcinoma, fusion oncogenes, molecular testing

(Am J Surg Pathol 2017;00:000–000)

Salivary gland tumors are relatively uncommon and morphologically highly diverse. Thus, the significant histologic overlap between tumor types with different biological behavior not only poses diagnostic challenges, but also continues to stimulate pathologists to look for new ancillary tests using immunohistochemistry (IHC) and

molecular techniques. IHC markers are useful supplementary aides for visualization of cell compartments and cell populations, thus contributing to improved salivary gland tumor classification.[1,2] Moreover, IHC also has an expanding role as surrogate markers of molecular alterations.[3,4]

Until recently, translocations and their resulting fusion oncogenes were thought to be rare in epithelial tumors. Typically, these somatic genetic aberrations were found in hematological and soft tissue neoplasms and thought to be rare or even absent in other tumor lineages.[5–7] Recently, however, the discovery of key molecular alterations in a variety of salivary gland tumors has significantly increased our knowledge about their molecular pathology and improved the classification of salivary gland neoplasms and also changed the way diagnoses are made.[8–11] Consequently, some existing tumor types have become more refined, and a few new salivary tumor entities have been characterized,[12,13] some of which have already been adopted in the new World Health Organization (WHO) Classification of Head and Neck Tumors.[14]

These genomic aberrations are recurrent and tumor type specific and may serve as powerful diagnostic tools in salivary gland diagnosis and classification. They also show promise as prognostic biomarkers and as new targets for therapy.[15] Some of these fusions have been found also in other tumor types that show little or no overlap with their salivary gland counterparts, but effectively they are specific within the salivary gland.[16–19]

In this review salivary carcinomas currently known to harbor translocations will be discussed, namely secretory carcinoma (SC) (also known as mammary analog secretory carcinoma [MASC]), hyalinizing clear cell carcinoma (HCCC), mucoepidermoid carcinoma (MEC), adenoid cystic carcinoma (AdCC), and 2 related low-grade salivary gland adenocarcinomas, namely polymorphous (low-grade) adenocarcinoma (PLGA/PAC) and cribriform adenocarcinoma of (minor) salivary gland origin (CASG). Finally, we will also discuss salivary duct carcinoma (SDC) (Table 1).

MAMMARY ANALOG SECRETORY CARCINOMA

MASC of salivary gland origin is a recently described tumor that harbors a characteristic balanced t(12;15)(p13;q25) chromosomal translocation resulting in an ETV6-NTRK3 fusion[20] identical to that commonly found in SC of the breast.[21] The Etv6-NTRK3 fusion gene encodes a chimeric tyrosine kinase with transforming activity in epithelial and myoepithelial cells in the mouse mammary gland.[22]

Over many years Skalova et al[20] began to identify a distinctive hitherto unrecognized neoplasm arising in the salivary glands characterized by morphologic and immunohistochemical features strongly reminiscent of those of SC of the breast. These salivary carcinomas are composed of microcystic and solid areas with abundant vacuolated colloid-like periodic acid Schiff-positive secretory material within the microcystic spaces (Fig. 1A). They had previously

TABLE 1. Key Molecular Alterations in Selected Salivary Gland Carcinomas

Tumor Type	Chromosomal Alteration	Gene Fusion/ Rearrangement	Prevalence (%)
MASC	t(12;15)(p13;q25)	ETV6-NTRK3	95-98
	t(12;X)	ETV6-RET	2-5
MEC	t(11;19)(q21;p13)	CRTC1-MAML2	40-80
	t(11;15)(q21;q26)	CRTC3-MAML2	5
HCCC	t(12;22)(q21;q12)	EWSR1-ATF1	80-90
AdCC	t(6;9)(q22-23;p23-24)	MYB-NFIB	25-80
	t(8;9)	MYBL1-NFIB	10-20
PLGA	14q12	Hotspot activating PRKD1 somatic point mutation (E710D)	20
CAS-Gs	t(1;14)(p36.11;q12)	ARID1A-PRKD1	24
	t(X;14)(p11.4;q12)	DDX3X-PRKD1	13
		PRKD2 and PRKD3 rearrangements	16
SDC	17q21.1	HER2 amplification	20-40
	3q26.32	PIK3CA mutation	20
	inv(10)(q11.21q11.22)	NCOA4-RET	<5

been categorized as either unusual variants of salivary acinic cell carcinoma (AciCC) or cystadenocarcinoma not otherwise specified.[20]

Skalova et al[20] initially recognized MASC as an entity different from AciCC on the basis of 3 major findings. First, MASC showed no basophilia in the cytoplasm in any of the constituent cells, which is the hallmark of the serous acinar cells of AciCC resulting from the presence of cytoplasmic zymogen granules. Second, these neoplasms had a completely different immunohistochemical profile, almost always expressing S100 protein, mammaglobin, vimentin, STAT5, and MUC4, all of which were rarely expressed in AciCC. Finally, unlike AciCC, most cases were found to harbor an ETV6-NTRK3 fusion gene due to a t(12;15)(p13;q25), a finding identical to SC of the breast.[21] Because of the morphologic and genomic similarities, Skalova et al,[20] proposed the designation "mammary analog secretory carcinoma (MASC) of salivary gland." The most recent version of the WHO Classification of Head and Neck Tumors, however, utilizes terminology "secretory carcinoma,"[23] for consistency and because SCs have been recently described at other sites, such as thyroid gland and skin.[24–26]

The near 100% rate of ETV6 gene rearrangements in MASC has been subsequently confirmed by many other studies.[27–30] Detection of ETV6 rearrangements by fluorescence in situ hybridization (Fig. 1B) or ETV6-NTRK3 fusion by reverse transcription polymerase chain reaction in formalin-fixed paraffin-embedded material (Fig. 1C) is technically straightforward, and >250 cases of MASC have been published since its original description in 2010.[20]

The presence of the ETV6-NTRK3 fusion gene has not been demonstrated in any other salivary gland tumor. However, the same fusion is found not only in SC of the breast,[21] but also in infantile fibrosarcoma,[31] congenital mesoblastic nephroma,[32] certain hematopoietic malignancies,[33] ALK-negative inflammatory myofibroblastic
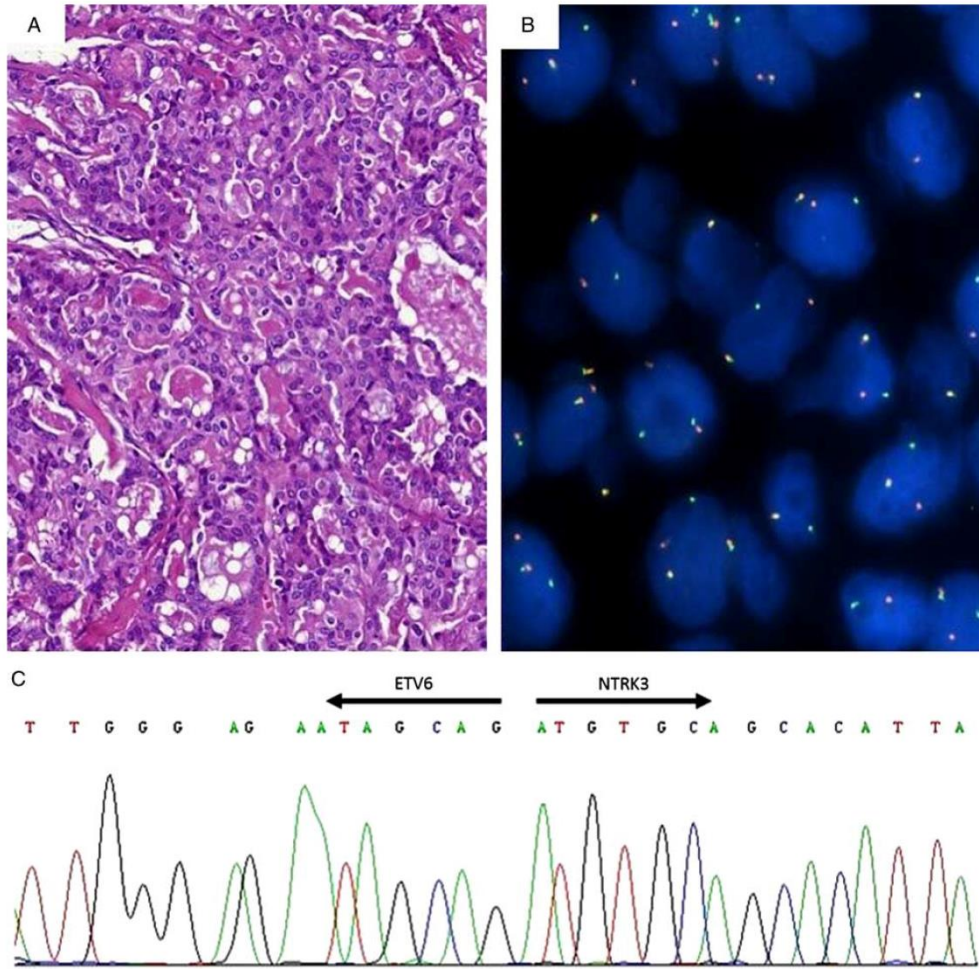
FIGURE 1. MASC of salivary gland. A, MASC is composed of microcystic and solid areas with abundant vacuolated colloid-like PAS-positive secretory material within the microcystic spaces. B, FISH analysis of ETV6 gene. C, Part of the ETV6-NTRK3 fusion transcript sequence. FISH indicates fluorescence in situ hybridization; PAS, periodic acid Schiff.

tumors,[34] and in radiation-induced papillary thyroid carcinomas.[35] MASCs of the thyroid gland have recently been reported also in patients without history of radiation exposure.[36–38] Moreover, *ETV6*-rearranged carcinomas with secretory features have been reported in the skin[26,39] and sinonasal mucosa.[40]

A small subset of MASCs show *ETV6* rearrangements with an as yet unknown partner(s) or may have atypical *ETV6-NTRK3* exon fusion junctions.[41] These atypical molecular features may be associated with more infiltrative histologic characteristics of MASC, and less

favorable clinical outcomes.[41,42] In addition, MASCs with *ETV6-X* gene fusion and other atypical fusion transcripts often demonstrate abundant fibrosclerotic stroma and particularly prominent, thick hyalinized fibrous septa.[41,42] The neoplastic cells may be embedded in a completely hyalinized central part of the tumor. Recently, next-generation sequencing using the ArcherDX analysis platform detected a novel ETV6-RET fusion transcript joining exon 6 of ETV6 gene and exon 12 of RET gene in 10 cases of salivary gland tumors displaying histologic and immunohistochemical features typical of SC (Figs. 2A–C).[43]
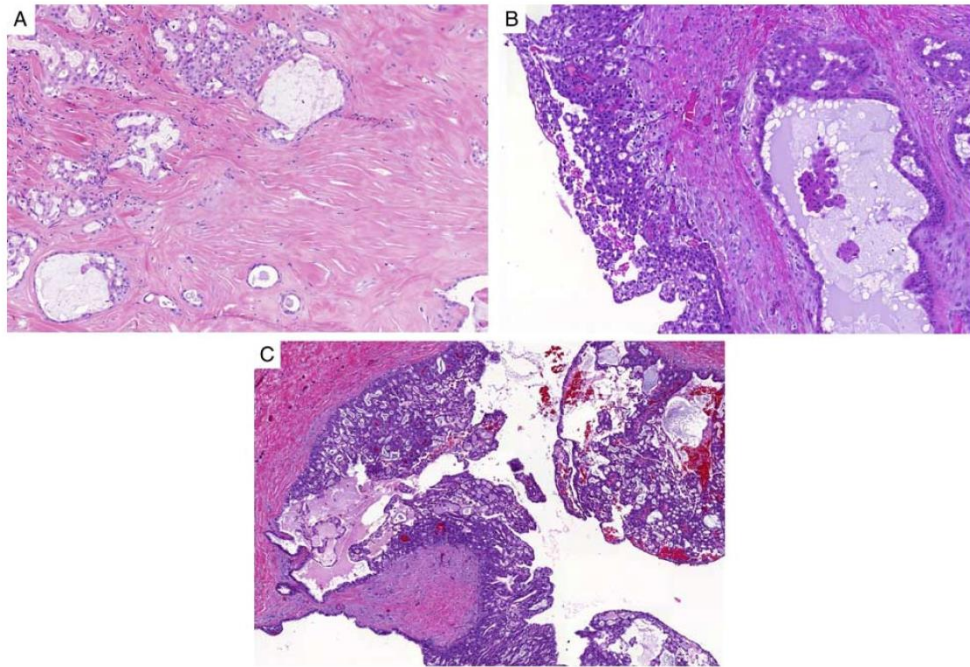
FIGURE 2. MASC of salivary gland. A, MASC has a prominent fibrosclerotic stroma with isolated tumor cells in small islands or trabeculae were seen in central part of the tumor. B, MASC is characterized by solid and microcystic growth with a multilobular structure. The cysts are lined by a double layer of cells with prominent apocrine features. C, MASC is well circumscribed and surrounded by a thick fibrous capsule enclosing predominantly multicystic growth pattern with multiple mural nodules.

Differential Diagnosis

The major differential diagnostic consideration is AciCC. The architectural patterns of MASC (ie, microcystic, papillary-cystic, follicular, and solid) overlap with those of AciCC. However, the large serous acinar cells with cytoplasmic periodic acid Schiff-positive zymogen-like granules typical of AciCC are completely absent in MASC.[20] Intraductal carcinoma, previously called "low-grade salivary duct carcinoma" is characterized by a prominent cystic tumor component associated with proliferation of bland eosinophilic ductal cells, frequent intraluminal secretions, and expression of S100 protein and mammaglobin, features that overlap with MASC.[36,44,45] In contrast to MASC, the epithelial structures of intraductal carcinoma are characteristically surrounded by an intact layer of p63-positive myoepithelial cells. Low-grade MEC is another potential consideration in the differential diagnosis of MASC because both tumor types can have a prominent cystic component, variable mucicarmine positivity together with cytologically bland cells that can be eosinophilic, clear, or vacuolated.[29] In contrast to MASC, MEC is consistently positive for p63 in the epidermoid foci and is negative for S100 and mammaglobin. In addition, low-grade MECs harbor a different chromosomal translocation, that is a t(11;19) resulting in a *CRTC1-MAML2* fusion.[46,47]

Clinical Features and Prognosis

MASC usually behaves indolently, but like other low-grade salivary gland carcinomas, there is some capacity for aggressive behavior including locoregional recurrence and distant metastasis. Particularly important is the rare occurrence of high-grade transformation (HGT) that may result in tumor-related death.[48,49]

The treatment of MASC has varied, ranging from simple excision to radical resection, neck dissection, adjuvant radiotherapy, and/or adjuvant systemic chemotherapy.[20,45,50] Recognizing MASC and testing for *ETV6* rearrangements may be of potential value in treatment decisions, because the *ETV6-NTRK3* fusion may serve as a target for treatment of tumors with this fusion at multiple anatomic sites, including the parotid gland.[51–53]

Application of Molecular Testing

For patients presenting with a locally advanced, recurrent, or metastatic MASC cases, the treatment options are currently limited and mainly palliative. Therefore, testing for *ETV6* rearrangements may be of potential
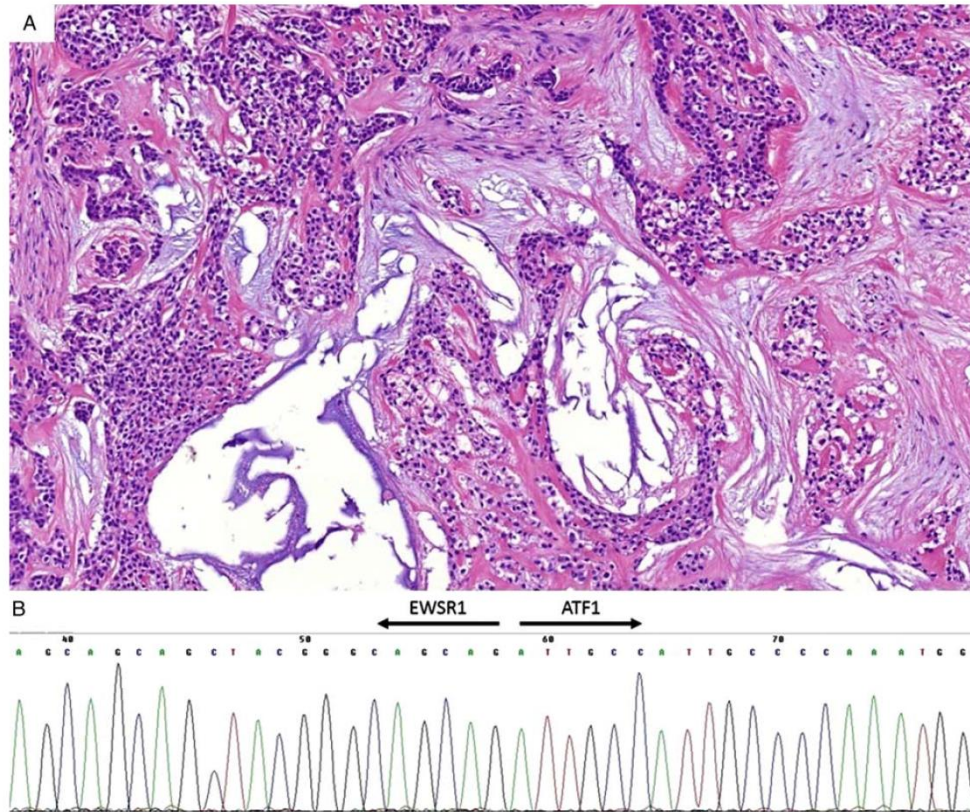
FIGURE 3. HCCC. A, The tumor is composed of cords and nests of clear cells in a hyalinized and myxoid stroma. B, Part of EWSR1-ATF1 transcript fusion sequence.

value in treatment decisions, because the *ETV6-NTRK3* and *ETV6-RET* fusions may serve as a target for therapy. MASC with *ETV6-RET* fusion must be clearly distinguished from MASCs with *ETV6-NTRK3* translocation, because drugs effective with various tumors driven with *RET* gene alterations, are being tested for the treatment. MASCs with *ETV6-RET* translocation might respond much better to these drugs, whereas entrectinib and similar inhibitors of tyrosine kinases TRKA/B/C will probably be ineffective.

HYALINIZING CLEAR CELL CARCINOMA

HCCC is a rare salivary gland malignancy with squamous differentiation and prominent clear cell morphology (Fig. 3A). Recently, it was discovered that most HCCCs have a recurrent t(12;22)(q13;q12) chromosomal translocation, leading to fusion of the *EWSR1* and *ATF1* genes (Fig. 3B). Notably, this rearrangement was not detected in myoepithelioma, PLGA, MEC, or epithelial-myoepithelial carcinoma (EMCA).[54,55]

EWSR1 rearrangements are also seen in a variety of epithelial and soft tissue tumors, including soft tissue myoepithelioma; however, the fusion partner genes that are common in myoepithelioma (*FUS, POU5F1, PBX1,* and *ZNF444*) does not seem to be involved in HCCC.[54,56] *EWSR1-ATF1*, which originally was identified in soft tissue clear cell sarcomas,[57] has also been described in 1 case of soft tissue myoepithelioma of the pelvis[58] and in angiomatoid fibrous histiocytoma.[59]

Initial studies failed to identify *EWSR1* rearrangements in other classic salivary gland tumors,[54] but more recently, Skalova et al[60] reported *EWSR1* rearrangements in 25 of 72 (34.7%) clear cell myoepithelial carcinomas (de novo and ex-pleomorphic adenoma [PA]) as well as in 1 of 11 (9%) EMCAs. Cases of *EWSR1*-rearranged myoepithelial carcinoma commonly had at least focal areas of necrosis, squamous pearls, and significant nuclear

pleomorphism. In cases where the differential diagnosis includes *EWSR1*-rearranged myoepithelial carcinoma and HCCC, the diagnosis depends more heavily on morphology and immunophenotypic markers because HCCC only infrequently shows focal myoepithelial differentiation with S100 positivity.

Differential Diagnosis

Although the finding of infiltrative nests of low-grade clear tumor cells with hyalinized and cellular fibrous stroma is quite characteristic of HCCC, several other tumor types, such as myoepithelial carcinoma, EMCA, and MEC, can enter into the differential diagnosis. In most instances the diagnosis is readily apparent, but cases with limited biopsy material or with only focal clear cell differentiation often require additional ancillary testing. In such cases, *EWSR1* FISH testing may be of great value. The current recommendation is that *EWSR1* FISH is not necessary in classic mucin-negative cases of HCCC. However, when abundant mucin is present or when there is minimal clear cell differentiation or hyalinization, confirmation can be useful. MECs showing similar features will generally have a higher grade than HCCC and potentially different treatment.[54,61] This is because most HCCCs lack cystic features, have highly infiltrative tumor fronts, and often show perineural invasion. With mucinous differentiation, these would be considered at least intermediate-grade, or even high-grade when using most traditional MEC grading schemes.[54,61]

Clinical Features and Prognosis

Although often indolent, HCCC shows occasional recurrences and/or metastases to lymph nodes in the neck.[54,62] They have a tendency to invade bone and show prominent perineural invasion in about half of the cases[54] and this can occasionally lead to pain or muscle atrophy.[61] Very rare examples of distant metastasis have been reported and occasional deaths due to the disease have been described.[55,61,63] These rates of morbidity and mortality are probably comparable with most other low-grade salivary gland carcinomas.

Application of Molecular Testing

Detection of *EWSR1* rearrangements in salivary gland tumors currently has no prognostic or predictive value but serves as good differential diagnostic tool and in refining classification criteria.

MUCOEPIDERMOID CARCINOMA

MEC is the most common salivary gland carcinoma and occurs approximately equally at major and minor salivary gland sites.[64] MEC is composed of 3 cell types: mucinous cells, often large and goblet like, which often line cystic spaces, epidermoid cells that are nonkeratinizing and may even look frankly squamous, and finally intermediate cells which are more basal or cuboidal (Fig. 4A). Atypia is unusual and the epidermoid/squamoid cells tend to be very bland akin to normal mucosal epithelium.[64]

MEC is associated with one of the most clinically useful translocations, involving the *MAML2* and *CRTC1 or CRTC3* genes (Fig. 4B). A recurrent t(11;19)(q21;p13) translocation, resulting in a *CRTC1-MAML2* fusion, was first described in MEC in 2003.[65,66] Later studies revealed that a small subset of MECs instead has t(11;15)(q21;q26) translocations generating molecularly similar *CRTC3-MAML2* fusions.[67,68] The use of *MAML2* FISH has been proposed as a useful ancillary test in the routine clinical diagnosis of salivary gland tumors in which MEC enters the differential diagnosis.[69] Recently, detection of AREG expression (downstream target of the *CRTC1-MAML2* fusion) has been reported to be useful for identifying *CRTC1-MAML2*-positive MECs and as a marker of favorable prognosis.[70]

The mutational profile of MEC is only partly known. *TP53* was the most commonly mutated gene in a whole-exome study of 18 MECs.[71] Other recurrently mutated genes were *POU6F2* (only seen in low-grade tumors), *IRAK1*, *MAP3K9*, *ITGAL*, *ERBB4*, *OTOGL*, *KMT2C*, and *OBSCN*. These observations were partly confirmed in a targeted resequencing study of 315 genes in 48 MECs identifying *TP53* as the most frequently mutated gene (41.7%). Recurrent genomic alterations were also found in *PI3KCA*, *BAP1*, *BRCA1/2*, and *ERBB2* (gene amplification).[72] Recurrent deletions of the tumor suppressor gene CDKN2A is also a characteristic feature of high-grade MECs.[72,73]

Differential Diagnosis

Clinically, detection of a *MAML2* rearrangement using break-apart FISH probes is helpful in several situations. In cases of low-grade MEC, differential diagnostic considerations can often include benign entities, such as metaplastic variant of Warthin tumor (WT),[74] or more rare lesions such as lymphadenoma. In such cases, detection of *MAML2* rearrangement confirms the diagnosis of MEC. Although some authors have reported *MAML2* translocations in WT[75] some even suggest that MEC can arise from WT,[76] others argue these cases may represent low-grade MEC mimicking WT, and most consider the finding of a *MAML2* rearrangement to strongly favor a diagnosis of MEC over WT.[77–83]

A particular scenario in which *MAML2* FISH can be extremely useful is the oncocytic variant of MEC, in which the prominent oncocytic morphology can mask the epidermoid phenotype, and mimic WT, oncocytic cystadenoma, or AciCC. Although p63 reactivity can be useful in many cases to suggest a diagnosis of MEC, detection of *MAML2* rearrangements confirms a diagnosis of MEC.[74,84,85] Although many of the oncocytic MECs that enter the differential diagnosis with benign mimickers (WT and oncocytic cystadenoma) will be low grade and unlikely to metastasize, the diagnosis of malignancy may nevertheless be important in highlighting the potential for more frequent recurrence.

At the other end of the spectrum, high-grade MEC can mimic a variety of other high-grade cancers, including metastatic squamous cell carcinoma, adenosquamous
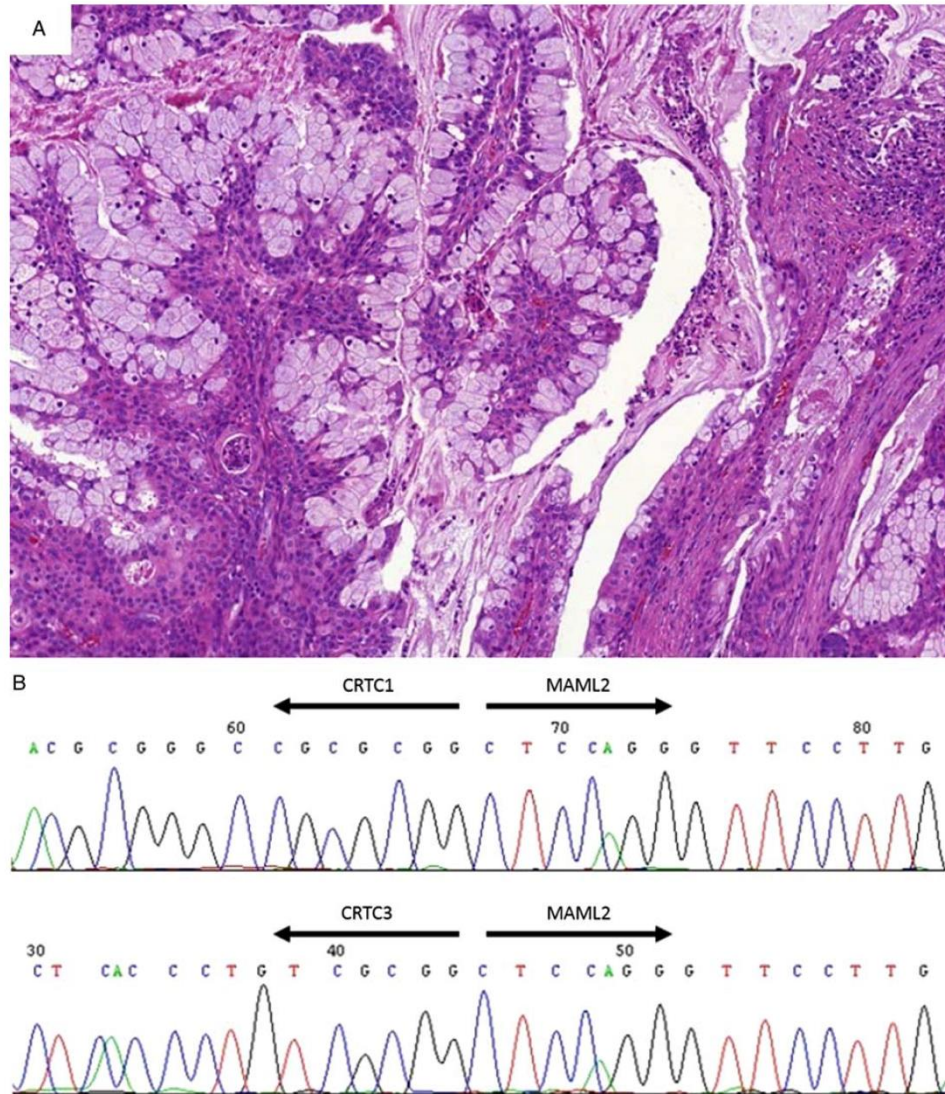
FIGURE 4. MEC. A, MEC is composed of large mucinous cells, epidermoid, and intermediate cells. B, Part of CRTC1-MAML2 and CRTC3-MAML2 transcript fusion sequence.

carcinoma, and SDC. In these instances, identification of a *MAML2*-rearrangement is diagnostic for MEC, which can be important because, in the parotid gland, this excludes the possibility of a metastasis. High-grade MECs are less likely to have *MAML2* rearrangements, hence the absence of a rearrangement does not rule out a diagnosis of MEC.[80,86,87] Differential diagnostic considerations for

such tumors include SDC, adenosquamous carcinoma, and even squamous cell carcinoma; all of which, in general, have a poorer prognosis than high-grade MEC. SDC frequently stains positive for androgen receptor (AR) and is p63 negative, which contrasts with MEC, which is usually AR-negative and has at least focal reactivity for p63. Adenosquamous and squamous cell carcinoma are

148

generally considered to arise from surface epithelium, in contrast to MEC, which does not have a surface in situ component. The presence of more than just focal keratinization favors a diagnosis of squamous cell carcinoma over MEC.

In addition to salivary gland MEC, *MAML2* rearrangement can also be detected in central (intraosseous) MEC[88] and MEC of the lacrimal gland,[89] thyroid,[90] thymus,[91] lung,[92,93] and cervix.[94] *CRTC1-MAML2* fusion has also been identified in cases of cutaneous clear cell hidradenoma.[95] *MAML2* can fuse with *KMT2A* (previously *MLL*) in some cases of acute myelogenous leukemia.[96] *MAML2*-rearrangements are not detected in glandular odontogenic cysts, which can enter the differential diagnosis, especially for a central (intraosseous) MEC.[97]

Clinical Features and Prognosis

The presence of *MAML2* rearrangement correlates with prognosis and stage because tumors with this rearrangement tend to be less aggressive and of lower histologic grade.[75,76,80,98] This statement only seems to hold in the absence of deletions inactivating the tumor suppressor gene *CDKN2A*.[99] *MAML2* rearrangements have been detected in up to three quarters of low-grade and intermediate-grade MECs, but fewer than one half of high-grade MECs seem to be fusion-positive. Among high-grade MECs there is recent evidence that fusion-negative tumors behave much more aggressively than fusion-positive ones. It has been proposed that *CRTC1-MAML2* fusion-negative high-grade carcinomas with MEC-like morphologic features and scanty mucin content actually represent a heterogenous group of other high-grade carcinomas which could relate to their more aggressive behavior.[73]

Application of Molecular Testing

The *CRTC1* and *CRTC3-MAML2* were originally considered prognostic markers in MEC,[68,78,98] however, more recent studies fail to show this, and in fact the original prognostic value may have been an artifact of misclassification of high-grade tumors. Detection of a *MAML2* rearrangement using break-apart FISH probes is helpful in differential diagnosis.

ADENOID CYSTIC CARCINOMA

AdCC is a common salivary gland carcinoma of both minor and major glands and the sinonasal mucosa. AdCC is characterized by its slow but relentless clinical progression. It is a morphologically bland but highly infiltrative and aggressive biphasic basaloid tumor composed of abluminal myoepithelial and luminal ductal cells arranged in tubular, cribriform, and solid growth patterns. The cells tend to have scant cytoplasm and angulated hyperchromatic nuclei (Figs. 5A, B). Perineural invasion is almost invariably present with adequate sampling.[100] Conventional AdCC is typically composed of all growth patterns in variable proportions, and is graded based on the extent of any solid growth component; >30% to 50%

solid component constitute grade 3.[101] AdCC with HGT is characterized by an overgrowth of the ductal component into a pleomorphic high-grade or undifferentiated adenocarcinoma.[102–104]

The most significant advance in the understanding of the molecular pathology of AdCC is the discovery and characterization of the t(6;9)(q22-23;p23-24) translocation (Fig. 5C).[105,106] The translocation results in an *MYB-NFIB* gene fusion which is the main genomic hallmark of AdCC.[11,15,107] The fusion is an oncogenic driver which activates several critical downstream targets with transforming potential.[15] Activation of the *MYB* oncogene by gene fusion or other mechanisms (eg, enhancer hijacking) has been shown by break-apart or fusion FISH or fusion transcript reverse transcription polymerase chain reaction in up to 80% of AdCCs.[108–110] Recently, a small subset of *MYB-NFIB* negative cases were shown to have t(8;9) translocations resulting in closely related *MYBL1-NFIB* fusions.[111,112]

Other genomic alterations in AdCC are variable with solid tumors showing a higher number of copy number alterations, including chromosomal losses involving 1p and 6q.[113] Interestingly, there is some evidence to suggest that 1p deletion correlates with poor prognosis.[114] Studies of the mutational landscape of >100 AdCCs have revealed a low exonic mutation rate and a wide mutational spectrum.[107,114,115] Although the frequency of mutations in individual genes seems to be very low, the mutations preferentially cluster in certain pathways, including those involved in chromatin regulation, DNA-damage/checkpoint signaling, FGF-IGF-PI3K-signaling and NOTCH-signaling, and axonal guidance. Interestingly, several of these are actionable mutations, calling for genetic testing of patients with AdCC to individualize and optimize the treatment.

Differential Diagnosis

AdCC is a biphasic salivary gland neoplasm consisting of a variety of architectural patterns. The abluminal myoepithelial cells often secrete a basement membrane-like material which is deposited in characteristic extracellular pseudocystic/cribriform myxoid and hyalinized extracellular matrix deposits. Although this might be a useful diagnostic clue, identical extracellular matrix deposits can be produced also by other biphasic salivary gland neoplasms, including PA, EMCA, basal cell adenoma/adenocarcinoma, and PLGA/PAC.[14] Distinguishing AdCC from its histomorphologic mimics is crucial for optimal treatment decisions.

The tumor border is important as pleomorphic and basal cell adenomas have well demarcated or even encapsulated edges, whereas basal cell adenocarcinoma and EMCA are multinodular, in sharp contrast to AdCC which is almost always frankly invasive. However, tumor borders are not apparent in small biopsies. In such cases, important clues to the diagnosis of AdCC are angulated hyperchromatic nuclei, as well as frequent mitotic figures and a Ki-67 index usually above 10%.[116] In addition, MYB protein expression by IHC shows strong nuclear
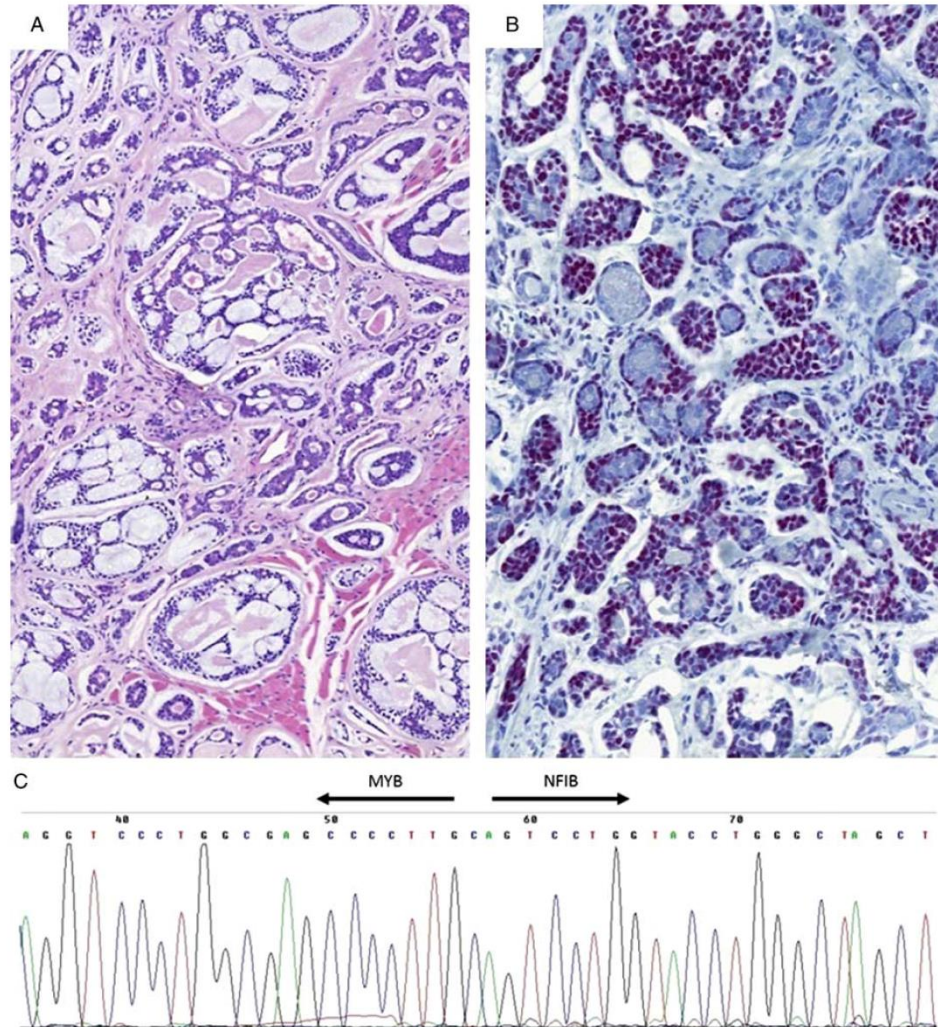
149

FIGURE 5. AdCC. A, AdCC is morphologically bland but highly infiltrative biphasic basaloid tumor, composed of abluminal myoepithelial and luminal ductal cells arranged in tubular, cribriform, and solid growth patterns. B, Nuclear expression of MYB antibody is seen in most cells of AdCC. C, Part of MYB-NFIB transcript fusion sequence.

staining in ≈90% of AdCCs irrespective of the mechanism of activation of *MYB*.[108] Although focal weak staining may occasionally be seen in other salivary gland tumors, MYB protein expression may still have utility in the diagnosis of difficult cases of AdCC.

Clinical Features and Prognosis

AdCC is characterized by its slow but relentless clinical progression with ultimate poor clinical outcome in most patients. Local recurrences and distant metastases are common but nodal disease is relatively rare in conventional AdCC,[100] especially for parotid gland primaries. The risk for nodal disease in AdCC is, however, distinctly higher in cases of AdCC with HGT.[103,104] HGT is an uncommon phenomenon among salivary carcinomas and is associated with increased tumor aggressiveness.[103] In AdCC with HGT, the clinical course tends to be accelerated, with a high propensity for lymph node metastasis.[104]

Because of the historically low incidence of occult nodal metastasis, neck dissection is only performed in case of clinically positive lymph nodes. Clinically obvious lymph node metastasis is not frequent in AdCC, especially not for parotid gland primaries.[117] However, for minor salivary gland subsites the incidence of lymph node involvement seems to be higher. Min et al[118] described a general incidence of lymph node metastases in AdCCs of the head and neck of almost 10%, which was mainly attributed to tumor sites such as base of tongue, mobile tongue, and floor of the mouth.[118] They also noted that primary tumor site and peritumoral lymphovascular invasion were significantly associated with cervical lymph node metastasis.

Recent rigorous reviews of the world literature by the International Head and Neck Scientific Group revealed high prevalence of lymph node metastasis in AdCC originating in the parotid (14.5%) the submandibular (23%), the sublingual glands (25%),[119] as well as in over 20% of AdCC arising in the minor salivary glands of the oral cavity and oropharynx.[120]

Treatment of AdCC includes surgery as well as radiation. Selective neck dissection should be considered for AdCC arising in minor salivary glands showing lymphovascular invasion. AdCCs are usually resistent to chemotherapy and targeted therapies.[121]

Application of Molecular Testing

MYB-status has not been shown consistently to correlate with prognosis or other clinicopathologic features, but the use of *MYB*-testing serves as robust ancillary test in the routine clinical diagnosis of salivary gland tumors in which AdCC enters the differential diagnosis.

POLYMORPHOUS (LOW-GRADE) ADENOCARCINOMA AND CRIBRIFORM ADENOCARCINOMA OF (MINOR) SALIVARY GLAND ORIGIN

PAC occurs most commonly in minor salivary glands, particularly in the palate, and displays a diversity of architectural growth patterns composed of monotonous tumor cells (Fig. 6). Recently, a similar tumor termed
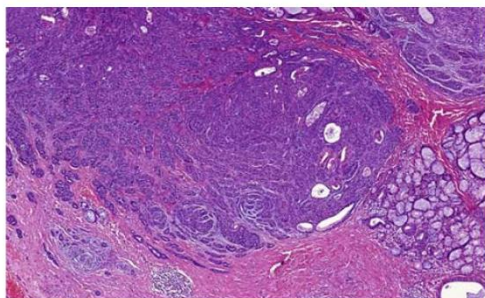
FIGURE 6. PLGA/PAC. PLGA displays a diversity of architectural growth patterns composed of monotonous tumor cells.
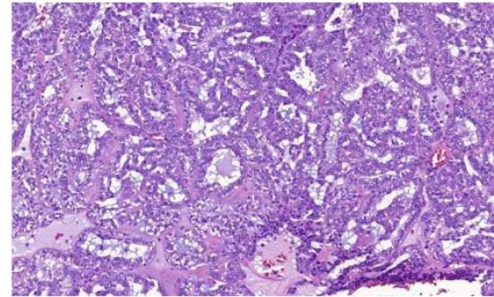
FIGURE 7. CASGs has a prominent solid growth often divided by fibrous septa into irregularly shaped and sized nodules composed of solid, cribriform, microcystic, and especially glomeruloid structures in variable proportions. The nuclei often overlap with one another, and are optically clear and vesicular with a ground glass appearance, strongly resembling those in papillary thyroid carcinoma.

CASG was described (Fig. 7).[122,123] There is currently an ongoing taxonomic debate as to whether these 2 are distinct entities or represent different ends of a morphologic spectrum. The most recent edition of the WHO Classification of Head and Neck Tumors prefers a designation "polymorphous adenocarcinoma" (PAC) for both tumor entities, referring to CASG as the "cribriform variant of PAC."[124]

However, CASG does have differences both morphologically and behaviorally from classic PAC. Unlike classic PAC, CASGs are more frequently extrapalatal, commonly at base of tongue, and have a higher propensity for nodal metastasis. Histologically they have more pronounced vesicular nuclei and tend to have a papillary, glomeruloid, and cribriform growth rather than a targetoid fascicular pattern seen in classic PAC.[123] They tend to demonstrate translocations involving the *PRKD* family of genes,[125] rather than the *PRKD1* point mutations [126,127] seen in classic PAC. Table 2 shows the key distinguishing features of PLGA/PAC and CASG.

Differential Diagnosis

The most important entity in the differential diagnosis of CASG is classic PAC.[124] PAC typically has a wide range of architectural appearances, including tubule and fascicle formation, as well as solid, cribriform, and sometimes small papillary structures. A prominent feature of PAC is the occurrence of streaming columns of single file or narrow trabeculae of cells forming concentric whorls, thereby creating a target-like (or "eye of storm") appearance. Perineural invasion is often seen, but does not indicate more aggressive behavior. The most striking feature of CASG is pronounced nuclear similarity to papillary carcinoma of the thyroid, and this is not seen to any great extent in PAC.

The main controversy in differentiating classic PAC (originally PLGA) from CASG has been stimulated by the approach of the editors of the recent issue of the WHO

TABLE 2. Comparison of PAC, Classic Variant (Originally Called PLGA) and CASGs

	CASG	PAC Classic Variant
Site	Minor salivary glands, base of tongue predominant	Minor salivary glands, palate, and buccal mucosa predominant
Growth	Cribriform and glomeruloid structures predominant, tubular, solid	Streaming columns of single file or narrow trabeculae of cells forming concentric whorls, target-like appearance, predominant, tubular, trabecular, papillary, solid, and cribriform
Nuclear features	Optically clear and vesicular with a ground glass appearance, papillary thyroid cancer-like nuclei	Vesicular and ovoid nuclei
Clinical features	Early cervical lymph node metastasis very common, occasionally bilaterally, no distant metastasis	Cervical lymph node metastasis only very rarely
Molecular alterations	*PRKD1-3* translocations, *ARID1A* and *DDX3X* partner genes	Hotspot activating *PRKD1* somatic point mutation (E710D)
Tissue invasion	Higher propensity for lymphatic invasion	Perineural invasion

Blue book who merged both entities to 1 single tumor type designated as PAC.[124] On the basis of clinical, morphologic, and molecular differences, however, many pathologists and clinicians still advocate for separation of CASG into a distinct entity.[122,123,128–136] There is, however, an ongoing discussion and controversy related to the morphologic and immunophenotypic overlap between these entities indicating that, the ultimate decision on separation of CASG and classic PAC will likely require additional studies.[2–4,12,13,124,137]

Clinical Features and Prognosis

CASG is a rare tumor; about 60 cases have been reported in the literature so far. Most CASGs are indolent neoplasms, but the local recurrence rates is 10% to 30%. Most importantly, about 70% of patients experience regional lymph node metastases often at the time of diagnosis. Nevertheless, there are no reported distant metastases and the only tumor-related deaths were due to late presentation and extensive local disease.[123,137]

Application of Molecular Testing

Although CASG and classic PAC have molecular alterations affecting the same gene loci, there are notable differences.[125–127] Molecular alterations of the *PRKD* gene family have been described in both entities. Weinreb et al[125] discovered recurrent translocations involving the *PRKD* genes in a series of 60 PAC and CASG cases, of which nearly one half showed a rearrangement of one of these genes, most commonly *PRKD1*. The fusion partner genes included *ARID1A* and *DDX3X*. Most cases with rearrangements were blindly classified as CASG or were judged to have indeterminate morphology, whereas only 1 case categorized as PAC showed rearrangement of *PRKD2*.[125] Hotspot activating E710D point mutations in *PRKD1* were also recently reported in nearly 3 quarters of PAC cases.[126] Mutations in *PRKD2* and *PRKD3* were not found in PAC.[127]

SALIVARY DUCT CARCINOMA

SDC is a primary, high-grade salivary gland adenocarcinoma, characterized by morphologic features akin to high-grade ductal carcinoma of the breast (Fig. 8A). SDCs are most commonly encountered in older

men and about half of the cases arise from preexisting PAs.[138] Morphologic variants are rare, including sarcomatoid, colloid (mucinous), basaloid, papillary, and micropapillary.[19,139] There is no role for grading in SDC because aggressive behavior is seen in most cases. When defined as a high-grade adenocarcinoma with apocrine phenotype, SDC almost uniformly expresses ARs,[140] although other large studies allow a broader morphologic phenotype in which AR positivity is seen in 67% to 83%.[141–144] The similarities between SDC and ductal breast carcinoma also include *HER2* (*ERBB2*) gene amplification. Amplification determined by FISH is found in 20% to 30% of SDCs.[141,143,145]

Additional common molecular alterations in SDC include mutations in *TP53*, *PIK3CA*, and *HRAS*, and loss or mutation of *PTEN*.[4,146–148] *BRAF*, *FBXW7*, *ATM*, and *NF1* mutations are also found in a small number of cases.[4,149–151] The majority of SDCs (74%) have alterations in either the MAPK pathway (*BRAF*, *HRAS*, and *NF1*) or in *ERBB2*, indicating that MAPK pathway activation and ERBB2 amplification are the major oncogenic drivers in SDC.[149] Notably, recent studies using RNA sequencing have revealed that also SDC may be added to the growing list of gene fusion-positive salivary carcinomas. Thus, *NCOA4-RET* fusions have been found in 2 SDCs[150] and there are also single cases of SDCs reported with *ETV6-NTRK3*, *BCL6-TRADD*, and *ABL1-PPP2R2C* gene fusions.[149]

Gene fusions involving the *PLAG1* and *HMGA2* oncogenes are specific for benign PAs[9,152] and as such have been used in differentiating PA from AdCC in fine needle aspiration cytology[153] and in differentiating carcinoma ex-PA from other de novo carcinomas.[154,155] Recently, *PLAG1* and *HMGA2* alterations have been described also in SDC (SDC-ex-PA) (Fig. 8B).[149,156] PLAG1 positivity, as determined by IHC, has also been encountered in 2 PLGAs.[157] The significance of this observation is unclear.

Differential Diagnosis

The histopathologic differential diagnosis of SDC includes primary oncocytic carcinoma, MEC, and myoepithelial carcinomas as well as metastatic melanoma, squamous, breast, and prostate carcinomas.[139]
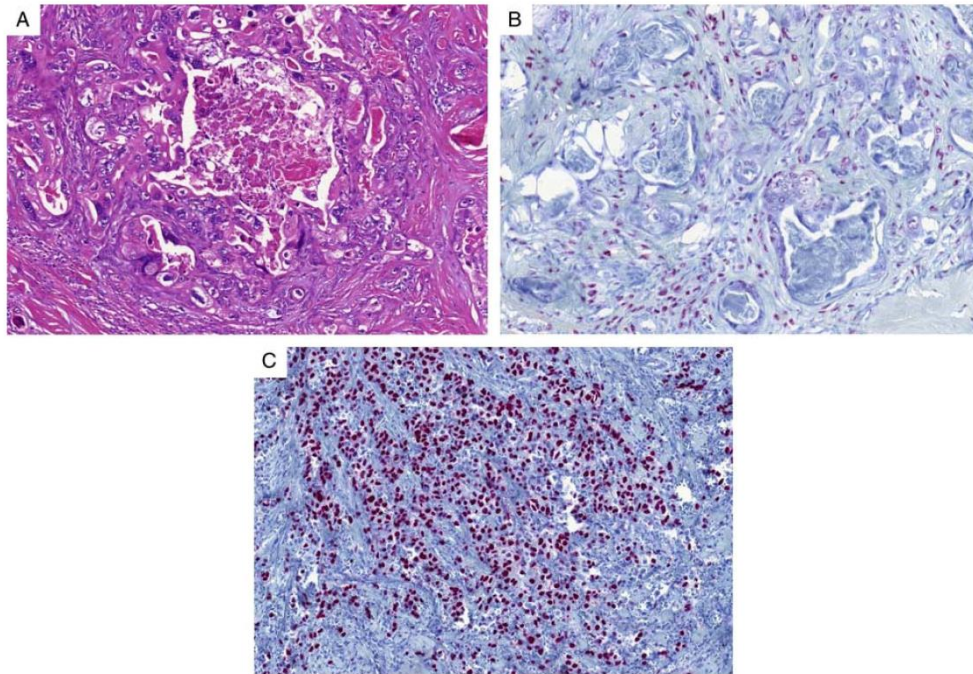
FIGURE 8. SDC. A, SDC is high-grade salivary gland carcinoma, characterized by morphologic features akin to high-grade ductal carcinoma of the breast. B, PLAG1 is expressed in residual structures of original PA and absent in most tumor cells of SDC. C, Strong nuclear expression of AR in SDC.

The oncocytic variant of SDC probably accounts for many cases previously diagnosed as oncocytic carcinoma, which is a rare and usually high-grade malignancy, unlikely to represent a single entity. High-grade MEC is also invasive and displays nuclear pleomorphism and increased mitotic activity. It is composed of mucinous goblet cells and cells with epidermoid and intermediate differentiation. In myoepithelial carcinoma, neoplastic lobules with central necrosis can bear a superficial resemblance to the ductal carcinoma in situ lesions of SDC, but these areas usually contain increased amounts of hyaline stromal material. The IHC profile is also very different. Metastatic melanoma with an epithelioid pattern can mimic a predominantly solid SDC, but can be excluded by appropriate immunomarkers. Metastatic squamous (poorly differentiated, nonkeratinizing), prostate or breast carcinoma all have the appearance of a high-grade salivary carcinoma. Squamous carcinoma lacks an infiltrating cribriform pattern and displays evidence of epidermoid differentiation such as intercellular bridges. Metastatic breast carcinoma is microscopically very similar to invasive SDC and differentiation can only be made on clinical grounds, although estrogen/progesterone receptor positivity would strongly favor a metastasis, particularly in the absence of sialodochodysplasia, the presence of which would support a primary salivary malignancy. Detection of AR expression by IHC is a useful diagnostic aid in resolving the differential diagnosis with other high-grade carcinomas (Fig. 8C).[139]

Clinical Features and Prognosis

SDC is one of the most aggressive salivary malignancies. At present, death occurs in 60% to 80% of the cases, usually within 5 years, with patients often developing distant metastases to the lungs, bone, liver, brain, and skin. The current standard treatment is complete surgical excision with radical neck dissection followed by radiotherapy to the tumor bed and possibly chemotherapy.[158] Several studies have shown benefit with androgen-deprivation therapy alone or in combination with conventional radiotherapy in some patients.[159,160] Because of the rarity of this carcinoma and the limited experience with androgen-deprivation therapy, correlation between the intensity of AR expression and response has not been determined and there is currently no accepted threshold to define AR positivity.

Treatment with anti-HER2 therapy in combination with bevacizumab and chemoradiation has resulted in

objective tumor response in some patients.[161,162] However, complete response to anti-HER2 therapy is rare in SDC and there is evidence that additional mutations involving *TP53*, *HRAS*, or loss of *PTEN* may decrease the efficacy of HER2 blockade.[4,146–148]

Application of Molecular Testing

SDC is a high-grade adenocarcinoma with morphologic and molecular features akin to invasive ductal carcinoma of the breast, including *HER2* gene amplification, mutations in *TP53*, *PIK3CA*, and *HRAS* and loss or mutation of *PTEN*. A subset of SDC with apocrine morphology is associated with overexpression of ARs. Molecular testing of SDC might provide information that leads to advances in personalized therapy for SDC.

CONCLUSIONS

Molecular examination in salivary gland pathology is becoming more common and can provide differential diagnostic, therapeutic, and prognostic information important not only for the purpose of classification of tumors but also for the management of patients with salivary gland carcinomas. The primary treatment of salivary gland neoplasms is surgical resection with or without postoperative radiotherapy. For patients presenting with locally advanced, recurrent, or metastatic disease the treatment options are currently limited and mainly palliative. However, the recent discovery of key molecular alterations in a variety of salivary gland tumor types has significantly increased our knowledge about their molecular pathology and improved the classification of salivary gland tumors. As these genetic alterations are recurrent they serve not only as powerful diagnostic tools, but also as promising prognostic biomarkers and new targets of therapy.

In this review we describe the clinicopathologic features of a selected group of salivary gland carcinomas with a focus on their distinctive molecular genetic characteristics. Importantly, we summarize the evidence and clinical utility of a tumor type-specific network of chromosome translocations and gene fusions in this group of diagnostically challenging carcinomas. We also discuss the clinical significance of the emerging landscape of oncogenic driver mutations in these carcinomas. Thus, MASC is characterized by *ETV6-NTRK3* fusions, HCCC by *EWSR1-ATF1* fusions, MEC by *CRTC1-MAML2* fusions, and AdCC by *MYB-NFIB* fusions. PLGA/PAC and CASG are related entities with partly differing clinicopathologic and genomic profiles; they are the subject of an ongoing taxonomic debate. PLGA/PACs are characterized by hot spot point E710D *PRKD1* mutations, whereas CASGs have translocations involving the *PRKD1-3* genes. SDC is a high-grade adenocarcinoma with morphologic and molecular features akin to invasive ductal carcinoma of the breast, including *HER2* gene amplification, mutations in *TP53*, *PIK3CA*, and *HRAS* and loss or mutation of *PTEN*. A subset of SDC with apocrine morphology is associated with overexpression of ARs.

Notably, an important number of salivary gland malignancies are still included in the group of adenocarcinomas not otherwise specified. We believe that detailed genomic and proteomic profiling and next-generation sequencing of a large cohort of these unspecified neoplasms may lead to the identification of novel gene fusions and driver mutations characterizing new clinically relevant subgroups of salivary gland carcinomas. Therefore, further molecular analyses of salivary gland tumors are warranted and deserve special attention.

REFERENCES

1. Zhu S, Schuerch C, Hunt J. Review and updates of immunohistochemistry in selected salivary gland and head and neck tumors. *Arch Pathol Lab Med.* 2015;139:55–66.
2. Griffith CC, Schmitt AC, Little JL, et al. New developments in salivary gland pathology. Clinically useful ancillary testing and new potentiall targetable molecular alterations. *Arch Pathol Lab Med.* 2017;141:381–395.
3. Seethala RR. Salivary gland tumors. Current concepts and controversies. *Surg Pathol.* 2017;10:155–176.
4. Seethala RR, Griffiths CC. Molecular pathology. Predictive, prognostic, and diagnostic markers in salivary gland tumors. *Surg Pathol.* 2016;9:339–352.
5. Mitelman F, Johansson B, Mertens F. Mitelman database of chromosome aberrations and gene fusions in cancer. 2013. Available at: http://cgap.nci.nih.gov/Chromosomes/Mitelman.
6. Mitelman F, Johansson B, Mertens F. The impact of translocations and gene fusions on cancer causation. *Nat Rev Cancer.* 2007;7: 233–245.
7. Aman P. Fusion oncogenes in tumor development. *Semin Cancer Biol.* 2005;15:236–243.
8. Stenman G. Fusion oncogenes and tumor type specificity—insight from salivary gland tumors. *Semin Cancer Biol.* 2005;15:224–235.
9. Stenman G. Fusion oncogenes in salivary gland tumors: molecular and clinical consequences. *Head Neck Pathol.* 2013;7(suppl 1): S12–S19.
10. Stenman G, Persson F, Andersson MK. Diagnostic and therapeutic implications of new molecular biomarkers in salivary gland cancers. *Oral Oncol.* 2014;50:683–690.
11. Andersson MK, Stenman G. The landscape of gene fusions and somatic mutations in salivary gland neoplasms—implications for diagnosis and therapy. *Oral Oncol.* 2016;57:63–69.
12. Skalova A, Michal M, Simpson RHW. Newly described salivary gland tumors. *Mod Pathol.* 2017;30:S27–S43.
13. Skalova A, Gnepp DR, Lewis JS Jr, et al. Newly described entities in salivary gland pathology. *Am J Surg Pathol.* 2017;41: e33–e47.
14. El-Naggar AK, Chan JKC, Grandis JR, et al. *WHO Classification of Head and Neck Tumours*, 4th ed. Lyon, France: IARC; 2017.
15. Andersson MK, Afshar MK, Andrén Y, et al. Targeting the oncogenic transcriptional regulator MYB in adenoid cystic carcinoma by inhibition of IGF1R-AKT signaling. *J Natl Cancer Inst.* 2017;109:djx017. Doi:10.1093/ jnci/djx017.
16. McCord C, Weinreb I, Perez-Ordonez B. Progress in salivary gland pathology: new entities and selected molecular features. *Diagn Histopathol.* 2012;18:253–260.
17. Skalova A, Vanecek T, Simpson RHW, et al. Molecular advances in salivary gland pathology and their practical application. *Diagn Histopathol.* 2012;18:388–396.
18. Weinreb I. Translocation-associated salivary gland tumors: a review and update. *Adv Anat Pathol.* 2013;20:367–376.
19. Simpson RHW, Skálová A, Di Palma S, et al. Recent advances in the diagnostic pathology of salivary glands. *Virchows Arch.* 2014; 465:371–384.
20. Skalova A, Vanecek T, Sima R, et al. Mammary analogue secretory carcinoma of salivary glands, containing the *ETV6-NTRK3* fusion gene: a hitherto undescribed salivary gland tumor entity. *Am J Surg Pathol.* 2010;34:599–608.

21. Tognon C, Knezevich SR, Huntsman D, et al. Expression of the *ETV6-NTRK3* gene fusion as a primary event in human secretory breast carcinoma. *Cancer Cell*. 2002;2:367–376.

22. Li Z, Tognon CE, Godinho FJ, et al. *ETV6-NTRK3* fusion oncogene initiates breast cancer from committed mammary progenitors via activation of AP1 complex. *Cancer Cell*. 2007;12: 542–558.

23. Skálová A, Bell D, Bishop JA, et al. Secretory carcinoma. In: El-Naggar A, Chan JKC, Grandis JR, Takata T, Slootweg PJ, eds. *World Health Organization (WHO) Classification of Head and Neck Tumours*, 4th ed. Lyon, France: IARC Press; 2017: 177–178.

24. Dogan S, Wang L, Ptashkin RN, et al. Mammary analog secretory carcinoma of the thyroid gland: a primary thyroid adenocarcinoma harboring *ETV6-NTRK3* fusion. *Mod Pathol*. 2016;29:985–995.

25. Reynolds S, Shaheen M, Olson G, et al. A case of primary mammary analog secretory carcinoma (MASC) of the thyroid masquerading as papillary thyroid carcinoma: potentially more than a one off. *Head Neck Pathol*. 2016;10:405–413.

26. Bishop JA, Taube JM, Su A, et al. Secretory carcinoma of the skin harboring *ETV6* gene fusion. A cutaneous analogue to secretory carcinomas of the breast and salivary glands. *Am J Surg Pathol*. 2017;41:62–66.

27. Griffith C, Seethala R, Chiosea SI. Mammary analogue secretory carcinoma: a new twist to the diagnostic dilemma of zymogen granule poor acinic cell carcinoma. *Virchows Arch*. 2011;459: 117–118.

28. Fehr A, Loning T, Stenman G. Mammary analogue secretory carcinoma of the salivary glands with *ETV6-NTRK3* gene fusion. letter to the editor. *Am J Surg Pathol*. 2011;35:1600–1602.

29. Connor A, Perez-Ordoñez B, Shago M, et al. Mammary analog secretory carcinoma of salivary gland origin with the *ETV6* gene rearrangement by FISH: expanded morphologic and immunohistochemical spectrum of a recently described entity. *Am J Surg Pathol*. 2012;36:27–34.

30. Chiosea SI, Griffith C, Assad A, et al. The profile of acinic cell carcinoma after recognition of mammary analog secretory carcinoma. *Am J Surg Pathol*. 2012;36:343–350.

31. Rubin BP, Chen CJ, Morgan TW, et al. Congenital mesoblastic nephroma t(12;15) is associated with ETV6-NTRK3 gene fusion: cytogenetic and molecular relationship to congenital (infantile) fibrosarcoma. *Am J Pathol*. 1998;153:1451–1458.

32. Knezevich SR, Garnett MJ, Pysher TJ, et al. *ETV6- NTRK3* gene fusions and trisomy 11 establish a histogenetic link between mesoblastic nephroma and congenital fibrosarcoma. *Cancer Res*. 1998;15:5046–5048.

33. Kralik JM, Kranewitter W, Boesmueller H, et al. Characterization of a newly identified ETV6-NTRK3 fusion transcript in acute myeloid leukemia. *Diagn Pathol*. 2011;6:19.

34. Alassiri AH, Ali RH, Shen Y, et al. *ETV6-NTRK3* is expressed in a subset of ALK-negative inflammatory myofibroblastic tumor. *Am J Surg Pathol*. 2016;40:1051–1061.

35. Leeman-Neill RJ, Kelly LM, Liu P, et al. *ETV6-NTRK3* is a common chromosomal rearrangement in radiation-associated thyroid cancer. *Cancer*. 2014;120:799–807.

36. Stevens TM, Kovalovsky AO, Velosa C, et al. Mammary analog secretory carcinoma, low-grade salivary duct carcinoma, and mimickers: a comparative study. *Mod Pathol*. 2015;28:1084–1100.

37. Seethala RR, Chiosea SI, Liu CZ, et al. Clinical and morphological features of ETV6-NTRK3 translocated papillary thyroid carcinoma in an adult population without radiation exposure. *Am J Surg Pathol*. 2017;41:446–457.

38. Dettloff J, Seethala RR, Stevens TM, et al. Mammary analog aecretory aarcinoma (MASC) involving the thyroid gland: A report of the first 3 cases. *Head Neck Pathol*. 2017;11:124–130.

39. Hyrcza MD, Ng T, Crawford RI. Detection of the *ETV6-NTRK3* translocation in cutaneous mammary-analogue secretory carcinoma. *Diagn Histopathol*. 2015;21:481–484.

40. Lurquin E, Jorissen M, Debiec-Rychter M, et al. Mammary analogue secretory carcinoma of the sinus ethmoidalis. *Histopathology*. 2015;67:749–751.

41. Skalova A, Vanecek T, Simpson RHW, et al. Mammary analogue secretory carcinoma of salivary glands. Molecular analysis of 25 *ETV6* gene rearranged tumors with lack of detection of classical *ETV6-NTRK3* fusion transcript by standard rt-pcr: report of 4 cases harboring *ETV6-X* gene fusion. *Am J Surg Pathol*. 2016;40:3–13.

42. Ito Y, Ishibashi K, Masaki A, et al. Mammary analogue secretory carcinoma of salivary glands: a clinicopathological and molecular study including 2 cases harboring *ETV6-X* fusion. *Am J Surg Pathol*. 2015;39:602–610.

43. Skalova A, Vanecek T, Martinek P, et al. Molecular profiling of mammary analogue secretory carcinoma revealed a subset of tumors harboring a novel *ETV6-RET* translocation: report of 10 cases. *Am J Surg Pathol*. 2017. In press.

44. Majewska H, Skálová A, Stodulski D, et al. Mammary analogue secretory carcinoma of salivary glands: first retrospective study of a new entity in Poland with special reference to *ETV6* gene rearrangement. *Virchows Arch*. 2015;466:245–254.

45. Pinto A, Nosé V, Rojas C, et al. Searching for mammary analogue secretory carcinoma among their mimicks. *Mod Pathol*. 2014;27: 30–37.

46. Tonon G, Modi S, Wu L, et al. t(11;19)(q21;p13) translocation in mucoepidermoid carcinoma creates a novel fusion product that disrupts a Notch signaling pathway. *Nat Genet*. 2003;33:208–213.

47. Okumura Y, Miyabe S, Nakayama T, et al. Impact of CRTC1/3– MAML2 fusions on histological classification and prognosis of mucoepidermoid carcinoma. *Histopathology*. 2011;59:90–97.

48. Skálová A, Vanecek T, Majewska H, et al. Mammary analogue secretory carcinoma of salivary glands with high-grade transformation: report of 3 cases with the *ETV6-NTRK3* gene fusion and analysis of TP53, beta-catenin, EGFR, and CCND1 genes. *Am J Surg Pathol*. 2014;38:23–33.

49. Luo W, Lindley SW, Lindley PH, et al. Mammary analog secretory carcinoma of salivary gland with high-grade histology arising in palate, report of a case and review of literature. *Int J Clin Exp Pathol*. 2014;7:9008–9022.

50. Bishop JA. Unmasking MASC: bringing to light the unique morphologic, immunohistochemical and genetic features of the newly recognized mammary analogue secretory carcinoma of salivary glands. *Head Neck Pathol*. 2013;7:35–39.

51. Chi HT, Ly BT, Kano Y, et al. *ETV6-NTRK3* as a therapeutic target of small molecule inhibitor PKC412. *Biochem Biophys Res Commun*. 2012;429:87–92.

52. Tognon CE, Somasiri AM, Evdokimova VE, et al. *ETV6-NTRK3*-mediated breast epithelial cell transformation is blocked by targeting the IGF1R signaling pathway. *Cancer Res*. 2011;71: 1060–1070.

53. Drilon A, Li G, Dogan S, et al. What hides behind the MASC: clinical response and acquired resistance to entrectinib after *ETV6-NTRK3* identification in a mammary analogue secretory carcinoma (MASC). *Ann Oncol*. 2016;27:920–926.

54. Antonescu CR, Katabi N, Zhang L, et al. *EWSR1-ATF1* fusion is a novel and consistent finding in hyalinizing clear-cell carcinoma of salivary gland. *Genes Chromosomes Cancer*. 2011;50:559–570.

55. Shah AA, LeGallo RD, van Zante A, et al. *EWSR1* genetic rearrangements in salivary gland tumors: a specific and very common feature of hyalinizing clear cell carcinoma. *Am J Surg Pathol*. 2013;37:571–578.

56. Antonescu CR, Zhang L, Chang NE, et al. *EWSR1-POU5F1* fusion in soft tissue myoepithelial tumors: a molecular analysis of sixty-six cases, including soft tissue, bone, and visceral lesions, showing common involvement of the *EWSR1* gene. *Genes Chromosomes Cancer*. 2010;49:1114–1124.

57. Zucman J, Delattre O, Desmaze C, et al. EWS and ATF1 gene fusion induced by t(12;22) translocation in malignant melanoma of soft parts. *Nat Genet*. 1993;4:341–345.

58. Flucke U, Mentzel T, Verdijk MA, et al. *EWSR1-ATF1* chimeric transcript in a myoepithelial tumor of soft tissue: a case report. *Hum Pathol*. 2012;43:764–768.

59. Chen G, Folpe AL, Colby TV, et al. Angiomatoid fibrous histiocytoma: unusual sites and unusual morphology. *Mod Pathol*. 2011;24:1560–1570.

155

60. Skalova A, Weinreb I, Hyrcza M, et al. Clear cell myoepithelial carcinoma of salivary glands showing *EWSR1* rearrangement: molecular analysis of 94 salivary gland carcinomas with prominent clear cell component. *Am J Surg Pathol*. 2015;39:338–348.
61. Tanguay J, Weinreb I. What the EWSR1-ATF1 fusion has taught us about hyalinizing clear cell carcinoma. *Head Neck Pathol*. 2013;7:28–34.
62. Solar AA, Schmidt BL, Jordan RC. Hyalinizing clear cell carcinoma: case series and comprehensive review of the literature. *Cancer*. 2009;115:75–83.
63. O'Regan E, Shandilya M, Gnepp DR, et al. Hyalinizing clear cell carcinoma of salivary gland: an aggressive variant. *Oral Oncol*. 2004;40:348–352.
64. Brandwein-Gensler M, Bell D, Inagaki H, et al. Mucoepidermoid carcinoma. In: El-Naggar A, Chan JKC, Grandis JR, Takata T, Slootweg PJ, eds. *World Health Organization (WHO) Classification of Head and Neck Tumours*, 4th ed. Lyon, France: IARC Press; 2017:163–164.
65. Tonon G, Modi S, Wu L, et al. t(11;19)(q21;p13) translocation in mucoepidermoid carcinoma creates a novel fusion product that disrupts a Notch signaling pathway (published correction appears in *Nat Genet* 2003;33(3):430] (letter). *Nat Genet*. 2003;33:208–213.
66. Enlund F, Behboudi A, Andrén Y, et al. Altered Notch signaling resulting from expression of a *WAMTP1-MAML2* gene fusion in mucoepidermoid carcinomas and benign Warthin's tumors. *Exp Cell Res*. 2004;292:21–28.
67. Fehr A, Roser K, Heidorn K, et al. A new type of MAML2 fusion in mucoepidermoid carcinoma. *Genes Chromosomes Cancer*. 2008;47:203–206.
68. Nakayama T, Miyabe S, Okabe M, et al. Clinicopathological significance of the CRTC3-MAML2 fusion transcript in mucoepidermoid carcinoma. *Mod Pathol*. 2009;22:1575–1581.
69. Chiosea SI, Dacic S, Nikiforova MN, et al. Prospective testing of mucoepidermoid carcinoma for the MAML2 translocation: clinical implications. *Laryngoscope*. 2012;122:1690–1694.
70. Shinomiya H, Ito Y, Kubo M, et al. Expression of amphiregulin in mucoepidermoid carcinoma of the major salivary glands: a molecular and clinicopathological study. *Hum Pathol*. 2016;57:37–44.
71. Kang H, Tan M, Bishop JA, et al. Whole-exome sequencing of salivary gland mucoepidermoid carcinoma. *Clin Cancer Res*. 2017;23:283–288.
72. Wang K, McDermott JD, Schrock AB, et al. Comprehensive genomic profiling of salivary mucoepidermoid carcinomas reveals frequent BAP1, PIK3CA, and other actionable genomic alterations. *Ann Oncol*. 2017;28:748–753.
73. Jee KJ, Persson M, Heikinheimo K, et al. Genomic profiles and *CRTC1-MAML2* fusion distinguish different subtypes of mucoepidermoid carcinoma. *Mod Pathol*. 2013;26:213–222.
74. Di Palma S, Simpson RHW, Skálová A, et al. Metaplastic (infarcted) Warthin's tumour of the parotid gland: a possible consequence of fine needle aspiration biopsy. *Histopathology*. 1999;35:432–438.
75. Tirado Y, Williams MD, Hanna EY, et al. CRTC1/MAML2 fusion transcript in high grade mucoepidermoid carcinomas of salivary and thyroid glands and Warthin's tumors: implications for histogenesis and biologic behavior. *Genes Chromosomes Cancer*. 2007;46:708–715.
76. Bell D, Luna MA, Weber RS, et al. CRTC1/MAML2 fusion transcript in Warthin's tumor and mucoepidermoid carcinoma: evidence for a common genetic association. *Genes Chromosomes Cancer*. 2008;47:309–314.
77. Martins C, Cavaco B, Tonon G, et al. A study of MECT1-MAML2 in mucoepidermoid carcinoma and Warthin's tumor of salivary glands. *J Mol Diagn*. 2004;6:205–210.
78. Okabe M, Miyabe S, Nagatsuka H, et al. MECT1-MAML2 fusion transcript defines a favorable subset of mucoepidermoid carcinoma. *Clin Cancer Res*. 2006;12:3902–3907.
79. Fehr A, Roser K, Belge G, et al. A closer look at Warthin tumors and the t(11;19). *Cancer Genet Cytogenet*. 2008;180:135–139.
80. Seethala RR, Dacic S, Cieply K, et al. A reappraisal of the MECT1/MAML2 translocation in salivary mucoepidermoid carcinomas. *Am J Surg Pathol*. 2010;34:1106–1121.
81. Clauditz TS, Gontarewicz A, Wang CJ, et al. 11q21 rearrangement is a frequent and highly specific genetic alteration in mucoepidermoid carcinoma. *Diagn Mol Pathol*. 2012;21:134–137.
82. Ishibashi K, Ito Y, Masaki A, et al. Warthin-like mucoepidermoid carcinoma: a combined study of fluorescence in situ hybridization and wholeslide imaging. *Am J Surg Pathol*. 2015;39:1479–1487.
83. Skalova A, Vanecek T, Simpson RHW, et al. *CRTC1-MAML2* and *CRTC3-MAML2* fusions were not detected in metaplastic Warthin's tumor and metaplastic pleomorphic adenoma of salivary glands. *Am J Surg Pathol*. 2013;37:1743–1750.
84. Garcia JJ, Hunt JL, Weinreb I, et al. Fluorescence in situ hybridization for detection of MAML2 rearrangements in oncocytic mucoepidermoid carcinomas: utility as a diagnostic test. *Hum Pathol*. 2011;42:2001–2009.
85. Weinreb I, Seethala RR, Perez-Ordoˇnez B, et al. Oncocytic mucoepidermoid carcinoma: clinicopathologic description in a series of 12 cases. *Am J Surg Pathol*. 2009;33:409–416.
86. Kass JI, Lee SC, Abberbock S, et al. Adenosquamous carcinoma of the head and neck: molecular analysis using CRTC-MAML FISH and survival comparison with paired conventional squamous cell carcinoma. *Laryngoscope*. 2015;125:E371–E376.
87. Chenevert J, Barnes LE, Chiosea SI. Mucoepidermoid carcinoma: a five decade journey. *Virchows Arch*. 2011;458:133–140.
88. Khan HA, Loya A, Azhar R, et al. Central mucoepidermoid carcinoma, a case report with molecular analysis of the TORC1/MAML2 gene fusion. *Head Neck Pathol*. 2010;4:261–264.
89. Von Holstein SL, Fehr A, Heegaard S, et al. CRTC1-MAML2 gene fusion in mucoepidermoid carcinoma of the lacrimal gland. *Oncol Rep*. 2012;27:1413–1416.
90. Shah AA, La Fortune K, Miller C, et al. Thyroid sclerosing mucoepidermoid carcinoma with eosinophilia: a clinicopathologic and molecular analysis of a distinct entity. *Mod Pathol*. 2017;30:329–339.
91. Roden AC, Erickson-Johnson MR, Yi ES, et al. Analysis of MAML2 rearrangement in mucoepidermoid carcinoma of the thymus. *Hum Pathol*. 2013;44:2799–2805.
92. Serra A, Schackert HK, Mohr B, et al. t(11;19)(q21; p12~p13.11) and MECT1-MAML2 fusion transcript expression as a prognostic marker in infantile lung mucoepidermoid carcinoma. *J Pediatr Surg*. 2007;42:E23–E29.
93. Achcar Rde O, Nikiforova MN, Dacic S, et al. Mammalian mastermind like 2 11q21 gene rearrangement in bronchopulmonary mucoepidermoid carcinoma. *Hum Pathol*. 2009;40:854–860.
94. Lennerz JK, Perry A, Mills JC, et al. Mucoepidermoid carcinoma of the cervix: another tumor with the t(11;19)-associated CRTC1-MAML2 gene fusion. *Am J Surg Pathol*. 2009;33:835–843.
95. Behboudi A, Winnes M, Gorunova L, et al. Clear cell hidradenoma of the skin-a third tumor type with a t(11;19)—associated TORC1-MAML2 gene fusion. *Genes Chromosomes Cancer*. 2005;43:202–205.
96. Nemoto N, Suzukawa K, Shimizu S, et al. Identification of a novel fusion gene MLL-MAML2 in secondary acute myelogenous leukemia and myelodysplastic syndrome with inv(11)(q21q23). *Genes Chromosomes Cancer*. 2007;46:813–819.
97. Bishop JA, Yonescu R, Batista D, et al. Glandular odontogenic cysts (GOCs) lack MAML2 rearrangements: a finding to discredit the putative nature of GOC as a precursor to central mucoepidermoid carcinoma. *Head Neck Pathol*. 2014;8:287–290.
98. Behboudi A, Enlund F, Winnes M, et al. Molecular classification of mucoepidermoid carcinomas-prognostic significance of the MECT1-MAML2 fusion oncogene. *Genes Chromosomes Cancer*. 2006;45:470–481.
99. Anzick SL, Chen WD, Park Y, et al. Unfavorable prognosis of CRTC1-MAML2 positive mucoepidermoid tumors with CDKN2A deletions. *Genes Chromosomes Cancer*. 2010;49:59–69.
100. Coca-Pelaz A, Rodrigo JP, Bradley PJ, et al. Adenoid cystic carcinoma of the head and neck—an update. *Oral Oncol*. 2015;51:652–661.
101. Seethala RR. An update on grading of salivary gland carcinomas. *Head Neck Pathol*. 2009;3:69–77.
102. Seethala RR, Hunt JL, Baloch ZW, et al. Adenoid cystic carcinoma with high grade transformation: a report of 11 cases and review of the literature. *Am J Surg Pathol*. 2007;31:1683–1694.

156

103. Hellquist H, Skalova A, Azadeh B. Salivary hybrid tumour revisited: could they represent high-grade transformation in a low-grade neoplasm? *Virchows Arch*. 2016;469:643–650.
104. Hellquist H, Skálová A, Barnes L, et al. Cervical lymph node metastasis in high-grade transformation of head and neck adenoid cystic carcinoma: a collective international review. *Adv Ther*. 2016;33: 357–368.
105. Persson M, Andren Y, Mark J, et al. Recurrent fusion of MYB and NFIB transcription factor genes in carcinomas of the breast and head and neck. *Proc Natl Acad Sci U S A*. 2009;106:18740–18744.
106. Stenman G, Sandros J, Dahlenfors R, et al. 6q and loss of the Y chromosome-two common deviations in malignant salivary gland tumors. *Cancer Genet Cytogenet*. 1986;22:283–293.
107. Ho AS, Kannan K, Roy DM, et al. The mutational landscape of adenoid cystic carcinoma. *Nat Genet*. 2013;45:791–798.
108. Brill LB 2nd, Kanner WA, Fehr A, et al. Analysis of MYB expression and MYB-NFIB gene fusions in adenoid cystic carcinoma and other salivary neoplasms. *Mod Pathol*. 2011;24: 1169–1176.
109. West RB, Kong C, Clarke N, et al. MYB expression and translocation in adenoid cystic carcinomas and other salivary gland tumors with clinicopathologic correlation. *Am J Surg Pathol*. 2011;35: 92–99.
110. Mitani Y, Li J, Rao PH, et al. Comprehensive analysis of the MYB-NFIB gene fusion in salivary adenoid cystic carcinoma: incidence, variability, and clinicopathologic significance. *Clin Cancer Res*. 2010;16:4722–4731.
111. Mitani Y, Liu B, Rao PH, et al. Novel MYBL1 gene rearrangements with recurrent MYBL1-NFIB fusions in salivary adenoid cystic carcinomas lacking t(6;9) translocations. *Clin Cancer Res*. 2016;22:725–733.
112. Brayer KJ, Frerich CA, Kang H, et al. Recurrent fusions in MYB and MYBL1 define a common transcription factor-driven oncogenic pathway in salivary gland adenoid cystic carcinoma. *Cancer Discov*. 2016;6:176–187.
113. Persson M, Andren Y, Moskaluk CA, et al. Clinically significant copy number alterations and complex rearrangements of MYB and NFIB in head and neck adenoid cystic carcinoma. *Genes Chromosomes Cancer*. 2012;51:805–817.
114. Stephens PJ, Davies HR, Mitani Y, et al. Whole exome sequencing of adenoid cystic carcinoma. *J Clin Invest*. 2013;123:2965–2968.
115. Rettig EM, Talbot CC Jr, Sausen M, et al. Whole-genome sequencing of salivary gland adenoid cystic carcinoma. *Cancer Prev Res (Phila)*. 2016;9:265–274.
116. Skálová A, Simpson RHW, Lehtonen H, et al. Assessment of proliferative activity using the MIB1 antibody helps to distinguish polymorphous low grade adenocarcinoma from adenoid cystic carcinoma of salivary glands. *Pathol Res Pract*. 1997;193:695–703.
117. Ferlito A, Shaha AR, Rinaldo A, et al. Management of clinically negative cervical lymph nodes in patients with malignant neoplasms of the parotid gland. *J Otorhinolaryngol Relat Spec*. 2001;63:123–126.
118. Min R, Siyi L, Wenjun Y, et al. Salivary gland adenoid cystic carcinoma with cervical lymph node metastasis: a preliminary study of 62 cases. *Int J Oral Maxillofac Surg*. 2012;41:952–957.
119. Silver CE, Bradley PJ, Barnes L, et al. Cervical lymph node metastasis in adenoid cystic carcinoma of the major salivary glands. *J Laryngol Otol*. 2017;131:96–105.
120. Suarez C, Barnes L, Silver CE, et al. Cervical lymph node metastasis in adenoid cystic carcinoma of oral cavity and oropharynx: a collective international review. *Auris Nasus Larynx*. 2016;43:477–484.
121. Carlson J, Licitra L, Locati L, et al. Salivary gland cancer: an update on present and emerging therapies. *Am Soc Clin Oncol Educ Book*. 2013:257–263.
122. Michal M, Skálová A, Simpson RHW, et al. Cribriform adenocarcinoma of the tongue: a hitherto unrecognized type of adenocarcinoma characteristically occurring in the tongue. *Histopathology*. 1999;35:495–501.
123. Skálová A, Sima R, Kaspirkova-Nemcova J, et al. Cribriform adenocarcinoma of the tongue and other minor salivary glands: characterization of new entity. *Am J Surg Pathol*. 2011;35:1168–1176.
124. Fonseca I, Assaad A, Catabi N, et al. Polymorphous adenocarcinoma. In: El-Naggar A, Chan JKC, Grandis JR, Takata T, Slootweg PJ, eds. *World Health Organization (WHO) Classification of Head and Neck Tumours*. Lyon, France: IARC Press; 2017:167–168.
125. Weinreb I, Zhang L, Tirunagari LM, et al. Novel PRKD gene rearrangements and variant fusions in cribriform adenocarcinoma of salivary gland origin. *Genes Chromosomes Cancer*. 2014;53: 845–856.
126. Weinreb I, Piscuoglio S, Martelotto LG, et al. Hotspot activating PRKD1 somatic mutations in polymorphous low-grade adenocarcinomas of the salivary glands. *Nat Genet*. 2014;46:1166–1169.
127. Piscuoglio S, Fusco N, Ng CK, et al. Lack of PRKD2 and PRKD3 kinase domain somatic mutations in PRKD1 wild-type classic polymorphous low-grade adenocarcinomas of the salivary gland. *Histopathology*. 2015;68:1055–1062.
128. Laco J, Kamarádová K, Vítková P, et al. Cribriform adenocarcinoma of minor salivary glands may express galectin-3, cytokeratin 19, and HBME-1 and contains polymorphisms of RET and H-RAS proto-oncogenes. *Virchows Arch*. 2012;461:531–540.
129. Pagano A, Dennis K. Cribriform adenocarcinoma of the minor salivary gland arising in the tonsil with metastasis to a cervical lymph node: a case report with description of fine needle aspiration cytology. *Diagn Cytopathol*. 2017;45:468–471.
130. Takhar AS, Simmons A, Ffolkes L, et al. Not just another paediatric neck lump: metastatic cribriform adenocarcinoma of the palate in an adolescent. *J Laryngol Otol*. 2015;129:194–197.
131. Gnepp DR. Salivary gland tumor "wishes" to add to the next WHO Tumor Classification: sclerosing polycystic adenosis, mammary analogue secretory carcinoma, cribriform adenocarcinoma of the tongue and other sites, and mucinous variant of myoepithelioma. *Head Neck Pathol*. 2014;8:42–49.
132. Brierley D, Green D, Spedight PM. Cribriform adenocarcinoma of the minor salivary glands arising in the epiglottis-a previously undocumented occurrence. *Oral Maxillofac Pathol*. 2015;120: e174–e176.
133. Gailey MP, Bayon R, Robinson RA. Cribriform adenocarcinoma of minor salivary gland: a report of two cases with an emphasis on cytology. *Diagn Cytopathol*. 2014;42:1085–1090.
134. Majewska H, Skalova A, Weinreb I, et al. Giant cribriform adenocarcinoma of the tongue showing *PRKD3* rearrangement. *Pol J Pathol*. 2016;67:84–90.
135. Cocek A, Hronkova K, Voldanova J, et al. Cribriform adenocarcinoma of the base of the tongue and low-grade, polymorphic adenocarcinomas of the salivary glands. *Oncol Lett*. 2011;2: 135–138.
136. Michal M, Kacerovska D, Kazakov DV. Cribriform adenocarcinoma of the tongue and minor salivary glands: a review. *Head Neck Pathol*. 2013;7:S3–S11.
137. Xu B, Aneja A, Ghossein R, et al. Predictors of outcome in the phenotypic spectrum of polymorphous low-grade adenocarcinoma (PLGA) and cribriform adenocarcinoma of salivary gland (CASG). A retrospective study of 69 patients. *Am J Surg Pathol*. 2016; 40:1526–1537.
138. Bahrami A, Perez-Ordoñez B, Dalton JD, et al. An analysis of PLAG1 and HMGA2 rearrangement in salivary duct carcinoma and examination of the role of precursor lesions. *Histopathology*. 2013;63:250–262.
139. Simpson RHW. Salivary duct carcinoma: new developments-morphological variants including pure in situ high grade lesions; proposed molecular classification. *Head Neck Pathology*. 2013;7: S48–S58.
140. Chiosea SI, Williams L, Griffith CC, et al. Molecular characterization of apocrine salivary duct carcinoma. *Am J Surg Pathol*. 2015;39: 744–752.
141. Masubuchi T, Tada Y, Maruya S, et al. Clinicopathological significance of androgen receptor, HER2, Ki-67 and EGFR expressions in salivary duct carcinoma. *Int J Clin Oncol*. 2015;20: 35–44.
142. Williams MD, Roberts D, Blumenschein GR Jr, et al. Differential expression of hormonal and growth factor receptors in salivary duct

carcinomas: biologic significance and potential role in therapeutic stratification of patients. *Am J Surg Pathol.* 2007;31:1645–1652.

143. Di Palma S, Simpson RHW, Marchiò C, et al. Salivary duct carcinomas can be classified into luminal androgen receptor-positive, HER2 and basal-like phenotypes. *Histopathology.* 2012;61:629–643.

144. Mitani Y, Rao PH, Maity SN, et al. Alterations associated with androgen receptor gene activation in salivary duct carcinoma of both sexes: potential therapeutic ramifications. *Clin Cancer Res.* 2014;20:6570–6581.

145. Skálová A, Stárek I, Vaněček T, et al. Expression of HER-2/neu gene and protein in salivary duct carcinoma of parotid gland as revealed by fluorescence in-situ hybridization and immunohistochemistry. *Histopathology.* 2003;42:348–356.

146. Griffith CC, Seethala RR, Luvison A, et al. PIK3CA mutations and PTEN loss in salivary duct carcinomas. *Am J Surg Pathol.* 2013;37:1201–1207.

147. Nardi V, Sadow PM, Juric D, et al. Detection of novel actionable genetic changes in salivary duct carcinoma helps direct patient treatment. *Clin Cancer Res.* 2013;19:480–490.

148. Qui W, Tong GX, Turk AT, et al. Oncogenic *PIK3CA* mutation and dysregulation in human salivary duct carcinoma. *Biomed Res Int.* 2014;810487. Doi:10.1155/2014/810487 [Epub January 8, 2014].

149. Dalin MG, Desrichard A, Katabi N, et al. Comprehensive molecular characterization of salivary duct carcinoma reveals actionable targets and similarity to apocrine breast cancer. *Clin Cancer Res.* 2016;22:4623–4633.

150. Wang K, Russell JS, McDermott JD, et al. Profiling of 149 salivary duct carcinomas, carcinoma ex pleomorphic adenomas, and adenocarcinomas, not otherwise specified reveals actionable genomic alterations. *Clin Cancer Res.* 2016;22:6061–6068.

151. Khoo TK, Yu B, Smith JA, et al. Somatic mutations in salivary duct carcinoma and potential therapeutic targets. *Oncotarget.* 2017. [Epub ahead of print].

152. Kas K, Voz ML, Roijer E, et al. Promoter swapping between the genes for a novel zinc finger protein and beta-catenin in pleomorphic adenomas with t(3;8)(p21;q12) translocations. *Nat Genet.* 1997;15:170–174.

153. Foo WC, Jo VY, Krane JF. Usefulness of translocation-associated immunohistochemical stains in the fine-needle aspiration diagnosis of salivary gland neoplasms. *Cancer Cytopathol.* 2016;124:397–405.

154. Bahrami A, Dalton JD, Shivakumar B, et al. *PLAG1* alteration in carcinoma ex pleomorphic adenoma: immunohistochemical and fluorescence in situ hybridization studies of 22 cases. *Head Neck Pathol.* 2012;6:328–335.

155. Katabi N, Ghossein R, Ho A, et al. Consistent *PLAG1* and *HMGA2* abnormalities distinguish carcinoma ex-pleomorphic adenoma from its de novo counterparts. *Hum Pathol.* 2015;46:26–33.

156. Chiosea SI, Thompson LD, Weinreb I, et al. Subsets of salivary duct carcinoma defined by morphologic evidence of pleomorphic adenoma, PLAG1 or HMGA2 rearrangements, and common genetic alterations. *Cancer.* 2016;122:3136–3144.

157. Rotellini M, Palomba A, Baroni G, et al. Diagnostic utility of PLAG1 immunohistochemical determination in salivary gland tumors. *Appl Immunohistochem Mol Morphol.* 2014;22:390–394.

158. Salovaara E, Hakala O, Bäck L, et al. Management and outcome of salivary duct carcinoma in major salivary glands. *Eur Arch Otorhinolaryngol.* 2013;270:281–285.

159. Soper MS, Iganej S, Thompson LD. Definitive treatment of androgen receptor-positive salivary duct carcinoma with androgen deprivation therapy and external beam radiotherapy. *Head Neck.* 2014;36:E4–E7.

160. Yamamoto N, Minami S, Fujii M. Clinicopathologic study of salivary duct carcinoma and the efficacy of androgen deprivation therapy. *Am J Otolaryngol.* 2014;35:731–735.

161. Falchook GS, Lippman SM, Bastida CC, et al. Human epidermal receptor 2-amplified salivary duct carcinoma: regression with dual human epidermal receptor 2 inhibition and anti-vascular endothelial growth factor combination treatment. *Head Neck.* 2014;36:E25–E27.

162. Limaye SA, Posner MR, Krane JF, et al. Trastuzumab for the treatment of salivary duct carcinoma. *Oncologist.* 2013;18:294–300.

Novinky v molekulární diagnostice karcinomů slinných žláz: „translokační karcinomy"

Alena Skálová [1,2]**, Petr Šteiner** [1,2]**, Tomáš Vaněček** [2]

[1] *Šiklův ústav patologie, Univerzita Karlova v Praze, Lékařská fakulta v Plzni, Plzeň*
[2] *Bioptická laboratoř, s.r.o., Plzeň*

SOUHRN

Objevy translokací a fúzních onkogenů, které jsou jejich produktem, změnily přístup ke klasifikaci salivárních karcinomů a do značné míry i diagnostické a interpretační postupy. Metody molekulární diagnostiky mají v patologii slinných žláz jak diferenciálně diagnostický význam, tak slouží v klasifikaci některých karcinomů, protože mnohé translokace jsou specifické pro určitou nádorovou jednotku. Průkaz fúzního transkriptu může mít také prognostický význam. V tomto přehledovém článku budou představeny 4 salivární karcinomy, u nichž byly dosud identifikovány onkogenní translokace, a to mukoepidermoidní karcinom, adenoidně cystický karcinom, sekreční karcinom mamárního typu, a hyalinizující světlobuněčný karcinom malých slinných žláz.

Klíčová slova: salivární karcinomy – fúzní onkogeny – *CRTC1/3-MAML2* – *MYB-NFIB* – *ETV6-NTRK3* – *EWSR1-ATF1*

New developments in molecular diagnostics of carcinomas of the salivary glands: "translocation carcinomas"

SUMMARY

In recent years the discovery of translocations and the fusion oncogenes that they result in has changed the way diagnoses are made in salivary gland pathology. These genetic aberrations are recurrent; and at the very least serve as powerful diagnostic tools in salivary gland tumors diagnosis and classification. They also show promise as prognostic markers and hopefully as targets of therapy. In this review the 4 carcinomas currently known to harbor translocations will be discussed, namely mucoepidermoid carcinoma, adenoid cystic carcinoma, mammary analogue secretory carcinoma, and hyalinizing clear cell carcinoma. The discovery and implications of each fusion will be highlighted and how they have helped to reshape the current classification of salivary gland tumors.

Keywords: salivary gland carcinoma – fusion oncogenes – *CRTC1/3-MAML2* – *MYB-NFIB* – *ETV6-NTRK3* – *EWSR1-ATF1*

Chromozomální aberace ve formě translokací mají ve většině případů za následek vznik fúzních genů, které mohou vykazovat onkogenní transformační a aktivační vlivy v různých buněčných liniích. V lidských nádorech bylo dosud identifikováno více než 800 fúzních onkogenů a mnohé z nich slouží jako vhodné diagnostické a prognostické biomarkery a potenciální cíle biologické léčby (1-3). Většina fúzních onkogenů byla nalezena v hematologických malignitách a sarkomech, naproti tomu v karcinomech jde o jev relativně vzácný (1,4).

Molekulární diagnostika pronikla v posledních několika letech i do onkopatologie slinných žláz (5-8). Objevy translokací a fúzních onkogenů, které jsou jejich produktem, změnily následně přístup ke klasifikaci salivárních karcinomů a do značné míry i diagnostické a interpretační postupy. Metody molekulární diagnostiky mají v patologii slinných žláz jak **diferenciálně diagnostický význam**, tak slouží v klasifikaci některých karcinomů, protože mnohé translokace jsou specifické pro určitou nádorovou jednotku. Nově popsaný sekreční karcinom slinných žláz mamárního typu (mammary analogue secretory carcinoma) (MASC) byl definován na základě detekce translokace t(12;15)(p13;q25) rezultující v genovou fúzi *ETV6-NTRK3* (9). Identický fúzní transkript *ETV6-NTRK3* byl sice již dávno před objevem MASC identifikován v řadě mesenchymálních (10-14), hematologických (15) a epiteliálních malignit (16-17), ale v onkologii slinných žláz je specifický pro MASC a nebyl nalezen v žádné jiné nádorové jednotce slinných žláz. Průkaz fúzního transkriptu může mít také **prognostický význam**. Příkladem je mukoepidermoidní karcinom malých a velkých slinných žláz. Přítomnost fúzního onkogenu *CRTC1-MAML2* který vzniká translokací t(11;19)(q14-21;p12-13) je spojena jednoznačně s příznivou prognózou (18).

V tomto přehledovém článku budou představeny 4 salivární karcinomy, u nichž byly dosud identifikovány onkogenní translokace, a to mukoepidermoidní karcinom s translokací t(11;19) (q21;p13) *CRTC1-MAML2* nebo translokací t(11;15) (q21;q26) *CRTC3-MAML2*, adenoidně cystický karcinom s translokací t(6;9) (q22-23;p23-24) generující fúzní transkript *MYB-NFIB*, sekreční karcinom mamárního typu s translokací t(12;15)(p13;q25) *ETV6-NTRK3* a hyalinizující světlobuněčný karcinom malých slinných žláz vykazující charakteristickou translokaci t(12;22)(q13;q12) s fúzním onkogenem *EWSR1-ATF1*.

✉ *Adresa pro korespondenci:*
Prof. MUDr. Alena Skálová, CSc.
Šiklův ústav patologie LF UK v Plzni
Fakultní nemocnice Bory
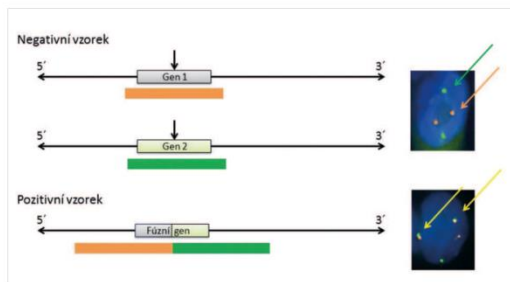*Ed. Beneše 13, 305 99 Plzeň, Česká republika*
tel.: +420 377 402 545
e-mail: skalova@fnplzen.cz

METODY DETEKCE ZLOMŮ A TRANSLOKACÍ

Pro detekci nádorově specifických fúzních onkogenů u salivárních karcinomů se využívají především **hybridizační techniky**, zejména tzv. hybridizace *in situ*. Hybridizace *in situ* je metoda DNA analýzy, která je založena na specifickém spojení komplementárních nukleotidových sekvencí pocházejících z vyšetřované jednořetězcové denaturované DNA a uměle připravené jednořetězcové DNA nebo oligo/poly- nukleotidového řetězce se známou sekvencí, tzv. sondy (próby), to vše přímo v jádrech buněk histologických řezů. Z důvodu vizualizace hybridizačního signálu je nutné, aby sonda byla značena a to buď přímo, zejména fluorescenčním barvivem - fluorochromem, nebo nepřímo, např. haptenem s následnou detekcí flourochromem značenou protilátkou nebo pomocí protilátek spřažených s enzymatickou reakcí. V současné době se k vyšetření specifických translokací u salivárních karcinomů používá v drtivé většině případů **fluorescenční in situ hybridizace (FISH)** s lokus specifickými sondami. Jedná se buď o sondy fúzní, kdy dochází po translokaci k fyzickému přiblížení dvou různobarevných sond komplementárních k dvěma konkrétním fúzním partnerům a tím vzniku signálu jiné barvy (obr. 1), nebo tzv. "break-apart" sondy, u kterých se různobarevné sondy komplementární k 5` a 3` konci jednoho konkrétního fúzního partnera po zlomu tohoto genu fyzicky oddělí za vzniku dvou různobarevných signálů (obr. 2). Detekce sond je pak provedena ve fluorescenčním mikroskopu s excitačním a emisním filtrem odpovídající vlnové délky.
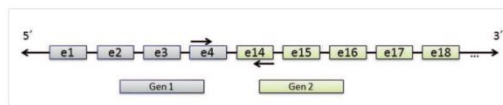
V molekulárně biologické diagnostice salivárních karcinomů se dále využívají **amplifikační techniky**, zejména polymerázová řetězová reakce (PCR), v těchto případech často spřažená s reverzní transkripcí (RT). PCR je metoda enzymatické syntézy spe-
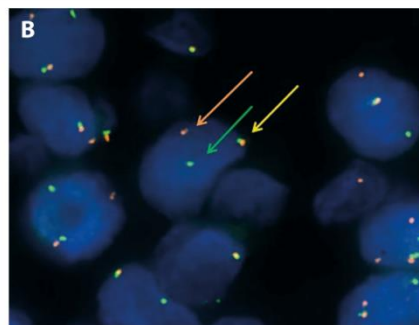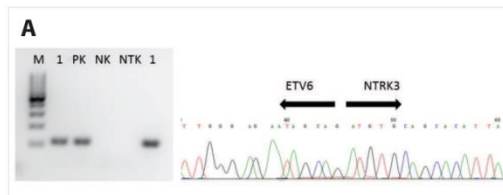
Obr. 3. Schematické zobrazení principu detekce fúzního transkriptu genů 1 a 2 pomocí RT-PCR. Zobrazena fúze mezi exonem 4 Genu 1 a exonem 14 Genu 2.

Obr. 4. A. Příklad agarózové elektroforézy a sekvenční analýzy fúzního transkriptu ETV6-NTRK3 u vzorku MASC. 1 – vzorek (v duplikátu), PK – pozitivní kontrola, NK – negativní kontrola, NTK – non-templátová kontrola. **B.** Příklad analýzy metodou fluorescenční *in situ* hybridizace s komerčně dostupnou break-apart sondou Vysis *ETV6* Break Apart FISH Probe (Vysis/Abbott Molecular) u vzorku MASC. Intaktní gen dává žlutý, zlomený pak červený a zelený signál.

Obr. 1. Schematické zobrazení fúzní FISH sondy, principu detekce translokace mezi dvěma geny (Gen1 a Gen 2) a jejich projev v jádře buňky po FISH analýze.

Obr. 2. Schematické zobrazení „break-apart" sondy, principu detekce zlomu určitého genu (Gen 1) a jejich projev v jádře buňky po FISH analýze.

cifických sekvencí DNA, kdy je díky mnohonásobné replikaci vytvořen dostatek materiálu pro další molekulárně genetické analýzy. RT-PCR pak umožňuje amplifikaci cDNA z výchozího RNA templátu, kdy se využívá reverzní transkripce RNA do prvního vlákna cDNA pomocí enzymu reverzní transkriptázy. RT – PCR slouží jako metoda k prokazování transkriptů fúzních onkogenů (obr. 3).

Aplikace těchto metodik pak tvoří silný nástroj pomáhající patologovi při vlastní diferenciální diagnostice. Detekce příslušných translokací a fúzních transkriptů v mnoha případech definuje příslušnost k určitým nádorovým jednotkám (obr. 4A, B)

FÚZNÍ ONKOGENY V KARCINOMECH SLINNÝCH ŽLÁZ

CRTC1-MAML2 a *CRTC3-MAML2* fúzní geny v mukoepidermoidním karcinomu

Mukoepidermoidní karcinom (MEC) patří k nejčastějším karcinomům slinných žláz; představuje asi 20% všech salivárních malignit (19). Mikroskopická struktura MEC je značně variabilní a diagnóza není vždy jednoduchá. MEC je většinou histologicky low-grade karcinom sestávající ze tří typů nádorových buněk, a to pohárkových buněk produkujících hlen (mucinozních), epidermoidních nekeratinizujících buněk a buněk intermediálního
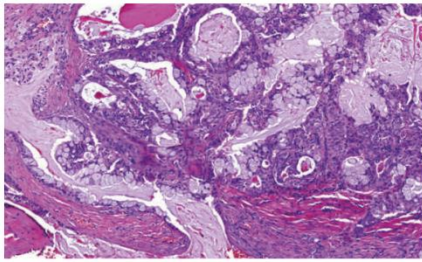
**Obr. 5.** Mukoepidermoidní karcinom (low-grade) konvenční struktury sestávající ze tří typů nádorových buněk, mucinózních, epidermoidních a buněk intermediálního typu (hematoxylin-eozin).
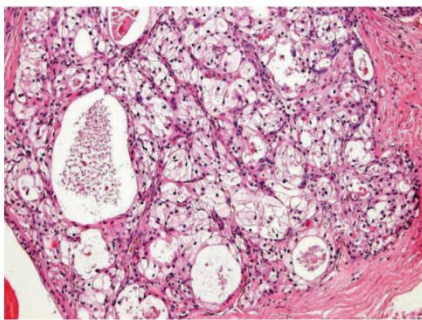
Obr. 6. Světlobuněčná varianta mukoepidermoidního karcinomu: nádorové buňky s vodojasnou cytoplasmou tvoří většinu nádoru (Hematoxylin-eosin).

typu, zastoupených v různých proporcích (obr. 5). Onkocytární a světlobuněčná varianta MEC mohou být diagnosticky velmi obtížné, protože nádorové buňky s onkocytární metaplázií nebo vodojasnou cytoplasmou mohou tvořit většinu nádoru (obr. 6). MEC mohou být převážně solidní, nebo mohou sestávat především z cystických ložisek vystlaných cylindrickými nebo kubickými mucinózními (pohárkovými) buňkami, které mají vodojasnou, eosinofilní nebo pěnitou cytoplasmu. V typických případech není diagnóza MEC problematická, ale vzhledem k variabilitě morfologie má MEC velký rozptyl diferenciálně diagnostických možností (20). Na low-grade straně histomorfologického spektra jsou multicystické nádory sestávající v převaze z mucinózních a intermediálních buněk s velkým množstvím hlenu. Tyto nádory je třeba odlišit od benigního mucinozního cystadenomu a duktektázií. MEC se středním (intermediálním) stupněm diferenciace (grade 2) může napodobovat MASC, acinický karcinom, celulární pleomorfní adenom nebo hyalinizující světlobuněčný karcinom malých slinných žláz. High-grade MEC je naopak třeba odlišit od metastatického squamozního (dlaždicového), salivárního duktálního karcinomu nebo vzácného adenosquamozního karcinomu slinných žláz (20).

Predikce prognozy pacientů s MEC je obtížná, neboť není dosud shoda na přesných kriteriích pro grading. Pro mukoepidermoidní karcinom bylo navrženo několik odlišných schémat a systémů, které nebudou v detailu diskutovány, ale všechny využívají procentuální zastoupení cystické komponenty, anaplázie, mitotické aktivity, přítomnosti nekroz, perineurální a lymfovaskulární invaze a některých dalších znaků (19), ale jejich použití je předmětem diskuzí. Teprve objev translokací t(11;19) (q21;p13) *CRTC1-MAML2* a t(11;15) (q21;q26) *CRTC3-MAML2* ve
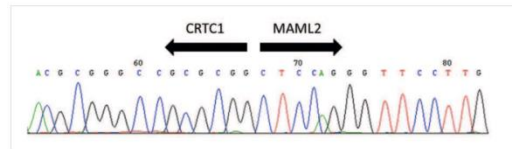
Obr. 7. Sekvenogram fúzního transkriptu *CRTC1-MAML2.* Šipky vyznačují místo fúze.

většině případů MEC představuje slibný diferenciálně diagnostický a prognostický indikátor. Fúzní transkript *CRTC1-MAML2* byl prvně popsán po mnoha letech cytogenetických studií, kdy Tonon et al. jako první identifikovali rekurentní translokaci t(11;19)(q14-21;p12-13) *CRTC1-MAML2* (syn. *MECT1-MAML2*) (obr. 7) ve skupině mukoepidermoidních karcinomů (21). Skutečným přelomem se staly následující publikace, v nichž byla prokázána nečekaně příznivá prognoza u pacientů s MEC s pozitivním fúzním transkriptem (18). Klinicko-patologické retrospektivní studie, prokázaly, že MEC s pozitivní fúzí mají nižší riziko recidiv a metastáz než MEC bez fúze (18, 22-23). Seethala *et al.* prokázali přítomnost *CRTC1-MAML2* translokace v 75 % všech MEC s nízkým a středně vysokým gradem, zatímco high-grade MEC byly pozitivní pouze ve 46 % (23). Důležité je však připomenout, že příznivou prognózu mají všechny translokované MEC, včetně pokročilých karcinomů s high-grade morfologií (23-24). Nový fúzní partner pro *MAML2* gen z rodiny CRTC byl popsán později (24). *CRTC3* je lokalizovaný na chromozomu 15q26.1 a jeho fúze s genem *MAML2* se vyskytuje velmi vzácně u mladých lidí a dětí. Podobně jako *CRTC1-MAML2* je také fúze *CRTC3-MAML2* spojená s excelentní prognózou (24,26).

Při zmíněné translokaci je u fúzního proteinu *CRTC1-MAML2* nahrazena N-terminální bazická doména genu *MAML2* CREB-binding (cAMP response element-binding) doménou genu *CRTC1*. Molekulární konsekvence této záměny nejsou dosud zcela objasněné, ale z dosavadních zjištění vyplývá, že fúzní protein nezávisle na vstupních signálech aktivuje jak CREB závislé geny, tak i Notch signální dráhu. Aktivace dvou nezávislých drah, zejména však CREB, pak významně přispívá k vlastnímu neoplastickému procesu (2). Obdobný mechanismus se pak zřejmě uplatňuje i u sesterského fúzního genu *CRTC3-MAML2*.

V literatuře přetrvávají určité kontroverze ohledně translokace *CRTC1-MAML2* ve Warthinovu tumoru (27-28), velmi pravděpodobně je však detekovaná translokace i v těchto vzácných případech specifická pro MEC vznikající ve Warthinově tumoru (mínění autorů textu) (29). Nepochybně mají obě translokace *CRTC1-MAML2* a *CRTC3-MAML2* pozitivní prognostický význam, translokované MEC se chovají příznivě. Translokaci nebo přestavbu genu *MAML2* lze také využít v diagnosticky obtížných případech, jako jsou onkocytární a světlobuněčná varianta MEC (30) nebo v neobvyklých lokalizacích, např. intraoseální (centrální) MEC (31).

MYB-NFIB fúzní gen v adenoidně cystickém karcinomu

Adenoidně cystický karcinom (AdCC) je low-grade bazaloidní nádor sestávající z epiteliálních a myoepiteliálních buněk ve variabilních morfologických strukturách (32). Jedná se o nejčastější karcinom hlavy a krku infiltrující nervy, s peri- a intraneurálním šířením ve 20 - 80 % případů (33). AdCC je většinou ohraničený, ale neopouzdřený nádor, hluboce infiltrující okolní tkáně především progresí kolem nervů. Je tvořen dvěma hlavními typy buněk, a to duktálními a modifikovanými myoepiteliálními. Jádra jsou hranatá a hyperchromní a cytoplazma často vodojasná. V AdCC se rozlišují se tři růstové struktury: tubulární, kribriformní a solidní (32) (obr. 8). Nejčastější kribriformní struktura je charakterizována hnízdy buněk s pseudocystickými

161
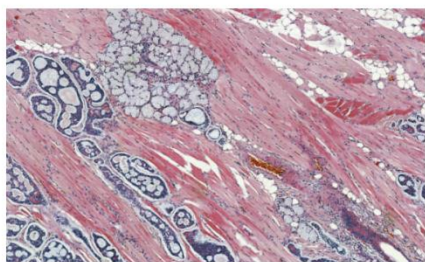
Obr. 8. Adenoidně cystický karcinom s typickou kribriformní strukturou a invazivním růstem (hematoxylin-eozin).
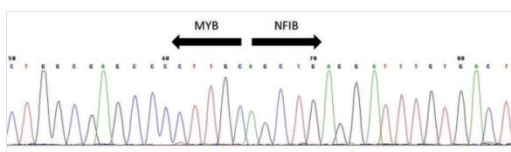
Obr. 9. Sekvenogram fúzního transkriptu *MYB-NFIB*. Šipky vyznačují místo fúze.

prostory, které jsou vyplněny hyalinní nebo bazofilní mukoidní extracelulární matrix. Tubulární struktura je tvořena dobře formovanými vývody a tubuly s centrálními luminy, které jsou lemovány uvnitř epiteliálními a zevně myoepiteliálními buňkami. Solidní (bazaloidní) struktura je formována uniformními malými bazaloidními buňkami s minimální cytoplazmou, které netvoří ani tubulární ani mikrocystické struktury (32). V kribriformní a solidní variantě nádoru se vyskytují i malé pravé vývody, které nemusejí být ihned patrné. Každá ze tří výše popsaných struktur může být v nádoru výrazně dominantní nebo častěji je jen jednou z komponent kompozitního tumoru. Nádorové stroma je obvykle hyalinizované (někdy i poměrně extenzivně s útlumem epiteliální komponenty) a může vykazovat i mucinózní nebo myxoidní rysy. Častým nálezem je perineurální a intraneurální invaze, která může dosahovat do značné vzdálenosti od klinických ale i radiologických hranic karcinomu.

Pro AdCC slinných žláz je typická chromozomální translokace t(6;9)(q22-23;p23-24), která generuje fúzní transkript *MYB-NFIB* (obr. 9) (34-36). *MYB–NFIB* fúzní onkogen byl poprvé popsán u AdCC Martou Perssonovou et al. v roce 2009 (37). Gen *MYB*, lokalizovaný v oblasti 6q22-23, kóduje transkripční faktor který hraje zásadní roli v regulaci buněčné proliferace, diferenciace a apoptózy, a tím pravděpodobně i v tumorogenezi. *MYB* je vysoce exprimován v nezralých a proliferujících epiteliálních, endoteliálních a hematopoetických buňkách a naopak down-regulován v době, kdy se tyto buňky stanou diferencovanými (34,36). Gen *NFIB* (Nuclear Factor I/B), lokalizovaný v oblasti 9p23-24, patří do rodiny dimerních DNA-vazebných proteinů fungujících jako buněčný transkripční faktor. Vznik fúzního onkogenu *MYB-NFIB* vede ke ztrátě 3´ konce *MYB* genu (exonu 15), místa, kde dochází k negativní regulaci *MYB* exprese (34,36). Následná zvýšená exprese fúzního transkriptu a proteinu pak aktivuje transkripci *MYB* cílových genů, které mají zasadní roli v onkogenní transformaci. *MYB-NFIB* fúze nebo přestavba *MYB* genu, které vedou k jeho aktivaci, a tím ke zvýšené expresi *MYB–NFIB* fúzního proteinu nebo *MYB* onkoproteinu, byly dosud ze salivárních karcinomů i jiných karcinomů hlavy a krku prokázány pouze u AdCC, a to ve více jak v 80 % případů (34,38). Jedná se tak o charakteristický znak těchto maligních sialomů, který se dá využít jako diagnostický marker, s výhodou především u vzdálených metastáz.

ETV6-NTRK3 fúzní gen v sekrečním karcinomu mammárního typu / Mammary analogue secretory carcinoma

Sekreční karcinom mamárního typu (MASC) je nově popsaný nádor slinných žláz, který vykazuje histologickou a imunohistochemickou podobnost se sekrečním karcinomem prsu (9). Podobně jako prsní sekreční karcinom, exprimuje MASC difúzně cytokeratiny, S-100 protein a mammaglobin, a je charakterizován translokací t(12;15) (p13;q25), která generuje fúzní transkript *ETV6-NTRK3* (9,16). Histologicky, jak sekreční karcinom salivární tak mamární, jsou většinou low-grade malignity, a jsou dobře ohraničené ale neopouzdřené s ložiskovým invazivním růstem. Nádorové buňky MASC jsou většinou uniformní, blandního vzhledu, s pravidelnými vesikulárními jádry, jedním centrálně lokalizovaným zřetelným jadérkem a eosinofilní vakuolizovanou nebo vodojasnou cytoplasmou (obr. 10A). Mikrocystická struktura je pro MASC typická, ale nádor je strukturálně variabilní, takže tubulární, solidní, makrocystická a kribriformní ložiska v různých proporcích nejsou výjimkou (obr. 10B). Velmi důležitým diferenciálně diagnostickým znakem je absence sekrečních zymogenních granul v cytoplasmě nádorových buněk, která MASC odlišuje od strukturálně podobného acinického karcinomu (9). MASC je karcinom, který typicky obsahuje tubulární a mikrocystické struktury s hojným homogenním nebo vakuolizovaným sekretem v lumen. Sekreční materiál je pozitivní při barvení mucikarmínem a PAS před i po natrávení diastázou.
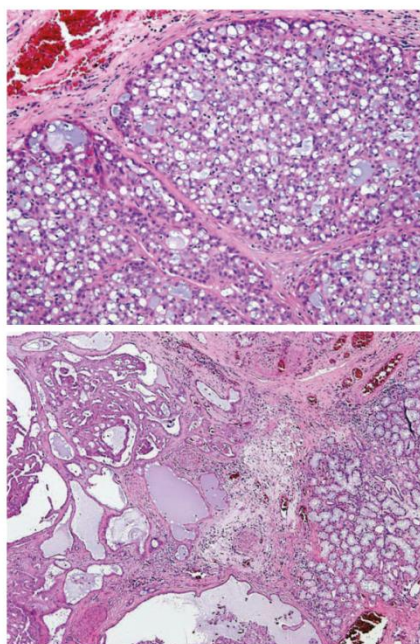
Obr. 10. Sekreční karcinom mamárního typu (MASC): typická mikrocystická struktura s uniformními nádorovými buňkami, blandního vzhledu, s pravidelnými vesikulárními jádry, jedním centrálně lokalizovaným zřetelným jadérkem a eosinofilní vakuolizovanou nebo vodojasnou cytoplasmou (**A**). MASC je nádor strukturálně variabilní, takže tubulární, solidní, makrocystická a kribriformní ložiska v různých proporcích nejsou výjimkou (**B**) (hematoxylin-eozin).

Imunoprofil MASC je charakterizován ko-expresí cytokeratinů (CK7, CK8, CK18), S-100 proteinu, SOX10, mammaglobinu a GATA3 (9). MASC nevykazuje na rozdíl od acinického karcinomu expresi markeru DOG1, který byl původně použit v diagnostice gastrointestinálního stromálního tumoru, ale v diagnostice karcinomů slinných žláz se využívá jeho exprese v normálních i nádorových buňkách s acinární diferenciací (39). Průkaz GCDFP 15 (gross cystic disease fluid protein) a EMA (epiteliální membránový protein) jsou velmi často v MASC pozitivní, zatímco p63 protein je zpravidla v nádorových buňkách negativní (9). Ložiskově a jen v některých případech, může jaderná exprese p63 dekorovat vrstvu bazálních buněk, a svědčí tak pro in situ lézi nebo fokální intraduktální komponentu MASC (40).

Pro MASC je typická rekurentní chromosomální translokace t(12;15)(p13;q28) generující fúzní transkript *ETV6-NTRK3* (9). Tato translokace byla popsána v řadě mezenchymálních nádorů (10-14), v různých hematologických malignitách (15) a dokonce nedávno v podskupině radiací indukovaných papilokarcinomů štítné žlázy (17), ale nevyskytuje se v žádném jiném nádoru slinných žláz než v MASC. Skutečně raritním je pozorování primárního sekrečního karcinomu mamárního typu (MASC) ve štítné žláze (41,42) napodobující papilokarcinom. To je skutečná diagnostická "past", protože léčba papilokarcinomu štítné žlázy je diametrálně odlišná od léčby MASC (42). Fúzní gen *ETV6-NTRK3* kóduje chimerický onkoprotein tyrosin kinázu, která aktivuje Ras-MAP kinázovou dráhu startující onkogenní transformaci (16, 43). Větší klinicko-patologické studie jsou dosud vzácné, ale ukazují, že MASC je u většiny pacientů low-grade malignita s relativně příznivou prognózou (44-45). U části pacientů může být však chování karcinomu velmi agresivní, včetně lokálních recidiv, vzdálených metastáz, případně s fatálním klinickým průběhem (46). Příkladem může být MASC s high-grade transformací (46) nebo MASC označovaný *ETV6-X*, u nichž FISH prokazuje zlom v *ETV6* genu nikoliv však genu *NTRK3* a ani žádného dalšího genu z NTRK rodiny, konkrétně *NTRK1* a *NTRK2* (47). MASC s high grade transformací jsou velmi agresivní karcinomy, které rychle generalizují a klinický průběh je často smrtelný, proto se u pacientů s takto agresivními formami MASC a s prokázanou translokací *ETV6-NTRK3* nabízí možnost cílené léčby inhibitory onkogenní tyrosin kinázy (46-48).

EWSR1-ATF1 fúzní gen v hyalinizujícím světlobuněčném karcinomu malých slinných žláz

Hyalinizující světlobuněčný karcinom malých slinných žláz (HCCC) byl prvně rozpoznán v roce 1994 Milchgrubovou *et al.* (49) jako samostatná nádorová jednotka odlišná od monomorfní světlobuněčné varianty myoepiteliálního karcinomu (50,51), epiteliálního-myoepiteliálního karcinomu a od světlobuněčných variant acinického a mukoepidermoidního karcinomu (20). Dle dosud platné WHO klasifikace nádorů hlavy a krku z roku 2005 (52) je sice HCCC klasifikován jako světlobuněčný adenokarcinom NOS (not otherwise specified), ale to je jistě chybná koncepce zvláště ve světle nových molekulárně genetických nálezů, které ukazují že HCCC je samostatná nádorová jednotka definovaná specifickou translokací t(12;22)(q13;q12) zahrnující geny *EWSR1* a *ATF1* (obr. 11) (53). Při této translokaci dochází k fúzi N-koncové transaktivační části genu *EWSR1* s DNA vazebnou doménou transkripčního faktoru *ATF1*, což vede k aktivaci exprese downstream cílových genů, které se účastní buněčného růstu (53). HCCC je low-grade karcinom s dobrou prognózou u většiny pacientů, ale vzácně s rizikem recidivy a regionálních uzlinových metastáz.

Histologicky je HCCC monofázický karcinom sestávající z uniformních buněk s eosinofilní nebo vodojasnou cytoplasmou typicky uspořádaných do malých hnízd, pruhů a trabekulárních struktur, oddělených od sebe hyalinizovanými vazivovými septy (obr. 12). Fokálně může být přítomna hlenotvorba a odlišení od
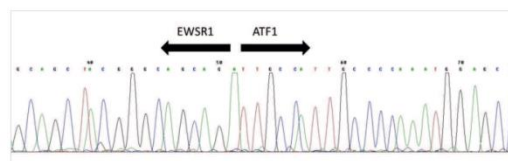
Obr. 11. Sekvenogram fúzního transkriptu *EWSR1-ATF1*. Šipky vyznačují místo fúze.
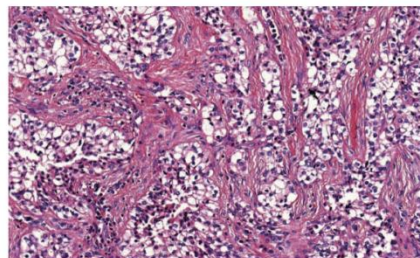
Obr. 12. Hyalinizující světlobuněčný karcinom malých slinných žláz sestává z uniformních buněk s eosinofilní nebo vodojasnou cytoplasmou typicky uspořádaných do malých hnízd, pruhů a trabekulárních struktur, oddělených od sebe hyalinizovanými vazivovými septy. (hematoxylin-eozin).

světlobuněčné varianty mukoepidermoidního karcinomu je tedy obtížné. Na základě absence S-100 proteinu a hladkosvalového aktinu byl HCCC již v původní práci definován jako karcinom, který postrádá myoepiteliální diferenciaci (49). Původní článek (49) a mnoho následujících studií však prokázaly, že HCCC vykazuje squamocelulární diferenciaci s difusní expresí vysokomolekulárních cytokeratinů a markeru p63 (54-56). Nicméně diferenciální diagnostika světlobuněčných lézí, především karcinomů, v dutině ústní byla vždy velmi problematická a zmatečná. Jednotlivé nádorové jednotky mohou mít podobné nebo shodné morfologické znaky, může se prolínat imunoprofil, kriteria pro odlišení nebyla svorně přijímána, a navíc pro diagnostiku lézí dutiny ústní je často k dispozici pouze malé množství tkáně v probatorní excizi. Proto byl nález specifické a rekurentní translokace t(12;22)(q13;q12), která generuje fúzní onkogen *EWSR1-ATF1* přijat s velkou nadějí, že bude spolehlivým diferenciálně diagnostickým markerem HCCC. Tato naděje se splnila pouze částečně, protože průkaz *EWSR1-ATF1* sice slouží k odlišení většiny ostatních světlobuněčných nádorů v ústní dutině, které HCCC napodobují (53,57), ale světlobuněčný odontogenní karcinom vykazuje identickou translokaci *EWSR1-ATF1* jako HCCC (58, 59), což svědčí pro biologickou příbuznost obou nádorů. My jsme nedávno dokonce identifikovali zlom v *EWSR1* genu u světlobuněčné varianty myoepiteliálního karcinomu (51). *EWSR1-ATF1* fúzní onkogen není specifický, již dříve byla identická translokace popsána u řady morfologicky velmi odlišných nádorů, jako jsou světlobuněčný sarkom, angiomatoidní fibrozní histiocytom, maligní gastrointestinální neuroektodermální tumor (60). Nedávno byl dokonce publikován případ angiosarkomu parotis s *EWSR1-ATF1* fúzí (61). Vzato celkově, průkaz přestavby genu *EWSR1* musí být interpretován vždy ve shodě s histomorfologií a imunoprofilem nádoru (62).

ZÁVĚRY

Nedávné objevy specifických translokací a fúzních onkogenů u několika salivárních karcinomů výrazně ovlivnily diagnostické

a interpretační postupy v klasifikaci salivárních karcinomů (63). Metody molekulární diagnostiky mají v onkopatologii slinných žláz v současné době především diferenciálně diagnostický význam, protože mnohé translokace jsou specifické pro určitou nádorovou jednotku. Nově popsaný sekreční karcinom slinných žláz mamárního typu (MASC) je chakterizován translokací t(12;15) a genovou fúzí *ETV6-NTRK3*, která je v onkologii slinných žláz specifická pro MASC a nebyla nalezena v žádné jiné nádorové jednotce slinných žláz. Podobně průkaz translokace t(12;22) s fúzním onkogenem *EWSR1-ATF1* je v kontextu příslušné histomorfologie diagnostický pro hyalinizující světlobuněčný karcinom malých slinných žláz a fúzní transkript *MYB-NFIB* pro adenoidně cystický karcinom. Průkaz fúzního transkriptu u mukoepidermoidního karcinomu má nejen diagnostický význam,

ale může být využit i v prognóze. Přítomnost fúzního onkogenu t(11;19) *CRTC1-MAML2* a t(11;15) *CRTC3-MAML2* je spojena jednoznačně s příznivou prognozou. S rozvojem technik molekulární biologie bude nepochybně v salivární patologii v dalších letech přibývat objevů translokací a dalších aberací. V neslední řadě, je naděje, že tyto nálezy bude možné v blízké budoucnosti využít k cílené biologické léčbě pacientů s karcinomy slinných žláz.

PROHLÁŠENÍ

Autor práce prohlašuje, že v souvislosti s tématem, vznikem a publikací tohoto článku není ve střetu zájmů a vznik ani publikace článku nebyly podpořeny žádnou farmaceutickou firmou. Toto prohlášení se týká i všech spoluautorů.

LITERATURA

1. **Mitelman F, Johansson B, Mertens F.** The impact of translocations and gene fusions on cancer causation. *Nat Rev Cancer* 2007; 7(4): 233-245.
2. **Stenman G.** Fusion oncogenes and tumor type specificity – insight from salivary gland tumors. *Semin Cancer Biol* 2005; 15(3): 224-235.
3. **Aman P.** Fusion oncogenes in tumor development. *Semin Cancer Biol* 2005; 15(3): 236-243.
4. **Mitelman F, Johansson B, Mertens F, eds.** Mitelman database of chromosome aberrations and gene fusions in cancer: http://cgap.nci.nih.gov/Chromosomes/Mitelman, 2013.
5. **Asp J, Persson F, Kost-Alimova M, Stenman G.** CHCHD7-PLAG1 and TCEA1-PLAG1 gene fusions resulting from cryptic, intrachromosomal 8q rearrangements in pleomorphic salivary gland adenomas. *Genes Chromosomes Cancer* 2006; 45(9): 820-828.
6. **Persson F, Winnes M, Andrén Y, et al.** High-resolution array CGH analysis of salivary gland tumors reveals fusion and amplification of the FGFR1 and PLAG1 genes in ring chromosomes. *Oncogene* 2008; 27(21): 3072-3080.
7. **Persson F, Andrén Y, Winnes M, et al.** High-resolution genomic profiling of adenomas and carcinomas of the salivary glands reveals amplification, rearrangement, and fusion of HMGA2. *Genes Chromosomes Cancer* 2009; 48(1): 69-82.
8. **Stenman G, Andersson MK, Andrén Y.** New tricks from an old oncogene: gene fusions and copy number alterations of MYB in human cancer. *Cell Cycle* 2010; 9(15): 2986-2995.
9. **Skalova A, Vaněček T, Šíma R, et al.** Mammary analogue secretory carcinoma of salivary glands, containing the ETV6-NTRK3 fusion gene: a hitherto undescribed salivary gland tumor entity. *Am J Surg Pathol* 2010; 34(5): 599–608.
10. **Knezevich SR, McFadden DE, Tao W, Lim JF, Sorensen PH.** A novel ETV6-NTRK3 gene fusion in congenital fibrosarcoma. *Nat Genet* 1998; 18(2): 184–187.
11. **Knezevich SR, Garnett MJ, Pysher TJ, Beckwith JB, Grundy PE, Sorensen PH.** *ETV6-NTRK3* gene fusions and trisomy 11 establish a histogenetic link between mesoblastic nephroma and congenital fibrosarcoma. *Cancer Res* 1998; 58(22): 5046–5048.
12. **Bourgeois JM, Knezevich SR, Mathers JA, Sorensen PH.** Molecular detection of the *ETV-6-NTRK3* gene fusion differentiates congenital fibrosarcoma from other childhood spindle cell tumors. *Am J Surg Pathol* 2000; 24(7): 937–946.
13. **Rubin BP, Chen CJ, Morgan TW, et al.** Congenital mesoblastic nephroma t(12;15) is associated with ETV6-NTRK3 gene fusion: cytogenetic and molecular relationship to congenital (infantile) fibrosarcoma. *Am J Pathol* 1998; 153(5): 1451–1458.
14. **Alassiri A, Lum A, Goytain A, et al.** ETV6-NTRK3 is expressed in a subset of ALK-negative inflammatory myofibroblastic tumors: case series of 20 patients. *Mod Pathol* 2015; 28(Supplement 2s): 13A.
15. **Kralik JM, Kranewitter W, Boesmueller H, et al.** Characterization of a newly identified ETV6 NTRK3 fusion transcript in acute myeloid leukemia. *Diagn Pathol* 2011; 6:19.
16. **Tognon CE, Knezevich SR, Huntsman D, et al.** Expression of the *ETV6-NTRK3* gene fusion as a primary event in human secretory breast carcinoma. *Cancer Cell* 2002; 2(5): 367–376.
17. **Leeman-Neill RJ, Kelly LM, Liu P, et al.** ETV-6-NTRK3 is a common chromosomal rearrangement in radiation-associated thyroid cancer. *Cancer* 2014; 120(6): 799–807.
18. **Behboudi A, Enlund F, Winnes M, et al.** Molecular classification of mucoepidermoid carcinoma – prognostic significance of the MECT1-MAML2 fusion oncogene. *Genes Chromosomes Cancer* 2006; 45(5): 470-481.
19. **Goode RK, El-Naggar AK.** Mucoepidermoid carcinoma. *In:* **Barnes L, Eveson J, Reichart P, Sidransky D**, eds. Pathology and genetics of head and neck tumours. World Health Organization classification of tumours. Lyon: IARC Press; 2005: 219-220.
20. **Hellquist H, Skalova A.** Histopathology of the salivary glands. Berlin, Heidelberg: Springer Verlag; 2014.
21. **Tonon G, Modi S, Wu L, et al.** t(11;19) (q21;p13) translocation in mucoepidermoid carcinoma creates a novel fusion product that disrupts a Notch signaling pathway. *Nat Genet* 2003; 33(2): 208-213.
22. **Okabe M, Miyabe S, Nagatsuka H, et al.** MECT1-MAML2 fusion transcript defines a favorable subset of mucoepidermoid carcinoma. *Clin Cancer Res* 2006; 12(13): 3902-3907.
23. **Seethala RR, Dacic S, Cieply K, Kelly LM, Nikiforova MN.** A reappraisal of the MECT1/MAML2 translocation in salivary mucoepidermoid carcinomas. *Am J Surg Pathol* 2010; 34(8): 1106-1121.
24. **Okumura Y, Miyabe S, Nakayama T, Fujiyoshi Y, Hattori H, Shimozato K, Inagaki H.** Impact of CRTC1 ∕ 3–MAML2 fusions on histological classification and prognosis of mucoepidermoid carcinoma. *Histopathology* 2011; 59(1): 90–97.
25. **Fehr A, Röser K, Heidorn K, Hallas C, Löning T, Bullerdiek J.** A new type of MAML2 fusion in mucoepidermoid carcinoma. *Genes Chromosomes Cancer* 2008; 47(3): 203-206.
26. **Nakayama T, Miyabe S, Okabe M, et al.** Clinicopathological significance of the CRTC3-MAML2 fusion transcript in mucoepidermoid carcinoma. *Mod Pathol* 2009; 22(12): 1575-1581.
27. **Bell D, Luna MA, Weber RS, Kaye FJ, El-Naggar AK.** CRTC1/MAML2 fusion transcript in Warthin's tumor and mucoepidermoid carcinoma: evidence for a common genetic association. *Genes Chromosomes Cancer* 2008; 47(4): 309–314.
28. **Fehr A, Roser K, Belge G, Löning T, Bullerdiek J.** A closer look at Warthin tumors and the t(11;19). *Cancer Genet Cytogenet* 2008; 180(2): 135–139.
29. **Skálová A, Vaněček T, Hauer L, et al.** *CRTC1-MAML2* and *CRTC3-MAML2* fusions were not detected in metaplastic Warthin´s tumor and metaplastic pleomorphic adenoma of salivary glands. *Am J Surg Pathol* 2013; 37(11): 1743-1750.
30. **García JJ, Hunt JL, Weinreb I, et al.** Fluorescence in situ hybridization for detection of MAML2 rearrangements in oncocytic mucoepidermoid carcinomas: utility as a diagnostic test. *Hum Pathol* 2011; 42(12): 2001–2009.
31. **Bell D, Holsinger CF, El-Naggar AK.** CRTC1/MAML2 fusion transcript in central mucoepidermoid carcinoma of mandible—diagnostic and histogenetic implications. *Ann Diagn Pathol* 2010; 14(6): 396–401.
32. **Barnes L, Eveson JW, Reichart P, Sidransky D**, eds. World Health Organization Classification of Tumours: Pathology and Genetics of Head and Neck Tumours. Lyon: IARC Press; 2005: 209–281.
33. **Amit M, Binenbaum Y, Trejo-Leider L, et al.** International collaborative validation of intraneural invasion as a prognostic marker in adenoid cystic carcinoma of the head and neck. *Head Neck* 2015; 37(7): 1038-1045.
34. **Stenman G.** Fusion oncogenes in salivary gland tumors: molecular and clinical consequences. *Head Neck Pathol* 2013; 7 Suppl 1: S12-S19.

35. **Stenman G, Persson F, Andersson MK.** Diagnostic and therapeutic implications of new molecular biomarkers in salivary gland cancers. *Oral Oncol* 2014; 50(8): 683-690.

36. **Bell D, Hanna EY.** Salivary gland cancers: biology and molecular targets for therapy. *Curr Oncol Rep* 2012; 14(2): 166-174.

37. **Persson M, Andrén Y, Mark J, Horlings HM, Persson F, Stenman G.** Recurrent fusion of MYB and NFIB transcription factor genes in carcinomas of the breast and head and neck. *Proc Natl Acad Sci U S A* 2009; 106(44): 18740-18744.

38. **Simpson RH, Skálová A, Di Palma S, Leivo I.** Recent advances in the diagnostic pathology of salivary carcinomas. *Virchows Arch* 2014; 465(4): 371-384.

39. **Chenevert J, Duvvuri U, Chiosea S, et al.** DOG1: a novel marker of salivary acinar and intercalated duct differentiation. *Mod Pathol* 2012; 25(7): 919–929.

40. **Laco J, Svajdler M, Jr, Andrejs J, et al.** Mammary analogue secretory carcinoma of salivary glands: a report of 2 cases with expression of basal/ myoepithelial markers (calponin, CD10 and p63 protein). *Pathol Res Pract* 2013; 209(3): 167-172.

41. **Stevens TM, Kovalovsky AO, Velosa C, et al.** Mammary analog secretory carcinoma,- low-grade salivary duct carcinoma, and mimickers: a comparative study. *Mod Pathol* 2015; 28(8): 1084-1100.

42. **Reynolds S, Shaheen M, Olson G, Barry M, Wu J, Bocklage T.** A case of primary mammary analog secretory carcinoma (MASC) of the thyroid masquerading as papillary thyroid carcinoma: potentially more than a one off. *Head Neck Pathol.* In press 2016.

43. **Lannon CL, Martin MJ, Tognon CE, Jin W, Kim SJ, Sorensen PH.** A highly conserved NTRK3 C-terminal sequence in the ETV6-NTRK3 oncoprotein binds the phosphotyrosine binding domain of insulin receptor substrate-1: an essential interaction for transformation. *J Biol Chem* 2004; 279(8): 6225-6234.

44. **Chiosea SI, Griffith C, Assaad A, Seethala RR.** Clinicopathological characterization of mammary analogue secretory carcinoma of salivary glands. *Histopathology* 2012; 61(3) :387–394.

45. **Majewska H, Skalova A, Stodulski D, et al.** Mammary analogue secretory carcinoma of salivary glands: a new entity associated with ETV6 gene rearrangement. *Virchows Arch* 2015; 466 (3): 245-254.

46. **Skálová A, Vanecek T, Majewska H, et al.** Mammary analogue secretory carcinoma of salivary glands with high-grade transformation: report of 3 cases with the ETV6-NTRK3 gene fusion and analysis of TP53, beta-catenin, EGFR, and CCND1 genes. *Am J Surg Pathol* 2014; 38(1): 23–33.

47. **Skálová A, Vaněček T, Simpson RHW, et al.** Mammary analogue secretory carcinoma of salivary glands: molecular analysis of 25 ETV6 gene rearranged tumors with lack of detection of classical ETV6-NTRK3 fusion transcript by standard RT-PCR: report of four cases harboring ETV6-X gene fusion. *Am J Surg Pathol* 2016; 40(1): 3-13.

48. **Drilon A, Li G, Dogan S, et al.** What hinds behind the MASC: Clinical response and acquired resistance to entrectinib after ETV6-NTRK3 identification in a mammary analogue secretory carcinoma (MASC). *Annals Oncol Advance.* In press 2016.

49. **Milchgrub S, Gnepp DR, Vuitch F, Delgado R, Albores-Saavedra J.** Hyalinizing clear cell carcinoma of salivary gland. *Am J Surg Pathol* 1994; 18(1): 74–82.

50. **Michal M, Skálová A, Simpson RH, Rychterová V, Leivo I.** Clear cell malignant myoepithelioma of the salivary glands. *Histopathology* 1996; 28(4): 309–315.

51. **Skálová A, Weinreb I, Hyrcza M, et al.** Clear cell myoepithelial carcinoma of salivary glands showing *EWSR1* rearrangement. Molecular analysis of 94 salivary gland carcinomas with prominent clear cell component. *Am J Surg Pathol* 2015; 39(3): 338–348

52. **Barnes L, Eveson JW, Reichart P, Sidransky D,** eds. World Health Organization Classification of Tumours: Pathology and Genetics of Head and Neck Tumours. Lyon: IARC Press; 2005.

53. **Antonescu CR, Katabi N, Zhang L, et al.** *EWSR1-ATF1* fusion is a novel and consistent finding in hyalinizing clear-cell carcinoma of salivary gland. *Genes Chromosomes Cancer* 2011; 50(7): 559–570.

54. **Weinreb I.** Translocation-associated salivary gland tumors: a review and update. *Adv Anat Pathol* 2013; 20(6): 367-377.

55. **Bilodeau EA, Hoschar AP, Barnes EL, Hunt JL, Seethala RR.** Clear cell carcinoma and clear cell odontogenic carcinoma: a comparative clinicopathologic and immunohistochemical study. *Head Neck Pathol* 2011; 5(2): 101-107.

56. **Dardick I, Leong I.** Clear cell carcinoma: review of its histomorphogenesis and classification as a squamous cell lesion. *Oral Surg Oral Pathol Oral Radiol Endod* 2009; 108(3): 399-405.

57. **Shah AA, LeGallo RD, van Zante A, et al.** *EWSR1* genetic rearrangements in salivary gland tumors: a specific and very common feature of hyalinizing clear cell carcinoma. *Am J Surg Pathol* 2013; 37(4): 571–578.

58. **Bilodeau EA, Weinreb I, Antonescu CR, et al.** Clear cell odontogenic carcinomas show *EWSR1* rearrangements: a novel finding & biologic link to salivary clear cell carcinomas. *Mod Pathol* 2012; 25 (Supplement 2s): 101:305A.

59. **Bilodeau EA, Bilodeau EA, Weinreb I, et al.** Clear cell odontogenic carcinomas show *EWSR1* rearrangements: a novel finding and biological link to salivary clear cell carcinomas. *Am J Surg Pathol* 2013; 37(7): 1001-1005.

60. **Stockman DL, Miettinen M, Suster S, et al.** Malignant gastrointestinal neuroectodermal tumor: clinicopathologic, immunohistochemical, ultrastructural, and molecular analysis of 16 cases with a reappraisal of clear cell sarcoma-like tumors of the gastrointestinal tract. *Am J Surg Pathol* 2012; 36(6): 857–868.

61. **Gru AA, Becker N, Pfeifer JD.** Angiosarcoma of the parotid gland with a t(12;22) translocation creating a *EWSR1-ATF1* fusion: a diagnostic dilemma. *J Clin Pathol* 2013; 66(5): 452–454.

62. **Tanguay J, Weinreb I.** What the *EWSR1-ATF1* Fusion has taught us about hyalinizing clear cell carcinoma. *Head and Neck Pathol* 2013; 7(1): 28–34.

63. **Simpson RWH, Skálová A, Di Palma S, Leivo I.** Recent advances in the diagnostic pathology of salivary carcinomas. *Virchows Arch* 2014; 465(4): 371-384.

165

Vážený pán

Mgr. Petr Šteiner
Bioptická laboratoř s.r.o.
Mikulášské náměstí 4, 326 00, Plzeň

V Praze dne 25.9.2017

Vážený pane magistře,

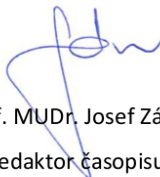s radostí Vám oznamujeme, že Váš rukopis

„Metody detekce molekulárních prognostických a prediktivních markerů v diagnostice adenoidně cystického karcinomu slinných žláz"

č. rukopisu: 296-2017

byl po recenzním řízení **přijat k publikaci**
v časopise Česko-slovenská patologie.

Děkujeme za spolupráci.

S pozdravem

Prof. MUDr. Josef Zámečník, Ph.D.
šéfredaktor časopisu Česko-slovenská patologie

Metody detekce molekulárních prognostických a prediktivních markerů v diagnostice adenoidně cystického karcinomu slinných žláz.

Petr Šteiner [1,2], Jaroslav Pavelka [3], Tomáš Vaněček [1,2], Markéta Miesbauerová [1,2], Alena Skálová [1,2]

[1] Šiklův ústav patologie, Univerzita Karlova v Praze, Lékařská fakulta v Plzni, Plzeň

[2] Bioptická laboratoř, s.r.o., Plzeň

[3] Západočeská Univerzita v Plzni, Pedagogická fakulta, Plzeň

Adresa pro korespondenci:

Mgr. Petr Šteiner

Bioptická laboratoř s.r.o.

Mikulášské náměstí 4, 326 00, Plzeň

Tel: +420 732 961 886

email.: steiner@biopticka.cz

SOUHRN

Adenoidně cystický karcinom slinných žláz (AdCC) je druhým nejčastějším salivárním karcinomem charakteristickým častými recidivami, perineurálním šířením a vysokou mortalitou v dlouhodobém horizontu. V léčbě AdCC je metodou volby chirurgická resekce s adjuvantní radioterapií, ale léčba velkých, invadujících a recidivujících karcinomů je zpravidla paliativní. AdCC charakterizuje vysoká incidence nádorově specifického onkogenu *MYB-NFIB*, který je v současné době diagnostickým markerem, ale mohl by v budoucnu sloužit jako cíl pro biologickou léčbu.

Ve studiu a diagnostice AdCC je využívána imunohistochemie a mnoho molekulárně-genetických metod. Některé metody, jako např. reverzně-transkripční PCR či fluorescenční in-situ hybridizace významnou měrou přispěly k identifikaci translokace t(6;9)(q22-23;p23-24) resultující ve fúzi transkripčních faktorů *MYB* a *NFIB*, která je pro AdCC mezi salivárními karcinomy unikátní a slouží při diagnostice histopatologicky obtížných případů. Komplexnější metody jako např. masivně paralelní sekvenování pak detekovaly další změny na molekulární úrovni a tím umožnily lepšímu pochopení vzniku a patogeneze tohoto v dlouhodobém horizontu často fatálně končícího onemocnění.

Tento přehledový článek shrnuje základní poznatky o tomto onemocnění, kterých bylo dosaženo použitím právě imunohistochemických a molekulárně-genetických metod, to je na úrovni genomu, transkriptomu či epigenomu.

Klíčová slova: Adenoidně cystický karcinom - salivární karcinom - *MYB-NFIB* – FISH – aCGH - NGS

Molecular methods for detection of prognostic and predictive markers in diagnosis of

adenoid cystic carcinoma of the salivary gland origin.

SUMMARY

Adenoid cystic carcinoma of salivary gland origin (AdCC) is second most common salivary carcinoma characterized by frequent recurrences, perineural invasion and high long-term mortality rate. The surgical resection of the tumor in combination with adjuvant radiotherapy is the only method of choice. AdCC has been studied, altogether with immunohistochemistry, by numerous molecular-genetic techniques. Some of them, e.g. reverse-transcription PCR or fluorescent in situ hybridization contributed to the identification of translocation t(6;9)(q22-23;p23-24), which results in fusion of two transcription factors *MYB-NFIB*. For AdCC is this fusion unique among salivary gland carcinomas and serves as a diagnostical tool in differential diagnosis of histopathologically difficult cases. More complex methods, such as next-generation sequencing helped to detect other molecular level changes; and hence improved understanding of a development, behavior and pathogenesis of this possibly fatal malignancy.

This review summarizes basic knowledge of AdCC on the genome, transcriptome and epigenetic level, which were achieved using molecular-genetic and immunohistochemical methods.

Keywords: adenoid cystic carcinoma - salivary carcinoma - *MYB-NFIB* – FISH - aCGH - NGS

Nádory slinných žláz jsou vzácné, představují jen asi 1 % všech lidských neoplázií. Jsou velmi variabilní, jak v mikroskopickém obraze a imunoprofilu, tak klinickým chováním. Adenoidně cystický karcinom (AdCC) je druhým nejčastějším maligním nádorem malých i velkých slinných žláz a představuje asi 10 % všech salivárních karcinomů. Jedná se o nejčastější karcinom hlavy a krku infiltrující nervy, s peri- a intraneurálním šířením až v 80 % případů (1). AdCC slinných žláz je charakteristický svým pomalým růstem, a přestože se histologicky jedná u většiny pacientů o dobře diferencovaný low-grade karcinom, jeho typickým projevem je prolongovaný klinický průběh trvající zpravidla roky, opakované recidivy, a variabilní riziko vzniku pozdních vzdálených metastáz. Klinický průběh onemocnění u pacientů postižených AdCC slinných žláz se často zdánlivě jeví indolentní, ale z dlouhodobého hlediska se jedná o jeden z nejagresivnějších a nejméně předvídatelných nádorů hlavy a krku. AdCC je také spojen s vysokou mortalitou (2). V individuálním případě je však velmi obtížné až nemožné predikovat klinický průběh nádorového onemocnění jen na základě histomorfologických nálezů.

Pro AdCC slinných žláz je typická chromozomální translokace t(6;9)(q22-23;p23-24), která generuje fúzní transkript *MYB-NFIB (3)*. *MYB–NFIB* fúzní onkogen byl poprvé popsán u AdCC Martou Persson a kol. v roce 2009 (4). Gen *MYB*, lokalizovaný v oblasti 6q22-23, kóduje transkripční faktor, který hraje zásadní roli v regulaci buněčné proliferace, diferenciace a apoptózy, a tím pravděpodobně i v tumorigenezi AdCC. *MYB* je vysoce exprimován v nezralých a proliferujících epiteliálních, endoteliálních a hematopoetických buňkách a naopak down-regulován v době, kdy se tyto buňky stanou diferencovanými (3, 5). Gen *NFIB* (Nuclear Factor I/B), lokalizovaný v oblasti 9p23-24, patří do rodiny dimerních DNA-vazebných proteinů fungujících jako buněčný transkripční faktor. Vznik fúzního onkogenu *MYB-NFIB* vede ke ztrátě 3´ konce *MYB* genu (od exonu 15 dále), místa, kde dochází k negativní regulaci *MYB* exprese (4). Následná zvýšená exprese fúzního transkriptu

a tím proteinu pak aktivuje transkripci MYB cílových genů, které mají zásadní roli v onkogenní transformaci. *MYB-NFIB* fúze nebo přestavba *MYB* genu, které vedou k jeho aktivaci, a tím ke zvýšené expresi *MYB–NFIB* fúzního proteinu nebo *MYB* onkoproteinu, byly dosud ze salivárních karcinomů i jiných karcinomů hlavy a krku prokázány pouze u AdCC (3, 6). Jedná se tudíž o charakteristický znak těchto maligních sialomů, který se dá využít jako diagnostický marker, s výhodou především u vzdálených metastáz. Zjištěné četnosti fúze *MYB-NFIB* u AdCC se však v různých studiích liší a závisí především na použité metodice (tab. 1).

V diagnostice AdCC se využívají imunohistochemické a molekulárně-genetické metody od relativně jednoduchých, jako jsou karyotypování, reverzně-transkripční PCR (RT-PCR), reverzně-transkripční PCR v reálném čase (Real-Time RT-PCR), fluorescenční in-situ hybridizace (FISH) až po ty komplexní, mezi které se řadí například komparativní genomová hybridizace na čipu (array comparative genomic hybridization - aCGH), či masivně paralelní sekvenování (Next Generation Sequencing - NGS).

IMUNOHISTOCHEMIE

V diagnostice AdCC lze využít jako nespecifickou skríningovou metodu detekci MYB proteinu (protilátka firmy AbCam v ředění 1:100), (obr. 1). Imunopozitivita na průkaz MYB proteinu se však vyskytuje i u některých AdCC případů, u kterých nebyl detekován zlom *MYB* genu, což naznačuje i jiné mechanismy aktivace *MYB* signální dráhy. Slabá až střední pozitivita barvení je také detekována až u 14 % jiných typů salivárních nádorů, což, na rozdíl od molekulárně-genetických technik, snižuje specifitu metody (7-9).

REVERZNĚ-TRANSKRIPČNÍ PCR

K detekci přítomnosti fúzního transkriptu v cDNA (reverzně přepsaná RNA) je využívána RT-PCR. Jedná se o metodu, kdy pomocí PCR za použití kombinace primerů nasedajících k jednomu i druhému fúznímu partnerovi dochází v přítomnosti fúzního transkriptu k jeho amplifikaci a tím možnosti jeho vizualizace, tj. detekce pomocí elektroforézy (obr. 2) (4). Vzhledem k variabilitě zlomových míst genů *MYB* a *NFIB* a faktu, že většina identifikovaných AdCC je dostupná ve formě parafinových bloků obsahujících více či méně degradovanou nukleovou kyselinu, je tato metoda zatížena rizikem falešně negativních výsledků. Studie provedená za použití této techniky detekovala přítomnost *MYB-NFIB* fúzního transkriptu v cca 30 % AdCC (10), což je výrazně méně než v případě detekce pomocí FISH metody (tab. 1).

Variantu RT-PCR, tzv. Real Time RT-PCR lze využít k relativní kvantifikaci exprese mRNA genu *MYB*. Pomocí této metody bylo zjištěno, že overexprese *MYB* mRNA byla detekována u většiny případů AdCC (89%) s tím, že u případů pozitivních na fúzi *MYB-NFIB* je tato overexprese signifikantně vyšší, než u případů bez této translokace (8, 10).

FLUORESCENČNÍ IN-SITU HYBRIDIZACE

V současnosti nejčastěji využívanou metodou v diagnostice AdCC je FISH analýza cílená na translokaci t(6;9)(q22-23;p23-24). Oproti konvenčním RT-PCR metodám není třeba znát přesnou nukleotidovou pozici zlomových míst, neboť FISH próba, zahrnující kompletní sekvenci studovaných genů a přilehlých oblastí, obsáhne celé široké spektrum možných aberací. Jako sondy se dříve hojně využívaly bakteriální arteficiální chromosomy (BAC). Jejich nevýhodou byly velmi často slabé signály na hůře fixovaném materiálu. V současnosti je dosahováno lepších výsledků s použitím polynukleotidových sond certifikovaných pro in-

vitro diagnostiku či oligonukleotidových necertifikovaných sond. Přítomnost fúzního genu pak lze prokazovat přímo - použitím kombinované fúzní sondy (jedna část sondy je cílena na *MYB* gen a druhá na gen *NFIB*) či nepřímo - detekcí zlomů jednotlivých zúčastněných genů s použitím tzv. break-apart sond (obr. 3).

Vedle analýzy translokace *MYB-NFIB* lze FISH použít i ke studiu dalších změn nalezených v AdCC, jako jsou např. numerické aberace genů. Takto byly popsány například relativně raritní amplifikace genu *KIT* (9) a genu *CCND1* (12).

Výše zmíněné metody jsou většinou cílené na jednu konkrétní oblast (například na fúzi *MYB-NFIB*). K detailnějšímu studiu nádorů je nutné využití komplexnějších analýz.

ARRAY-KOMPARATIVNÍ GENOMOVÁ HYBRIDIZACE

V případě studia početních chromosomálních změn je metodou volby komparativní genomová hybridizace na čipu založená na kompetitivní hybridizaci různě fluorescenčně značené (např. Cy3 a Cy5) nádorové a nenádorové DNA jednoho vzorku na čipu, který obsahuje obvykle 25-70 nt dlouhé oligonukleotidy (sondy) se známou přesnou genomickou lokalizací. Po hybridizaci je čip skenován pro zjištění intensit fluorescencí, kdy z případné převahy intenzity konkrétní barvy lze usuzovat na zisk nebo ztráty jednotlivých regionů korespondujících k daným sondám (13).

V práci Bernheima a kol. (14) byly pomocí aCGH detekovány rekurentní numerické aberace u bronchiálních a salivárních AdCC. Šlo o parciální ztráty v oblastech 1p35, 6q22-25, 8q12-13, 9p21, 12q12-13, 17p11-13 a zisky (gain) v oblastech 7p15.2, 17q21-25, 22q11-13. Do minimálních oblastí vykazujících deleci se řadily oblasti obsahující tumor-supresorové geny *CDKN2A*/*CDKN2B*, *TP53* a *LIMA1*. Minimální oblast s amplifikací byla oblast HOXA

genového clusteru (14). V jiných studiích však byla nalezena řada dalších změn v genomu (tab. 2).

EXPRESNÍ ANALÝZA

Komplexnější alternativou k měření exprese pomocí Real-Time RT-PCR je cDNA expresní čip schopný analýzy míry exprese mRNA až celého transkriptomu. Jde o variantu aCGH, kdy jsou na čip, obsahující oligonukleotidy z kódujících oblastí genomu, nahybridizovány fluorescenčně značené cDNA tumoru a zdravé tkáně k detekci rozdílů exprese (15). Touto metodou byla u AdCC například potvrzena zvýšená exprese genu *SOX10* (16, 17) a obecně upregulace genů ze SOX, NOTCH a WNT genových rodin (18).

MASIVNĚ PARALELNÍ SEKVENOVÁNÍ

V současnosti zřejmě nejkomplexnější metodou s nejvyšší informační výtěžností je masivně paralelní sekvenování nebo také sekvenování nové generace (anglicky next-generation sequencing – NGS).

NGS je schopna nejen prosté analýzy sekvencí nukleotidů v kompletním genomu či jeho vybrané části, ale může detekovat i případné strukturální varianty. Tímto v sobě zahrnuje mimo jiné i jistou náhradu aCGH, Real-Time RT-PCR či expresních arrayí. V případě celogenomového či RNA (transkriptomového) sekvenování je izolována DNA či RNA, která se přepíše do cDNA. Takto připravená DNA je pak různými metodami fragmentována na kratší úseky vhodné pro další zpracování. U cíleného sekvenování vybraných částí genomu či transkriptomu se po izolaci DNA či RNA (přepsané do cDNA) nejprve vychytávají hybridizací či obohacují amplifikací konkrétní oblasti zájmů. Pak již, pro oba přístupy

společně, následuje ligace adapterů a amplifikace produktu s použitím primerů nasedajících ke komplementárním sekvencím na adapterech. Po přečištění amplifikátu je vzniklý produkt – knihovna připraven k vlastnímu sekvenování a následně k analýze dat. V současné době jsou nejrozšířenějšími postupy „Sequence-by-synthesis" metody využívající fluorescenční značení a metody využívající analýzu změny pH (19, 20).

NGS metody se také významně zapsaly do molekulární charakterizace AdCC. V roce 2016 byl celogenomovým sekvenováním odhalen gen *MYBL1* jako alternativní fúzní partner *NFIB* u 5 z 12 *MYB-NFIB* negativních případů (21). Přibližně ve stejné době pak Brayer a kol. získali obdobnou informaci pomocí RNA sekvenování (22). Mimo to bylo těmito skupinami identifikováno několik nových vzácně se vyskytujících fúzí – genů *YTHDF3* a *RAD51B* s *MYBL1* genem, dále genů *XRCC4*, *NKAIN2*, *PTPRD* a *AIG1* genů s genem *NFIB*.

Tyto studie, stejně jako některé další, také potvrdily nízkou frekvenci genových mutací (substitucí, krátkých delecí, inzercí apod.) u AdCC. Pokud již byly mutace nalezeny, jako ve studii Stephens a kol. (23), zasahovaly především geny z NOTCH signální dráhy. Příkladem je gen *SPEN* mutovaný u 20,8 % pacientů. Gen *SPEN* je lokalizovaný na lokusu 1p36. Kóduje represor transkripce s RNA SPOC (Spen paralog and ortholog C-terminal) vazebnými doménami, regulující především NOTCH signální dráhu. Všechny nalezené mutace vyústily ve zkrácený protein s chybějící regulační SPOC doménou. Ve stejné studii byla v 8,3 % případů také identifikována aktivující mutace *FGFR2* analogická k mutacím nalezeným u ovariálních a endometriálních nádorů, poukazující na možnosti léčebného využití u této podskupiny pacientů (23). Ve studii Ho a kol. (24) byly použitím kombinace celogenomového a exomového sekvenování na kohortě 60 případů detekovány mutace zasahující chromatin remodelující geny, dále i geny z FGF/IGF/PI3K, PKA a NOTCH signálních drah. V malém

procentu případů negativních na *MYB-NFIB* fúzi pak byly pozorovány pravděpodobně aktivující mutace genu *MYB* (24).

Expresní studie využívající jak čipovou, tak NGS technologii přinesly další vhled do karcinogeneze AdCC. Prokázaly například, že u tumorů s fúzemi *MYB-NFIB* a *MYBL1-NFIB* nejsou signifikantní rozdíly v expresích analyzovaných genů. Naproti tomu, klastrová analýza expresních profilů odlišila vzorky s translokacemi zasahujícími exon 11 nebo vyšší v *MYB*, popř. *MYBL1* genu od vzorků s translokacemi zasahujícími exony 8 nebo 9 těchto genů (21). Bell a kol. (25) pak zkoumali transkriptom AdCC se zaměřením na rozdíly mezi epiteliálně (E-AdCC) a myoepiteliálně (M-AdCC) dominantními AdCC. Nalezli 430 transkriptů specifických pro E-AdCC, 392 pro M-AdCC a 424 transkriptů, které byly společné pro oba typy. Jejich detailní analýza pak ukázala na možné použití *DLX-6* genu jako biomarkeru pro E-AdCC a *KRT16*, *SOX11* a *MYB* genů pro M-AdCC (25).

METODY PRO DETEKCI METYLACÍ PROMOTORŮ GENŮ

Výše zmíněné studie se zabývaly strukturou vlastní nukleové kyseliny, popř. mírou její exprese. Významnou funkci v karcinogenezi má však též epigenetika, tj. ovlivnění exprese genů beze změny nukleotidové sekvence. Toto se na úrovni DNA děje nejčastěji prostřednictvím metylací promotorových oblastí genů vyúsťujících v potlačení exprese daných genů a je tedy logicky dalším předmětem zájmu při charakterizaci nádorových onemocnění.

 Metylační status promotorů genů lze zjišťovat řadou odlišných způsobů. Nejčastěji používaným způsobem je metylačně sensitivní PCR, při které se metylované cytosiny v DNA nejprve konvertují bisulfidovou reakcí na uracil a takto konvertovaný templát je pak amplifikován pomocí PCR za použití primerů specifických jak k metylované tak

nemetylované sekvenci (tzv. metylačně-specifická PCR – MSP). V pozitivním případě vzniká v reakci obsahující primery pro metylovaný promotor elektroforeticky či fluorescenčně detekovatelný produkt amplifikace.

Maruya a kol. (26) pomocí MSP detekovali metylaci promotoru E-cadherinu (*CDH1*) u 70 % případů AdCC. V obdobné studii Zhang a kol. (27) identifikovali metylovaný promotor *CDH1* u 57% pacientů, zde však, na rozdíl od výše zmíněné studie, metylační status promotoru *CDH1* koreloval s pokročilejším stádiem tumoru a také perineurálním šířením AdCC. V dalších studiích využívajících MSP pak byla zjištěna zvýšená metylace promotorů genů *p16* u 49,1% (28) a 46,7% (29) pacientů, dále genů *RASSF1A* celkem u 33,8% pacientů, *DAPK* u 20,9%, *MGMT* u 5,8% (29, 30), *RARβ2* u 3,8% (30) a genu *RUNX3* u 75% pacientů, jehož nízká exprese korelovala s vyšší agresivitou AdCC (31). Ve studii Shao a kol. (32) byla studována metylace genu *MYB* s negativním výsledkem u všech 18-ti analyzovaných případů AdCC. V práci Tan a kol. (33) pak byla detekována hypometylace Aquaporinu-1 u 75,3 % AdCC pacientů, avšak nekorelující s klinickými parametry.

Další metodou, použitou ke studiu metylačního profilu AdCC byla Metylated CpG Island Amplification (MCIA), která je založena na štěpení DNA 2 různými metylačně sensitivními restrikčními enzymy s následnou amplifikací PCR. Nádorová a kontrolní DNA jsou poté označeny Cy3 a Cy5 a hybridizovány na čipu. Porovnáním intensity výsledných barev (princip aCGH) lze zjistit míru metylace daných promotorů.

Ve studiích jež používali MCIA metody pak bylo identifikováno 32 hypermetylovaných genů, mezi nimi např. *EN1*, *FOXE1*, *GBX2*, *FOXL1* a 7 hypometylovaných genů, jako např. *FBXO17*, *PHKG1*, *LOXL1*, *DOCK1* a *PARVG*. Nejvýznamnějším z těchto výsledků byla hypermetylace *EN1* – genu ovlivňujícím vývoj CNS, která koreluje se stádiem, lokalizací a klinickým chováním nádoru (34, 35).

ZÁVĚR

Na základě našich zkušeností s detekcí translokací *MYB-NFIB*, popř. *MYBL1-NFIB* lze říci, že především FISH analýza za použití break-apart a fúzních sond představuje spolehlivý diagnostický nástroj u jinak obtížně diagnostikovatelných AdCC různých tkání. Oproti tomu RT-PCR dává často falešně negativní výsledky kvůli využívání parafinových bločků a tím degradované RNA, či pro možný výskyt alternativních zlomových míst. Jako slibný prognostický marker AdCC se dle našich závěrů jeví delece lokusu 1p36, která výrazně koreluje s nižším přežíváním pacientů.

Adenoidně cystický karcinom je druhým nejčastějším maligním nádorem slinných žláz, je diagnosticky obtížný, neúprosně progredující a v mnoha případech fatálně končící nádor. Metody molekulární biologie, vedle histopatologie a imunoprofilu, významně pomáhají lepšímu pochopení vzniku, chování a vývoji tohoto onemocnění, což v budoucnu může vyústit v objev nové, účinnější léčby.

PODĚKOVÁNÍ

Prohlášení

Autor práce prohlašuje, že v souvislosti s tématem, vznikem a publikací tohoto článku není ve střetu zájmu a vznik ani publikace článku nebyly podpořeny žádnou farmaceutickou firmou. Toho prohlášení se týká i všech spoluautorů.

LITERATURA

1. **Amit M, Binenbaum Y, Trejo-Leider L, et al.** International collaborative validation of intraneural invasion as a prognostic marker in adenoid cystic carcinoma of the head and neck. *Head Neck* 2015; 37(7): 1038-1045.

2. **Stenam G, Licitra L, Said-Al-Naief N, van Zante A, Yarbrough WG.** Adenoid Cystic Carcinoma. In: El-Naggar AK, Chan JKC, Grandis JR, Takata T, Slootweg PJ, eds. World Health Organization (WHO) Classification of Head and Neck Tumours. (4th ed). Lyon, France: IARC Press; 2017: 164-165.

3. **Stenman G.** Fusion oncogenes in salivary gland tumors: molecular and clinical consequences. *Head Neck Pathol* 2013; 7 Suppl 1: S12-19.

4. **Persson M, Andrén Y, Mark J, Horlings HM, Persson F, Stenman G.** Recurrent fusion of MYB and NFIB transcription factor genes in carcinomas of the breast and head and neck. *Proc Natl Acad Sci U S A* 2009; 106(44): 18740-18744.

5. **Stenman G, Persson F, Andersson MK.** Diagnostic and therapeutic implications of new molecular biomarkers in salivary gland cancers. *Oral Oncol* 2014; 50(8): 683-690.

6. **Simpson RH, Skálová A, Di Palma S, Leivo I.** Recent advances in the diagnostic pathology of salivary carcinomas. *Virchows Arch* 2014; 465(4): 371-384.

7. **West RB, Kong C, Clarke N, et al.** MYB expression and translocation in adenoid cystic carcinomas and other salivary gland tumors with clinicopathologic correlation. *Am J Surg Pathol* 2011; 35(1): 92-99.

8. **Brill LB, Kanner WA, Fehr A, et al.** Analysis of MYB expression and MYB-NFIB gene fusions in adenoid cystic carcinoma and other salivary neoplasms. *Mod Pathol* 2011; 24(9): 1169-1176.

9. **Rooney SL, Robinson RA.** Immunohistochemical expression of MYB in salivary gland basal cell adenocarcinoma and basal cell adenoma. J Oral Pathol Med. In press 2017.

10. **Mitani Y, Li J, Rao PH, et al.** Comprehensive analysis of the MYB-NFIB gene fusion in salivary adenoid cystic carcinoma: Incidence, variability, and clinicopathologic significance. *Clin Cancer Res* 2010; 16(19): 4722-4731.

11. **Freier K, Flechtenmacher C, Walch A, et al.** Differential KIT expression in histological subtypes of adenoid cystic carcinoma (ACC) of the salivary gland. *Oral Oncol* 2005; 41(9): 934-939.

12. **Greer RO, Said S, Shroyer KR, Marileila VG, Weed SA.** Overexpression of cyclin D1 and cortactin is primarily independent of gene amplification in salivary gland adenoid cystic carcinoma. *Oral Oncol* 2007; 43(8): 735-741.

13. **Szuhai K, Vermeer M.** Microarray Techniques to Analyze Copy-Number Alterations in Genomic DNA: Array Comparative Genomic Hybridization and Single-Nucleotide Polymorphism Array. *J Invest Dermatol* 2015; 135(10): e37.doi:10.1038/jid.2015.308

14. **Bernheim A, Toujani S, Saulnier P, et al.** High-resolution array comparative genomic hybridization analysis of human bronchial and salivary adenoid cystic carcinoma. *Lab Invest* 2008; 88(5): 464-473.

15. **Ylstra B, van den Ijssel P, Carvalho B, Brakenhoff RH, Meijer GA.** BAC to the future! or oligonucleotides: a perspective for micro array comparative genomic hybridization (array CGH). *Nucleic Acids Res* 2006; 34(2): 445-450.

16. **Ohtomo R, Mori T, Shibata S, et al.** SOX10 is a novel marker of acinus and intercalated duct differentiation in salivary gland tumors: a clue to the histogenesis for tumor diagnosis. *Mod Pathol* 2013; 26(8): 1041-1050.

17. **Ivanov SV, Panaccione A, Nonaka D, et al.** Diagnostic SOX10 gene signatures in salivary adenoid cystic and breast basal-like carcinomas. *Br J Cancer* 2013; 109(2): 444-451.

18. **Chen W, Zhang HL, Shao XJ, et al.** Gene expression profile of salivary adenoid cystic carcinoma associated with perineural invasion. *Tohoku J Exp Med* 2007; 212(3): 319-334.

19. **Ambardar S, Gupta R, Trakroo D, Lal R, Vakhlu J.** High Throughput Sequencing: An Overview of Sequencing Chemistry. *Indian J Microbiol* 2016; 56(4): 394-404.

20. **Apaga DL, Dennis SE, Salvador JM, Calacal GC, De Ungria MC.** Comparison of Two Massively Parallel Sequencing Platforms using 83 Single Nucleotide Polymorphisms for Human Identification. *Sci Rep* 2017; 7(1): 398.

21. **Mitani Y, Liu B, Rao PH, et al.** Novel MYBL1 Gene Rearrangements with Recurrent MYBL1-NFIB Fusions in Salivary Adenoid Cystic Carcinomas Lacking t(6;9) Translocations. *Clin Cancer Res* 2016; 22(3): 725-733.

22. **Brayer KJ, Frerich CA, Kang H, Ness SA.** Recurrent Fusions in MYB and MYBL1 Define a Common, Transcription Factor-Driven Oncogenic Pathway in Salivary Gland Adenoid Cystic Carcinoma. *Cancer Discov* 2016; 6(2): 176-187.

23. **Stephens PJ, Davies HR, Mitani Y, et al.** Whole exome sequencing of adenoid cystic carcinoma. *J Clin Invest* 2013; 123(7): 2965-2968.

24. **Ho AS, Kannan K, Roy DM, et al.** The mutational landscape of adenoid cystic carcinoma. *Nat Genet* 2013; 45(7): 791-798.

25. **Bell D, Bell AH, Bondaruk J, Hanna EY, Weber RS.** In-depth characterization of the salivary adenoid cystic carcinoma transcriptome with emphasis on dominant cell type. *Cancer* 2016; 122(10): 1513-1522.

26. **Maruya S, Kurotaki H, Wada R, Saku T, Shinkawa H, Yagihashi S.** Promoter methylation and protein expression of the E-cadherin gene in the clinicopathologic assessment of adenoid cystic carcinoma. *Mod Pathol* 2004; 17(6): 637-645.

27. **Zhang CY, Mao L, Li L, et al.** Promoter methylation as a common mechanism for inactivating E-cadherin in human salivary gland adenoid cystic carcinoma. *Cancer* 2007; 110(1): 87-95.

28. **Guo XL, Sun SZ, Wei FC.** [Mechanisms of p16 gene inactivation salivary adenoid cystic carcinoma]. *Hua Xi Kou Qiang Yi Xue Za Zhi* 2005; 23(5): 418-420.

29. **Li J, El-Naggar A, Mao L.** Promoter methylation of p16INK4a, RASSF1A, and DAPK is frequent in salivary adenoid cystic carcinoma. *Cancer* 2005; 104(4): 771-776.

30. **Williams MD, Chakravarti N, Kies MS, et al.** Implications of methylation patterns of cancer genes in salivary gland tumors. *Clin Cancer Res* 2006; 12(24): 7353-7358.

31. **Sasahira T, Kurihara M, Yamamoto K, Bhawal UK, Kirita T, Kuniyasu H.** Downregulation of runt-related transcription factor 3 associated with poor prognosis of adenoid cystic and mucoepidermoid carcinomas of the salivary gland. *Cancer Sci* 2011; 102(2): 492-497.

32. **Shao C, Bai W, Junn JC, et al.** Evaluation of MYB promoter methylation in salivary adenoid cystic carcinoma. *Oral Oncol* 2011; 47(4): 251-255.

33. **Tan M, Shao C, Bishop JA, et al.** Aquaporin-1 promoter hypermethylation is associated with improved prognosis in salivary gland adenoid cystic carcinoma. *Otolaryngol Head Neck Surg* 2014; 150(5): 801-807.

34. **Bell A, Bell D, Weber RS, El-Naggar AK.** CpG island methylation profiling in human salivary gland adenoid cystic carcinoma. *Cancer* 2011; 117(13): 2898-2909.

35. **Bell D, Bell A, Roberts D, Weber RS, El-Naggar AK.** Developmental transcription factor EN1--a novel biomarker in human salivary gland adenoid cystic carcinoma. *Cancer* 2012; 118(5): 1288-1292.

36. **Nordkvist A, Mark J, Gustafsson H, Bang G, Stenman G.** Non-random chromosome rearrangements in adenoid cystic carcinoma of the salivary glands. *Genes Chromosomes Cancer* 1994; 10(2): 115-121.

37. **Mitani Y, Rao PH, Futreal PA, et al.** Novel chromosomal rearrangements and break points at the t(6;9) in salivary adenoid cystic carcinoma: association with MYB-NFIB

chimeric fusion, MYB expression, and clinical outcome. *Clin Cancer Res* 2011; 17(22): 7003-7014.

38. **Hudson JB, Collins BT.** MYB gene abnormalities t(6;9) in adenoid cystic carcinoma fine-needle aspiration biopsy using fluorescence in situ hybridization. *Arch Pathol Lab Med* 2014; 138(3): 403-409.

39. **Rettig EM, Tan M, Ling S, et al.** MYB rearrangement and clinicopathologic characteristics in head and neck adenoid cystic carcinoma. *Laryngoscope* 2015; 125(9): E292-299.

40. **Tian Z, Li L, Zhang CY, Gu T, Li J.** Differences in MYB expression and gene abnormalities further confirm that salivary cribriform basal cell tumors and adenoid cystic carcinoma are two distinct tumor entities. *J Oral Pathol Med* 2016; 45(9): 698-703.

41. **Argyris PP, Wetzel SL, Greipp P, et al.** Clinical utility of myb rearrangement detection and p63/p40 immunophenotyping in the diagnosis of adenoid cystic carcinoma of minor salivary glands: a pilot study. *Oral Surg Oral Med Oral Pathol Oral Radiol* 2016; 121(3): 282-289.

42. **Hauer L, Skálová A, Šteiner P, et al.** Adenoidně cystický karcinom slinných žláz. Soubor 27 pacientů. *Česká Stomatologie* 2016; 116(3): 57 - 65.

43. **Rao PH, Roberts D, Zhao YJ, et al.** Deletion of 1p32-p36 is the most frequent genetic change and poor prognostic marker in adenoid cystic carcinoma of the salivary glands. *Clin Cancer Res* 2008; 14(16): 5181-5187.

44. **Oga A, Uchida K, Nakao M, et al.** Loss of 6q or 8p23 is associated with the total number of DNA copy number aberrations in adenoid cystic carcinoma. *Oncol Rep* 2011; 26(6): 1393-1398.

45. **Freier K, Flechtenmacher C, Walch A, et al.** Copy number gains on 22q13 in adenoid cystic carcinoma of the salivary gland revealed by comparative genomic hybridization and tissue microarray analysis. *Cancer Genet Cytogenet* 2005; 159(1): 89-95.

Tabulka 1: Počty detekovaných fúzí *MYB-NFIB* v různých studiích použitím FISH a/nebo pomocí RT-PCR

Publikace	Primární materiál	FISH	RT-PCR
Nordkvist et al. (36)	Kult.	2/10 (20 %)	NP
Persson et al. (4)	NFT	(6/6) (100 %)	11/11 (100 %)
Mitani et al. (37)	NFT	34/82 (41 %)	21/82 (26 %)
Brill et al. (8)	FT	NP	14/32 (44 %)
Brill et al. (8)	NFT	NP	25/29 (86 %)
Ho et al. (24)	FT	34/60 (57 %)	NP
Hudson et al. (38)	NFT	4/10 (40 %) [ba]	NP
Rettig et al. (39)	FT	59/91 (65 %) [ba]	NP
Tian et al. (40)	FT	9/20 (45 %) [ba]	NP
Argyris et al. (41)	FT	5/5 (100 %)	NP
Hauer et al. (42)	FT	19/24 (79 %)	5/18 (28 %) (nepublikováno)

Vysvětlivky: [ba] – provedena pouze MYB break-apart sonda, FT – fixovaná tkáň, Kult. – kultivát primární tkáně, NFT – nefixovaná tkáň, NP – neprovedeno.

**Tabulka 2**: Nalezené chromosomální aberace v různých studiích pomocí aCGH.

Publikace	počet vzorků ve studii	Lokus se ztrátou (četnost v %)	Lokus se ziskem (četnost v %)
Rao et al. (43)	53	1p32-36 (44 %)	chr.8 (38 %)
		6q23-27 (32 %)	chr.18 (11 %)
		12q12-14 (18 %)	
Oga et al. (44)	10	6q25 (80 %)	6p (30 %)
		8p23 (50 %)	6q23 (30 %)
			8p23 (30 %)
			22q12-3 (30 %)
Freier et al. (45)	27	6q (22 %)	22q13 (33 %)
			16p (26 %)
			17q (15 %)

**Obrázek 1:** A. Typická histologická struktura AdCC s převahou kribriformních a pseudocystických struktur, HE barvení, zvětšení 200x. B. Imunohistochemická exprese MYB s nukleární pozitivitou, zvětšení 200x.

Obrázek 2: Výsledek sekvenace amplifikačního produktu RT-PCR k průkazu fúzního transkriptu *MYB-NFIB*.

Obrázek 3: Ukázka pozitivního FISH preparátu s A. *MYB* break-apart sondou a B. *MYB-NFIB* Dual-Fusion sondou, zvětšení 1000x.

A. Negativní alela je reprezentována složeným oranžovo-žluto-zeleným signálem, zlom je reprezentován separátním oranžovým a zeleným signálem. B. Zdravé alely jsou reprezentovány separátními oranžovými a zelenými signály, fúze je reprezentována složeným oranžovo-žluto-zeleným signálem (viz. žluté šipky).
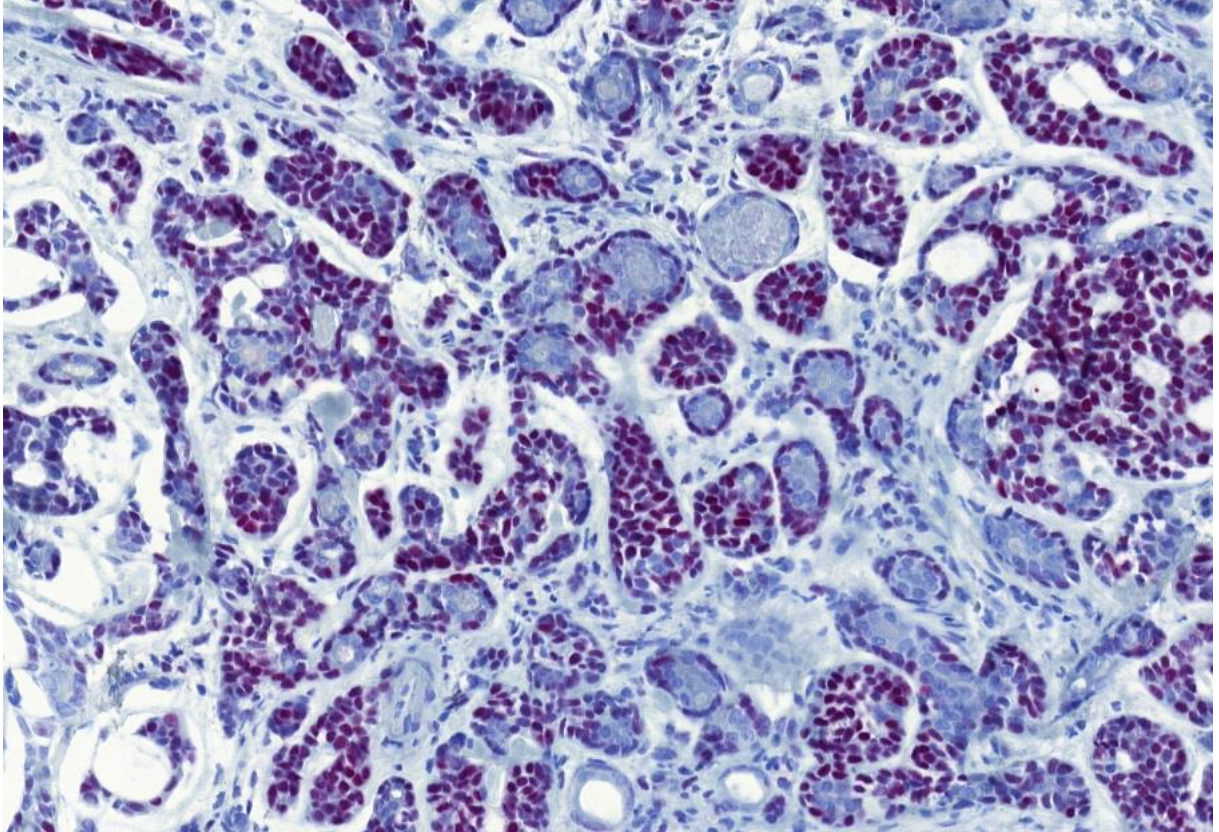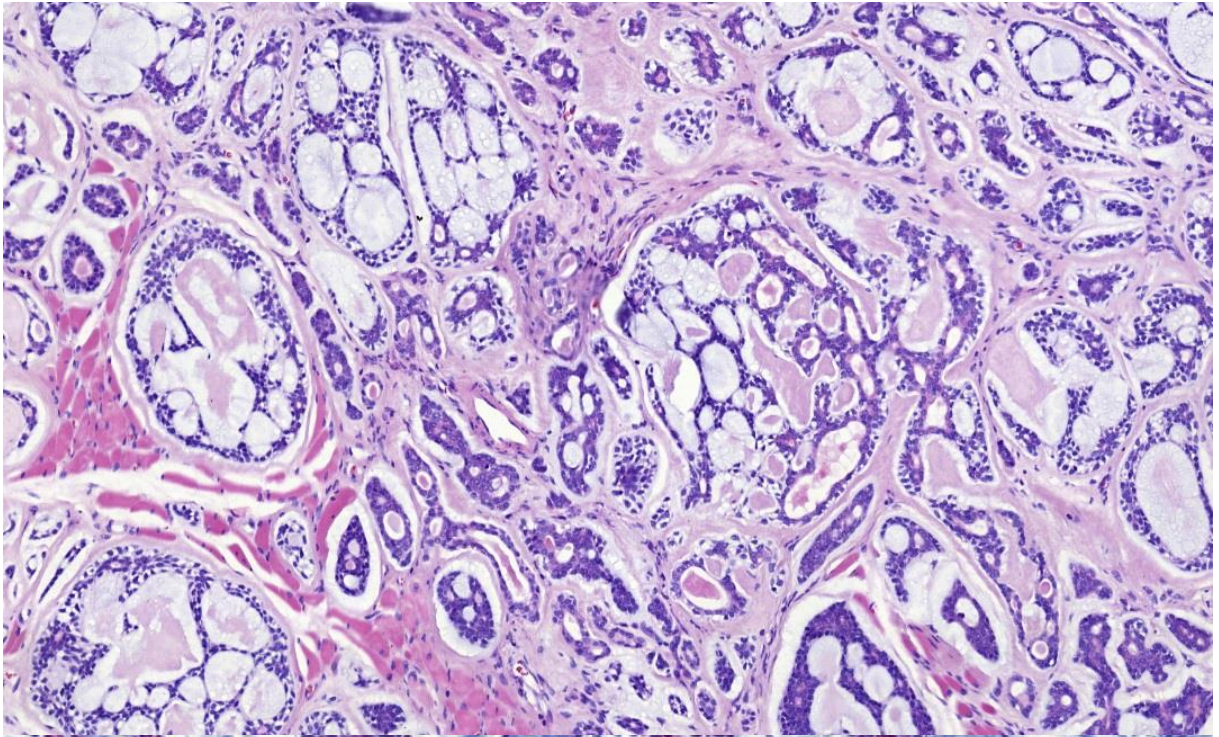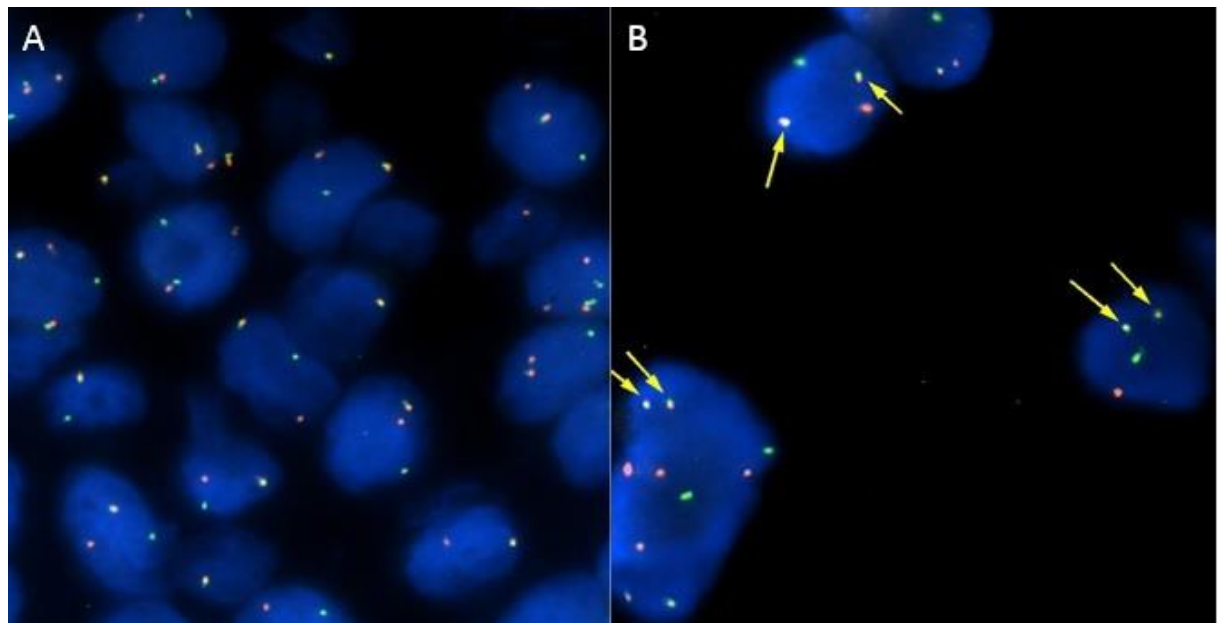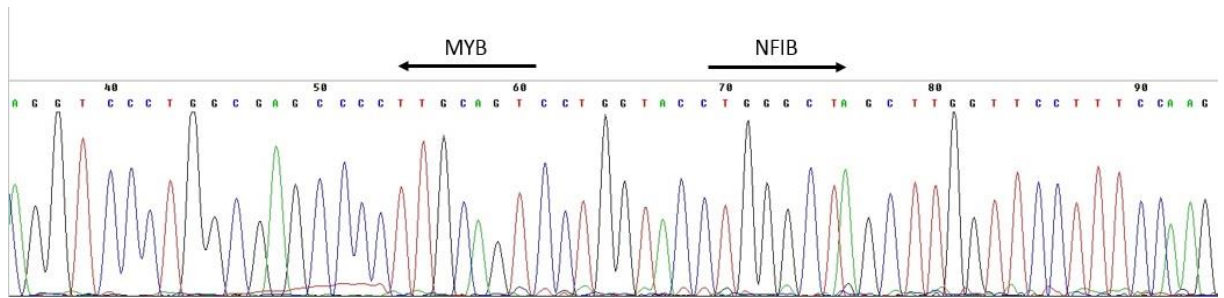
4. část - Světlobuněčný myoepiteliální karcinom slinných žláz vykazující přestavbu *EWSR1*: Molekulární analýza 94 karcinomů slinných žláz s nápadnou světlobuněčnou komponentou

V této studii „*Clear Cell Myoepithelial Carcinoma of Salivary Glands Showing EWSR1 Rearrangement: Molecular Analysis of 94 Salivary Gland Carcinomas With Prominent Clear Cell Component*" [28] byl metodou FISH studován zlom genu *EWSR1* u 94 světlobuněčných myoepiteliálních salivárních karcinomů. *EWSR1* gen, lokalizovaný na 22q12.2, kóduje RNA vazebný protein účastnící se různých buněčných procesů, včetně regulace genové exprese, buněčné signalizace, sestřihu a transportu RNA [57]. Jeho zlom byl prvně popsaný u Ewingova sarkomu [58, 59], nicméně bylo zjištěno, že fúzuje u více typů tumorů s různými fúzními partnery, například s geny *FLI1*, *ERG*, *POU5F1*, *ETV1*, *ETV4*, *FEV*, *NFATc2* a *SMARCA5* [60-64], včetně fúzí s geny *ATF1* [5] a *POU5F1* [65] identifikovanými u salivárních karcinomů.

Náš soubor myoepiteliálních salivárních karcinomů vyšetřovaných na průkaz zlomu genu *EWSR1* zahrnoval 51 myoepiteliálních karcinomů de novo, 21 myoepiteliálních karcinomů vznikajících z pleomorfního karcinomu, 11 epiteliálních-myoepiteliálních karcinomů, 6 epiteliálních-myoepiteliálních karcinomů s přerůstáním solidní světlobuněčné myoepiteliální komponenty, 5 případů hyalinizujících světlobuněčných karcinomů malých slinných žláz, 10 myoepiteliálních karcinomů bez světlobuněčných změn a 12 benigních myoepiteliomů. Celkem u 25 případů světlobuněčných myoepiteliálních karcinomů byl metodou FISH detekován zlom *EWSR1* genu. *EWSR1-ATF1* fúzní onkogen není specifický, již dříve byla identická translokace popsána u hyalinizujícího světlobuněčného karcinomu malých slinných žláz [5] a u světlobuněčného odontogenního nádoru [66]. Naše práce ukázala, že průkaz přestavby genu *EWSR1* musí být interpretován vždy ve shodě s histomorfologií a imunoprofilem nádoru.

Clear Cell Myoepithelial Carcinoma of Salivary Glands Showing *EWSR1* Rearrangement

Molecular Analysis of 94 Salivary Gland Carcinomas With Prominent Clear Cell Component

Alena Skálová, MD, PhD,* Ilan Weinreb, MD,† Martin Hyrcza, MD, PhD,‡
Roderick H.W. Simpson, MD,§ Jan Laco, MD, PhD,‖ Abbas Agaimy, MD,¶ Marina Vazmitel,
MD, PhD,# Hanna Majewska, MD, PhD,** Tomas Vanecek, RNDr, PhD,†† Peter Talarčik,
MD,‡‡ Spomenka Manajlovic, MD, PhD,§§ Simona N. Losito, MD,‖‖ Petr Šteiner, MSc,††
Adela Klimkova, MSc,†† and Michal Michal, MD*

Abstract: This study examines the presence of the *EWSR1* rearrangement in a variety of clear cell salivary gland carcinomas with myoepithelial differentiation. A total of 94 salivary gland carcinomas with a prominent clear cell component included 51 cases of clear cell myoepithelial carcinomas de novo (CCMC), 21 cases of CCMCs ex pleomorphic adenoma (CCMCexPA), 11 cases of epithelial-myoepithelial carcinoma (EMC), 6 cases of EMC with solid clear cell overgrowth, and 5 cases of hyalinizing clear cell carcinoma of minor salivary glands. In addition, 10 cases of myoepithelial carcinomas devoid of clear cell change and 12 cases of benign myoepithelioma were included as well. All the tumors in this spectrum were reviewed, reclassified, and tested by fluorescence in situ hybridization (FISH) for the

EWSR1 rearrangement using the Probe Vysis *EWSR1* Break Apart FISH Probe Kit. The *EWSR1* rearrangement was detected in 20 of 51 (39%) cases of CCMC, in 5 of 21 (24%) cases of CCMCexPA, in 1 of 11 (9%) cases of EMC, and in 4 of 5 (80%) cases of hyalinizing clear cell carcinoma. The 25 *EWSR1*-rearranged CCMCs and CCMCexPAs shared similar histomorphology. They were arranged in nodules composed of compact nests of large polyhedral cells with abundant clear cytoplasm. Necrosis, areas of squamous metaplasia, and hyalinization were frequent features. Immunohistochemically, the tumors expressed p63 (96%), cytokeratin CK14 (96%), and S100 protein (88%). MIB1 index varied from 10% to 100%, with most cases in the 20% to 40% range. Clinical follow-up information was available in 21 cases (84%) and ranged from 3 months to 15 years (mean 5.2 y); 4 patients were lost to follow-up. Ten patients are alive with no evidence of recurrent or metastatic disease in the follow-up period from 3 months to 15 years (mean 5 y), 3 patients are alive with recurrent and metastatic disease, and 8 died of disseminated cancer 9 months to 16 years after diagnosis (mean 6 y). Lymph node metastasis appeared in 5 patients within 5 months to 4 years after diagnosis (mean 22 mo), distant metastases were noted in 7 patients with invasion of orbit (2 cases), and in 1 case each metastasis to the neck soft tissues, liver, lungs, mediastinum, and thoracic vertebra was noted. We describe for the first time *EWSR1* gene rearrangement in a subset of myoepithelial carcinomas arising in minor and major salivary glands. The *EWSR1*-rearranged CCMC represents a distinctive aggressive variant composed predominantly of clear cells with frequent necrosis. Most *EWSR1*-rearranged CCMCs of salivary glands are characterized by poor clinical outcomes.

Key Words: salivary gland, clear cell myoepithelial carcinoma, *EWSR1* rearrangement

(Am J Surg Pathol 2015;39:338–348)

The Ewing sarcoma breakpoint region 1 *(EWSR1)* is translocated in many sarcomas. As is apparent from the name, rearrangements involving the *EWSR1* region

were first described in Ewing sarcoma.[1,2] However, there is a growing body of evidence that *EWSR1* is a promiscuous gene, with rearrangements involving a number of partner genes, such as *POU5F1, PBX1, ATF1, CREB1,* etc. present in a number of tumor entities. *EWSR1* translocations have been identified in such morphologically distinct soft tissue tumors as extraskeletal myxoid chondrosarcoma, desmoplastic small round cell tumor, clear cell sarcoma, angiomatoid malignant fibrous histiocytoma, clear cell sarcoma–like gastrointestinal tumor, and soft tissue myoepithelial tumors (SMETs), etc.[3–6]

Rarely, *EWSR1* rearrangements were also identified in nonmesenchymal tumors. Antonescu et al[7] have recently identified a consistent *EWSR1-ATF1* fusion in hyalinizing clear cell carcinoma (HCCC) of minor salivary glands. Similar *EWSR1* and *ATF1* rearrangements have been also identified in clear cell odontogenic carcinoma providing molecular evidence of link between HCCC and clear cell odontogenic carcinoma.[8] More recently, *EWSR1* rearrangements were described in SMET but not in salivary gland carcinomas with myoepithelial phenotype.[9] We decided to investigate whether *EWSR1* rearrangement might be present in the rare clear cell variant of salivary myoepithelial carcinoma we have defined earlier.[10]

In this study we have undertaken a systematic analysis of *EWSR1* rearrangements using FISH in a large spectrum of myoepithelial tumors of salivary glands with clear cell morphology.

MATERIALS AND METHODS

Histopathologic Diagnosis

Cases were retrieved from our consultation files (A.S. and M.M.) by searching the following key words "clear cell myoepithelial carcinoma," "hyalinizing clear cell carcinoma," "epithelial-myoepithelial carcinoma," as well as all the tumors of salivary glands that contained combination of words "clear cell" and "myoepithelial carcinoma." Ninety-four cases of salivary gland carcinomas with available tissue for molecular analysis were retrieved from surgical pathology and consultation files of the authors (A.S., M.M., I.W., R.H.W.S., M.V., J.L., S.M., H.M., and A.A.). Hematoxylin-eosin and immunohistochemistry slides were retrieved for all cases. Minimum criteria for confirming histologic diagnosis of myoepithelial carcinoma included coexpression of cytokeratins (AE1/AE3, OSCAR, CAM5.2, CK14) and/or EMA together with S100 protein and/or other myoepithelial markers, such as smooth muscle actin, GFAP, calponin, p63, and CD10.

A total of 116 cases of salivary gland tumors were studied by FISH for the *EWSR1* rearrangement; these included HCCC (N = 5), myoepithelial carcinoma with predominant clear cell component (CCMC) (N = 51), clear cell myoepithelial carcinoma ex pleomorphic adenoma (CCMCexPA) (N = 21), epithelial-myoepithelial carcinoma (EMC) with solid myoepithelial clear cell overgrowth (N = 6), pure EMC (N = 11), non-CCMC

(N = 10), and benign myoepithelioma (N = 12). All the tumors in this spectrum were reviewed, reclassified if necessary (A.S. and M.H.) without the knowledge of FISH test results, and then tested by FISH for the *EWSR1* rearrangement using the Probe Vysis *EWSR1* Break Apart FISH Probe Kit.

For conventional microscopy, the excised tissues were fixed in formalin, routinely processed, embedded in paraffin, cut, and stained with hematoxylin-eosin.

For immunohistochemical studies, 4-μm-thick sections were cut from paraffin blocks, mounted on slides coated with 3-aminopropyltriethoxy-silane (Sigma, St Louis), deparaffinized in xylene, and rehydrated in descending grades (100% to 70%) of ethanol. Sections were then subjected to heat-induced epitope retrieval by immersion in a CC1 solution at pH 8, at 95°C. Endogenous peroxidase was blocked by a 5-minute treatment with 3% hydrogen peroxide in absolute methanol. The slides were then stained by immunostainer BenchMark ULTRA (Roche). The primary antibodies used are summarized in Table 1. The bound antibodies were visualized using the Histofine Simple Stain MAX PO (Multi) Universal Immuno-peroxidase Polymer, Anti-Mouse and Rabbit (Nichirei Biosciences Inc., Tokyo, Japan), and 3,3′-diaminobenzidine (Sigma) as chromogen. The slides were counterstained with Mayer hematoxylin. Appropriate positive and negative controls were used.

Clinical follow-up information was obtained from the patients, their physicians, or from referring pathologists.

FISH Testing

The 4-μm-thick formalin-fixed paraffin-embedded sections were placed onto a positively charged slide. Hematoxylin and eosin–stained slides were examined for determination of areas for cell counting. The unstained slides were routinely deparaffinized and incubated in the ×1 Target Retrieval Solution Citrate pH 6 (Dako, Glostrup, Denmark) for 40 minutes at 95°C and subsequently cooled for 20 minutes at room temperature in the same solution and washed in deionized water for 20 minutes. The slides were digested in protease solution with pepsin (0.5 mg/mL) (Sigma Aldrich) in 0.01 M HCl at 37°C for 15 minutes. The slides were then rinsed in deionized water for 5 minutes, dehydrated in a series of ethanol solution (70%, 85%, 96% for 2 min each), and air-dried. Probe Vysis EWSR1 Break Apart FISH Probe Kit (Abbott Molecular, IL) was mixed with water and LSI/WCP Hybridization buffer (Abbott) in a 1:2:7 ratio. Appropriate amounts of this probe mix were applied, covered with a glass cover slip and sealed with rubber cement. The slides were incubated in the ThermoBrite instrument (StatSpin/Iris Sample Processing, Westwood, MA) with codenaturation parameters 85°C for 8 minutes and hybridization parameters 37°C for 16 hours. Rubber cemented cover slips were then removed, and the slides were placed in posthybridization wash solution (2×SSC/0.3% NP-40) at 72°C for 2 minutes. The slides were air-dried in the dark, counterstained with 4′,6′-diamidino-2-phenylindole DAPI (Abbott), covered with slip and immediately examined.

TABLE 1. Antibodies Used for Immunohistochemical Study

Antibody Specificity	Clone	Dilution	Source
S100 protein	Polyclonal	1:2000	DakoCytomation
AE1-AE3	AE1-AE3 + PCK26	RTU	Ventana
Cytokeratin OSCAR	OSCAR	1:100	Covance
Cytokeratin CAM5.2	CAM5.2	RTU	Ventana
CK7	OV-TL 12/30	1:200	DakoCytomation
CK8	35 beta H11	RTU	DakoCytomation
CK19	RCK 108	1:200	DakoCytomation
CK18	DC10	RTU	DakoCytomation
CK14	NCL-LL002	1:40	Novocastra
CK5/6	D5/16B4	1:50	DakoCytomation
EMA	E29	1:400	DakoCytomation
SMA	1A4	1:1000	DakoCytomation
Muscle actin	HHF35	1:200	DakoCytomation
Ki-67	30-9	RTU	Ventana
P63	4A4	RTU	Ventana
Calponin	EP798y	RTU	Ventana
GFAP	polyclonal	RTU	DakoCytomation

EMA indicates epithelial membrane antigen; RTU, ready to use; SMA, smooth muscle actin.

FISH Interpretation

The specimens were examined with an Olympus BX51 fluorescence microscope using a × 100 objective and filter sets Triple Band Pass (DAPI/Green/Orange), Dual Band Pass (FITC/Orange), and Single Band Pass (Green or Orange). One hundred randomly selected non-overlapping tumor cell nuclei were counted. The presence of yellow (normal) or separated orange and green (chromosomal breakpoint) fluorescent signals was examined (Fig. 1). Positivity cutoff value was set to > 10% of all nuclei showing chromosomal breakpoint signals.[11]

RESULTS

FISH Findings

A total of 94 salivary gland tumors with prominent clear cell component and/or myoepithelial differentiation were analyzed for *EWSR1* gene break by FISH. The *EWSR1* rearrangement was detected in 20 of 51 (39%) cases of CCMC de novo, in 5 of 21 (24%) cases of CCMCexPA, in 1 of 11 (9%) cases of EMC, together 26 cases of myoepithelial-derived carcinomas with prominent clear cell change showed rearranged *EWSR1*. In addition, 4 of 5 HCCCs of minor salivary glands (80%) showed *EWSR1* gene rearrangement as well.

Intact *EWSR1* was noted in 46 cases of tumors with prominent clear cell component and/or myoepithelial differentiation, whereas in 17 cases DNA was not sufficient for analysis; namely 6 EMCs with solid overgrowth (4 negative, 2 nonanalyzable), 10 pure EMCs (4 negative, 6 nonanalyzable), and 47 cases of CCMC and CCMCexPA (38 negative, 9 nonanalyzable). In all 12 benign myoepitheliomas and 10 non-CCMCs, and in 1 single case of HCC, the *EWSR1* gene was intact.

Clinical Findings

The clinical and pathologic data of 25 *EWSR1*-positive CCMC cases are summarized in Table 2. The

patients included 15 female and 10 male individuals with age ranging from 33 to 87 years (mean 60.3 y). The majority of tumors were located in the parotid with a total of 14 cases (56%). The remaining tumors occurred in the palate (5), submandibular gland (3), sublingual gland (1), maxillary sinus (1), and lung (1). The tumors ranged in size from 1.0 to 9.0 cm (mean 4.5 cm).

The only 1 *EWSR1*-positive EMC displayed histologic features of conventional biphasic low-grade EMC with a prominent clear cell myoepithelial layer, and it was completely devoid of necrosis and squamous metaplasia.

Treatment and Follow-up Period

Data on treatment were available for all 25 patients. All tumors of the submandibular gland were treated by resection of the gland (N = 3). All 14 carcinomas of the parotid gland were removed surgically, in 5 patients by radical parotidectomy, in 5 cases by subtotal parotidectomy, and the other 4 patients underwent nonradical
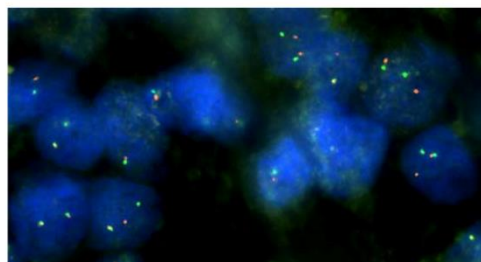

FIGURE 1. FISH analysis using EWSR1 dual-color, break apart probe. Visualization under Triple Band Pass filter. Yellow signals indicate intact *EWSR1* gene region, separated green and red signals represent rearranged *EWSR1* gene region. Several nuclei positive for *EWSR1* break are shown.

TABLE 2. Clinical and Pathologic Findings in 25 Cases of CCMC With *EWSR1* Rearrangement

Case	Sex/Age (y)	Site	Size (cm)	TNM Stage	Therapy	Outcome	Follow-up (y)	Margins	LVI	Perineural Invasion
1	F/51	Parotid	5×4×4.5	pT3pN1M0	SP, ND, RT	Recur (2 y) LN mts (2 y)	Alive with tu (5 y)		Yes	No
2	F/43	Palate	3.5×4.0×2.0	pT3N0M0	Excision, RT, CHT	1. recur (2 y), 2. Recur to orbit (3 y), tu progression (4 y), 3. recur to orbit (4 y), soft tissue mts (4 y)	Alive with tu (7 y)		No	No
3	M/60	Parotid	7.5×6.5×6.0	pT4a,N0M0	Excision, CP of recurrence, RT, CHT	Recur (4 mo), lung mts (12 mo)	DOD (14 mo)	Pos	Yes	Yes
4	F/35	Parotid	9×6×5	pT4aN1M1	RP, CHT	Recur (1 y), LN mts (1 y), mts liver (1 y)	DOD (3 y)		Yes	Yes
5	F/74	Parotid	4×3×2	pT2pN1M0	RP, ND, RT	NED	NED (5 y)		No	No
6	M/60	Palate	5×4×4	pT4bN0M0	PMax, CHT, RT	1. recur (11 mo), 2. recur (5 y) invasion of orbit, 3. multifocal recur (6 y) invasion of ethmoid sinus, nasal cavity	DOD (8 y)		No	No
7	F/67	Parotid	8×4×2.5	pT2cN0cM0	SP, CHT	NED	NED (12 y)	Neg	Yes	No
8	F/46	Palate	1.0×1.3×1.2	pT1cN0cM0	Surgery	NED	NED (10 y)	Neg	No	No
9	M/53	Parotid	1×1.5×1.2	pT1cN0cM0	Excision, RT	Recur (1 y)	DOD (3 y)	Pos	No	No
10	F/67	Parotid	4×5×3	pT3cN1cM0	SP,RT	NED	NED (15 y)		No	No
11	F/81	Parotid	3	pT2cN0cM0	SP	NA	NA	NA	No	No
12	F/34	Parotid	2.5	pT2cN0cM	SP	NA	NA	NA	No	No
13	F/67	Submand	12×8×7	pT4,pN1cM0	Excision of SG, refused RT, recur cured by radical excision + ND	Recur (3 y), LN mts (2 y)	NED (3 y) Lost of follow-up	Neg	Yes	Yes
14	F/67	Sublingual	2×0.8×0.5	pT1cN0cM0	Excision, refused RT	Recur (4 y),LN mts (4 y)	Alive with tu (5 y) Lost for follow-up	Pos	No	Yes
15	M/56	Parotid	1.5	pT1cN0pM1	Excision	Recur (10 y), mts mediastinum, Th skelet (13 y)	DOD (16 y)	Neg	No	No
16	M/73	Palate	10×5.5×5	pT3NxMx	BPMa	NA	NA	Pos	Yes	Yes
17	M/70	Palate	2	pT1NxMx	CL, RMa after 2. Recur, RT	1. Recur (6 y), 2. recur (9 y), 3. recur (10 y)	DOD (10 y)		No	No
18	F/55	Maxill.sinus	8	pT4bMxMx	RMa	NED	Alive NED (3 mo)	Pos	Yes	Yes
19	M/66	Lung	8×5×5.5	pT3N1M0, Pl0	Surgery	NED	Alive NED (14 mo)	Neg	Yes	No
20	F/87	Parotid	5.5×5×3.5	pT3N0M0	RP	NED	Alive NED (14 mo)	Pos	No	Yes
21	F/54	Submand	2.2×1.7×1.5	pT2N0M0	Excision	NED	Alive NED (11 mo)	Neg	No	No
22	F/33	Parotid	2.4×2×2	pT2pN1M0	Excision	NED	Alive NED (5 mo)	Neg	Yes	No
23	M/69	Parotid	2	pT1N0M0	Excision	Recur (5 y)	DOD (6 y 4 mo)	Pos	No	Yes
24	M/78	Parotid	2.5	pT3pN1M0	RP, RT	LN mets (5 mo), mts in floor of mouth and gingiva (50 mo)	DOD (9 mo)	Neg	Yes	Yes
25	M/63	Submand	5.6	pT3pN2cM0	Excision, RT	NA	NA	Neg	Yes	No

BPMa indicates bilateral partial maxillectomy; CHT, chemotherapy; CL, Caldwell-Luc procedure; DOD, dead of disease; F, female; LVI, lymphovascular invasion; M, male; NA, not available; ND, neck dissection; NED, no evidence of disease; Pl0, no infiltration of pleura; PMa, partial maxillectomy; RMa, radical maxillectomy; RP, radical parotidectomy; RT, radiotherapy; SP, subtotal parotidectomy (conservative, partial, superficial, lateral).
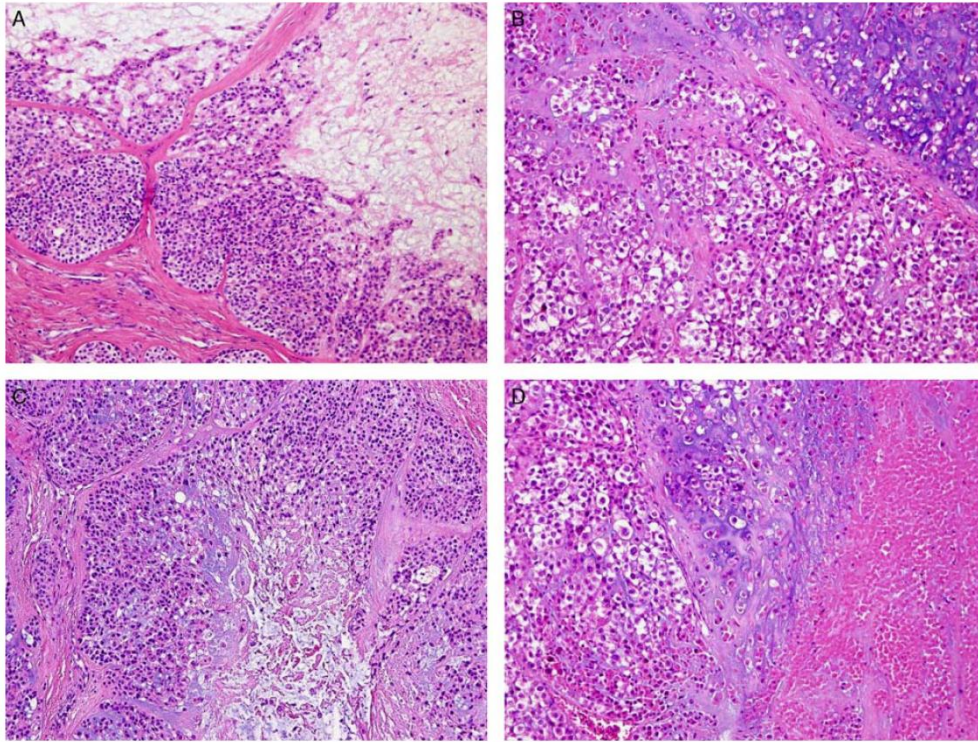
194

FIGURE 2. A, *EWSR1*-rearranged myoepithelial carcinomas are composed of compact nests of clear neoplastic cells divided by fibrous septa. B, Large polyhedral cells with abundant water-clear cytoplasm and focal necrotic islands are seen. Necrosis is a nearly universal feature, although its extent varies widely from large and irregularly shaped necrotic areas (C) to foci in the centers of tumor islands resembling comedo necrosis (D).

excision of the tumor. The patients with carcinoma of the palate were treated by partial maxillectomy (N = 2), by radical excision with clear margins (N = 2), and by the Caldwell-Luc procedure (N = 1), followed by radical maxillectomy after second recurrence of the tumor. One patient with CCMC located in the sublingual gland underwent simple nonradical excision, and the remaining 1 patient with CCMC arising in minor salivary glands of maxillary sinus underwent radical maxillectomy. Neck dissection was performed in 2 patients, 10 received radiotherapy postoperatively, and 5 patients were treated by adjuvant chemotherapy.

Clinical follow-up information was available in 21 cases (84%) and ranged from 3 months to 15 years (mean 5.2 y); 4 patients were lost to follow-up. Ten patients of 21 (48%) are alive with no evidence of recurrent or metastatic disease in the follow-up period from 3 months to 15 years (mean 5 y), 3 patients are alive with recurrent and metastatic disease (14%), and 8 died of disseminated cancer (38%) 9 months to 16 years after diagnosis (mean

6 y). Lymph node metastasis appeared in 5 patients (24%) within 5 months to 4 years after diagnosis (mean 22 mo), distant metastases occurred in 7 patients (33%) and involved the orbit (2 cases), and in 1 case each metastasis to the neck soft tissues, the liver, the lungs, the mediastinum, and the thoracic vertebra was noted.

In our series, a total of 47 cases of CCMC and CCMCexPA included 38 tumors with intact *EWSR1* and 9 nonanalyzable cases. Clinical follow-up data of patients with intact *EWSR1* were available in 35 of 38 cases (92%) and ranged from 1 to 14 years (mean 5.7 y); 3 patients were lost to follow-up. Seventeen patients of 35 (49%) are alive with no evidence of recurrent or metastatic disease, 14 patients are alive with recurrent and metastatic disease (40%), and 2 died of disseminated cancer (5.5%) 2 years after diagnosis. Two patients died of other causes without evidence of tumor.

Ten cases of spindle cell myoepithelial carcinomas of both minor and major salivary glands devoid of clear cell component were studied for *EWSR1* gene break for
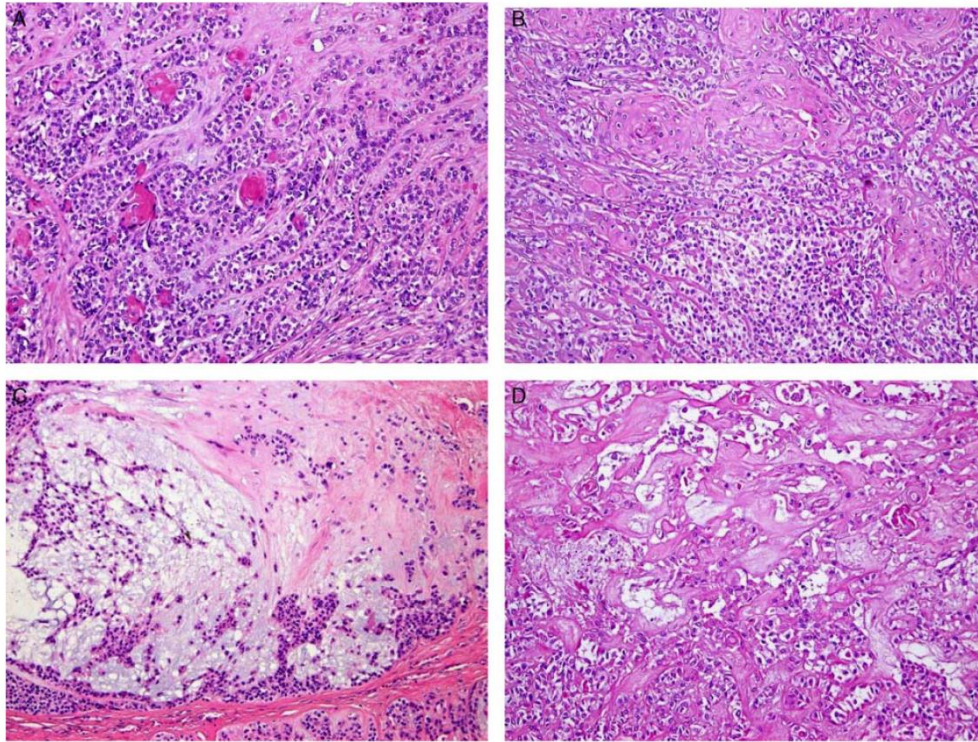
195

FIGURE 3. Squamous pearls (A) and/or areas of overt squamous differentiation are seen (B). C, Myxoid stroma was noted at least focally in all cases. D, Various degrees of hyalinization were observed in most cases.

comparison. Three patients of 10 (30%) experienced locoregional recurrence, 1 of these patients died of disseminated tumor 2 years after diagnosis with multiple lung metastases. The remaining 7 patients (70%) are free of disease in the follow-up period between 1 and 10 years (mean 3.4 y).

Histopathologic Findings

The 25 *EWSR1*-rearranged clear cell carcinomas shared similar histomorphology. Microscopic examination showed a complete or partial fibrous capsule in 12 of the 25 cases. Nineteen cases showed either well-delineated or at least broad pushing borders, whereas the remaining 6 cases demonstrated infiltrative growth of the tumor islands into the surrounding tissues. The *EWSR1*-rearranged myoepithelial carcinomas were composed of compact nests of large polyhedral cells with abundant clear cytoplasm divided by fibrous septa (Fig. 2A). Clear cells were observed as a prominent component in 23 of the 25 cases examined (Fig. 2B). The remaining 2 cases showed classical spindle cell and rhabdoid cytology, respectively, with minor clear cell component. The extent of clear cell morphology varied

from the entire or nearly the entire tumor in more than half of the cases to just a few islands constituting < 5% of the tumor (in 2 cases). Necrosis was a nearly universal feature, present in 22 of the 25 cases, although its extent varied widely from large necrotic areas (Fig. 2C) to foci in the centers of tumor islands resembling comedo necrosis (Fig. 2D), to occasional small foci requiring a careful search. Squamous pearls and/or areas of overt squamous differentiation were seen in 14 cases (Figs. 3A, B). The amount of stroma varied widely among the cases. Myxoid stroma was noted at least focally in 17 cases including all 5 cases of myoepithelial carcinomas ex pleomorphic adenoma (Fig. 3C). Various degree of hyalinization was observed in 24 cases (Fig. 3D). This varied from thickened basement membranes (Fig. 4A), to hyaline stromal deposits accumulating between the cells (in 13 cases) (Fig. 4B), to overt collagenous spherulosis-like formations (in 7 cases) (Fig. 4C). In 2 cases well-developed collagenous crystalloids were observed (Fig. 4D). Tubule formation was noted in 7 cases; however, it was a minor finding in all cases, and, in 1 of those cases, the myoepithelial carcinoma arose in pleomorphic adenoma, leading to a possibility the tubules
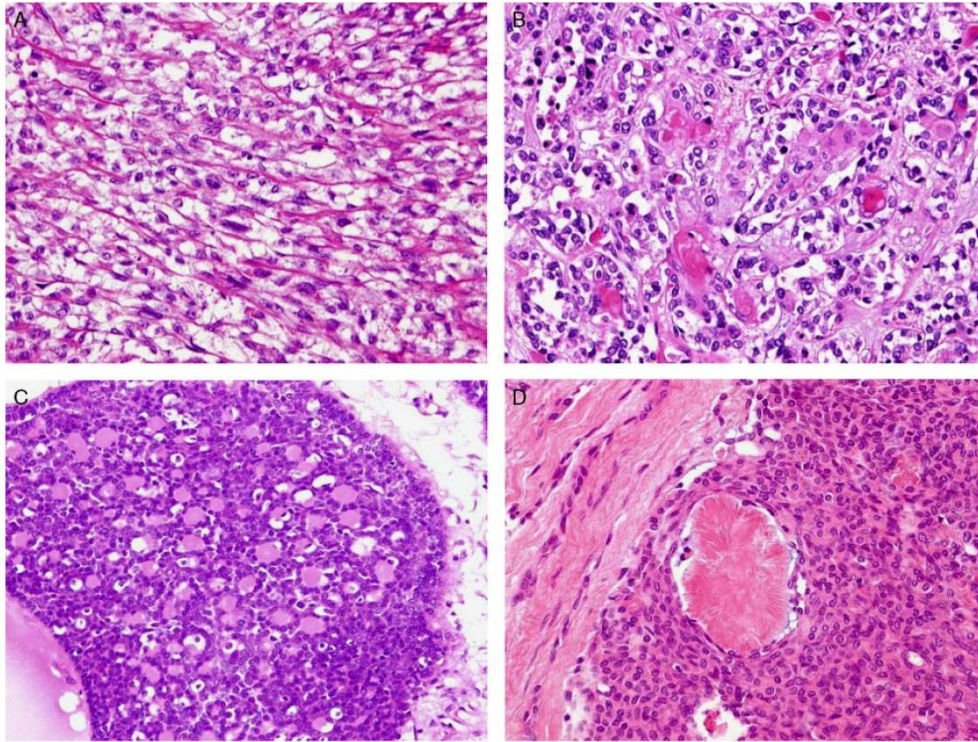
196

FIGURE 4. Hyalinized extracellular matrix deposits differs in morphology from thickened basement membranes (A), to hyaline stromal deposits accumulating between the cells (B), to overt collagenous spherulosis-like formations (C). D, In 2 cases, well-developed collagenous crystalloids were present.

were found in the PA remnants. In the remaining 5 cases the tubules were found in high-grade tumors, suggesting a possibility they represented residual normal structures. Fifteen cases showed significant nuclear pleomorphism (Fig. 5A), reflecting the high-grade nature of the tumors. A spindle cell component was observed in 9 cases, however, in only a single case was the spindle cell morphology predominant (Fig. 5B). The above-mentioned distinctive histomorphology was not generally seen in CCMC with intact *EWSR1*. Other findings included: calcification (3 cases), ossification (1 case), cartilage formation (1 case), intratumoral inflammatory component (2 cases), tumor clefting (5 cases), and pseudocystic structures with peripheral nuclear palisading (1 case) (Fig. 5C). Perineural invasion was noted in 9 cases (36%) and lymphovascular invasion in 11 cases (44%).

Immunohistochemical Findings

A summary of the immunohistochemical profiles of all *EWSR1*-rearranged cases is presented in Table 3. For 24 of the 25 cases, we obtained a minimum set of 4 immunostains S100, p63, CK14, and MIB1 (Ki-67) (Figs. 6A–D). In the remaining

case, only EMA, S100, and actin were available. Most of the cases had additional immunostains performed, including: CK7 (21 cases), actin (20 cases), and calponin (15 cases).

Twenty-two of the 25 cases (88%) showed a substantial degree of nuclear/cytoplasmic S100 immunostaining (Fig. 6A). Twenty-three cases (96% of the 24 examined) were positive for p63 (Fig. 6C), with a majority of cases showing diffuse positivity. CK14 was focally or diffusely positive in 23 cases (Fig. 6D) (96% of 24 examined). CK7 was at least focally positive in 13 of 21 cases examined (62%). No tumors showed diffuse actin or calponin positivity; however, weak and/or focal positivity for actin was noted in 10 of 20 tumors examined (50%) (Fig. 6B) and for calponin in 7 of 15 tumors (60%). Finally, MIB1 (Ki-67) index ranged from 10% to 100% with a mean of 42%.

DISCUSSION

EWSR1 has been identified as a translocation partner in a wide variety of clinically and histomorphologically diverse tumors, such as the Ewing family of tumors,[12] desmoplastic small round cell tumor,[13] clear cell sarcoma of soft
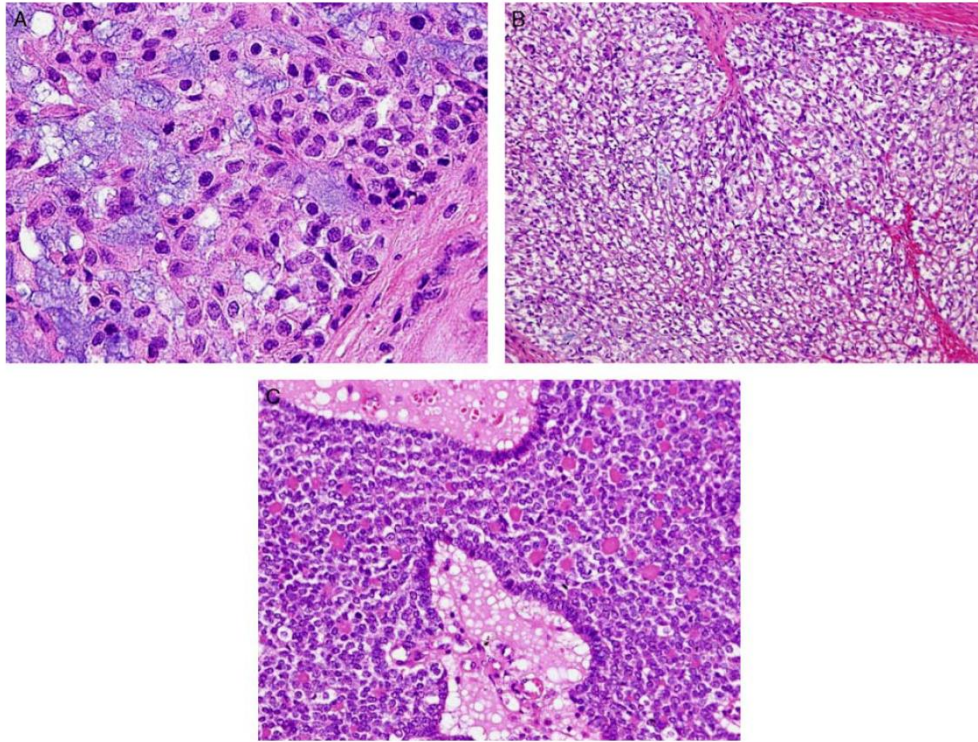
FIGURE 5. A, Significant nuclear pleomorphism reflecting the high-grade nature of the tumors is seen. B, Spindle cell component was focally observed, in only a single case was the spindle cell morphology predominant. C, Pseudocystic change and palisading was seen in 1 case.

tissue,[14,15] angiomatoid fibrous histiocytoma,[3] myxoid liposarcomas,[16] extraskeletal myxoid chondrosarcoma,[17] primary myoepithelial tumors of skin, soft tissue and bone[9,18] and many other soft tissue tumors (for more data see Fisher[6]). *EWSR1* is a highly promiscuous gene with a propensity for fusing with a great number of different partners resulting thus in many different gene fusions, such as *EWSR1-WT1*, *EWSR1-CREB1*, *EWSR1-ATF1*, *EWSR1-DDIT3*, *EWSR1-POU5F1*, *EWSR1-PBX1*, *EWSR1-ZNF444*, etc.[6] Interestingly, many of these translocations in soft tissue sarcomas are associated with unique tumor entities or/and may be shared between different entities; and the tumors differ considerably in morphology and clinical behavior. The diversity of the soft tissue tumor types and their specific *EWSR1* gene rearrangements were recently reviewed.[6] The best examples of this phenomenon are *EWSR1-CREB1* and *EWSR1-ATF1* gene fusions, 1 or both of which have been described in histopathologically and behaviorally diverse mesenchymal neoplasms, such as angiomatoid fibrous histiocytoma, conventional clear cell sarcoma of tendons and aponeuroses, clear cell sarcoma–like tumor of gastrointestinal tract, and primary pulmonary myxoid sarcoma.[19] Although *EWSR1-CREB1* and *EWSR1-ATF1* fusions are described with increasing frequency in more soft tissue tumor entities, the mechanisms by which they contribute to oncogenesis are still not known.

Approximately one third of sarcomas harbor balanced translocations, resulting in new gene fusions. In contrast, oncogenic translocation is a very rare event in epithelial malignancies. The *EWSR1-ATF1* fusion has been recently described in HCCC of minor salivary glands[7,20] and in odontogenic clear cell carcinomas.[8] In contrast to phenotypically diverse *EWSR1*-rearranged soft tissue tumors, most *EWSR1*-rearranged carcinomas seem to share in many cases phenotypical features, such as nested appearance divided by hyalinized fibrous septa, focal necrosis, collagenous spherulosis, foci of squamous metaplasia, and particularly clear cell cytomorphology.[7,8,10,19,21]

Recently, the presence of *EWSR1* gene rearrangement has been also demonstrated in 45% of SMET with a variety of fusion partners.[9] Interestingly, the tumors harboring

TABLE 3. Immunohistochemistry and FISH Results of the 25 Myoepithelial Carcinoma Cases Showing *EWSR1* Rearrangement

	S100	p63	CK14	CK7	Actin	Calponin	MIB1%	Positive Nuclei (%)	Note
Case 1	+	+	+	+/−	+	+	40	21	
Case 2a	+	+	+	−	+/−	−	30	19	
Case 2b	+	+	+	+/−	ND	ND	30	31	
Case 3	+	−	−	−	−	−	90	15	
Case 4	+	+	+	+	−	+/−	50	30	
Case 5	+	+	+	−	−	−	30	52	
Case 6	+	+	+	ND	ND	+/−	30	29	
Case 7	+	+	−/+	+	−/+	ND	15	23	
Case 8	+	+	+	+	−/+	−/+	30	28	
Case 9	−	+	+	−	+/−	−	30	33	
Case 10	+	−/+	−/+	−/+	−	ND	90	24	
Case 11	+	ND	ND	ND	−	ND	ND	27	
Case 12	+	+	+/−	−	−	−/+	15	14	
Case 13	+	+/−	+	+/−	+	−/+	25	35	
Case 14a	+	+	+/−	+/−	−/+	ND	15	95	
Case 14b	−	+	+	+/−	−/+	ND	30	35	
Case 15	+	+	+	−/+	−/+	ND	40	12	
Case 16	+	+	+	ND	ND	ND	20	65	
Case 17	+	+	+/−	−	ND	ND	40	12	
Case 18	+	+	+	ND	ND	ND	10	21	
Case 19	+	+	−/+	−	−	−	90	22	
Case 20	−	+	+	+	+	ND	100	26	Ampl
Case 21	+	+	+	−	+	+	70	37	Ampl
Case 22	+	+	+	+	−	−	20	11	Ampl
Case 23	+	+	−/+	+	ND	ND	35	24	
Case 24	−	+	+	+	−	−	45	20	Ampl
Case 25	+	+	+/−	−	−	−	70	22	Ampl
	88%	96%	96%	62%	50%	47%	42%		

For S100, substantial degree of staining was noted as a positive result (+). For p63, CK14, CK7, actin, and calponin, cases were scored as diffusely positive, or reported as positive (+); focally positive in > 50% of cells (+/−); focally positive in < 50% of cells (−/+); and negative (−). MIB1 (Ki-67) labeling index is given as a percentage of positive cells. The lowest line reports the percentage of cases with any positivity, or, in the case of MIB1, the average labeling index.
    Ampl indicates *EWSR1* gene amplification; ND, not done.

EWSR1-POU5F1 fusion were composed predominantly of clear cells and had a distinctive nested morphology.[9] Furthermore, a similar *EWSR1-POU5F1* fusion has also been reported in cutaneous hidradenoma and a single case of "poorly differentiated" mucoepidermoid carcinoma.[21] However, a control group of 5 salivary myoepithelial carcinomas ex pleomorphic adenoma (histologic pictures were not provided) in their series all showed an intact *EWSR1* gene; therefore the authors concluded that there is no pathogenetic relationship between salivary myoepithelial tumors and SMETs.[9] This paper by Antonescu et al[9] immediately attracted our attention as we had earlier published a short series of 5 CCMCs of salivary glands displaying an apparent solid and nested growth pattern, separated by thin fibrous septa, and predominant clear cell morphology.[10] This raises the question of whether CCMCs of salivary glands could have similar genetic aberrations as SMET. Therefore, we decided to test for *EWSR1* rearrangements using FISH in a large spectrum of myoepithelial tumors of salivary glands with clear cell morphology. A total of 94 salivary gland tumors each with a prominent clear cell component and evidence of myoepithelial differentiation were analyzed for *EWSR1* gene break by FISH. The *EWSR1* rearrangement was detected in 25 of 72 "monomorphic" CCMCs (35%). The 25 *EWSR1*-rearranged clear cell carcinomas all shared a similar histomorphology. Necrosis was a nearly universal feature, seen in 22 of the 25 cases, although its extent varied widely from large necrotic areas, to foci in the centers of tumor islands resembling comedo necrosis, to occasional small foci requiring a careful search. Given that not all sections were available for all the cases, it is possible that the remaining 3 cases might very well have harbored necrotic foci that were simply absent in the material available for examination. A nested growth pattern, hyalinized extracellular matrix forming septa, hyaline droplets, foci of squamous metaplasia, and prominent clear cell morphology[10] were seen in all *EWSR1*-rearranged CCMC. In addition, collagenous spherulosis[22,23] and collagenous crystalloids[24] were noted in some cases. Tissue material from all 5 cases of CCMC previously reported[10] was available, but the quality of DNA, however, was not sufficient, and the cases were nonanalyzable. The above-mentioned distinctive histomorphology was not generally seen in CCMC with intact *EWSR1*. Interestingly, a recently published case report of a rhabdoid variant of soft tissue myoepithelial carcinoma with *EWSR1* rearrangement showed focal clear cell change and the presence of prominent coagulative necrosis[25] and in our opinion could represent the same entity.

Myoepithelial carcinomas of salivary glands are locally aggressive neoplasms with diverse clinical outcomes.[26] A previous study of 25 salivary myoepithelial carcinomas found only a weak statistical correlation for outcome with
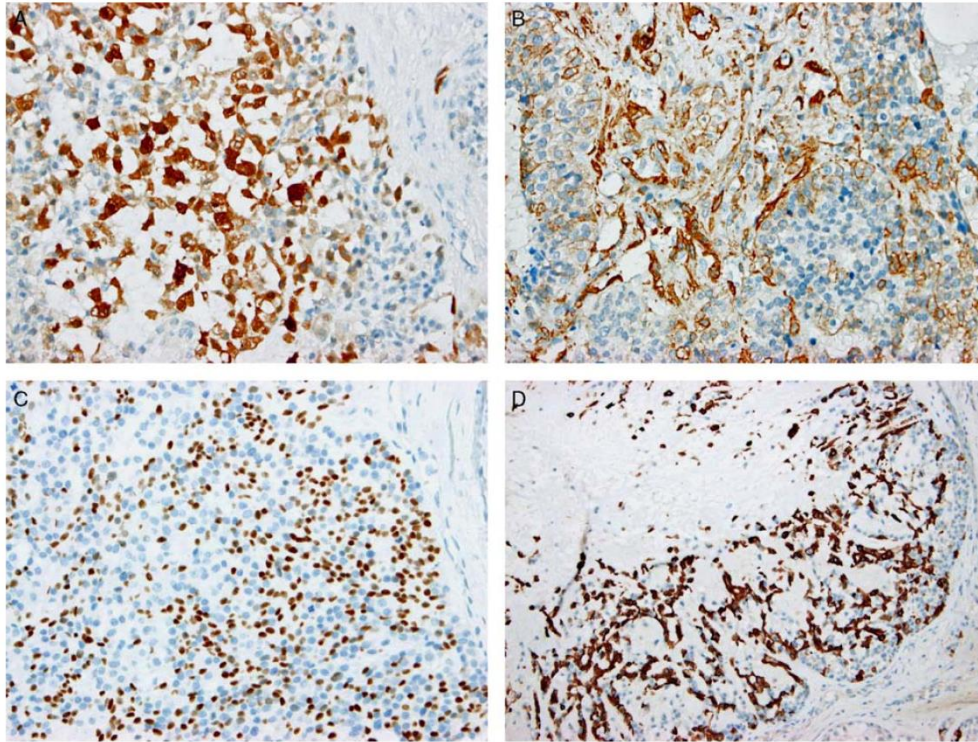
FIGURE 6. Tumor cells are immunoreactive with antibodies to S100 protein (A), smooth muscle actin (B), p63 (C), and CK14 (D).

cytologic atypia (high grade), but other parameters (tumor size, site, cell type, mitotic rate, presence of benign tumor, necrosis, perineural and vascular invasion) showed no relationship.[27] In our present series, 7 of 21 patients (33%) with *EWRS1*-rearranged CCMC developed distant metastases, and lymph node metastasis appeared in 5 patients (24%). Eight patients died of disseminated cancer (38%), and 3 patients are alive with recurrent and metastatic disease (14%). The prognosis of CCMC with *EWSR1* rearrangement is rather poor, and it seems that the acquisition of *EWSR1* rearrangement may be the driver of the high-grade malignant phenotype and hence aggressive clinical behavior.

In the differential diagnosis, HCCC must be considered. Myoepithelial carcinomas in our series, in contrast to HCCC, expressed S100 protein, cytokeratins, and EMA, with varying combination of actin, calponin, p63, and glial fibrillary acidic protein. Although the immunoprofile may vary considerably between cases, the minimal requirement for the inclusion to the family of myoepithelial carcinomas of salivary gland origin encompassing the coexpression of cytokeratin/EMA, S100

protein, and/or at least 1 other myoepithelial marker was present in all our cases (Table 3).

In summary, our study has demonstrated that CCMCs of salivary gland harbor *EWSR1* rearrangement in a subset of cases and therefore may be genetically related to *EWSR1*-rearranged cutaneous myoepithelial tumors.[28] Regarding the partner fusion genes of *EWSR1* in salivary CCMC, further investigations are mandatory.

REFERENCES
1. Aurias A, Rimbaut C, Buffe D, et al. Translocation of chromosome 22 in Ewing sarcoma. *C R Seances Acad Sci III.* 1983;296: 1105–1107.
2. Turc-Carel C, Philip I, Berger MP, et al. Chromosome study of Ewing sarcoma (ES) cell lines. Consistency of reciprocal translocation t(11;22)(q24;q12). *Cancer Genet Cytogenet.* 1984;12:1–19.

3. Antonescu CR, Dal Cin P, Nafa K, et al. *EWSR1-CREB1* is the predominant gene fusion in angiomatoid fibrous histiocytoma. *Genes Chromosomes Cancer*. 2007;46:1051–1060.

4. Attwooll C, Tariq M, Harris M, et al. Identification of a novel fusion gene involving hTAFII68 and CHN from a t(9;17)(q22;q11.2) translocation in an extraskeletal myxoid chondrosarcoma. *Oncogene*. 1999;18:7599–7601.

5. Antonescu CR, Nafa K, Segal NH, et al. *EWSR1-CREB1*: a recurrent variant fusion in clear cell sarcoma-association with gastrointestinal location and absence of melanocytic differentiation. *Clin Cancer Res*. 2006;12:5356–5362.

6. Fisher C. Diversity of soft tissue tumours with *EWSR1* gene rearrangements: a review. *Histopathology*. 2014;64:134–150.

7. Antonescu CR, Katabi N, Zhang L, et al. *EWSR1-ATF1* fusion is a novel and consistent finding in hyalinizing clear-cell carcinoma of salivary gland. *Genes Chromosomes Cancer*. 2011;50:559–570.

8. Bilodeau EA, Weinreb I, Antonescu CR, et al. Clear cell odontogenic carcinomas show *EWSR1* rearrangements: a novel finding and biologic link to salivary clear cell carcinomas. *Am J Surg Pathol*. 2013;37:1001–1005.

9. Antonescu CR, Zhang L, Chang NE, et al. *EWSR1-POU5F1* fusion in soft tissue myoepithelial tumors. A molecular analysis of sixty-six cases, including soft tissue, bone, and visceral lesions, showing common involvement of the *EWSR1* gene. *Genes Chromosomes Cancer*. 2010;49:1114–1124.

10. Michal M, Skálová A, Simpson RH, et al. Clear cell malignant myoepithelioma of the salivary glands. *Histopathology*. 1996;28: 309–315.

11. Ventura RA, Martin-Subero JI, Jones M, et al. FISH analysis for the detection of lymphoma-associated chromosomal abnormalities in routine paraffin-embedded tissue. Review. *J Mol Diagn*. 2006;8:141–151.

12. Arvand A, Denny CT. Biology of EWS/ETS fusions in Ewing's family tumors. *Oncogene*. 2001;20:5747–5754.

13. Ladanyi M, Gerald W. Fusion of the *EWS* and *WT1* genes in the desmoplastic small round cell tumor. *Cancer Res*. 1994;54: 2837–2840.

14. Hisaoka M, Ishida T, Kuo TT, et al. Clear cell sarcoma of soft tissue: a clinicopathologic, immunohistochemical, and molecular analysis of 33 cases. *Am J Surg Pathol*. 2008;32:452–460.

15. Wang WL, Mayordomo E, Zhang W, et al. Detection and characterization of *EWSR1/ATF1* and EWSR1/CREB1 chimeric transcripts in clear cell sarcoma (melanoma of soft parts). *Mod Pathol*. 2009;22:1201–1209.

16. Panagopoulos I, Hoglund M, Mertens F, et al. Fusion of the EWS and CHOP genes in myxoid liposarcoma. *Oncogene*. 1996;12:489–494.

17. Clark J, Benjamin H, Gill S, et al. Fusion of the *EWS* gene to *CHN*, a member of the steroid/thyroid receptor gene superfamily, in a human myxoid chondrosarcoma. *Oncogene*. 1996;12:229–235.

18. Fletcher CD. Cutaneous syncytial myoepithelioma: clinicopathologic characterization in a series of 38 cases. *Am J Surg Pathol*. 2013;37:710–718.

19. Thway K, Fisher C. Tumors with *EWSR1-CREB1* and *EWSR1-ATF1* fusions: the current status. *Am J Surg Pathol*. 2012;36:e1–e11.

20. Shah AA, LeGallo RD, van Zante A, et al. *EWSR1* genetic rearrangements in salivary gland tumors: a specific and very common feature of hyalinizing clear cell carcinoma. *Am J Surg Pathol*. 2013;37:571–578.

21. Moller E, Stenman G, Mandahl N, et al. *POU5F1*, encoding a key regulator of stem cell pluripotency, is fused to *EWSR1* in hidradenoma of the skin and mucoepidermoid carcinoma of the salivary glands. *J Pathol*. 2008;215:78–86.

22. Michal M, Skálová A. Collagenous spherulosis. A comment on its histogenesis. *Pathol Res Pract*. 1990;186:365–370.

23. Skálová A, Leivo I. Extracellular collagenous spherules in salivary gland tumors. Immunohistochemical analysis of laminin and various types of collagen. *Arch Pathol Lab Med*. 1992;116:649–653.

24. Skálová A, Leivo I, Michal M, et al. Analysis of collagen isotypes in crystalloid structures of salivary gland tumors. *Hum Pathol*. 1992;23:748–755.

25. Thway K, Bown N, Miah A, et al. Rhabdoid variant of myoepithelial carcinoma, with *EWSR1* rearrangement: expanding the spectrum of *EWSR1*-rearranged myoepithelial tumors. *Head Neck Pathol*. 2014. [Epub ahead of print].

26. Skálová A, Jakel KT. Myoepithelial carcinoma. In: Barnes L, Eveson JW, Reichart P, Sidransky D, eds. *World Health Organization Classification of Tumours. Pathology and Genetics of Head and Neck Tumours*. Lyon: IARC Press; 2005:240–241.

27. Savera AT, Sloman A, Huvos AG, et al. Myoepithelial carcinoma of salivary glands: a clinicopathologic study of 25 patients. *Am J Surg Pathol*. 2000;24:761–774.

28. Flucke U, Palmedo G, Blankenhorn N, et al. *EWSR1* gene rearrangement occurs in a subset of cutaneous myoepithelial tumors: a study of 18 cases. *Mod Pathol*. 2011;24:1444–1450.

201

Seznam vlastních publikací

1. Hes O, Vanecek T, Petersson F, Grossmann P, Hora M, Perez Montiel DM, **Steiner P**, Dvořák M, Michal M. Mutational Analysis (c.402C>G) of the *FOXL2* gene and Immunohistochemical Expression of the FOXL2 protein inTesticular Adult Type Granulosa Cell Tumors and Incompletely Differentiated Sex Cord Stromal Tumors. *Appl Immunohistochem Mol Morphol.* 2011; 19(4):347-51.

2. Petersson F, Vanecek T, Michal M, Martignoni G, Brunelli M, Halbhuber Z, Spagnolo D, Kuroda N, Yang X, Cabrero IA, Hora M, Branzovsky J, Trivunic S, Kacerovska D, **Steiner P**, Hes O. A disctinctive translocation carcinoma of the kidney, "rosette forming", t(6;11), HMB45 positive renal tumor: a histomorphologic, immunohistochemical, ultrastructural and molecular genetic study of 4 cases. *Human Pathol.* 2011; 43(5): 726-36.

3. Grossmann P, Vanecek T, **Steiner P**, Kacerovska D, Spagnolo DV, Cribier B, Rose C, Vazmitel M, Carlson JA, Emberger M, Martinek P, Pearce RL, Pearn J, Michal M, Kazakov DV. Novel and recurrent germline and somatic mutations in a cohort of 67 patients from 48 families with Brooke-Spiegler syndrome including the phenotypic variant of multiple familial trichoepitheliomas and correlation with the histopathological findings in 379 biopsy specimens. *Am J Dermatopathol.* 2013; 35(1): 34-44.

4. **Steiner P**, Hora M, Stehlik J, Martinek P, Vanecek T, Petersson F, Michal M, Korabecna M, Travnicek I, Hes O. Tubulocystic renal cell carcinoma: is there a rational reason for targeted therapy using angiogenic inhibition? Analysis of seven cases. *Virchows Arch.* 2013; 462(2): 183-192.

5. Majewska H, Skálová A, Stodulski D, Klimková A, **Steiner** P, Stankiewicz C, Biernat W. Mammary analogue secretory carcinoma of salivary glands: a new entity associated with ETV6 gene rearrangement. *Virchows Arch.* 2015; 466(3): 245-254.

6. Skálová A, Weinreb I, Hyrcza M, Simpson RH, Laco J, Agaimy A, Vazmitel M, Majewska H, Vanecek T, Talarčik P, Manajlovic S, Losito SN, **Šteiner P,** Klimkova A, Michal M. Clear cell myoepithelial carcinoma of salivary glands showing EWSR1 rearrangement: molecular analysis of 94 salivary gland carcinomas with prominent clear cell component. *Am J Surg Pathol.* 2015; 39(3): 338-348.

7. Skálová A, Vanecek T, Simpson RH, Laco J, Majewska H, Baneckova M, **Steiner** P, Michal M. Mammary Analogue Secretory Carcinoma of Salivary Glands: Molecular Analysis of 25 ETV6 Gene Rearranged Tumors With Lack of Detection of Classical ETV6-NTRK3 Fusion Transcript by Standard RT-PCR: Report of 4 Cases Harboring ETV6-X Gene Fusion. *Am J Surg Pathol*. 2015; 40(3): 3-13.

8. Skálová A, Sar A, Laco J, Metelková A, Misbauerová M, **Šteiner P**, Švajdler M, Michal M. The Role of SATB2 as a Diagnostic Marker of Sinonasal Intestinal-type Adenocarcinoma. *Appl Immunohistochem Mol Morphol*. 2016; 26(2): 140-146.

9. Hauer L, Skálová A, **Šteiner P**, Hrušák D, Andrle P, Hostička L, Sebera O. Adenoidně cystický karcinom slinných žláz. Soubor 27 pacientů. *Česká Stomatologie* 2016; 116(3): 57-65.

10. Broz M, **Steiner P**, Salzman R, Hauer L, Starek I. The incidence of MYB gene breaks in adenoid cystic carcinoma of the salivary glands and its prognostic significance. *Biomed Pap Med FacUnivPalacky* 2016; 160(3): 417-422.

11. Skálová A, **Šteiner P**, Vaněček T. New developments in molecular diagnostics of carcinomas of the salivary glands: "translocation carcinomas". *Cesk Patol.* 2016; 52(3): 139-45.

12. Korabecna M, Geryk J, Hora M, **Steiner P**, Seda O, Tesar V. Genome-Wide methylation analysis of tubulocystic and papillary renal cell carcinomas. *Neoplasma* 2016; 63(3): 402 – 10.

13. Korabecna M, **Steiner P**, Jirkovská M. DNA from microdissected tissues may be extracted and stored on microscopic slides. *Neoplasma* 2016; 63(4): 518 - 22.

14. Michal M, Kazakov DV, Agaimy A, Hosova M, Michalova K, Grossmann P, **Steiner P**, Skenderi F, Vranic S, Michal M. Whorling cellular perineuroma: A previously undescribed variant closely mimicking monophasic fibrous synovial sarcoma. *Ann Diag. Pathol* 2017; 27: 74 – 78.

15. Michal M, Kazakov DV, Hadravsky L, Michalova K, Grossmann P, **Steiner P**, Vanecek T, Renda V, Suster S, Michal M. Lipoblasts in Spindle Cell and Pleiomorphic Lipomas: a Close Scrutiny. *Hum Pathol.* 2017; 65: 140 - 146.

16. Skalova A, Vanecek T, Martinek P, Weinreb I, Stevens TM, Simpson RH, Hyrcza M, Rupp NJ, Baneckova M, Michal M Jr., Slouka D, Svoboda T, Metelkova A, Etebarian A, Pavelka J, Potts SJ, Christiansen J, **Steiner P**, Michal M. Molecular profiling of mammary analogue secretory carcinoma revealed a subset of tumors harboring a novel ETV6-RET translocation: report of 10 cases. *Am J Surg Pathol.* 2017; 42: 234 - 246.

17. Skalova A, Stenman G, Simpson RHW, Hellquist H, Slouka D, Svoboda T, Bishop J, Hunt JL, Nibu K-I, Rinaldo A, Poorten VV, Devaney KO, **Steiner P**, Ferlito A. The Role of Molecular Testing in the Differential Diagnosis of Salivary Gland Carcinomas. *Am J Surg Pathol.* 2017; 42(2): e11 – e27.

18. **Šteiner P**, Pavelka J, Vaněček T, Misbauerová M, Skálová A. Metody detekce molekulárních prognostických a prediktivních markerů v diagnostice adenoidně cystického karcinomu slinných žláz. *Cesk Patol.* 2018; [v tisku].

19. Andreasen S, Tan Q, Agander TK, **Steiner P**, Bjørndal K, Høgdal E, Larsen SR, Erentaite D, Olsen CH, Ulhøi BP, von Holstein SL, Wessel I, Heegaard S, Homøe P. Adenoid Cystic Carcinoma of the Salivary Gland, Lacrimal Gland, and Breast are Morphologically and Genetically Similar but have Distinct microRNA Expressional Profiles. *Mod Pathol* 2018; [v tisku].

20. Kazakov DV, Kyrpychova L, Martinek P, Grossmann P, **Steiner P**, Vanecek T, Pavlovsky M, Bencik V, Michal M, Michal M. ALK Gene Fusions in Epithelioid Fibrous Histiocytoma: A Study of 14 Cases, With New Histopathological Findings. *Am J Dermatopathol* 2018; [v tisku].

21. Kyrpychova L, Vanecek T, Grossmann P, Martinek P, **Steiner P**, Hadravsky L, Belousova IE, Shelekhova KV, Svaidler M, Michal M, Kazakov DV. A small subset of adenoid cystic carcinoma of the skin is associated with alterations of the *MYBL1* gene similar to their extracutaneous counterparts. *Am J Dermatopathol* 2018; [v tisku].

22. Michalova K, **Steiner P**, Alaghehbandan R, Trpkov K, Martinek P, Grossmann P, Perez Montiel D, Sperga M, Suster S, Straka L, Prochazkova K, Cempirkova D, Horava V, Bulimbasic S, Pivovarcikova K, Daum O, Ondic O, Rotterova P, Michal M, Hes O. Papillary Renal Cell Carcinoma with Cytologic and Molecular Genetic Features of Renal Oncocytoma: Analysis of 10 Cases. *Ann Diag Pathol* 2018; [v tisku].

23. Andreasen S, Tan Q, Klitmøller Agander T, Hansen van Overeem T, **Steiner P**, Bjørndal K, Høgdall E, Rosenkilde Larsen S, Erentaite D, Holkmann Olsen C, Parm Ulhøi B, Heegaard S, Wessel I, Homøe P. MicroRNA dysregulation in adenoid cystic carcinoma of the salivary gland in relation to prognosis and gene fusion status: A cohort study. *Virchows Arch.* 2018; [v tisku].

24. Baneckova M, Agaimy A, Andreasen S, Vanecek T**, Steiner P**, Slouka D, Svoboda T, Miesbauerova M, Michal M Jr, Skalova A. Mammary analogue secretory carcinoma of the sinonasal tract. *Am J Surg Pathol* 2018; [v tisku].

25. **Šteiner P**, Andreasen S, Grossmann P, Hauer L, Vaněček T, Miesbauerová M, Santana T, Kiss K, Slouka D, Skálová A. Prognostic significance of 1p36 locus deletion in adenoid cystic carcinoma of the salivary glands. *Virchows Arch.* 2018; [v tisku].

26. Ronen S, Aguilera-Barrantes I, Giorgadze T, **Šteiner P**, Grossmann P, Suster S. Polymorphous Sweat Gland Carcinoma: An Immunohistochemical and Molecular Study. *Am J Dermatopathol* 2018; [v tisku].

Závěr

V průběhu studia bylo dosaženo několika prioritních pozorování a publikačních výstupů. V případě adenoidně cystického karcinomu naše práce přispěly k lepší charakterizaci translokací zahrnujících geny *MYB*, *NFIB* a *MYBL1*, dále k identifikaci prvního prognostického markeru – delece lokusu 1p36, k identifikaci miRNA, které by mohly sloužit jako diferenciálně diagnostické, popř. prognostické markery AdCC a k popsání prvních případů s přestavbou *MYBL1* u kožních adenoidně cystických karcinomů [24, 29, 31-34]. V případě sekrečního karcinomu mamárního typu byly identifikovány nové případy vykazující klasickou přestavbu *ETV6* genu, byly prioritně popsány případy, kde *ETV6* fúzuje s jiným fúzním partnerem než *NTRK3*, posléze k identifikaci fúzního partnera - genu *RET* a nakonec byly publikovány první dva případy sekrečního karcinomu v nosní sliznici [9, 26, 27, 30]. Dále došlo k sepsání celkem tří přehledových článků [23, 25, 35] a nakonec ke zjištění, že detekci přestavby *EWSR1* genu nelze použít jako specifického diagnostického markeru hyalinizujícího světlobuněčného karcinomu slinných žláz, ale že molekulární nálezy musí být interpretovány vždy v korelaci s histomorfologií daného tumoru [28].

Celkem bylo sepsáno 14 publikací, z toho 2 prvoautorské články (jeden v časopise s impakt faktorem), 12 spoluautorských článků (z toho 9 v časopisech s faktorem impaktu - IF) a dalších osm publikací nesouvisejících s tématem dizertační práce.

Seznam použité literatury

1. Neville BW, Allen CM, Damm DD, Chi AC. *Oral and maxillofacial pathology.*3rd edition, Saunders, 2009, 473-477.
2. Stenman G, Licitra L, Said-Al-Naeief N,van Zante A, Yarbrough WG. Adenoid cystic carcinoma. in *World Health Organization Classification of Head and Neck Tumours* Ed. El-Naggar AK, Chan JKC, Grandis JR, Takata T, Slootweg PJ. IARC Press, Lyon, 2017, pp. 164-165.
3. Skálová A, Vanecek T, Sima R, Laco J, Weinreb I, Perez-Ordonez B, Starek I, Geierova M, Simpson RH, Passador-Santos F, Ryska A, Leivo I, Kinkor Z, Michal M. Mammary analogue secretory carcinoma of salivary glands, containing the ETV6-NTRK3 fusion gene: a hitherto undescribed salivary gland tumor entity. *Am J Surg Pathol* 2010; 34(5): 599-608.
4. Tognon C, Knezevich SR, Huntsman D, Roskelley CD, Melnyk N, Mathers JA, Becker L, Carneiro F, MacPherson N, Horsman D, Poremba C, Sorensen PH. Expression of the ETV6-NTRK3 gene fusion as a primary event in human secretory breast carcinoma. *Cancer Cell* 2002; 2(5): 367-376.
5. Antonescu CR, Katabi N, Zhang L, Sung YS, Seethala RR, Jordan RC, Perez-Ordoñez B, Have C, Asa SL, Leong IT, Bradley G, Klieb H, Weinreb I. EWSR1-ATF1 fusion is a novel and consistent finding in hyalinizing clear-cell carcinoma of salivary gland. *Genes Chromosomes Cancer* 2011; 50(7): 559-570.
6. Persson M, Andrén Y, Mark J, Horlings HM, Persson F, Stenman G. Recurrent fusion of MYB and NFIB transcription factor genes in carcinomas of the breast and head and neck. *Proc Natl Acad Sci U S A* 2009; 106(44): 18740-18744.
7. Tonon G, Modi S, Wu L, Kubo A, Coxon AB, Komiya T, O'Neil K, Stover K, El-Naggar A, Griffin JD, Kirsch IR, Kaye FJ. t(11;19)(q21;p13) translocation in mucoepidermoid carcinoma creates a novel fusion product that disrupts a Notch signaling pathway. *Nat Genet* 2003; 33(2): 208-213.
8. Martins C, Cavaco B, Tonon G, Kaye FJ, Soares J, Fonseca I. A study of MECT1-MAML2 in mucoepidermoid carcinoma and Warthin's tumor of salivary glands. *J Mol Diagn* 2004; 6(3): 205-210.
9. Skalova A, Vanecek T, Martinek P, Weinreb I, Stevens TM, Simpson RHW, Hyrcza M, Rupp NJ, Baneckova M, Michal M, Slouka D, Svoboda T, Metelkova A, Etebarian A, Pavelka J, Potts SJ, Christiansen J, Steiner P. Molecular Profiling of Mammary Analog Secretory Carcinoma Revealed a Subset of Tumors Harboring a Novel ETV6-RET Translocation: Report of 10 Cases. *Am J Surg Pathol* 2018; 42(2): 234-246.
10. Skálová A, Laco J, Uro-Coste E, Martinek P, Thompson LD, R, Badoual C, Santana T, Miesbauerová M, Vaněček T, Michal M. Molecular profiling of intraductal carcinoma of parotid gland revealed a subset of tumors harboring a NC*OA4-RET an*d n*ovel* TRIM*27-RET fus*ions: report of 3 cases. USCAP 2018. Vancouver, Canada, 2018.
11. Amit M, Binenbaum Y, Trejo-Leider L, Sharma K, Ramer N, Ramer I, Agbetoba A, Miles B, Yang X, Lei D, Bjørndal K, Godballe C, Mücke T, Wolff KD, Eckardt AM, Copelli C, Sesenna E, Palmer F, Ganly I, Patel S, Gil Z. International collaborative validation of intraneural invasion as a prognostic marker in adenoid cystic carcinoma of the head and neck. *Head Neck* 2015; 37(7): 1038-1045.

12.   Nordkvist A, Mark J, Gustafsson H, Bang G, Stenman G. Non-random chromosome rearrangements in adenoid cystic carcinoma of the salivary glands. *Genes Chromosomes Cancer* 1994; 10(2): 115-121.

13.   Mitani Y, Liu B, Rao PH, Borra VJ, Zafereo M, Weber RS, Kies M, Lozano G, Futreal PA, Caulin C, El-Naggar AK. Novel MYBL1 Gene Rearrangements with Recurrent MYBL1-NFIB Fusions in Salivary Adenoid Cystic Carcinomas Lacking t(6;9) Translocations. *Clin Cancer Res* 2016; 22(3): 725-733.

14.   Brayer KJ, Frerich CA, Kang H, Ness SA. Recurrent Fusions in MYB and MYBL1 Define a Common, Transcription Factor-Driven Oncogenic Pathway in Salivary Gland Adenoid Cystic Carcinoma. *Cancer Discov* 2016; 6(2): 176-187.

15.   Stephens PJ, Davies HR, Mitani Y, Van Loo P, Shlien A, Tarpey PS, Papaemmanuil E, Cheverton A, Bignell GR, Butler AP, Gamble J, Gamble S, Hardy C, Hinton J, Jia M, Jayakumar A, Jones D, Latimer C, McLaren S, McBride DJ, Menzies A, Mudie L, Maddison M, Raine K, Nik-Zainal S, O'Meara S, Teague JW, Varela I, Wedge DC, Whitmore I, Lippman SM, McDermott U, Stratton MR, Campbell PJ, El-Naggar AK, Futreal PA. Whole exome sequencing of adenoid cystic carcinoma. *J Clin Invest* 2013; 123(7): 2965-2968.

16.   Skalova A. Mammary analogue secretory carcinoma of salivary gland origin: an update and expanded morphologic and immunohistochemical spectrum of recently described entity. *Head Neck Pathol* 2013; 7 Suppl 1: S30-36.

17.   Stenman G. Fusion oncogenes in salivary gland tumors: molecular and clinical consequences. *Head Neck Pathol* 2013; 7 Suppl 1: S12-19.

18.   Skálová A, Vanecek T, Majewska H, Laco J, Grossmann P, Simpson RH, Hauer L, Andrle P, Hosticka L, Branžovský J, Michal M. Mammary analogue secretory carcinoma of salivary glands with high-grade transformation: report of 3 cases with the ETV6-NTRK3 gene fusion and analysis of TP53, β-catenin, EGFR, and CCND1 genes. *Am J Surg Pathol* 2014; 38(1): 23-33.

19.   Luo W, Lindley SW, Lindley PH, Krempl GA, Seethala RR, Fung KM. Mammary analog secretory carcinoma of salivary gland with high-grade histology arising in hard palate, report of a case and review of literature. *Int J Clin Exp Pathol* 2014; 7(12): 9008-9022.

20.   Chi HT, Ly BT, Kano Y, Tojo A, Watanabe T, Sato Y. ETV6-NTRK3 as a therapeutic target of small molecule inhibitor PKC412. *Biochem Biophys Res Commun* 2012; 429(1-2): 87-92.

21.   Tognon CE, Somasiri AM, Evdokimova VE, Trigo G, Uy EE, Melnyk N, Carboni JM, Gottardis MM, Roskelley CD, Pollak M, Sorensen PH. ETV6-NTRK3-mediated breast epithelial cell transformation is blocked by targeting the IGF1R signaling pathway. *Cancer Res* 2011; 71(3): 1060-1070.

22.   Drilon A, Li G, Dogan S, Gounder M, Shen R, Arcila M, Wang L, Hyman DM, Hechtman J, Wei G, Cam NR, Christiansen J, Luo D, Maneval EC, Bauer T, Patel M, Liu SV, Ou SH, Farago A, Shaw A, Shoemaker RF, Lim J, Hornby Z, Multani P, Ladanyi M, Berger M, Katabi N, Ghossein R, Ho AL. What hides behind the MASC: clinical response and acquired resistance to entrectinib after ETV6-NTRK3 identification in a mammary analogue secretory carcinoma (MASC). *Ann Oncol* 2016; 27(5): 920-926.

23.   Šteiner P, Pavelka J, Vaněček T, Miesbauerová M, Skálová A. Metody detekce molekulárních prognostických a prediktivních markerů v diagnostice adenoidně cystického karcinomu slinných žláz. *Cesk Patol* 2018; [v tisku].

24.   Šteiner P, Andreasen S, Grossmann P, Hauer L, Vaněček T, Miesbauerova M, Santana T, Kiss K, Slouka D, Skálová A. Prognostic significance of 1p36 locus deletion in adenoid cystic carcinoma of the salivary glands. *Virchows Arch* 2018; [v tisku].

25.   Skálová A, Stenman G, Simpson RHW, Hellquist H, Slouka D, Svoboda T, Bishop JA, Hunt JL, Nibu KI, Rinaldo A, Vander Poorten V, Devaney KO, Steiner P, Ferlito A. The Role of Molecular Testing in the Differential Diagnosis of Salivary Gland Carcinomas. *Am J Surg Pathol* 2017; 42(2): e11-e27.

26.   Majewska H, Skálová A, Stodulski D, Klimková A, Steiner P, Stankiewicz C, Biernat W. Mammary analogue secretory carcinoma of salivary glands: a new entity associated with ETV6 gene rearrangement. *Virchows Arch* 2015; 466(3): 245-254.

27.   Skálová A, Vanecek T, Simpson RH, Laco J, Majewska H, Baneckova M, Steiner P, Michal M. Mammary Analogue Secretory Carcinoma of Salivary Glands: Molecular Analysis of 25 ETV6 Gene Rearranged Tumors With Lack of Detection of Classical ETV6-NTRK3 Fusion Transcript by Standard RT-PCR: Report of 4 Cases Harboring ETV6-X Gene Fusion. *Am J Surg Pathol* 2016; 40(1): 3-13.

28.   Skálová A, Weinreb I, Hyrcza M, Simpson RH, Laco J, Agaimy A, Vazmitel M, Majewska H, Vanecek T, Talarčik P, Manajlovic S, Losito SN, Šteiner P, Klimkova A, Michal M. Clear cell myoepithelial carcinoma of salivary glands showing EWSR1 rearrangement: molecular analysis of 94 salivary gland carcinomas with prominent clear cell component. *Am J Surg Pathol* 2015; 39(3): 338-348.

29.   Andreasen S, Tan Q, Klitmøller Agander T, Hansen van Overeem T, Steiner P, Bjørndal K, Høgdall E, Rosenkilde Larsen S, Erentaite D, Holkmann Olsen C, Parm Ulhøi B, Heegaard S, Wessel I, Homøe P. MicroRNA dysregulation in adenoid cystic carcinoma of the salivary gland in relation to prognosis and gene fusion status: A cohort study. *Virchows Arch* 2018; [v tisku].

30.   Baneckova M, Agaimy A, Andreasen S, Vanecek T, Steiner P, Slouka D, Svoboda T, Miesbauerova M, Michal M, Skálová A. Mammary Analog Secretory Carcinoma of the Nasal Cavity: Characterization of 2 Cases and Their Distinction From Other Low-grade Sinonasal Adenocarcinomas. *Am J Surg Pathol* 2018; [v tisku].

31.   Andreasen S, Tan Q, Agander TK, Steiner P, Bjørndal K, Høgdall E, Larsen SR, Erentaite D, Olsen CH, Ulhøi BP, von Holstein SL, Wessel I, Heegaard S, Homøe P. Adenoid cystic carcinomas of the salivary gland, lacrimal gland, and breast are morphologically and genetically similar but have distinct microRNA expression profiles. *Mod Pathol* 2018; [v tisku].

32.   Kyrpychova L, Vanecek T, Grossmann P, Martinek P, Steiner P, Hadravsky L, Belousova IE, Shelekhova KV, Svajdler M, Dubinsky P, Michal M, Kazakov DV. Small Subset of Adenoid Cystic Carcinoma of the Skin Is Associated With Alterations of the MYBL1 Gene Similar to Their Extracutaneous Counterparts. *Am J Dermatopathol* 2018; [v tisku].

33.   Broz M, Steiner P, Salzman R, Hauer L, Starek I. The incidence of MYB gene breaks in adenoid cystic carcinoma of the salivary glands and its prognostic significance. *Biomed Pap Med Fac Univ Palacky Olomouc Czech Repub* 2016; 160(3): 417-422.

34.   Hauer L, Skálová A, Šteiner P, Hrušák D, Andrle P, Hostička L, Sebera O. Adenoidně cystický karcinom slinných žláz. Soubor 27 pacientů. *Česká Stomatologie* 2016; 116(3): 57 - 65.

35.   Skálová A, Šteiner P, Vaneček T. [New developments in molecular diagnostics of carcinomas of the salivary glands: "translocation carcinomas"]. *Cesk Patol* 2016; 52(3): 139-145.

36.   Korabecna M, Steiner P, Jirkovska M. DNA from microdissected tissues may be extracted and stored on microscopic slides. *Neoplasma* 2016; 63(4), 518-522.

37.   Korabecna M, Geryk J, Hora M, Steiner P, Seda O, Tesar V. Genome-wide methylation analysis of tubulocystic and papillary renal cell carcinomas. *Neoplasma* 2016; 63(3): 402-410.

38.   Michal M, Kazakov DV, Hadravsky L, Michalova K, Grossmann P, Steiner P, Vanecek T, Renda V, Suster S. Lipoblasts in Spindle Cell and Pleomorphic Lipomas: a Close Scrutiny. *Hum Pathol* 2017; 65: 140-146.

39.   Michal M, Kazakov DV, Agaimy A, Hosova M, Michalova K, Grossmann P, Steiner P, Skenderi F, Vranic S. Whorling cellular perineurioma: A previously undescribed variant closely mimicking monophasic fibrous synovial sarcoma. *Ann Diagn Pathol* 2017; 27, 74-78.

40.   Kazakov DV, Kyrpychova L, Martinek P, Grossmann P, Steiner P, Vanecek T, Pavlovsky M, Bencik V, Michal M. ALK Gene Fusions in Epithelioid Fibrous Histiocytoma: A Study of 14 Cases, With New Histopathological Findings. *Am J Dermatopathol* 2018; [v tisku].

41.   Michalova K, Steiner P, Alaghehbandan R, Trpkov K, Martinek P, Grossmann P, Perez Montiel D, Sperga M, Suster S, Straka L, Prochazkova K, Cempirkova D, Horava V, Bulimbasic S, Pivovarcikova K, Daum O, Ondic O, Rotterova P, Michal M, Hes O. Papillary Renal Cell Carcinoma with Cytologic and Molecular Genetic Features of Renal Oncocytoma: Analysis of 10 Cases. *Ann Diag Pathol* 2018; [v tisku].

42.   Skalova A, Sar A, Laco J, Metelkova A, Miesbauerova M, Steiner P, Švajdler M, Michal M. The Role of SATB2 as a Diagnostic Marker of Sinonasal Intestinal-type Adenocarcinoma. *Appl Immunohistochem Mol Morphol* 2016; 26(2): 140-146.

43.   Ronen S, Aguilera-Barrantes I, Giorgadze T, Šteiner P, Grossmann P, Suster S. Polymorphous Sweat Gland Carcinoma: An Immunohistochemical and Molecular Study. *Am J Dermatopathol* 2018; [v tisku].

44.   Mitani Y, Roberts DB, Fatani H, Weber RS, Kies MS, Lippman SM, El-Naggar AK. MicroRNA profiling of salivary adenoid cystic carcinoma: association of miR-17-92 upregulation with poor outcome. *PLoS One* 2013; 8(6): e66778.

45.   Hall JS, Taylor J, Valentine HR, Irlam JJ, Eustace A, Hoskin PJ, Miller CJ, West CM. Enhanced stability of microRNA expression facilitates classification of FFPE tumour samples exhibiting near total mRNA degradation. *Br J Cancer* 2012; 107(4): 684-694.

46.   Xi Y, Nakajima G, Gavin E, Morris CG, Kudo K, Hayashi K, Ju J. Systematic analysis of microRNA expression of RNA extracted from fresh frozen and formalin-fixed paraffin-embedded samples. *RNA* 2007; 13(10): 1668-1674.

47.   Knezevich SR, McFadden DE, Tao W, Lim JF, Sorensen PH. A novel ETV6-NTRK3 gene fusion in congenital fibrosarcoma. *Nat Genet* 1998; 18(2): 184-187.

48.   Knezevich SR, Garnett MJ, Pysher TJ, Beckwith JB, Grundy PE, Sorensen PH. ETV6-NTRK3 gene fusions and trisomy 11 establish a histogenetic link between mesoblastic nephroma and congenital fibrosarcoma. *Cancer Res* 1998; 58(22): 5046-5048.

49.   Bourgeois JM, Knezevich SR, Mathers JA, Sorensen PH. Molecular detection of the ETV6-NTRK3 gene fusion differentiates congenital fibrosarcoma from other childhood spindle cell tumors. *Am J Surg Pathol* 2000; 24(7): 937-946.
50.   Rubin BP, Chen CJ, Morgan TW, Xiao S, Grier HE, Kozakewich HP, Perez-Atayde AR, Fletcher JA. Congenital mesoblastic nephroma t(12;15) is associated with ETV6-NTRK3 gene fusion: cytogenetic and molecular relationship to congenital (infantile) fibrosarcoma. *Am J Pathol* 1998; 153(5): 1451-1458.
51.   Alassiri AH, Ali RH, Shen Y, Lum A, Strahlendorf C, Deyell R, Rassekh R, Sorensen PH, Laskin J, Marra M, Yip S, Lee CH, Ng TL. ETV6-NTRK3 Is Expressed in a Subset of ALK-Negative Inflammatory Myofibroblastic Tumors. *Am J Surg Pathol* 2016; 40(8): 1051-1061.
52.   Kralik JM, Kranewitter W, Boesmueller H, Marschon R, Tschurtschenthaler G, Rumpold H, Wiesinger K, Erdel M, Petzer AL, Webersinke G. Characterization of a newly identified ETV6-NTRK3 fusion transcript in acute myeloid leukemia. *Diagn Pathol* 2011; 6, 19.
53.   Leeman-Neill RJ, Kelly LM, Liu P, Brenner AV, Little MP, Bogdanova TI, Evdokimova VN, Hatch M, Zurnadzy LY, Nikiforova MN, Yue NJ, Zhang M, Mabuchi K, Tronko MD, Nikiforov YE. ETV6-NTRK3 is a common chromosomal rearrangement in radiation-associated thyroid cancer. *Cancer* 2014; 120(6): 799-807.
54.   Li GG, Somwar R, Joseph J, Smith RS, Hayashi T, Martin L, Franovic A, Schairer A, Martin E, Riely GJ, Harris J, Yan S, Wei G, Oliver JW, Patel R, Multani P, Ladanyi M, Drilon A. Antitumor Activity of RXDX-105 in Multiple Cancer Types with RET Rearrangements or Mutations. *Clin Cancer Res* 2017; 23(12): 2981-2990.
55.   Sabari JK, Siau ED, Drilon A. Targeting RET-rearranged lung cancers with multikinase inhibitors. *Oncoscience* 2017; 4(3-4): 23-24.
56.   Drilon A, Siena S, Ou SI, Patel M, Ahn MJ, Lee J, Bauer TM, Farago AF, Wheler JJ, Liu SV, Doebele R, Giannetta L, Cerea G, Marrapese G, Schirru M, Amatu A, Bencardino K, Palmeri L, Sartore-Bianchi A, Vanzulli A, Cresta S, Damian S, Duca M, Ardini E, Li G, Christiansen J, Kowalski K, Johnson AD, Patel R, Luo D, Chow-Maneval E, Hornby Z, Multani PS, Shaw AT, De Braud FG. Safety and Antitumor Activity of the Multitargeted Pan-TRK, ROS1, and ALK Inhibitor Entrectinib: Combined Results from Two Phase I Trials (ALKA-372-001 and STARTRK-1). *Cancer Discov* 2017; 7(4): 400-409.
57.   Cantile M, Marra L, Franco R, Ascierto P, Liguori G, De Chiara A, Botti G. Molecular detection and targeting of EWSR1 fusion transcripts in soft tissue tumors. *Med Oncol* 2013; 30(1): 412.
58.   Aurias A, Rimbaut C, Buffe D, Dubousset J, Mazabraud A. [Translocation of chromosome 22 in Ewing's sarcoma]. *C R Seances Acad Sci III* 1983; 296(296): 1105-1107.
59.   Turc-Carel C, Philip I, Berger MP, Philip T, Lenoir GM. Chromosome study of Ewing's sarcoma (ES) cell lines. Consistency of a reciprocal translocation t(11;22)(q24;q12). *Cancer Genet Cytogenet* 1984; 12(1): 1-19.
60.   Uren A, Toretsky JA. Ewing's sarcoma oncoprotein EWS-FLI1: the perfect target without a therapeutic agent. *Future Oncol* 2005; 1(4): 521-528.
61.   Ladanyi M. EWS-FLI1 and Ewing's sarcoma: recent molecular data and new insights. *Cancer Biol Ther* 2002; 1(4): 330-336.
62.   Deng FM, Galvan K, de la Roza G, Zhang S, Souid AK, Stein CK. Molecular characterization of an EWSR1-POU5F1 fusion associated with a t(6;22) in an undifferentiated soft tissue sarcoma. *Cancer Genet* 2011; 204(8): 423-429.

63. Antonescu CR, Zhang L, Chang NE, Pawel BR, Travis W, Katabi N, Edelman M, Rosenberg AE, Nielsen GP, Dal Cin P, Fletcher CD. EWSR1-POU5F1 fusion in soft tissue myoepithelial tumors. A molecular analysis of sixty-six cases, including soft tissue, bone, and visceral lesions, showing common involvement of the EWSR1 gene. *Genes Chromosomes Cancer* 2010; 49(12): 1114-1124.

64. Fisher C. The diversity of soft tissue tumours with EWSR1 gene rearrangements: a review. *Histopathology* 2014; 64(1), 134-150.

65. Möller E, Stenman G, Mandahl N, Hamberg H, Mölne L, van den Oord JJ, Brosjö O, Mertens F, Panagopoulos I. POU5F1, encoding a key regulator of stem cell pluripotency, is fused to EWSR1 in hidradenoma of the skin and mucoepidermoid carcinoma of the salivary glands. *J Pathol* 2008; 215(1): 78-86.

66. Bilodeau EA, Weinreb I, Antonescu CR, Zhang L, Dacic S, Muller S, Barker B, Seethala RR. Clear cell odontogenic carcinomas show EWSR1 rearrangements: a novel finding and a biological link to salivary clear cell carcinomas. *Am J Surg Pathol* 2013; 37(7): 1001-1005.